論文 / 著書情報
Article / Book Information

題目(和文)	
Title(English)	Influencing factors and driving mechanisms for greenhouse gas emissions in eutrophic lakes of the middle and lower Yangtze River Basin
著者(和文)	ZhouChuanqiao
Author(English)	Chuanqiao Zhou
出典(和文)	学位:博士(工学), 学位授与機関:東京科学大学, 報告番号:甲第343号, 授与年月日:2025年3月26日, 学位の種別:課程博士, 審査員:木内 豪,吉村 千洋,中村 恭志,藤井 学,中村 隆志
Citation(English)	Degree:Doctor (Engineering), Conferring organization: Institute of Science Tokyo, Report number:甲第343号, Conferred date:2025/3/26, Degree Type:Course doctor, Examiner:,,,,
学位種別(和文)	博士論文
Type(English)	Doctoral Thesis

Influencing factors and driving mechanisms for greenhouse gas emissions in eutrophic lakes of the middle and lower Yangtze River Basin

Chuanqiao Zhou

(22D58340)

A dissertation submitted for the Degree of Doctor of Engineering

Global Engineering for Development, Environment and Society (GEDES)

School of Environment and Society

Institute of Science Tokyo

March 2025

Abstract

Lake ecosystems are interconnected with multiple ecosystems on the Earth's surface, playing a crucial role in the circulation of carbon and other substances on the regional and global scale. With the continuous impact of human activities and climate warming, eutrophication has become a severe environmental issue facing lake ecosystems. The intensification of lake eutrophication has led to the cyanobacteria blooms, which through subsequent biochemical processes, has increased greenhouse gas (GHG) emissions and altered the role of lakes as sources or sinks. However, the factors driving GHG emissions in eutrophic lakes and the potential mechanisms remain unclear. This study focuses on the lake groups in the middle and lower reaches of the Yangtze River Basin in China, an area with a high potential for increased eutrophication. Through field investigation and laboratory simulation experiments, this study tracked the spatiotemporal patterns of eutrophication and GHG emissions in typical lakes of this region, identified the potential influencing factors, and elucidated the mechanism of the eutrophication-altered GHG emission. These findings provide a theoretical and policy basis for lake management and GHG emission assessment.

The main conclusions were summarized as follows:

(1) Results indicated that GHG production and emissions from lake ecosystems in this region are significantly higher than in other areas and positively correlated with eutrophication levels. On the spatial scale, the average CH_4 production potential, dissolved CH_4 concentrations, and CH_4 release fluxes in eutrophic lakes were 268.6, 0.96 $\mu mol \cdot L^{-1}$, and 587.6 $\mu mol \cdot m^{-2} \cdot h^{-1}$, respectively, while they were 215.8, 0.79$\mu mol \cdot L^{-1}$, and 548.6 $\mu mol \cdot m^{-2} \cdot h^{-1}$ on the temporal scale. Factors including physical and chemical conditions, and nutrient concentrations significantly influence GHG emission. The study revealed that ignoring temporal and spatial variations in factors such as DO and temperature can result in inaccuracies in gross carbon emission estimates, and using summer data leads to an overestimation of gross carbon emissions.

(2) The multiple sources of dissolved organic matter (DOM) in typical eutrophic lakes contribute to the complexity of DOM composition. Lignins constituted the majority of DOM compounds, surpassing 40% of the total, while the organic carbon content was predominantly composed of humic acids (1.02–3.01 g kg 1). The high amounts of lignin oxidative cleavage led to CHO being the main molecular structure in the DOM of the Lake Taihu basin. The elevated DOM concentration, coupled with its intricate

composition, contributed to the increases in GHG production and emission. Experiments showed that the unit carbon emission efficiency was highest in the mixed group, reaching 160.9μmol·C_g^{-1}, which also exhibited a significantly different carbon pool. The co-metabolic processes induced by the decomposition of multi-source DOM are considered potential driving factors.

(3) Unexpectedly high concentrations of dissolved GHG were observed in the overlying water, accompanied by a significant amount of particulate organic carbon (POC). The carbon isotopic analysis showed that the $\delta^{13}C_{poc}$ ranged from -30.28‰ to -21.14‰, indicating that cyanobacteria-derived carbon is an important source of POC. Therefore, the intensification of eutrophication and the resulting increase in POC concentration is a potential driver for the increased GHG flux. Additionally, the methane paradox was observed, characterized by high concentrations of dissolved CH_4 in oxic waters.

(4) Cyanobacteria decomposition in eutrophic lakes altered the carbon storage structure in sediments, leading to the shift of hotspot areas for GHG production. In lakes with hyper-eutrophic conditions, a slight increase in the dissolved CO_2 concentrations in the pore-water of surface sediments (-4-0 cm) was observed. Isotope tracing in simulation experiments indicated that cyanobacteria-derived carbon altered the physicochemical environment and organic carbon concentration in surface sediments, resulting in significantly higher CH_4 and CO_2 concentrations in the pore-water of surface sediment compared to the deeper layer. In the microcosm simulation with the most severe cyanobacteria accumulation, average CH_4 and CO_2 concentrations in surface sediments reached 6.9 and 2.3 mol·L^{-1}, respectively, surpassing the 4.7 and 1.4 mol·L^{-1} observed in bottom sediments, indicating upward migration of CH_4 and CO_2 hotspots from deeper to surface layers, which improved emission efficiency.

(5) Sulfate (SO_4^{2-}) concentration in the overlying water of lakes in the middle and lower reaches of the Yangtze River basin is on the rise and showed a positive correlation with the lake eutrophication levels across spatiotemporal scales. The increasing sulfate concentrations intensify sulfate reduction reactions, leading to the proliferation of sulfate reduction bacteria (SRB). A random forest model was applied to assess the impact of SO_4^{2-} concentrations on CH_4 emissions, revealing a significant negative effect. Microcosmic experiments showed a strong negative correlation between CH_4 concentrations and initial SO_4^{2-} levels (R^2=0.83), indicating that higher initial SO_4^{2-} concentrations led to lower final CH_4 concentrations. This was attributed to the

competition for cyanobacteria-supplied substrates between SRB, and methane production archaea (MPA).

Key words: Greenhouse gas; microbial activities; organic carbon mineralization; lakes; eutrophication

Contents

1. Introduction

1.1 Background

Lakes are significant natural sources of GHG emissions, especially for (methane) CH_4, whose emissions range from 8 to 48 Tg/yr worldwide, accounting for 6-16% of total natural CH_4 emissions (Bastviken et al., 2011). In recent years, under the pressures of intensified human activities and climate change, lake ecosystems have been facing severe eutrophication problems (Ho et al., 2019). Numerous studies have demonstrated a bidirectional positive feedback relationship between intensified lake eutrophication and increased GHG emissions, with eutrophication-induced cyanobacteria blooms playing a pivotal role in this process (Yan et al., 2017).

Frequent cyanobacteria blooms in eutrophic lakes significantly promote GHG emissions (Jiang et al., 2015). The severe accumulation of cyanobacteria alters the physicochemical environment of lakes, particularly contributing to the formation of anaerobic conditions, which creates a suitable environment for anaerobic metabolism driven by microorganisms (Qi et al., 2020). GHG emissions from lakes to the atmosphere are the consequence of a series of microbial processes; therefore, the abundance and activity of microorganisms have a significant impact on GHG emissions (Xu et al., 2015). The increase in primary productivity due to lake eutrophication enhances microbial activity and leads to more vigorous microbial metabolism (Yan et al., 2017). The presence of highly labile carbon components in cyanobacteria-derived carbon significantly drives increased GHG emissions in eutrophic lakes (Deng et al., 2023). Cyanobacteria-derived carbon inputs exacerbate the instability of lake carbon cycling, as substantial amounts of reactive organic carbon are mineralized into CH_4 and CO_2 and subsequently released into the atmosphere (Ma et al., 2024). Studies have identified that cyanobacteria-derived organic carbon induces co-metabolism effects, where the addition of “readily degradable fresh carbon” alters the metabolic rates of pre-existing organic carbon in lake ecosystems, particularly through microbial pathways (Ma et al., 2020). This discovery further underscores the critical impact of cyanobacteria blooms on GHG emissions (Deng et al., 2022). The cyanobacteria blooms also influence GHG production and emissions by altering organic carbon metabolic pathways, with research indicating that severe cyanobacteria accumulation can shift methane production pathways, inducing methanogenesis via methylated

substrates, a potential contributor to elevated GHG emissions in lakes (Zhou et al., 2022a). Furthermore, the coupling of organic carbon mineralization with other biogeochemical processes, such as the regulatory role of nitrogen in organic carbon metabolism and the coupling of anaerobic methane oxidation with nitrate metabolism, is believed to affect GHG emissions (Zhou et al., 2020). Recently, increasing sulfate concentrations in freshwater lakes have gained attention for their effects on lake ecosystems, such as promoting internal phosphorus release and influencing iron reduction processes, though their impact on organic carbon mineralization and GHG emissions remains poorly understood (Zhao et al., 2019).

Lake sediments are the primary reservoirs of organic carbon in lakes, with organic carbon mineralization processes predominantly occurring in sediment carbon pools (Xu et al., 2015). As eutrophication intensifies, the input of cyanobacteria-derived organic carbon and other biogeochemical processes significantly impact the storage and structural composition of sediment carbon pools, exacerbating their instability and influencing GHG production and emissions (Bartosiewicz et al., 2021; Ma et al., 2024). Studies have shown that cyanobacterial blooms profoundly alter the physicochemical environment of sediments, with severe cyanobacterial accumulation forming a "cyanobacterial detritus mat" in surface sediments (Qi et al., 2020). This mat increases the organic carbon load in sediment carbon pools and obstructs oxygen exchange at the sediment-water interface, ultimately creating anaerobic conditions (Braeckman et al., 2019; Qi et al., 2020). Furthermore, driven by physical processes such as gravitational settling and diffusion, cyanobacteria-derived organic carbon infiltrates deeper into sediments as dissolved organic matter, further destabilizing sediment carbon pools (Deng et al., 2023). This effect is particularly pronounced in the numerous shallow lakes of the middle and lower Yangtze River Basin, where hydrodynamic movements and wind-induced disturbances facilitate the deeper penetration of algal-derived organic carbon into sediment layers (Liu et al., 2019). Therefore, it is imperative to analyze the impacts of cyanobacterial blooms in eutrophic lakes on the physicochemical environment of sediments, organic carbon load, and structural composition, as well as their effects on sediment carbon pools and the driving mechanisms of GHG production and emissions. It is essential for advancing the understanding and management of carbon emissions and prediction in lake ecosystems.

1.2 Purpose and structure of this study

Distinguished from net emissions, which incorporate the effects of carbon sink processes, gross emissions refer to the total GHG released into the atmosphere from a given region, excluding considerations of absorption or removal. This thesis focuses on the current states and influencing factors of GHG gross emissions from lakes in the middle and lower reaches of the Yangtze River Basin under the context of increasing eutrophication, our research objectives and structure are as follows.

1.2.1 Research objectives

Our study focuses on the GHG gross emissions from lakes, the objectives are as follows,
(1) By selecting typical lakes in the middle and lower reaches of Yangtze River Basin, this study conducted field investigation to reveal the current state of nutrient loads and GHG gross emissions in typical lakes under the pressures of activities and climate change on spatial and temporal scale.
(2) Based on the field investigation, combined with laboratory simulation experiments to explore the potential factors driving GHG gross emissions from lakes and evaluate their contributions.
(3) Laboratory simulation experiments were designed to integrate multidisciplinary approaches, including biological, chemical, data science, and geographic techniques. The study aims to elucidate the driving mechanisms of GHG gross emissions from lakes by investigating various influencing factors including changes in physicochemical environments, increased endogenous carbon, exogenous carbon inputs, the impact of cyanobacteria blooms on sediment carbon pool, and the coupling biogeochemical process between sulfur and carbon.

1.2.2 Structure of the thesis

This thesis consists of seven chapters to elaborate on the main research contents and results, as follows,
(1) Chapter 1 introduces the current states and limitations of research on GHG gross emissions from lakes and their driving mechanisms, emphasizing the objectives and key focuses of this study.
(2) Chapter 2 examines the current GHG gross emissions from lakes and their

relationship with lake trophic states, analyzing the spatiotemporal responses of lake GHG gross emissions to trophic status and physicochemical environmental changes.

(3) Chapter 3 investigates the composition and sources of exogenous organic carbon, revealing its impact on lake GHG gross emissions and the driving mechanisms behind these effects.

(4) Chapter 4 analyzes the concentrations of dissolved GHG in overlying water, uncovering the reasons for their elevation, particularly in the context of increasing POC concentrations, and proposes potential explanations for the methane paradox.

(5) Chapter 5 elucidates the impact of cyanobacteria-derived organic carbon inputs on the structural composition and physicochemical environment of sediment carbon pools, further revealing the driving mechanisms behind the organic carbon mineralization processes that produce GHG in sediment carbon pools.

(6) Chapter 6 addresses the current rise in sulfate concentrations in lakes, analyzing the spatiotemporal drivers of sulfate increases and examining the coupled processes of sulfate reduction and organic carbon mineralization on GHG gross emissions and their driving mechanisms.

(7) Chapter 7 summarizes the conclusions of this study based on its findings, highlights the existing limitations and gaps in research, and proposes directions and priorities for future studies.

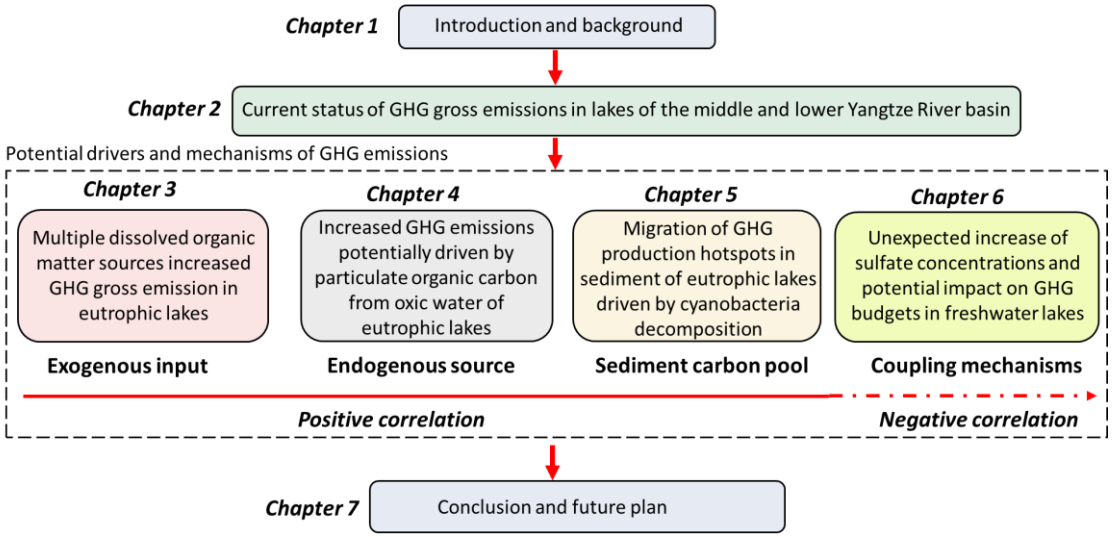

Fig. 1.1. The structure of the thesis

2. Current state of GHG emissions in lakes of middle and lower Yangtze River Basin

2.1 Background

The rapid rise of GHG in the atmosphere is one of the important causes of global warming (Bastviken et al., 2011; IPCC, 2014). CH_4 and CO_2 from freshwater ecosystems significantly contribute to the imbalance of the GHG in the atmosphere (Bastviken et al., 2008; Holgerson and Raymond., 2016). Although the total area of freshwater lakes worldwide is only 2% of the Earth's surface area, freshwater lakes have been considered important natural sources of CH_4 and CO_2 emissions (Holgerson and Raymond., 2016). It has been reported that the increase in lacustrine eutrophication will intensify CH_4 and CO_2 emissions (Yan et al., 2017; Ho et al., 2019). However, there is still great uncertainty about the production and emission of CH_4 and CO_2 from eutrophic lakes under the dual influence of anthropogenic activities and climate change.

Widespread evidence has revealed that multiple environmental factors control the production and emission of CH_4 and CO_2 (Borrel et al., 2011; He et al., 2019). Carbon release (CH_4 and CO_2) from lakes to the atmosphere is the consequence of a series of microbial processes; therefore, the abundance and activity of microorganisms have a significant impact on the carbon emissions (Kumar et al., 2022; Zhou et al., 2022a). In addition, organic matter concentration, oxygen concentration, and temperature change predominantly affect microbial activities (Shamrin et al., 2019). In eutrophic lakes, eutrophication mainly causes cyanobacterial blooms (Pelechata et al., 2016), which can lead to the imbalance of the carbon pool and an increase in carbon emissions (Yan et al., 2019; Ma et al., 2020). The decomposition of cyanobacteria releases a large amount of organic matter into lake sediments and induces the co-metabolism effect which facilitates the transformation of lake sediments from a carbon sink to a carbon source (Shi et al., 2021). It has been shown that the sediment carbon production potential in the area, where cyanobacteria is intensively accumulated, is much higher than in the open lake area (Zhou et al., 2022a). The mineralization of cyanobacteria-derived organic carbon results in CH_4 and CO_2 production in lake sediments and release into the overlying water (Zhou et al., 2022b). The dissolved CH_4 and CO_2 concentrations in the overlying water increase significantly with the intensification of eutrophication in freshwater lakes (Zhou et al., 2018). The mass balances for the production and

consumption of CH_4 and CO_2 is a universal phenomenon in lakes. CH_4, an incomplete organic carbon mineralization production, is oxidized to CO_2 easily in the overlying water (Zhou et al., 2022b). Therein, dissolved CH_4 is easily oxidized up to 50%, and in the extreme case up to 90%, in the overlying water (Yao et al., 2016). CH_4-oxidizing microorganisms play an important role in mitigating CH_4 emissions from lakes effectively (Musenze et al., 2016). A part of the free CO_2 is absorbed by cyanobacteria in the overlying water and re-participates in the carbon cycling process of lakes, which leads to the instability in carbon emissions (Wang, et al., 2020; Zhou et al., 2022a). Therefore, the carbon emissions from freshwater lakes are affected by many factors, especially the further intensification of eutrophication in freshwater lakes.

Recently, CH_4 and CO_2 emissions from freshwater lakes have been statistically analyzed and predicted on different spatial scales (Zhou et al., 2020; Zhou et al., 2021). It has been reported that the global CH_4 emission from lakes to the atmosphere is about 63.9 Tg/yr (Bastviken et al., 2011); however, this estimate potentially overestimates or underestimates the emissions from eutrophic lakes (Kumar et al., 2022). Predicting carbon emissions on different spatial scales usually ignores the influence of lake physicochemical environment changes on the seasonal or temporal scale (Li et al., 2018). Intensive current studies have used the carbon emissions of lakes with different trophic states on the spatial scale to replace the carbon emissions on the evolution process of lake trophic state on the temporal scale, thus estimating the carbon emissions from the freshwater lakes at a region or even global scale (Walter et al., 2007; Bertolet et al., 2020). The absence of spatial or temporal variability will lead to biases in the total CH_4 flux budget (Kumar et al., 2022). For instance, high temperature promotes CH_4 and CO_2 production due to organic matter fixation in both the surface and deep sediments (Li et al., 2018a). In addition, the growth and reproduction of algae and plants in summer will significantly change a dissolved oxygen (DO) concentration in eutrophic lakes (Zhang et al., 2021). Theoretically, an anaerobic environment promotes organic carbon mineralization and CH_4 production (Townsend-Small et al., 2016); however, it has been proposed that the lake CH_4 paradox exists, i.e., the surface aerobic water of the lake appears CH_4 unsaturation phenomenon (Fernandez et al., 2016). The evidence proves that DO is an important factor affecting carbon emission. Therefore, spatial and temporal discrepancies should be considered for predicting carbon emissions in lakes.

In this study, to test the effect of widely used space-for-time substitution on lake carbon emissions, we collected water, sediment, and gas samples from eight freshwater lakes along the Yangtze River basin and Lake Taihu, one of the typical eutrophic lakes worldwide. Year-round sampling and monitoring campaigns were conducted to investigate dissolved CH_4 and CO_2 concentrations in the overlying water and their release fluxes. The physicochemical indexes in the overlying water and sediments were synchronously monitored to find the primary drivers of carbon emissions. In addition, a series of microcosms were established to explore the carbon production potential in sediments of different lakes. The findings of this study benefit the accurate evaluation of the carbon emission underlying the influence of eutrophication degree in freshwater lakes.

2.2 Materials and methods

2.2.1 Study site and sample collection

Eight sampling shallow freshwater lakes (< 7 m deep) in the middle and lower reaches of the Yangtze River basin were selected based on the *TLI* (Fig.2.1). These lakes were classified into five trophic states including oligotrophic ($TLI < 30$), mesotrophic ($30 < TLI < 50$), eutrophic ($50 < TLI < 60$), middle-eutrophic ($60 < TLI < 70$), and hyper-eutrophic ($TLI > 70$). All samples were collected from three sampling sites in each lake in July 2021. A typical eutrophic lake, Lake Taihu, was selected from the surveyed lakes and investigated for one year during 2021-2022.

The sediment samples were collected using a gravity core sampler. After being transported to the laboratory, they were blended thoroughly, homogenized, and sieved (100 mesh), and then placed in a polyethylene bag. The *in situ* dissolved oxygen (DO) and oxidation-reduction potential (ORP) in the overlying water were measured by using YSI ProfessionalPlus (A Xylem, USA). Triplicate overlying water samples (30 cm below the water surface) were collected to measure nutrient concentrations. In order to measure dissolved CH_4 and CO_2 concentrations, water sample (300 mL) was slowly poured into anaerobic bottles, and excess gas was removed by N_2 blowing. Anaerobic bottles were oscillated for 5 min, and the headspace gas was extracted with a syringe and injected into an airbag (E-Switch, China) for storage. Gas release flux samples were collected via a light-shielded floating static chamber (38.5 cm × 30.5 cm × 18.5 cm)

every 10 min for 1 h, which has been previously shown to provide unbiased measurements of water-gas exchange (Peng et al., 2022).

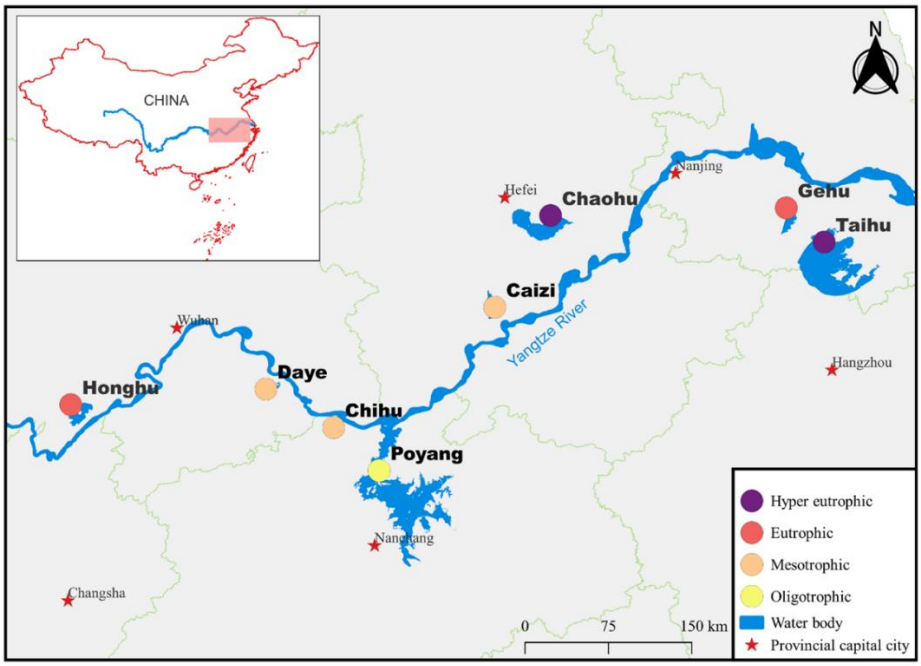

Fig. 2.1. Sampling sites in different trophic state lakes along the Yangtze River.

2.2.2 Calculated trophic state index

The trophic state of lakes was evaluated using the trophic state index (*TLI*) developed by Carlson (1977) and modified by Jin (1995), which is more suitable for Asian freshwater lakes (Equation (1)). The total nitrogen (TN), total phosphorus (TP) and chl-*a* concentrations are used as a criterion to evaluate the lake trophic state by *TLI* (Zhou et al., 2021). The lake trophic state was further classified into mesotrophic ($30 < TLI \leq 50$), eutrophic ($50 < TLI \leq 60$), middle-eutrophic ($60 < TLI \leq 70$), and hyper-eutrophic ($TLI > 70$) based on the *TLI* value.

$$TLI = \sum_{j=1}^{m} wj \times TLI(j), \quad (1)$$

$$W_j = \frac{r_{ij}^2}{\sum_{j=1}^{m} r_{ij}^2}, \quad (2)$$

$$TLI(chl-a) = 10 \times \left(2.46 + \frac{\ln(ch-a)}{\ln(2.5)}\right), \quad (3)$$

$$TLI(TN) = 10 \times (5.453 + 1.694 \times \ln(\mathrm{TN})), \quad (4)$$

$$TLI(TP) = 10 \times (9.436 + 1.624 \times \ln(\mathrm{TP})), \quad (5)$$

where *TLI* is the integrated trophic level index; *TLI* (j) is the trophic level index of j; W_j is the correlative constant for the *TLI* of j; r_{ij} is the relative coefficient, which was

described by Zhou et al. (2021); j and m represent the parameters (*i.e.,* chl-*a*, TP, and TN) and the number of parameters, respectively.

2.2.3 Carbon production potential via incubation microcosms

To measure the carbon production potential from eight lakes along the Yangtze River basin, a series of microcosm systems were set up with six replicates for each lake, *i.e.*, 48 anaerobic bottles (diameter 7.5 cm and height 50 cm). In order to measure the seasonal changes of carbon production potential in Lake Taihu, the same series of microcosm systems were set up with six replicates in four seasons, *i.e.*, in total 24 anaerobic bottles (diameter 7.5 cm and height 50 cm). Hundred grams of sediment was added to each anaerobic bottle, followed by the lake water to submerge the sediment. The headspace in each anaerobic bottle was filled with N_2 gas, and each treatment ensured that the carbon in the anaerobic bottle only came from the sediment. All the anaerobic bottles were placed in a biochemical incubator at a temperature of 25℃ with darkness condition. Gas samples were collected in a time series of 1, 2, 3, 4, 5, 6, 7, 8, 9, 11, 13, 15, 17, 21, 25, 29, 33, 37, 41, 45, 49, 55, 61, 67, 73, 79 and 85 days.

2.2.4 Chemical analytical methods

The overlying water samples were used to determine the concentrations of total phosphorus (TP), total nitrogen (TN), total organic carbon (TOC), and chlorophyll-*a* (chl-*a*). TP was measured using the ammonium molybdate spectrophotometric method after digestion with $K_2S_2O_8$+NaOH (Ebina et al., 1983). TN was measured by an ultraviolet spectrophotometry method through a UV-Visible spectrophotometer (UV-6100, Mapada, China). TOC concentrations in the water and sediments were analyzed using a TOC analyzer (AnlaytikJena HT1300, Germany). Water samples for chl-*a* measurement were filtered through a Mili CA membrane (0.45 μm) at a low pressure. Then, filters were frozen and extracted using 10 mL of 95% acetone (Sinopharm Chemical ReagentCo, China, AR). The optical densities of the extracts at 630, 645, 663, and 750 nm were determined using a UV-vis spectrophotometer (UV-6100, Mapada, China) with a 1 cm matched cell. The microbial biomass carbon (MBC) concentrations were measured by a fumigation extraction method (Li et al., 2018b). The accuracy of TN, TP, TOC, Chl-*a,* and MBC concentrations was up to 0.1 mg/L level.

The CH_4 and CO_2 release fluxes (F) were estimated by a floating static chamber

(size: 38.5 cm × 30.5 cm × 18.5 cm). During each gas sampling event, six gas samples were collected at every 10 min for 1 h. The gas was measured by a gas chromatography (GC-2014, Shimadzu, Japan). The CH_4 and CO_2 release fluxes (F) estimated by a static chamber method are calculated as follows:

$$F = \frac{M}{V_0}\frac{P}{P_0}\frac{T_0}{T}H\frac{dC}{dt} \quad (1)$$

where F is the CH_4 and CO_2 release fluxes ($\mu g \cdot m^{-2} \cdot min^{-1}$); M is the molar mass of the CH_4 and CO_2 ($g \cdot mol^{-1}$); P is the pressure at sampling (Pa), T is the temperature at sampling (K); V_0, P_0, and T_0 are the molar volume of the CH_4 and CO_2, the absolute air pressure and the temperature of the air under the standard state; H is the height above the water surface of the static box (m); dC/dt is the slope of gas concentration changing with time during sampling; it is obtained by linear regression of gas concentration at a different time and corresponding time interval.

Gas samples from both field and microcosm collections in eight different lakes and Lake Taihu during one year were measured by a gas chromatography (GC-2014, Shimadzu, Japan). Five mL of gas was withdrawn from the microsystems. The chamber temperature and FID detector temperatures were 55°C and 200°C, respectively. The rate of the carrier gas was 2 mL/min by 99.999% high purity nitrogen. High purity hydrogen and air were used as the gas at a flow rate of 40 mL/min and 400 mL/min, respectively. The gas concentrations were tested by GC columns CBP1-S25-050 (length: 25.0 m, inner diameter: 0.32 mm, thickness: 0.50 μm) and CBP1-W12-100 (length: 12.0 m, inner diameter: 0.53 mm, thickness: 1.00 μm), respectively. The detection limit was 0.2 ppm for CH_4 and 4 ppm for CO_2 with an error range of ±1%.

2.2.5 Statistical analysis

Bivariate correlation analysis was used for correlation analysis. One-way analysis of variance (ANOVA) was and independent sample *t*-test were used to analyze significant differences each index, respectively. All of the statistical analysis were conducted using the Statistical Package for the Social Sciences 18.0 (SPSS Inc., Chicago, USA).

2.3 Results

2.3.1 The physicochemical characteristics of water

The concentrations of TN, TP, chl-*a*, and TOC exhibited significant differences in different trophic state lakes along the Yangtze River basin (Fig.2.2a,b,c,d). The highest concentrations of TN, TP, chl-*a*, and TOC appeared in Lake Taihu with their values of 6.3 mg/L, 0.7 mg/L, 124.8 μg/L, and 18.8 mg/L, respectively. The lowest concentrations of chl-*a* and TP were 0.06 μg/L and 0.03 mg/L in Lake Caizi and Lake Poyang, respectively. TN and TOC in the overlying water of Lake Caizi were also the lowest concentrations among the surveyed lakes, which were 1.2 and 3.7 mg/L, respectively.

The concentrations of TN, TP, chl-*a*, and TOC in the overlying water of Lake Taihu displayed significant seasonal differences in the entire year (Fig.2.3a,b,c,d). The highest concentration of TP was 1.3 mg/L in October and the lowest concentration of TP was 0.15 mg/L in December. The TN concentration in the overlying water was the highest in summer and the lowest in spring. The highest TN concentration was 9.49 mg/L in June, and the lowest TN concentration was only 1.12 mg/L in February. The TOC concentration in winter was significantly higher than that in other seasons. TOC concentrations in October, November, and December were 71.21, 84.52, and 76.54 mg/L, respectively. The distribution of chl-*a* was fan-shaped and the highest chl-a concentration occurred in June, which reached 172.5 μg/L. The chl-*a* concentration was the lowest in winter, and the chl-*a* concentrations in January and December were 2.53 and 2.51 μg/L, respectively.

2.3.2 The TOC and MBC concentrations in sediments

All the TOC concentrations in sediments of different trophic state lakes were more than 20 g/kg in the lakes along the Yangtze River basin (Fig. 2.2e). Among the eight surveyed lakes, the highest concentration of TOC in sediments was 60.9 g/kg in Lake Taihu and the lowest concentration of TOC in sediment was 24.5 g/kg in Lake Poyang. The concentrations of MBC in different lakes were significantly different ranging from 278.3 to 1126.5 mg/kg (Fig. 2.2f). The MBC concentrations in hyper-eutrophication lakes were significantly higher than in other lakes.

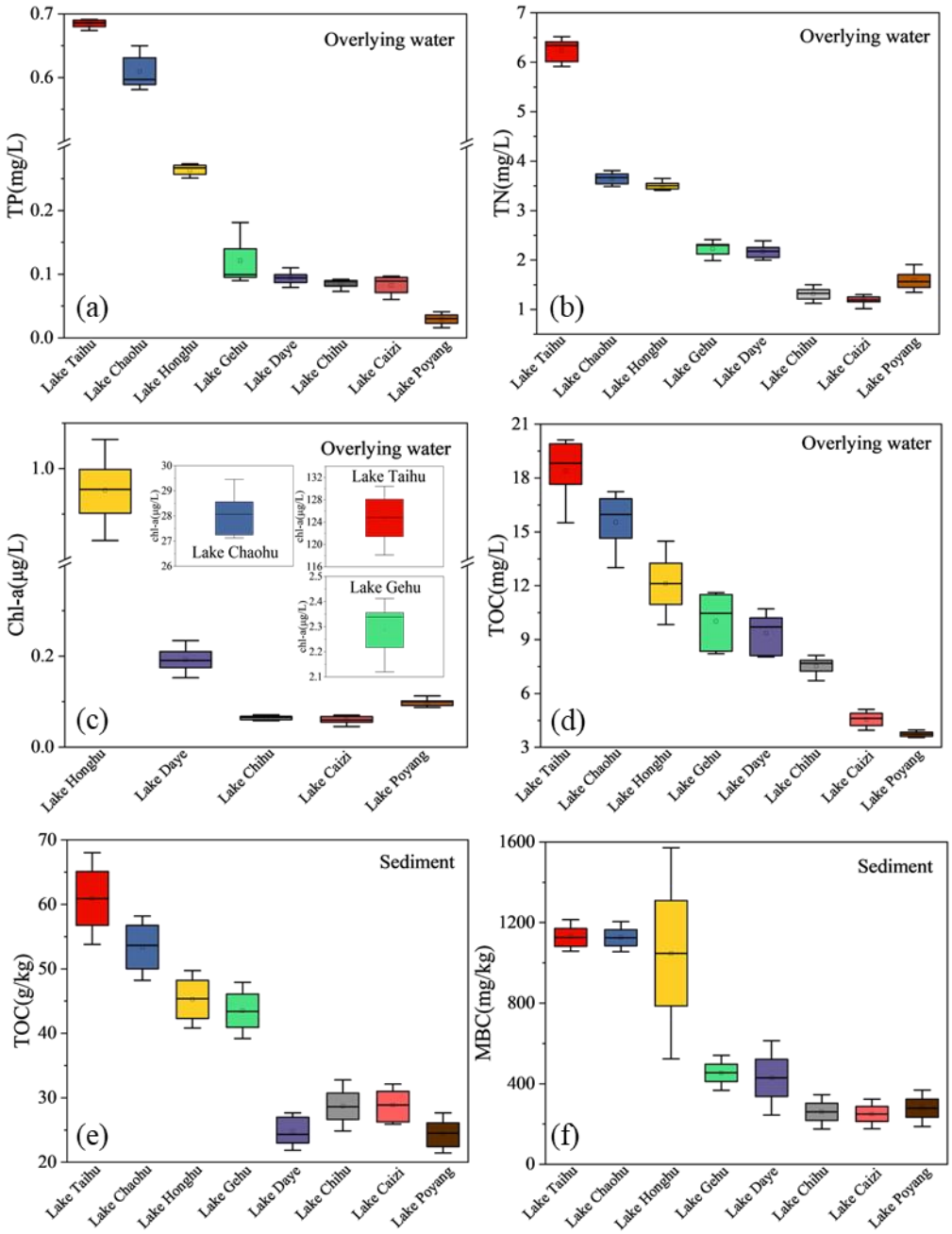

Fig. 2.2. The TP (a), TN (b), TOC (c) and chl-a (d) concentrations in overlying water and TOC (e) and MBC (f) concentrations in sediments in summer of different lakes along the Yangtze River.

The variation of TOC and MBC concentrations in Lake Taihu was different in a year (Fig. 2.3e). The TOC in sediment changed little and the highest TOC concentration in sediment was 60.9 g/kg in July. The TOC concentration in February was the lowest, 29.2% lower than that in July, and its concentration was 43.13 g/kg. The MBC concentration showed a fan-shaped distribution, with the highest MBC concentration in summer, and the MBC concentrations in June, July, and August were 1079, 1126.5,

and 1156.9 mg/kg, respectively (Fig. 2.3f).

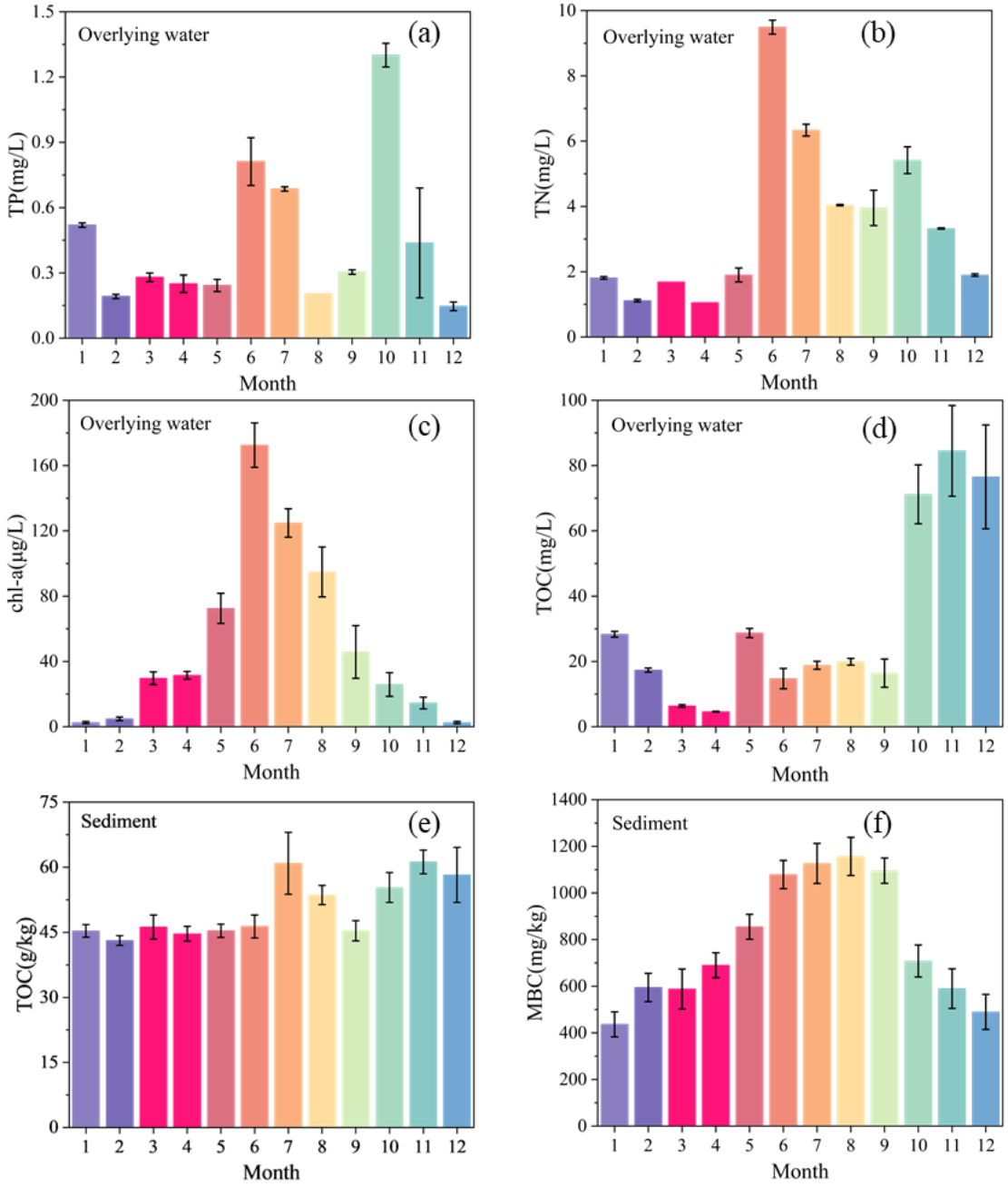

Fig. 2.3. Monthly variations of TP (a), TN (b), TOC (c), and chl-a (d) concentrations in overlying water and TOC (e) and MBC (f) concentrations in sediments of Lake Taihu.

2.3.3 In situ CH_4 and CO_2 release fluxes

The CH_4 and CO_2 release fluxes were the main forms of carbon output from lakes to the atmosphere. There was a great difference in CH_4 release fluxes between different lakes, while all these lakes acted as a source of carbon emissions in the lakes along the

Yangtze River basin (Fig. 2.4a). The CH_4 release fluxes ranged from 17.2 to 929.9 $\mu mol \cdot m^{-2} \cdot h^{-1}$. In hyper-eutrophic lakes, the CH_4 release flux was 929.9 $\mu mol \cdot m^{-2} \cdot h^{-1}$ in Lake Taihu, and it was 830.9 $\mu mol \cdot m^{-2} \cdot h^{-1}$ in Lake Chaohu. The CO_2 release fluxes not only acted as a source of emission in some lakes but also displayed as a sink for Lake Caizi with the value of 0.34 $\mu mol \cdot m^{-2} \cdot h^{-1}$ (Fig. 2.4b). The highest CO_2 release flux was 7222.5 $\mu mol \cdot m^{-2} \cdot h^{-1}$ in hyper-eutrophic Lake Taihu.

The *in situ* CH_4 and CO_2 release fluxes showed the same distribution with the dissolved CH_4 and CO_2 concentrations in Lake Taihu in the entire year (Fig. 2.5a,b). The release fluxes (CH_4 and CO_2) in Lake Taihu were the highest in July which was consistent with the dissolved CH_4 and CO_2 concentrations. The CH_4 and CO_2 release fluxes were 38.5 and 7222.5 $\mu mol \cdot m^{-2} \cdot h^{-1}$ in July, respectively. The CH_4 and CO_2 release fluxes were the lowest in spring, 229.9 and 1997.7 $\mu mol \cdot m^{-2} \cdot h^{-1}$ in January.

2.3.4 In situ dissolved CH_4 and CO_2 concentrations

The mean dissolved CH_4 concentrations across all lakes ranged from 0.26 to 2.1 μmol/L and showed a significant correlation with *TLI* in the lakes along the Yangtze River basin (Fig.2.4c). The highest concentration of dissolved CH_4 was 2.5 μmol/L in Lake Taihu. The mean dissolved CO_2 concentrations showed a positive correlation with *TLI*, and the dissolved CO_2 ranged from 26.6 to 98.9 μmol/L (Fig. 2.4d). In hyper-eutrophic lakes, the concentration of dissolved CO_2 in Lake Taihu was 98.9 μmol/L, much higher than Lake Chaohu of 76.5 μmol/L. Lake Poyang was the only oligotrophic lake in this study, and the concentration of dissolved CO_2 was 27.3 μmol/L.

The mean dissolved CH_4 and CO_2 concentrations in Lake Taihu in a year showed a fan-shaped distribution which was consistent with the chl-*a* distribution (Fig. 2.5c,d). The highest dissolved CH_4 and CO_2 concentrations of 2.1 and 98.9 μmol/L occurred in July, respectively. The lowest dissolved CH_4 and CO_2 were 0.32 and 32.5 μmol/L, respectively. Overall, the dissolved CH_4 and CO_2 concentrations in the overlying water were the highest in summer and the lowest in winter. This trend is similar to the distribution of TOC concentration in sediments.

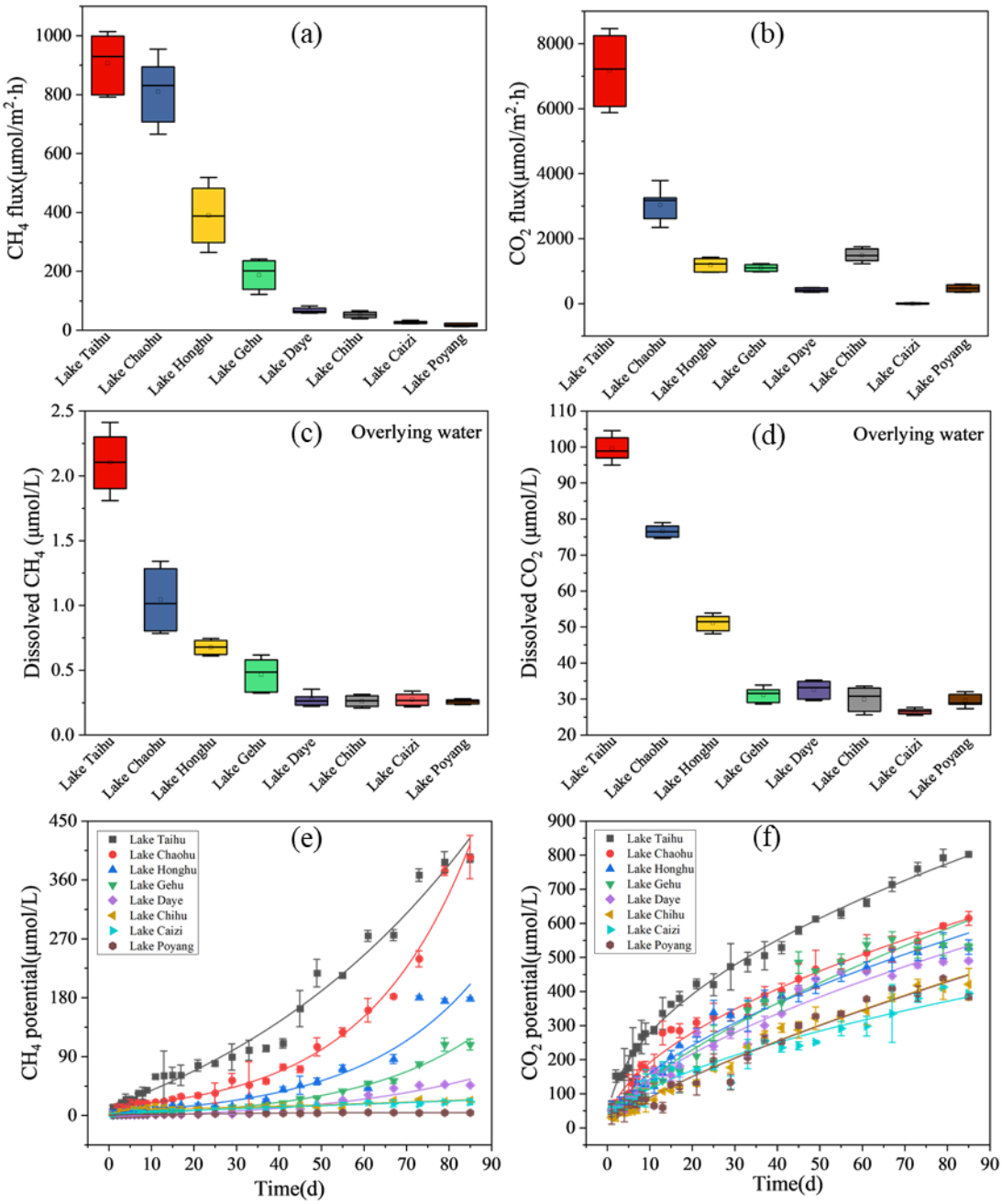

Fig. 2.4. The release flux (a,b), dissolved concentration (c,d), and production potential (e,f) of CH_4 and CO_2 from different lakes in summer along the Yangtze River.

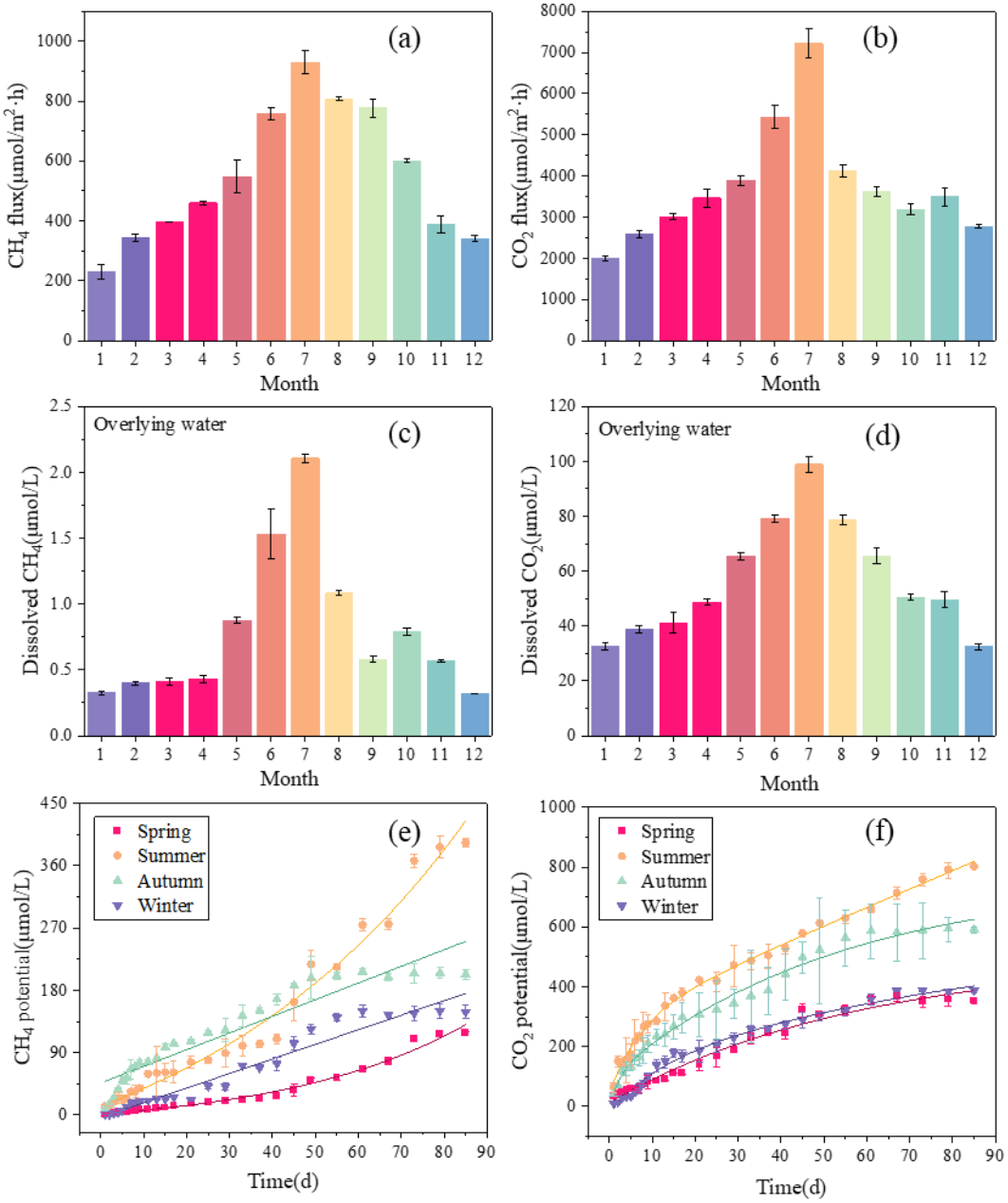

Fig. 2.5. Monthly variations of release flux (a,b), dissolved concentration (c,d) and production potential (e,f) of CH_4 and CO_2 from Lake Taihu.

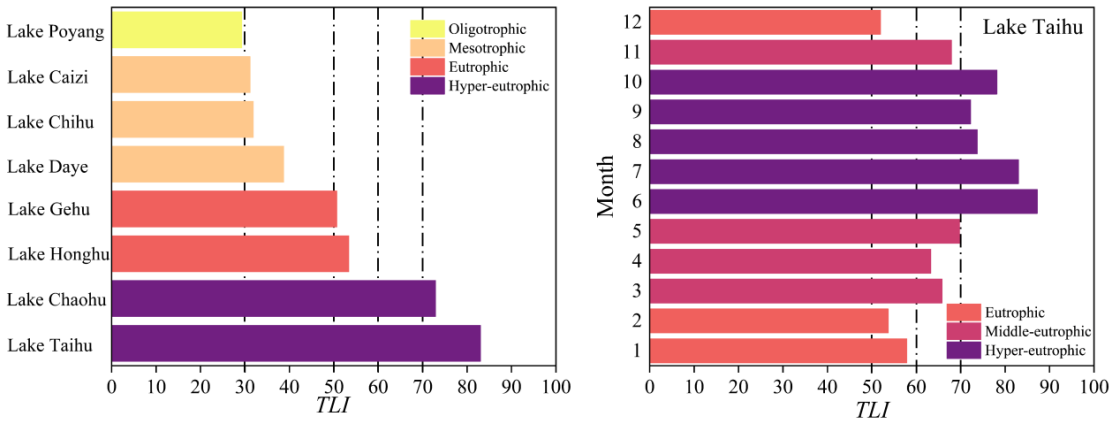

Fig. 2.6. The *TLI* of different lakes in summer along the Yangze River (left) and seasonal variations (right) of *TLI* in Lake Taihu.

2.3.5 Carbon production potential from the sediments

The CH_4 and CO_2 production potential from the sediments of freshwater lakes along the Yangtze River basin was significantly different (Fig. 2.4e,f). The potential of CH_4 production was 392.9 and 394.8 μmol/L in hyper-eutrophic lakes of Lake Taihu and Lake Chaohu, respectively. Among the eight surveyed lakes, the CH_4 and CO_2 production potentials in Lake Poyang were the lowest with their values of 4.2 and 384.3 μmol/L, respectively. The highest CO_2 production potential was 802.2 μmol/L in Lake Taihu among all the surveyed lakes.

There were significant monthly differences in the CH_4 and CO_2 production potential of sediments in Lake Taihu (Fig. 2.5e,f). The overall carbon production potential (CH_4 and CO_2) first increased and then converged. The carbon production potential was the highest in summer, and the CH_4 and CO_2 concentrations were 392.9 and 802.2 μmol/L, respectively. The CH_4 production potential in winter was the lowest, 62.2% lower than that in summer, and its concentration was 148.5 μmol/L. The CO_2 production potential was also the lowest in winter, with a final concentration of 386.9 μmol/L.

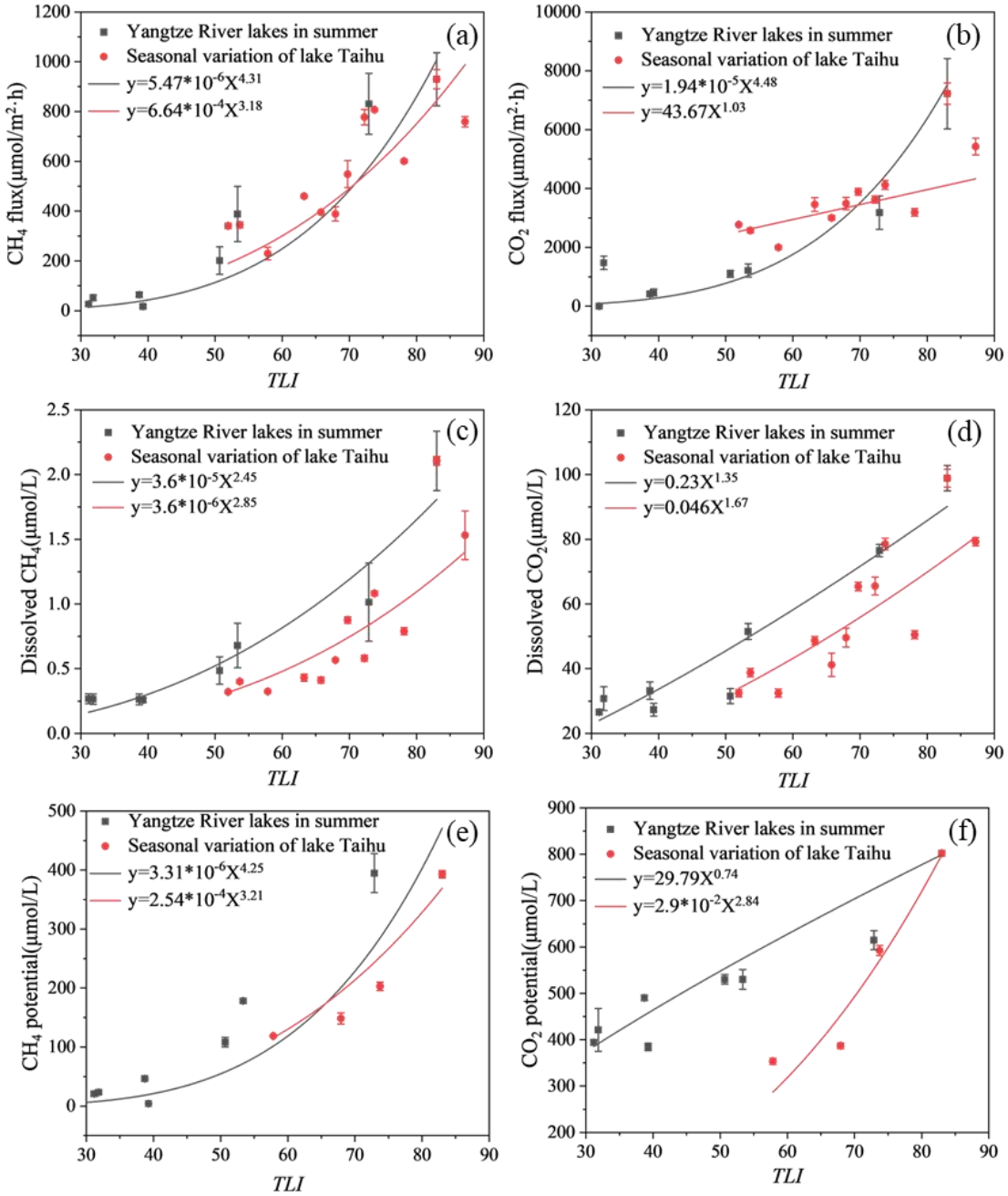

Fig. 2.7. The correlation analysis of release flux (a,b), dissolved concentration (c,d), and production potential (e,f) of CH_4 and CO_2 with *TLI*, respectively.

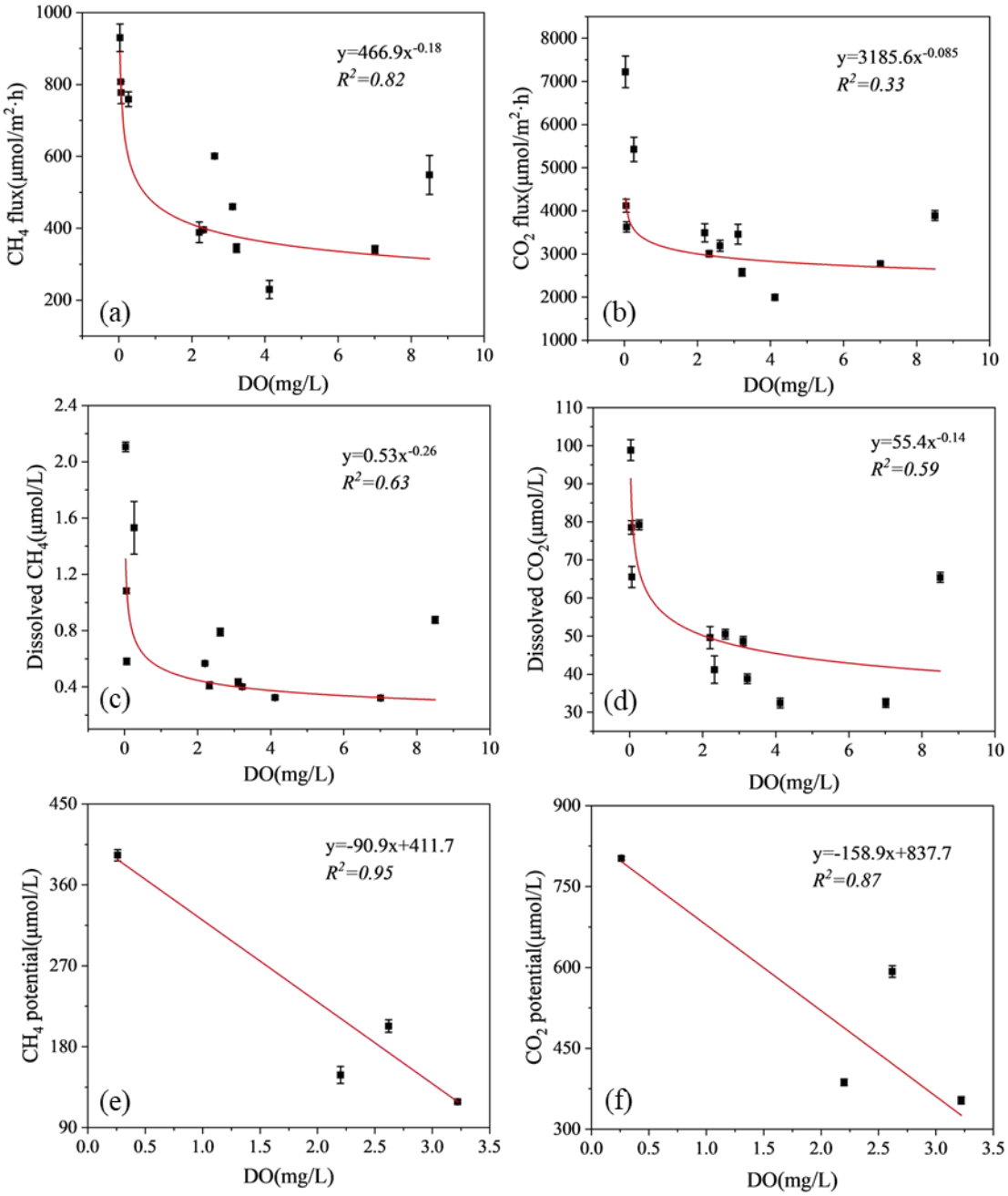

Fig. 2.8. The correlation analysis of carbon (CH_4 and CO_2) release flux (a,b), dissolved concentration (c,d), production potential (e,f) with DO, respectively.

2.4 Discussion

Freshwater lakes make up only a tiny part of the land surface; however, they are one of the largest sources of natural carbon emissions (Tranvik et al., 2009; Bastviken et al., 2011). Owing to anthropogenic activities, a large amount of nutrients (C, N, P, etc.) was released into freshwater ecosystems (Fig. 2.2), leading to a serious ecological

problem, *e.g.*, eutrophication (Fig. 2.6). Eutrophication in freshwater lakes promoted the increase of carbon production potential, dissolved carbon concentrations, and carbon release fluxes (Fig. 2.7). However, obtaining an accurate calculation of carbon emissions on a long-term time scale is difficult; a spatiotemporal substitution on regional and even global scale of lakes is generally deemed an effective method (Bastviken et al., 2011). Although the evolution of a lacustrine trophic state is a long-time process, the trophic state of different lakes at the same spatial scale can replace the trophic state of the same lake at different temporal scales (Bastviken et al., 2011). Theoretically, the most important consideration is the effect of the gradient change of cyanobacterial biomass on carbon emissions in lakes with different trophic states (Yan et al., 2017). However, this study claims that the previously used spatiotemporal substitution overestimas the influence of eutrophication on carbon emissions in shallow lakes (Fig. 2.7). Especially, this overestimation is more serious in higher *TLI* index, i.e., higher eutrophic state.

Recent report underscores that the impact of a time scale should be considered to assess the carbon emission capacity in eutrophic lakes (Kumar et al., 2022; Xiao et al., 2022). The year-round survey implemented in this study showed the significance of the monthly variations of DO concentration and water temperature in eutrophic Lake Taihu (Figs. 2.8 and 2.9). On the other hand, the organic carbon mineralization in sediments was driven by microorganisms (Figs. 2.2f and 2.3f), and the carbon emission was the final result of microbial production and oxidation processes (Roland et al., 2017). Microbial activity is greatly affected by temperature and DO concentrations; therefore, seasonal changes in DO and temperature should be considered for assessing carbon emissions from eutrophic lakes (Yan et al., 2017). An anaerobic environment and high water temperature promote organic carbon conversion to CO_2 and CH_4 (Li et al., 2018a). Both spatial and temporal scale investigations in this study proved that physicochemical environments were an important factor affecting carbon emissions in eutrophic lakes (Figs. 2.8 and 2.9). DO was negatively correlated with the carbon production potential, dissolved carbon concentrations, and carbon release fluxes. The field observation and the highest chl-*a* concentration in summer demonstrated a breakout of cyanobacteria bloom (Fig. 2.3c). The decay and decomposition of cyanobacteria consume a large amount of oxygen, creating anaerobic environments (Zhao et al., 2021), which allowed anaerobic bacteria to further decompose the remaining organic carbon. Therefore, the

formation of anaerobic environments is the reason that carbon emission in summer was greater than those in the other seasons (Zhang et al., 2018). Water temperature significantly influences the physicochemical processes of lakes, especially eutrophic shallow lakes (Paerl and Pual., 2012). High water temperature promotes organic matter decomposition, causes the rise of partial pressure of carbon dioxide (pCO_2) in water, and eventually increases the CO_2 emissions from water to the atmosphere (Yan et al., 2017). Meanwhile, the increase in water temperature stimulates the microbial activity, and reduces the residence time of the gas in water (Wadham et al., 2012; Kumar et al., 2022). This study proved that there was a positive relationship between temperature and carbon emissions, and the increasing water temperature promoted the carbon production potential, dissolved carbon concentrations, and carbon release fluxes (Fig. 2.9). Summer was the season with the highest water temperature, and its carbon emission capacity was higher than the other seasons (Figs. 2.5 and 2.9). Therefore, when carbon emissions from shallow lakes are assessed, changes in other influencing factors on the time scale should not be ignored; otherwise, carbon emissions are likely overestimated.

The CH_4 and CO_2 emissions are complex processes in eutrophic lakes, including being produced from sediments, released to overlying water, and eventually released into the atmosphere (Roland et al., 2017). The impact of lake eutrophication on carbon emissions is manifested including the change in physicochemical environments and the increase of nutrient concentrations (Dai et al., 2009; Tian et al., 2019). This study demonstrated that the CH_4 and CO_2 production potential, dissolved CH_4 and CO_2 concentrations, and CH_4 and CO_2 release fluxes in eutrophic lakes were positively correlated (Figs. 2.10 and 2.11). Both spatial and temporal scale investigations proved that freshwater lakes were facing severe eutrophication (Fig. 2.6). And the carbon emission showed a positive correlation with the degree of eutrophication (Fig. 2.7). In eutrophic lakes, cyanobacteria blooms occur frequently, and after the decay, they settle from the overlying water to the surface sediments and contribute to the sedimentary organic pool, increasing TOC concentration in sediments (Figs.2.2e and 2.3e) (Xing et al., 2005; Shao et al., 2013). The amount of organic matter in sediments is the most important factor in determining carbon production potential (Zhou et al., 2022a). As a fragile source, cyanobacteria-derived organic matter provides a substrate requiring microbial growth and utilization, as evidenced by the high correlation between MBC

concentrations and CH_4 emission on the spatial and temporal scales (R^2=0.93; 0.97) (Figs. 2.10 and 2.11). The mineralization of organic carbon in sediments produces CH_4 and CO_2, which are released into the overlying water (Yan et al., 2017). The eutrophication had positive correlations with the dissolved CH_4 and CO_2 in the overlying water (Fig. 2.7c,d), consistent with previous studies (Zhou et al., 2020). The dissolved CH_4 and CO_2 in the overlying water are emitted into the atmosphere through ebullition, diffusion, storage, etc. (Bastviken et al., 2004). Intensifying eutrophication promoted carbon release fluxes (CH_4 and CO_2), especially for CH_4 release flux, which showed a positive correlation with *TLI* on the spatial and temporal scales (R^2=0.98; 0.84) (Figs. 2.7a,b , 2.10, 2.11).

Collectively, a conceptual diagram is described to clarify the mechanism of eutrophication promoting carbon emissions and the reasons for differences in carbon emission capacity at temporal and spatial scales (Fig. 2.12). Eutrophication triggered cyanobacteria bloom, which provided a large amount of organic carbon to promote microbial decomposition. As a result, the produced CH_4 and CO_2 were released into lake water to enhance their CH_4 and CO_2 dissolved concentrations, and eventually, the CH_4 and CO_2 release fluxes from the water to the atmosphere were increased. The carbon emission capacity (CH_4 and CO_2) was different at temporal and spatial scales, and the spatiotemporal substitution overestimated the influence of eutrophication on carbon emissions. The carbon emission process from the lake was also affected by other factors, especially the physicochemical environment changes on the temporal scale. Seasonal changes can lead to changes in DO and water temperature, which can affect the activity and abundance of microorganisms involved in carbon emissions. These results suggest that the inhibitory effect of DO concentration rise and the promoting effect of temperature needs to be considered on the spatial scale for assessing the carbon emission in eutrophic lakes, especially the further intensification of eutrophication.

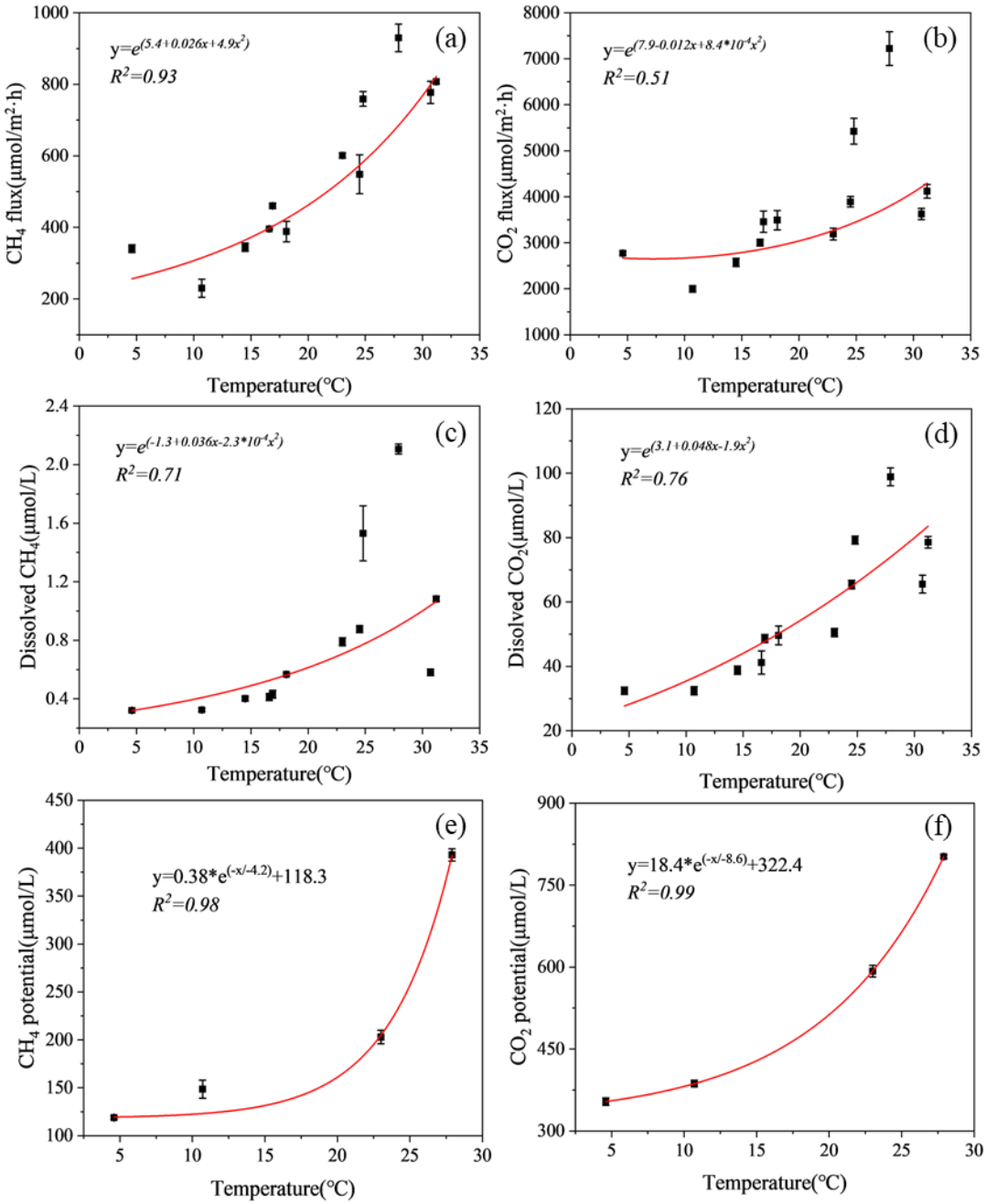

Fig. 2.9. The correlation analysis of carbon (CH_4 and CO_2) release flux (a,b), dissolved concentration (c,d), production potential (e,f) with temperature.

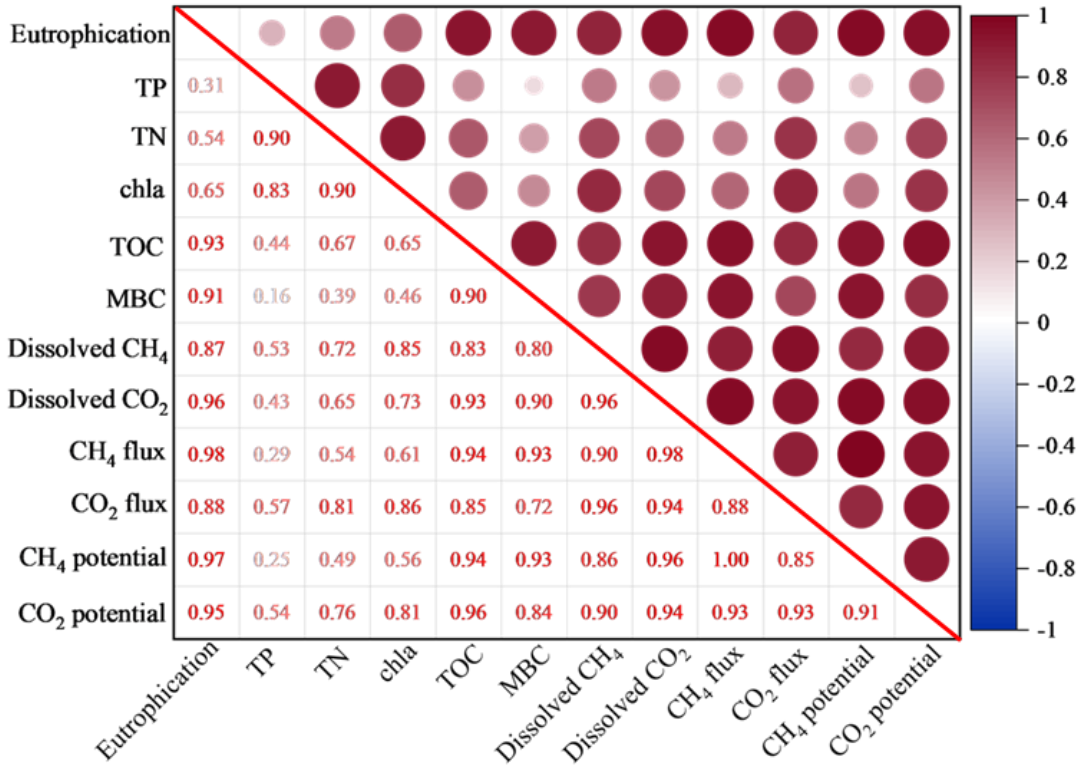

Fig. 2.10. Correlation analysis of each index in different lakes along the middle and lower reaches of Yangtze River Basin

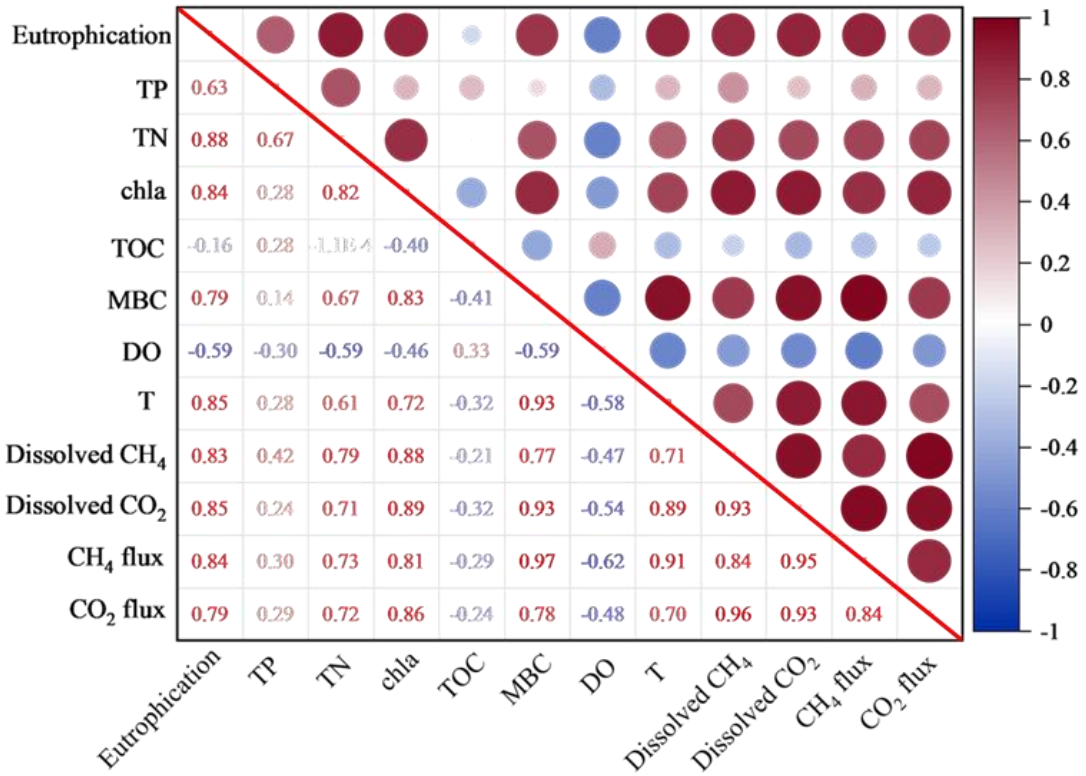

Fig. 2.11. Correlation analysis of each index in Lake Taihu during one year

2.5 Summary

Spatiotemporal scale investigations showed that eutrophication was a severe ecological problem in shallow lakes along the Yangtze River basin, and the nutrient concentrations (TN, TP, and TOC) were high in the overlying water. Increased eutrophication promoted the carbon production potential, dissolved carbon concentrations, and the subsequent carbon release fluxes. The correlation between carbon emission capacity and eutrophication was different at spatial and temporal scales. This study proved that the variations of DO and water temperature caused by seasonal changes also affected carbon emission capacity (carbon production potential, dissolved carbon concentrations, and carbon release fluxes), negatively correlated with DO, and positively correlated with water temperature. Therefore, ignore temporal and spatial variations in factors such as DO and temperature can result in inaccuracies in gross carbon emission estimates. This study demonstrates that using summer data leads to an overestimation of gross carbon emissions, which is important for the accurate assessment of the carbon gross emissions in freshwater lakes.

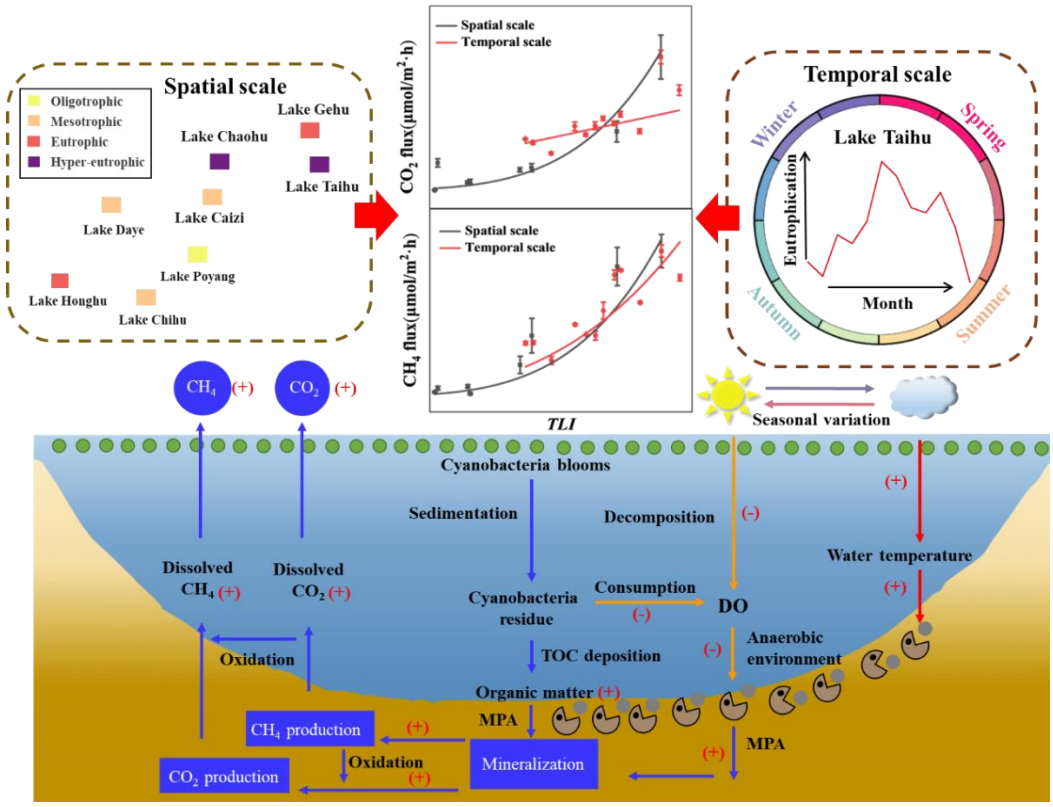

Fig. 2.12. A conceptual diagram of differences in the estimation of carbon (CH_4 and CO_2) flux at spatial and temporal scales.

3. Multiple dissolved organic matter sources increased GHG emission in eutrophic lakes

3.1 Background

Although lakes are only 1.38% the size of the ocean, they are estimated to take up 25% ~ 58% as much carbon, therefore, lakes play disproportionately large roles in the biogeochemical cycling of organic matter (Tranvik et al., 2009; Guillemette et al., 2017). The fate and reactivity of organic matter in lakes vary depending on specific drivers, such as organic matter concentration and composition (Zhou et al., 2022b). Surface runoff, especially via rivers, are crucial sources of organic matter in lakes and, can destabilize the carbon cycle in lake sediment (Xu et al., 2019). With escalating eutrophication and the intensification of dissolved organic carbon (DOM) input (Liu et al., 2019), it has become imperative to identify the factors associated with surface runoff that cause instability in lake carbon pools.

The origins of DOM in river systems are primarily terrigenous and autogenic endogenous, and can exhibit significant variability in terms of source and composition across different rivers (Xu et al., 2023). It has been shown that rapid urbanization processes and the significant reduction of forest, grassland, and farmland cover have contributed to rivers becoming the main repositories of organic matter (Lambert et al., 2022). In basins characterized by extensive forest and farmland coverage, terrigenous input determines the organic matter content in water, with discernibly higher degrees of humification, higher aromaticity values, and higher molecular weights (Ma et al., 2021; Liu et al., 2022). As human activities intensify, the primary component of organic matter carried by land runoff shifts from humic to proteoid substances (Williams et al., 2016; Song et al., 2021). This is because the organic matter carried in domestic sewage is mainly composed of proteoid material, which can enter rivers and affect the composition of organic matter, a process that is especially apparent in eutrophic lake basins (Hosen et al., 2014; Guo et al., 2018). Proteoid matter is readily utilized by microbes, so elevated proteoid content can promote microorganism growth and the associated organic metabolism rates (Yu et al., 2020). The utilization of organic matter by microorganisms directly contributes to carbon cycling in eutrophic lake basins and the CH_4 and CO_2 produced are the main drivers of climate warming (Zhou et al., 2022a; Zhou et al., 2023b). Persistent elevated concentrations of organic carbon in lakes have

been established through field studies conducted in various lakes basin across China (Song et al., 2018; Zhang et al., 2020). These periods of high organic carbon concentrations have been associated with the release of organic matter from sediments, especially in shallow water depths and disturbed water environments (Zhou et al., 2019).

The rivers within the Lake Taihu basin are estimated to transport 2.2×105 t· yr^{-1} of dissolved organic carbon and 6.7×104 t· yr^{-1} of inorganic carbon into Lake Taihu annually (Song et al., 2008). The inflow of DOM transported by rivers has been identified as a significant driver of carbon emissions within eutrophic lakes (Zhou et al., 2018; Jin et al., 2018). In recent years, there has been a substantial upsurge in carbon emissions emanating from lakes worldwide, and in China this has manifested in the average CH_4 emissions reaching 531.5 mmol·m^{-2}·yr^{-1} (Zhou et al., 2022b). Hydrologic dynamics are important factors contributing to the input of DOM into lakes and can enhance the function of lakes as carbon sinks (Ejarque et al., 2018). Moreover, the complexity of organic components transported via rivers into lakes can trigger a series of biogeochemical processes, including co-metabolic interactions, that contribute to the release of carbon from lake sediments to the atmosphere (Deng et al., 2023). These biogeochemical processes can transform the respective roles of different sources and sinks within the carbon pools of lakes (Ma et al., 2020; Deng et al., 2022). To date, most research efforts have examined the carbon cycling processes in lakes (Davidson et al., 2015), while the impact of carbon inputs from rivers on lake carbon pools and carbon emissions remain unclear. Understanding these impacts is especially important as human activities intensify.

In this study, to test the effect of multi-DOM sources on carbon output in the Lake Taihu basin, the water, sediment, and gas samples were collected from seven different rivers entering Lake Taihu, a typical eutrophic lake. The isotope tracer technique and Fourier Transform Ion Cyclotron Resonance Mass Spectrometry (FT-ICR-MS) were used to determine the organic carbon compounds entering Lake Taihu. Meanwhile, a series of microcosms was established to explore the mechanism of multi-source DOM on carbon emissions. These findings provide important insights into the organic carbon content and composition in eutrophic lake basins, and shed light on the influence of multi-source DOM on carbon emissions in lakes, which offers a theoretical basis for accurately assessing carbon output in lake basins.

3.2 Materials and methods

3.2.1 Study site and sample collection

In December 2021, we conducted a study on seven rivers that feed into Lake Taihu, which serves as a representative eutrophic lake. Lake Taihu, located in the lower reaches of the Yangtze River, covers an area of 2338 km^2 with an average depth of 1.89 m. The region experiences a subtropical monsoon climate, with a long-term average temperature of 15–17 ℃ and annual precipitation of 1177 mm. Around 60% of the precipitation occurs from May to September, while the average annual evaporation stands at 821.7 mm. The population density in the Lake Taihu basin is 1500 people per km^2, which is more than 10 times the national average in China. Consequently, human activities have a significant impact on the ecological environment of the basin (Yu et al., 2013).

The specific sampling sites are illustrated in Fig. 3.1. Surface sediment (0-10 cm depth below the water-sediment surface), and water (30 cm below the air-water interface) were obtained respectively from seven rivers entering Lake Taihu, and each sample was collected three times. The sample tanks with ice packs were used to store water and sediment samples, and immediately transported back to laboratory for analysis. Dissolved oxygen (DO), oxidation-reduction potential (ORP), temperature (T), the potential of hydrogen (pH), total dissolved solids (TDS), and electrical conductivity (Ec) were measured in situ using the YSI Professional Plus multi-parameter meter (A Xylem, USA). To quantify dissolved CH_4, CO_2, and N_2O concentrations in water, the anaerobic bottle added 300 ml of water and produced the gas with excessed N_2. The anaerobic bottle was shaken vigorously for 5 minutes, a syringe was used to extract the gas in the headspace, and then stored in the airbag (E-Switch, China).

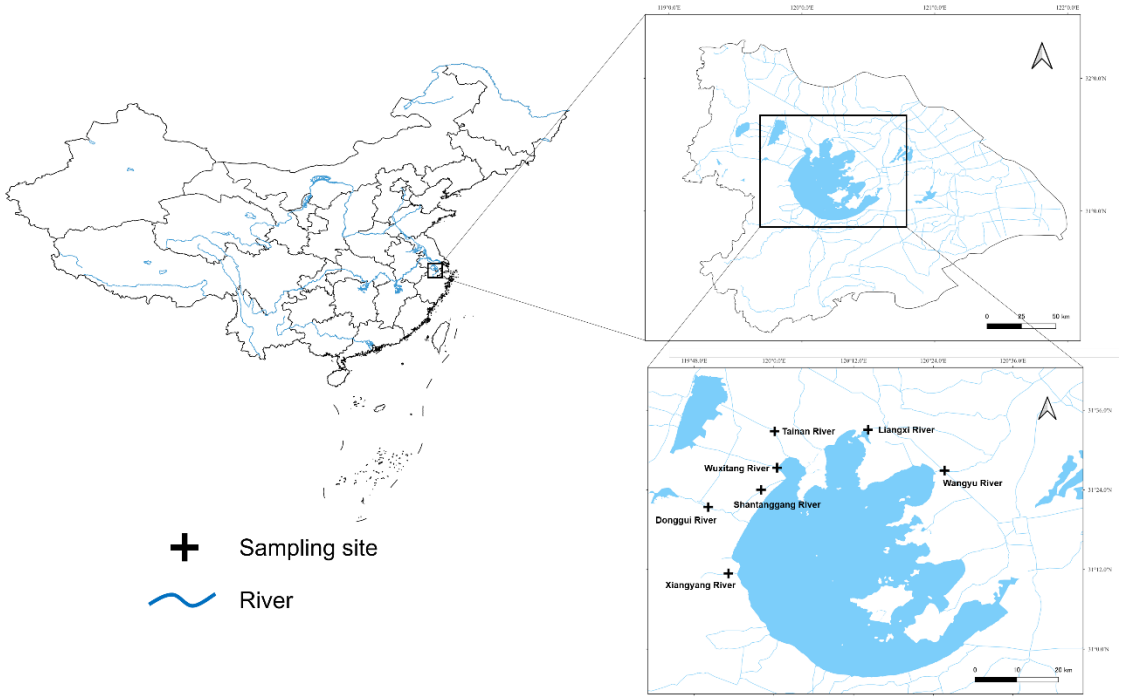

Fig. 3.1. Sampling site information in 7 rivers entering lake Taihu

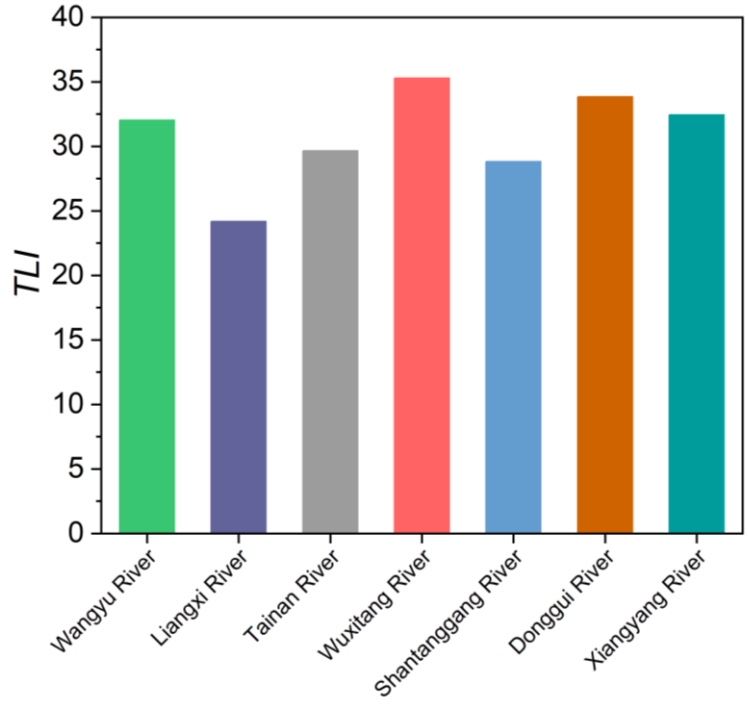

Fig. 3.2. The trophic level index (TLI) from 7 rivers entering Lake Taihu in water.

3.2.2 Laboratory simulation experiment

A series of microcosm system was used to test the effect of organic carbon input on the sediment pool and carbon emissions. The microcosm system experiment consisted of 51 anaerobic bottles (Φ 75 mm, length 180 mm, volume 500 ml) divided

among three treatment groups (cyanobacteria; sediment; and cyanobacteria + sediment) with three replicates for each treatment. According to the ecological environment of Lake Taihu studied by Zhang et al., each anaerobic bottle was added with 0.11 g cyanobacteria powder, 200 mL water, and 100 g sediment, and was incubated in an incubator at 25 °C in darkness condition. Nitrogen purging was performed to ensure the absence of interference from other gas sources. Each anaerobic bottle was sampled at day 1, 2, 3, 4, 5, 6, 7, 9, 11, 14, 18, 23, 28, 33, 38, 43, and 348 of incubation, with a total of 17 destructive samples. The samples of gas and sediment were collected by destructive sampling for each time. The sediment was placed in a refrigerator at 0-4 ℃, and the gas was extracted by syringe from the anaerobic bottle and analyzed within 24 h.

3.2.3 Chemical analysis of samples

All water samples were filtered through 0.45 μm Nylon filters before determining the concentrations of total dissolved carbon (DTC), total dissolved inorganic carbon (DIC), total dissolved organic carbon (DOC), total nitrogen (TN), total phosphorus (TP), ammonia nitrogen (NH_4^+-N), and nitrate (NO_3^--N). The concentrations of TP and TN were quantified using ultraviolet spectrophotometry, employing a UV-Visible spectrophotometer (UV-6100, Mapada, Shang Hai Shi, China) (Peng, et al., 2022). The concentrations of DTC, DOC, and DIC in water samples were determined utilizing a carbon analyzer (Anlaytik HT1300, Jena, Germany) (Zhou, et al., 2023a). The NH_4^+-N and NO_3^--N concentrations of water were measured using a continuous flow analyzer (AutoAnalyzer 3, SEAL, Germany) (Zhou, et al., 2021). The sediment sample acidified to pH < 2.0, and then a multi-N/C analyzer (HT 1300, Analytikjena) was used to measure the TOC concentration.

Dissolved gas concentrations in the overlying water samples collected from the seven rivers were assessed using a gas chromatograph (GC-2014, Shimadzu, Tokyo, Japan). Gas samples of 5 mL were extracted from the microsystems and introduced into the analyzer. The chamber, Electron Capture Detector (ECD) and Flame Ionization Detector (FID) were set at temperatures of 55 ℃, 300 ℃, and 200 ℃, respectively. The gas utilized were high-purity N_2 and air, and the flow rate were reached to 40 and 400 $mL \cdot min^{-1}$, respectively. The high-purity N_2, which reached to 99.999% purity, was be used as the carrier gas, and the flow rate was reached to 2 $mL \cdot min^{-1}$. The detection limits

of CH_4, CO_2, and N_2O were 0.2 ppm, 4.0 ppm, and 0.01 ppm, respectively, with an error range of ±1%.

The particle size analysis of the samples was conducted using the Mastersizer 2000 laser particle size analyzer. The instrument was first allowed to warm up for 15–20 minutes before activating the gas control system. A standardized test program, referred to as the SOP program, was then established. The sample was added to the sample cell and the SOP program was executed. This program included predefined test conditions encompassing factors such as refractive index and test duration. After the measurement, the particle size volume percentages were determined within various subintervals spanning the range from 0.01 to 3000 μm. Furthermore, parameters such as D10, D50, D90, and other particle size fineness metrics were obtained. Additionally, the cumulative particle-size distribution curve was generated as part of the analysis.

After 24 hours, the larger particles in the sediment were eliminated and subsequently subjected to drying in a vacuum freeze dryer (Biosafer-10A, Nanjing, Jiangsu, China). Then, the sediment samples were subsequently sieved through 100 mesh screens, followed by acidification with a 1 $mol \cdot L^{-1}$ HCl solution for 24 hours. They were then rinsed to neutrality and precisely weighed on a 0.1 mg analytical balance. Sediment subsamples, weighing 0.05 g each, were allocated for the assessment of carbon (C) and nitrogen (N) contents, which were analyzed utilizing a carbon/nitrogen analyzer (Analytic Jena HT1300). An elemental analyzer (FLASH 2000, Thermo Fisher, Monza, Italy) was used to test the values of $\delta^{13}C$ and $\delta^{15}N$ in sediment (Xu et al., 2015).

The organic carbon composition in sediment was determined using the sodium pyrophosphate leaching-potassium dichromate oxidation method. Soil humus is composed of humic acid, fulvic acid, and humin in residue. A solution consisting of 0.1 $mol \cdot L^{-1}$ sodium pyrophosphate and 0.1 $mol \cdot L^{-1}$ sodium hydroxide is employed as leaching agents to extract humus. This is due to their potent complexing capability in highly alkaline conditions, which enables them to bind the insoluble and readily soluble humus components in the soil into a water-soluble sodium humus salt. The resulting humus can be more completely leached into the solution for measurement. The carbon content ($g \cdot kg^{-1}$) of a portion of the leached solution was measured to determine the total amounts of humic acid and phosphoric acid. Another portion of the leached solution was acidified so that the humic acid would precipitate and separate the rich acids. The

precipitate was then dissolved in sodium hydroxide and its carbon content ($g \cdot kg^{-1}$) was determined using the same method as for the humic acid content ($g \cdot kg^{-1}$). Phosphoric acid can be calculated as the difference between these measurements. Humin (i.e., the organic matter remaining in the soil residue) was calculated by subtracting the carbon content of humic acid and fulvic acid ($g \cdot kg^{-1}$) from the total carbon content of the humus ($g \cdot kg^{-1}$). The carbon was determined using the potassium dichromate oxidation external heating method.

A 0.5 g portion of each sediment sample was measured and placed into a centrifuge tube. Subsequently, 30 ml of ultra-pure water was introduced. The sample was agitated at 25 ± 1 ℃ for 8 hours, followed by centrifugation at 4200 rpm for 20 minutes. The resulting supernatant was then passed through a 0.22 μm filter membrane, and subsequently subjected to Solid Phase Extraction (SPE) using an Agilent Bond Elut PPL kit from the USA. 200 μl of the extracted solution was taken for mass spectrometric analysis using the Bruker SolariX FT-ICR MS. The ion source used in this study was an electrospray ionization source (ESI) operating in the negative ion mode. The primary detection parameters were as follows: continuous infusion was employed for sample introduction at a flow rate of 120 $\mu L \cdot h^{-1}$, the capillary entrance voltage was maintained at -4.0 kV, the ion accumulation time was set to 0.2 seconds, and data collection was conducted within a mass range of 100 to 1600 Da. A total of 4 million 32-bit data points were collected and the time-domain signal was averaged over 300 scans to improve the signal-to-noise ratio. Before sample analysis, instrument calibration was performed using a 10 $mmol \cdot L^{-1}$ sodium formate solution, and post-analysis an internal standard calibration was conducted using a known soluble organic compound with a known molecular formula. After calibration, the mass error for all detected ions was found to be less than 1 ppm.

An ultra-low temperature freezer of -80 ℃ was used to store sediment samples. The E.Z.N.A. ®Soil DNA Kit (Omega Bio-Tek, Norcross, GA, USA) was used to extract the total genomic DNA from each sediment sample. The nucleic acid quality was assessed using 1% agarose gel electrophoresis, and the nucleic acid concentration was assessed a NanoDrop 2000 UV spectrophotometer (Thermo Scientific, USA), respectively. The bacterial community in the sediments was quantified through 16S rRNA gene analysis. The quantitative polymerase chain reaction (qPCR) method was used to quantify the microorganisms in the sediments, with the following primers:

Primer F = Illumina adapter sequence 1 + GTGCCAGCMGCCGCGG, and Primer R = Illumina adapter sequence 2 + CCGTCAATTCMTTTRAGTTI. The procedures were conducted according to the MIQE guidelines.

3.2.4 Statistical analysis

The data statistical analysis was performed with Origin 2023 and Social Sciences 18.0 (SPSS 18.0). The structural equation modelling was finished by SPSS AMOS 21.0. A bivariate correlation analysis was conducted to determine if there were correlations in the data. One-way analysis of variance (ANOVA) and independent sample t-test were used to analyze significant differences between each index, respectively. In the ANOVA tests, the *p* values lower than 0.05 or 0.01 were considered statistically significant.

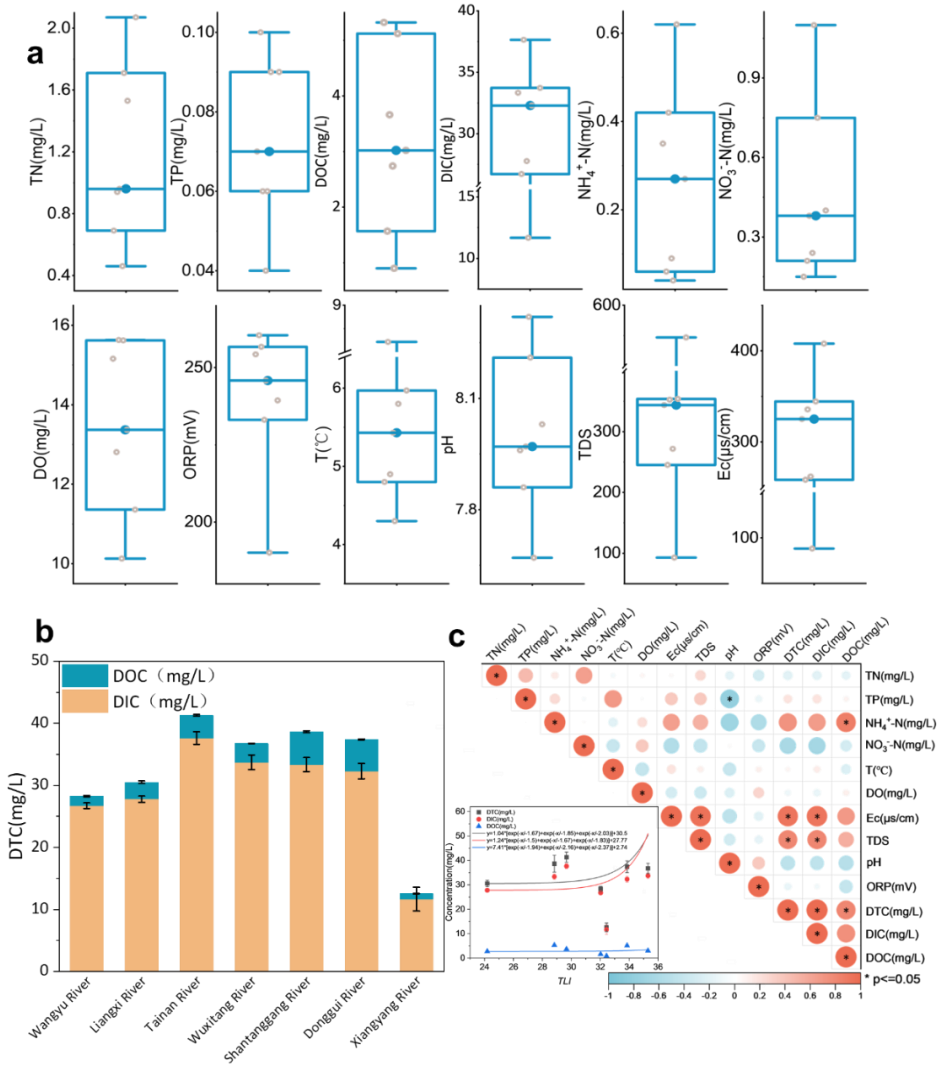

Fig. 3.3. (a) Physical and chemical properties in 7 rivers entering Lake Taihu. (b) The concentration and composition of DTC in 7 rivers entering Lake Taihu. (c)

Correlation analysis of physicochemical properties and correlation between carbon form concentration and TLI.

3.3 Results

3.3.1 Concentrations of nutrients in the water samples

The concentrations of various parameters in the overlying water from the seven rivers entering Lake Taihu displayed a significant variability, encompassing TP, TN, DTC, DOC, DIC, NH_4^+-N, and NO_3^--N (Fig. 3.1). Wuxitang River exhibited the highest level of eutrophication, as indicated by its trophic level index (TLI) of 35.3 (Fig. 3.2). Additionally, the TN and TP concentrations of Wuxitang River were 2.07 and 0.09 $mg \cdot L^{-1}$, respectively (Fig. 3.3a). Donggui River exhibited the highest concentrations of NH_4^+-N (0.62 $mg \cdot L^{-1}$) and NO_3^--N (0.75 $mg \cdot L^{-1}$) among the samples (Fig. 3.3a). The DO concentrations were greater than 10 $mg \cdot L^{-1}$ (Fig.3.3a) in all investigated rivers, indicating that the streams were aerobic environments. DIC was the predominant form of carbon in all rivers and was highest in Tainan River at 37.65 $mg \cdot L^{-1}$ (Fig. 3.3a). As eutrophication intensified in the rivers, carbon (i.e., DTC, DOC, and DIC) concentrations increased, as evidenced by their correlation (Fig. 3.3c).

3.3.2 The concentrations of dissolved CH_4, CO_2, and N_2O in water

The concentrations of dissolved GHGs in the seven rivers entering Lake Taihu displayed notable variability, as shown in Table 3.1. The concentrations of dissolved CH_4 in the investigated rivers ranged from 0.3 to 1.21 $\mu mol \cdot L^{-1}$, with the highest dissolved CH_4 concentration occurring in Donggui River. The dissolved CO_2 concentrations were consistently greater than the dissolved CH_4 concentrations, but they exhibited similar distributions and trends. The concentrations of dissolved CO_2 in seven rivers were 34.12 to 59.48 $\mu mol \cdot L^{-1}$, and the highest concentration occurring in Donggui River. The dissolved N_2O concentration in the water of the seven rivers entering Lake Taihu ranged from 0.03 to 0.07 $\mu mol \cdot L^{-1}$, with a mean of 0.04 $\mu mol \cdot L^{-1}$.

3.3.3 Particle size, C, N, $\delta^{13}C$, and $\delta^{15}N$ in sediment

The particle size distribution of the samples showed that sand (particle size

between 63 and 2200 μm) made up the largest proportion of the surface sediments of the investigated rivers, except for Shatanggang River, and Liangxi River had the highest proportion of sand at 91.35% (Fig. 3.4). Furthermore, Shantanggang River had the highest proportion of particles between 2 and 63 μm in size, which made up 66.86% of its sediment. The particle size distribution analysis revealed relatively low proportions of particles smaller than 2 μm in all investigated rivers. Among them, Liangxi River had the lowest proportion at 0.37%.

The C, N, $\delta^{13}C$, and $\delta^{15}N$ contents in the sediments from seven rivers are presented in Table 3.2. The C values of the sediments ranged from 0.6% to 3.59% in the seven rivers. The lowest C content occurred in the surface sediments of Xiangyang River at 0.6%, which coincided with the lowest DTC concentration in the overlying water in Xiangyang River. The N contents of the surface sediments ranged from 0.06% to 0.4% in the seven rivers. The distribution of N was consistent with that of C, and the lowest value also appeared in Xiangyang River at 0.06%. The $\delta^{13}C$ in the surface sediments ranged from -25.82‰ to -21.51‰, while $\delta^{15}N$ ranged from -29.35‰ to -0.17‰. The lowest values of $\delta^{13}C$ and $\delta^{15}N$ both occurred in Xiangyang River.

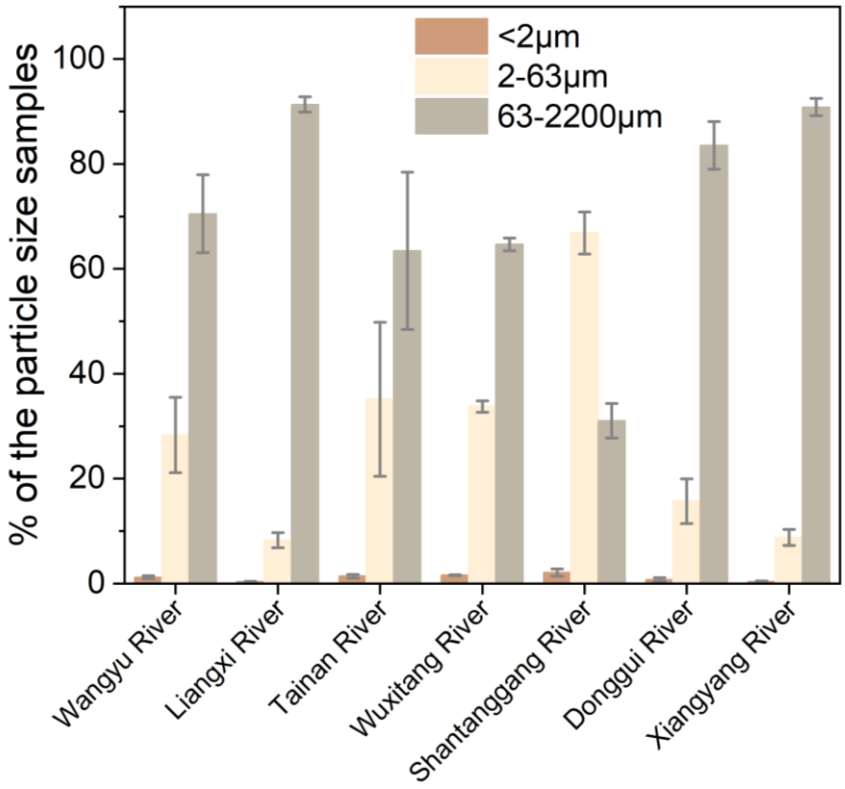

Fig. 3.4. Particle size distribution from 7 rivers entering Lake Taihu in sediment.

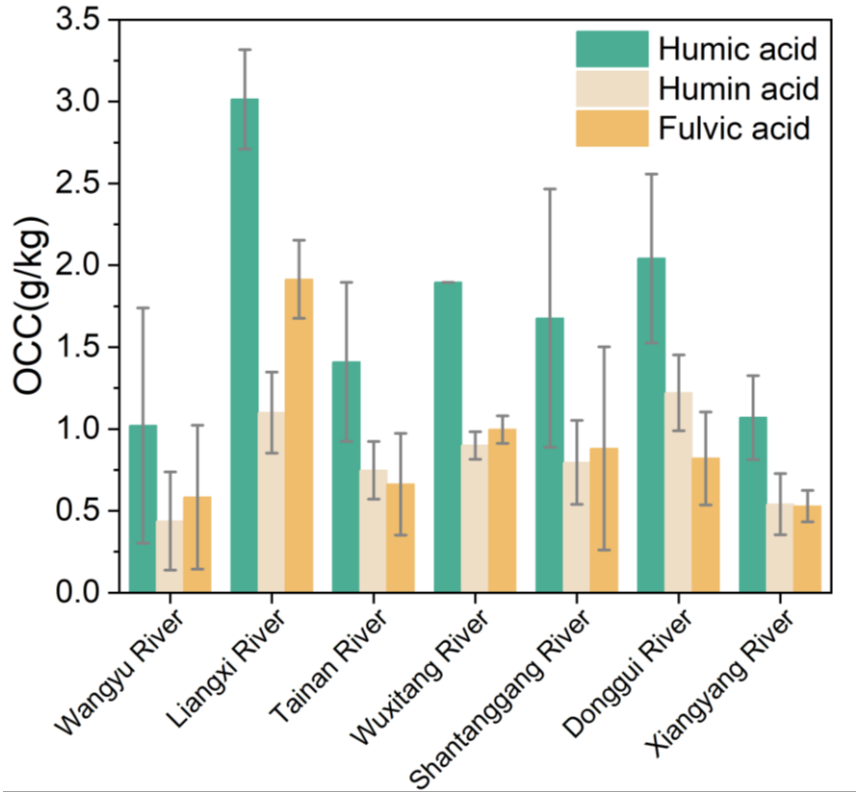

Fig. 3.5. Organic carbon content (OCC) of different fractions of humic acid, Humin acid, and Fulvic acid extracted from 7 rivers entering Lake Taihu in sediment.

Table. 3.1. The dissolved CH_4, CO_2, and N_2O concentration from 7 rivers entering Lake Taihu in water.

Sample Site	CH_4 (μmol/L)	CO_2 (μmol/L)	N_2O (μmol/L)
1	0.13 ± 0.05	34.12 ± 4.33	0.03 ± 0.001
2	1.18 ± 0.13	46.44 ± 3.16	0.03 ± 0.001
3	0.53 ± 0.18	40.9 ± 3.24	0.04 ± 0.001
4	0.48 ± 0.07	51.65 ± 7.66	0.07 ± 0.02
5	0.72 ± 0.13	43.84 ± 5.93	0.04 ± 0.01
6	1.21 ± 0.29	59.48 ± 3.91	0.05 ± 0.01
7	0.3 ± 0.1	55.93 ± 4.7	0.05 ± 0.01

Table. 3.2. The $\delta^{13}C$, $\delta^{15}N$ values, C%, N%, and C/N from 7 rivers entering Lake Taihu in sediment.

Sample Site	$\delta^{13}C$ (‰)	$\delta^{15}N$ (‰)	C%	N%	C/N
1	-21.51 ± 3.23	-4.09 ± 2.48	1.93	0.16	11.85
2	-21.88 ± 2.52	-0.17 ± 5.08	3.23	0.4	8.07
3	-25.79 ± 0.57	-9.85 ± 7.53	1.33	0.14	9.74
4	-24.73 ± 0.44	-14.09 ± 12.99	1.45	0.15	9.9
5	-22.59 ± 4.7	-14.98 ± 10.64	1.39	0.14	9.72
6	-25.26 ± 0.85	-6.1 ± 6.88	3.59	0.4	8.98
7	-25.82 ± 1.89	-29.35 ± 18.46	0.6	0.06	9.45

Table. 3.3. The Chao1, ACE, Shannon, Simpson, and coverage of microorganism from 7 rivers entering Lake Taihu in sediment.

Sample Site	Chao1	ACE	Shannon	Simpson	Coverage (%)
1	4026.9	4026.26	7.35	2.15×10^{-3}	99.93
2	3510.94	3514.97	7.02	3.18×10^{-3}	99.96
3	5059.06	5046.04	7.56	1.81×10^{-3}	99.91
4	4638.09	4630.94	7.36	2.81×10^{-3}	99.94
5	3779.28	3766.08	7.44	1.69×10^{-3}	99.9
6	3948.44	3939.99	7.33	2.22×10^{-3}	99.93
7	5301.9	5289.9	7.78	9.17×10^{-4}	99.92

3.3.4 Organic carbon content (OCC) of sediment

The OCC of the surface sediments of the seven rivers entering Lake Taihu were similar and humic acid made up the largest proportion in each (Fig. 3.5). Among the sampling sites, Liangxi River had the highest concentration of humic acid at 3.01 $g\cdot kg^{-1}$, while Wangyu River had the lowest concentration at 1.02 $g\cdot kg^{-1}$. In this study, the concentrations of fulvic acid were generally higher than humin, except in Samples 6 and 7. In Donggui River, the concentration of fulvic acid was 0.82 $g\cdot kg^{-1}$, while the concentration of humin acid was 1.22 $g\cdot kg^{-1}$. Wangyu River, on the other hand, had the lowest concentration of humin acid at 0.44 $g\cdot kg^{-1}$, whereas Xiangyang River had the lowest concentration of fulvic acid at 0.53 $g\cdot kg^{-1}$.

3.3.5 Composition of organic molecular and compounds in sediments

The complexity of DOM was analyzed in seven river samples, with molecular formulas ranging from 2381 to 6051. The predominant molecular formulas observed were CHO, CHON, CHOS, and CHONS (Figs. 3.6 and 3.7). This indicated that CHO, CHON, and CHONS were the primary molecular components of DOM entering Lake Taihu. Furthermore, the molecular components of DOM varied significantly among different rivers. Wangyu River had the fewest molecular formulas, while Shantanggang River had the most. Except for Wuxitang River, the DOM was dominated by CHO in all sampling sites, accounting for proportions from 34.74% to 51.56%. Notably, Wuxitang River had the largest proportion of CHOS at 45.42%. The number of molecular formulas of CHO, CHON, and CHOS ranged from 1165 to 2462 (accounting

for 48.93% to 40.69%), 506 to 1497 (accounting for 21.25% to 24.74%), and 574 to 2018 (accounting for 24.11% to 35.27%), respectively.

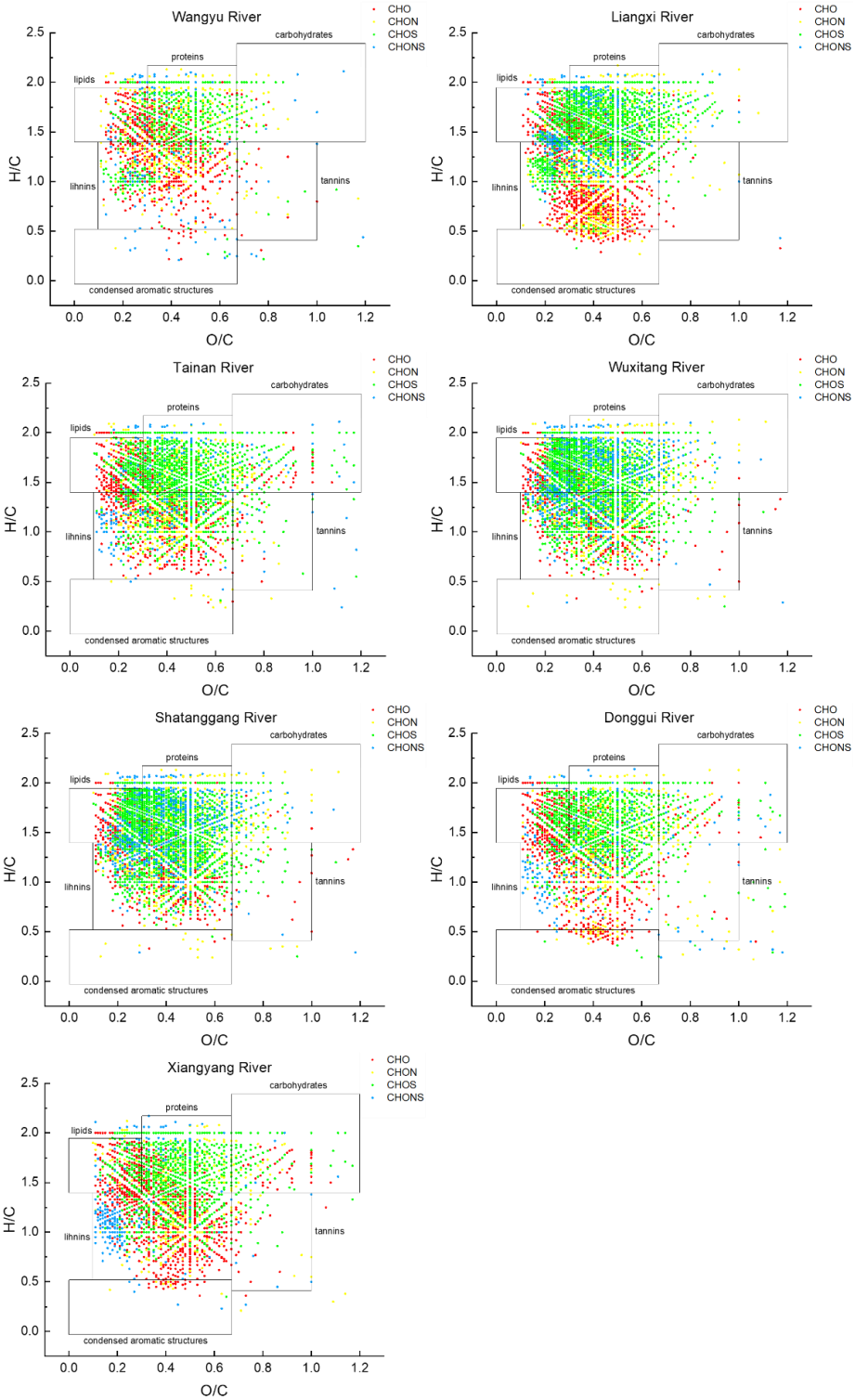

Fig. 3.6. FTMS-derived van Krevelen diagrams of common compound compositions observed in overlying water from 7 rivers entering Lake Taihu, and color-coded according to CHO (red), CHNO (yellow), CHOS (green), and CHONS (blue) compound series.

The DOM compounds in the investigated rivers encompassed a wide range of substances, including lignins, proteins, lipids, tannins, carbohydrates, and condensed aromatic structures, as revealed by the values of H/C and O/C, highlighting the complexity of DOM (Figs. 3.6 and 3.8). Lignin compounds constituted the majority of DOM compounds in all sample sites, surpassing 40% in all cases. Among them, Shatanggang River had the highest abundance of lignin compounds, where they accounted for 60.42% of the DOM. Protein and lipid compounds followed lignin in terms of prevalence, while tannin, carbohydrate, and condensed aromatic structure compounds accounted for the lowest proportions of DOM in the seven sample sites. Together, the lowest three compound categories made up only 5.31% to 12.95% of the DOM in the samples.

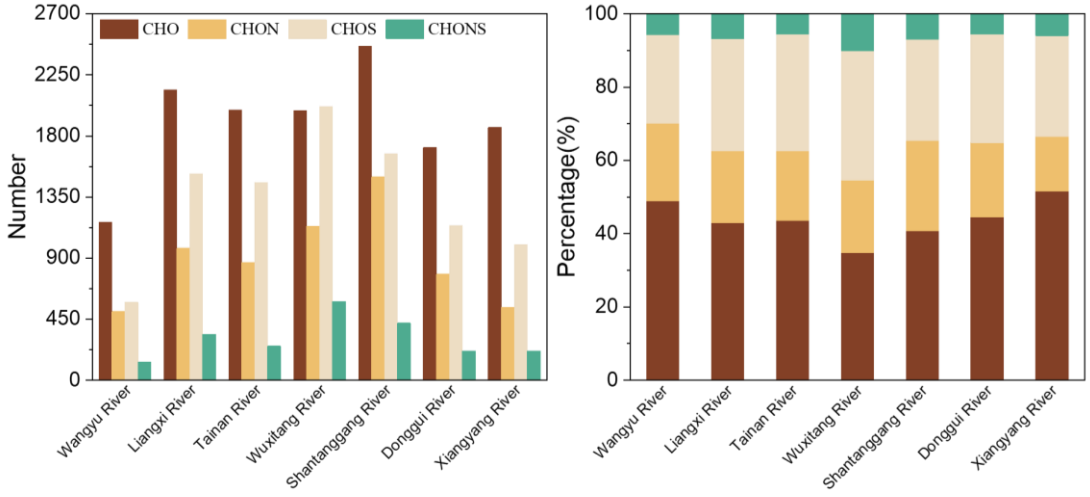

Fig. 3.7. Molecular composition (left) and proportion (right) of DOM in sediment from 7 rivers entering Lake Taihu.

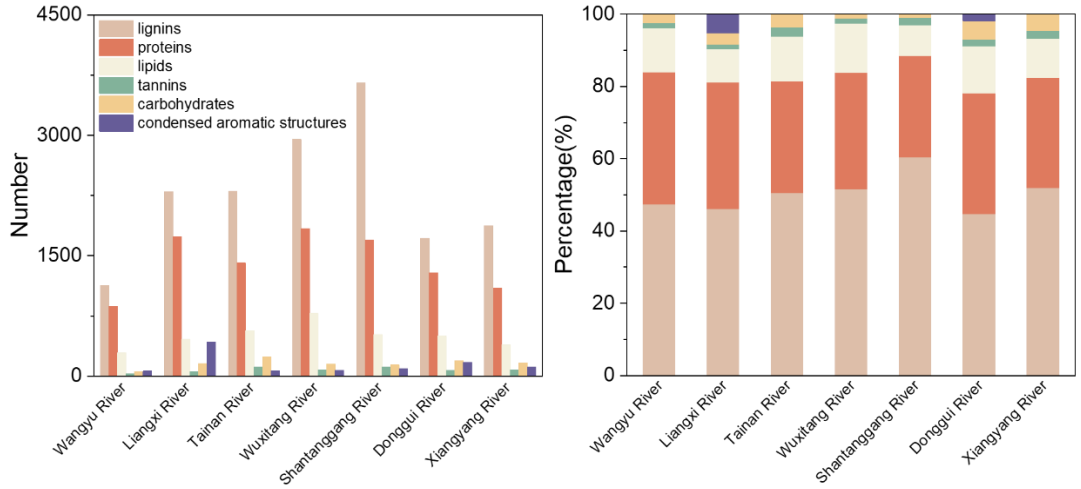

Fig. 3.8 Compound composition (left) and proportion (right) of DOM in sediment from 7 rivers entering Lake Taihu.

3.3.6 Microbial communities in sediments

The microbial community structure exhibited remarkable similarity across the seven rivers, and the species coverage within these microbial communities was found to be highly diverse and abundant, encompassing a rich assortment of taxa (Fig. 3.9; Table 3.2). At the phylum level, the sediment harbors a total of 15 distinct microbial species. Among all the samples, Proteobacteria exhibited the highest proportion, with Tainan River displaying the highest proportion of 43.73%. The proportions of Acidobacteria and Chloroflexi demonstrated a similar pattern across the sediment of the seven rivers.

3.3.7 Dynamic changes in carbon emissions during incubation

Carbon was emitted in the forms of CH_4 and CO_2, with more of the former being emitted (Fig. 3.10). The CH_4 concentration was the highest in the mixed treatment, which reached 640.2 $\mu mol \cdot L^{-1} \cdot C_g^{-1}$, while the highest CO_2 concentration occurred in the cyanobacteria treatment, which reached 228.1 $\mu mol \cdot L^{-1} \cdot C_g^{-1}$. The carbon emission efficiency was highest in the mixed treatment, where the carbon emission per unit reached 160.9 $\mu mol \cdot C_g^{-1}$. The sediment treatment had the lowest carbon emission efficiency, with carbon emissions per unit of 9.3 $\mu mol \cdot L^{-1} \cdot C_g^{-1}$. The cyanobacteria decomposition resulted in significant alterations to the sediment carbon pool, with the TOC concentration in sediment increasing sharply and then decreasing. In the mixed treatment, the TOC concentration in sediment peaked at 57.6 $g \cdot kg^{-1}$ and generally remained stable.

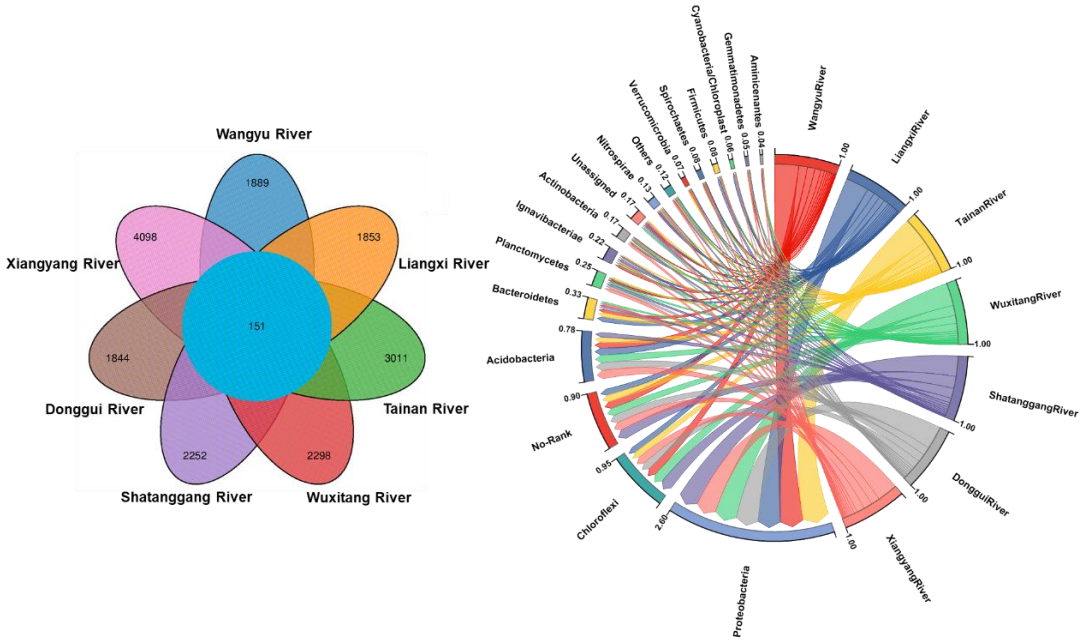

Fig. 3.9. The similarities of bacterial communities (left) and the community structure (right) in sediment from 7 rivers entering Lake Taihu.

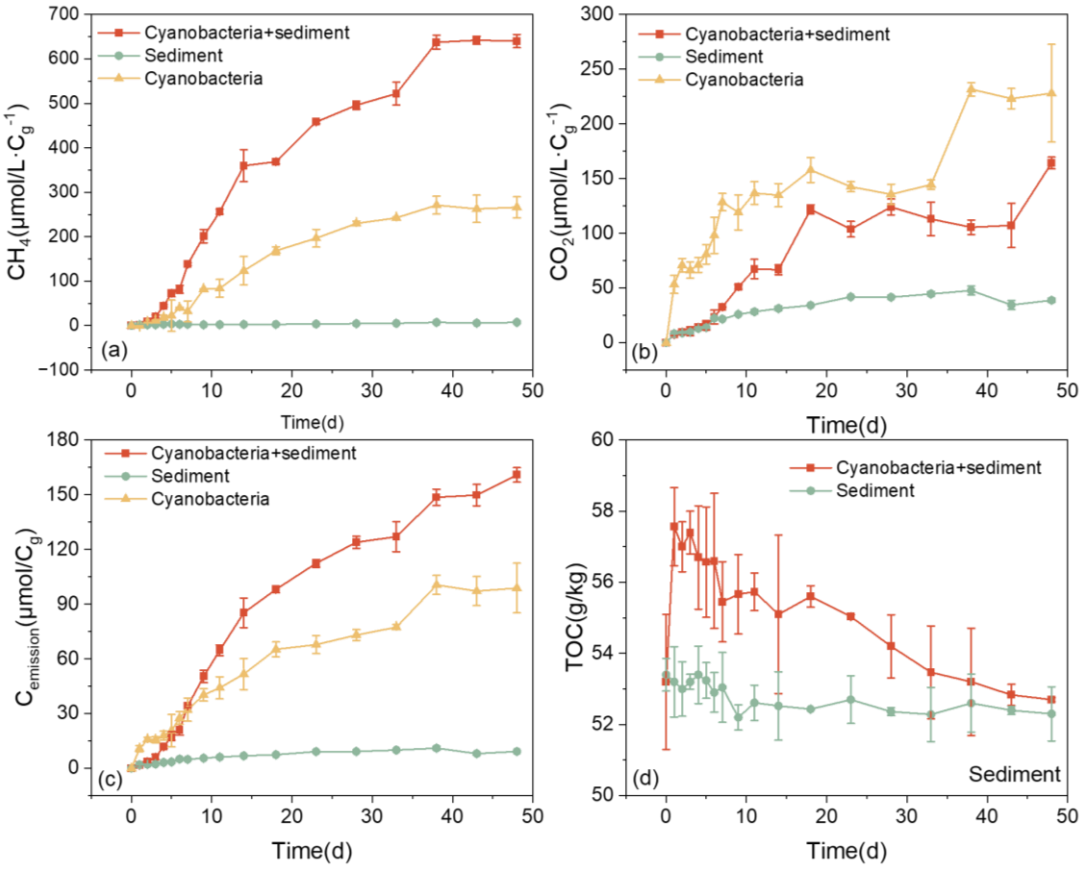

Fig. 3.10. The dynamic change of CH_4 (a), CO_2 (b), total carbon emission (c) under the condition for per gram of carbon input ($C_{emission}=CH_4+CO_2$), and the dynamic changes of TOC concentration in sediment (d).

3.4 Discussion

3.4.1 Trophic status of rivers

During the winter season, the rivers entering the lake carried relatively low nutrient loads, resulting in oligotrophic and mesotrophic conditions (Fig. 3.2). Inputs of exogenous nutrients including nitrogen and phosphorus are the main drivers of increases in nutrient loads in freshwater lake basins (Xu et al., 2010). Elevated levels of nutrients serve as substrates for the growth of microorganisms, which undertake their metabolic processes in sediments (Fig. 3.9). Eutrophication in freshwater lake basins typically occurs during the summer and, as such, exhibits notable seasonal variability (Tong et al., 2021). Surface runoff plays a crucial role in the introduction of terrestrial nutrients into freshwater lake basins (Diaz-Torres et al., 2022). As such, reductions in precipitation in winter restrict the influx of terrestrial nutrients from the surrounding terrestrial environment (Culbertson et al., 2016). This trend was apparent in the nitrogen and phosphorus loads of the seven rivers entering Lake Taihu in this study conducted in winter, which were at low concentrations, consistent with previous research (Fig. 3.3a).

In this study during winter, the water temperatures of the seven rivers entering Lake Taihu were low (Fig. 3.3a). Low water temperatures limit the activities of microorganisms and plants and slows the biotransformation of nutrients (Hopkins et al., 2006). This low temperature inhibitory effect, like the reduced nutrient loads, also reduces the consumption of DO by the microorganisms and cyanobacteria (Ya et al., 2022). Additionally, the lower water temperatures during winter increase the solubility of oxygen in water, resulting in higher dissolved oxygen concentrations (Martin et al., 2013). Due to the various effects of low water temperatures, the overlying water observed in this study had high DO concentrations and all rivers were in aerobic states (Fig. 3.3a).

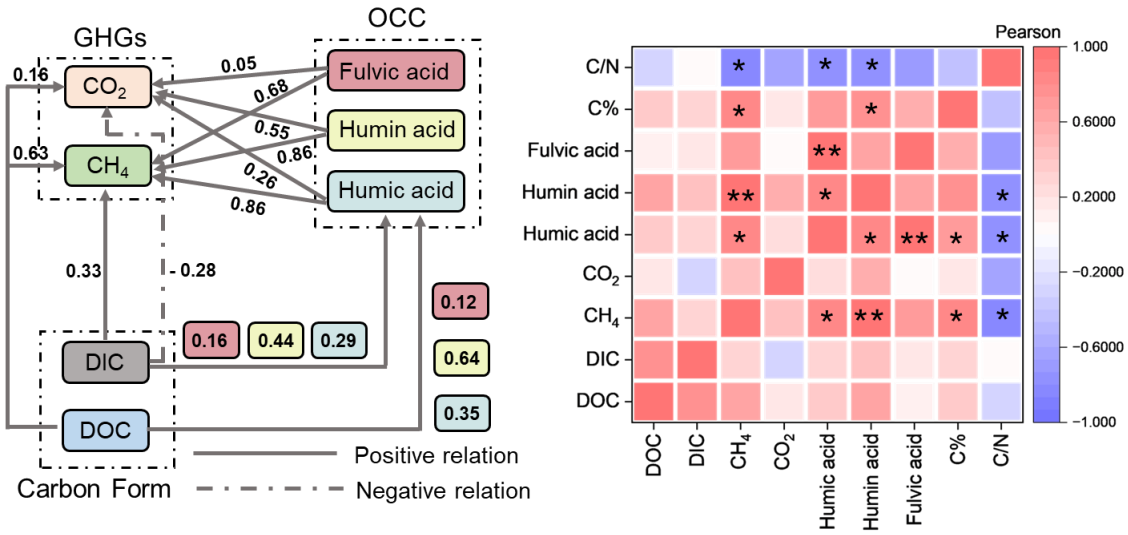

Fig. 3.11. The contribution of organic carbon components to CH_4 and CO_2 emissions (left) and correlation analysis between different indexs (right) (* and ** indicate the significant differences between expected and observed values at $P < 0.05$ and $P < 0.01$, respectively).

3.4.2 Composition and source of DOM in rivers

The composition of DOM in the seven rivers exhibited significant variability (Figs. 3.6, 3.7, and 3.8). The complex nature of DOM in rivers was due to the large variety of contributing sources (Medeiros et al., 2015; Li et al., 2020). The composition of the DOM in rivers comprised a range of organic molecules originating from the remnants of living organisms, which encompassed proteins, carbohydrates, lipids, lignin, tannins, and humic substances (Figs. 3.5 and 3.8). In this study, humic acid dominated the humus of organic carbon content (Fig. 3.5), which was due to the highly diverse microbial community structure in river sediments (Fig. 3.9; Table 3.3). Humus, including humic acid, humic acid, and fulvic acid, has the longest retention time in rivers and constitutes the predominant fraction of DOM (Luo et al., 2022). The decomposition and transformation of animal and plant matter in sediments is an important source of humus (Gontijo et al., 2021).

The sources of DOM in rivers fall into two main categories: terrestrial sources and in-stream sources (Lambert et al., 2017; Luo et al., 2022). The Lake Taihu basin was found to have a main source of organic matter from terrestrial input, as indicated by carbon isotope analysis (Table 3.2). During the winter, when biological activity in the basin is generally low, the contribution of terrestrial sources to organic matter becomes

more significant (Gontijo et al., 2021; Bai et al., 2023). The reduced biological activity during winter highlights the importance of terrestrial inputs as sources of organic matter during this period (Gontijo et al., 2021; Luo et al., 2022). In this study, whether the molecular composition was dominated by CHO or the compound composition was dominated by lignins, the DOM in the rivers was mainly derived from plants, specifically, from terrestrial plants (Figs. 3.7 and 3.8). Lignin in rivers can be released through the dissolution of terrestrial organic matter, like plant residues, dead leaves, trees, and plant debris (Jung et al., 2015). During winter in the Lake Taihu basin, there is an extensive die-off of aquatic plants, which also contributes to the increased proportion of organic matter from terrestrial plant litter (Bai et al., 2023). The high primary productivity of Lake Taihu basin leads to high microbial activity and contributed to the variety observed in the microbial community structures (Fig. 3.9). Proteins, as vital organic compounds within organisms, are produced through organismal metabolic processes and released the degradation of cell debris (Habicht et al., 2011). The decomposition of aquatic organisms such as algae, plants, and plankton, along with microbial metabolism and organic carbon decomposition collectively contribute to the high concentration of proteins in freshwater lakes (Bianchini et al., 2018). This finding was consistent with the observations in this study, where proteins were found to be an important component of the DOM, second only to lignins (Fig. 3.8). Furthermore, CHON was an important molecular component of DOM, indicating that microbial activity was an important source of DOM in the Lake Taihu basin (Fig. 3.7). In terms of molecular composition, CHON is strongly correlated with microbial activity (Zhang et al., 2021; Hong et al., 2023).

3.4.3 Links between DOM composition and carbon emission

The elevated concentration of DOM, accompanied by its complex composition, collectively contributed to the elevated levels of dissolved GHGs in rivers (Fig. 3.11; Table 3.1). Several studies have highlighted the importance of DOM in determining the distributions of dissolved GHGs (Begum et al., 2021; Hassan et al., 2023). In this study, different components of DTC showed different contributions to the production of dissolved CH_4 and CO_2, and the DIC concentration was negatively correlated with dissolved CO_2 (Figs. 3.3 and 3.11). These findings highlight the impact of DOM characteristics on the distribution of GHGs.

Overall, the presence of humic-like substances originating from both terrestrial and in-stream sources be associated with the concentrations of dissolved CH_4 and CO_2 in the Lake Taihu basin (Figs. 3.6, 3.10; Table 3.1). The input of multi-source DOM may induce the co-metabolism effect of different components, which has been proved to promote the decomposition of humic-like substances (Farjalla et al., 2009). The degradation of humic-like substances releases GHGs (CH_4, CO_2, etc.), while also providing a substrate for microbial activity (Shirokova et al., 2015). Studies have demonstrated that humic acid can act as both a source and medium for the production of CH_4 and CO_2, significantly impacting their distributions and release within water bodies (Gontijo et al., 2021). The presence of biodegradable organic carbon within humic acids plays a pivotal role driving these production patterns (Luo et al., 2022). Fulvic acid in aquatic environments primarily originates from plant litter and soil secretion, and it typically encompasses a notable proportion of aromatic carbon resulting from the degradation of lignin (Ni et al., 2022). In agreement with these trends, this study also observed that lignins were the main component of DOM (Fig. 3.8). Several studies have shown that terrestrial aromatic compounds make significant contributions to the pCO_2 values in aquatic systems (Gontijo et al., 2021; Luo et al., 2022).

The complex composition of DOM compounds can also contribute to the substantial fluctuations in dissolved GHGs concentrations in lakes (Valle et al., 2018). The proteins and lipids in DOM made up significant components of the organic carbon in this study (Fig. 3.8), and their presence played a crucial role in influencing the degradation and decomposition of DOM, consequently impacting the release of GHGs. Among the GHGs, dissolved N_2O was strongly related to the proteins, showing a positive correlation (Fig. 3.12). This result aligns with the conclusion of a previous study that investigated shallow estuaries (Begum et al., 2021). Proteins consist of nitrogen-enriched molecules with low aromaticity. Additionally, the concentrations of low molecular weight organic compounds can impact the rate of denitrification (Begum et al., 2021; Luo et al., 2022). The collective terrestrial inputs establish the positive correlation between carbon emissions and DOM in freshwater lakes (Deirmendjian et al., 2020). In this study, terrestrial lignin was predominant in the river DOM of Lake Taihu basin (Fig. 3.8; Tables 3.2 and 3.3). The structural complexity and relative stability of lignin make it highly resistant to degradation (Smith et al., 2013). This study

revealed a weak positive correlation between lignin content and both dissolved CH_4 and CO_2 concentrations (Fig. 3.12). The degradation of lignin is influenced by a multitude of environmental factors and microbial processes (Zhang et al., 2018; Song et al., 2020). Numerous studies have demonstrated that co-metabolic effects in eutrophic lakes promote the decomposition of refractory substance (Ma et al., 2020), and microbial-produced enzymes (such as lignin enzymes) play crucial roles in the decomposition of lignins (Hall et al., 2015). The rivers in the Taihu Basin harbored a diverse array of microbial species, presenting a favorable environment for lignin decomposition (Fig. 3.9). Overall, the DOM content and components in Lake Taihu basin were likely to be closely related to the generation of GHGs, but the complexity of the components may obscure the relationships between GHGs and their underlying drivers.

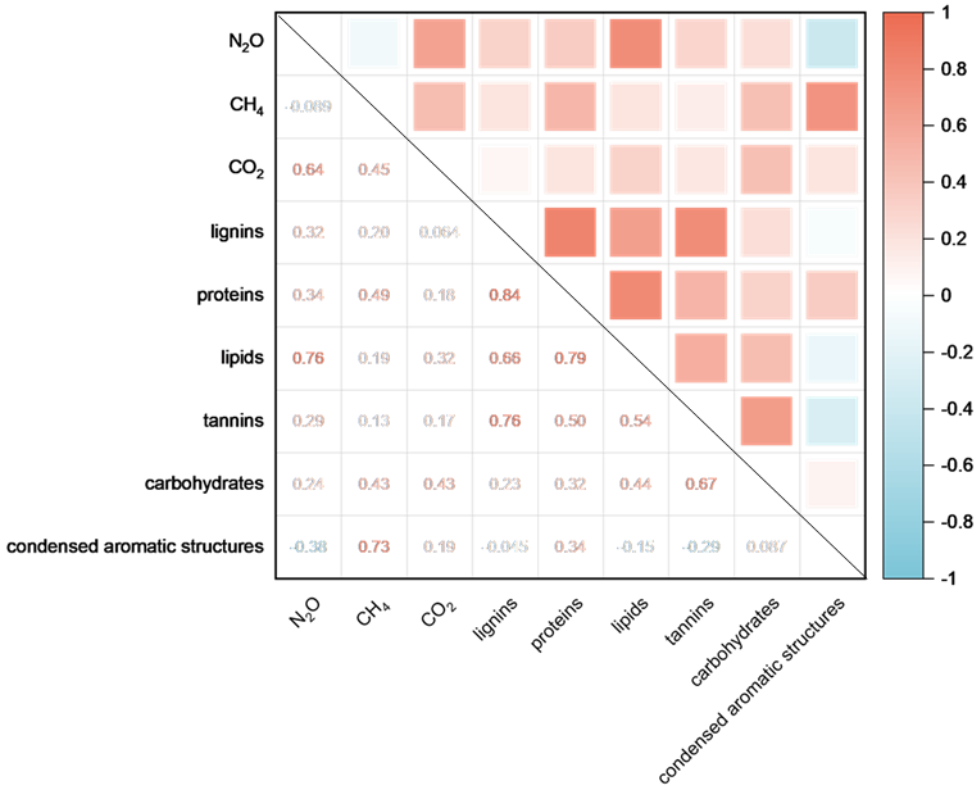

Fig. 3.12. The correlation analysis between compound components of DOM and indexes.

3.4.4 Potential effects of multiple carbon sources on sediment carbon pool

The presence of multiple carbon sources created potential instability in lake sediments (Fig. 3.12). This study showed that the sources of organic carbon to the rivers

of the Lake Taihu basin were complex (exogenous and endogenous) (Table 3.2). The input of diverse carbon sources, such as terrestrial organic matter, aquatic plant material, and algal biomass, can exert a substantial influence on both the quantity and composition of organic matter in river sediments (Wang et al., 2022). The organic carbon components and nutrient availability in the sediment carbon pool play vital roles in determining microbial activity, which in turn can impact the stability of the carbon pool (van der Kooij et al., 2017). Microbial activity, driven by the availability of organic carbon, drives the decomposition and transformation of organic matter in sediments (Wan et al., 2023). The mixed metabolism of cyanobacteria-derived DOM and sediment-released DOM showed that the input of exogenous organic carbon into the lake led to the instability in the sediment carbon pool. This, in turn, stimulated the mineralization of organic carbon, leading to a significant increase in carbon emissions (Fig. 3.10). Previous studies have proposed that the microbial co-metabolic processes induced by the mixing of multiple carbon sources promote metabolic efficiency, ultimately leading to the intensification of GHGs emissions (Ma et al., 2020; Deng et al., 2022).

Here, the CO_2 emission flux patterns in the Lake Taihu basin exhibited significant instability, characterized by a notably high fluxes of CO_2 emissions (Fig. 3.13). The variety of sources of DOM has been shown to significantly influence the oxidation-deoxidation environment in lake sediments (Zhao, et al., 2022). Specifically, a rich variety of DOM inputs in organic matter can complicate the oxidation-deoxidation environment of sediments and exacerbate the degradation and release of organic carbon (Mostofa et al., 2018). It has been shown that the mixing of organic carbon from multiple sources can induce co-metabolic processes in lake basins, particularly the multi-source mixing of DOM (Ma et al., 2021; Deng et al., 2023). This mechanism may have contributed to the increased carbon emissions from the lake ecosystem investigated here (Fig. 3.13). Co-metabolism can shift the roles of sources and sinks in the lake sediment carbon pool, further intensifying the instability in the sediment carbon pool (Ma et al., 2022). Microbial activity plays a leading role during organic carbon mineralization (Wasswa et al., 2022). Clearly, multi-source inputs of DOM into shallow lakes intensifies the degradation and release of carbon in sediment carbon pools, potentially contributing to increased emissions of carbon from lakes.

3.5 Summary

The variety of sources of carbon in lake basins result in complex DOM compositions, which can potentially drive instability in sediment carbon pools. In this study, the nutrient load in Lake Taihu basin during winter was relatively low and the water environment was aerobic. Exogenous inputs increased the carbon concentration, especially the DOM concentration. The mixing of multiple sources of organic carbon enhanced the carbon emission efficiency, induced co-metabolic processes, and drove drastic changes in sediment carbon pool. The organic carbon content in Lake Taihu basin consisted predominantly of humic acid, with lignins being the predominant compound. This was related to the decomposition of terrestrial plants and some aquatic plants in winter. These observations were further supported by the analysis of carbon and nitrogen isotopes in the sediments. The concentrations of dissolved CH_4 and CO_2 in the Lake Taihu basin were positively correlated with organic matter concentrations, and increases in the organic carbon load promoted carbon emissions. The elevated concentrations and intricate nature of DOM instigated processes of microbial organic carbon mineralization, ultimately contributing to the destabilization of the sediment carbon reservoir within the lake basin. These findings offer crucial insights into assessing the impact of diverse DOM sources on carbon emissions and the overall carbon emissions within freshwater lakes.

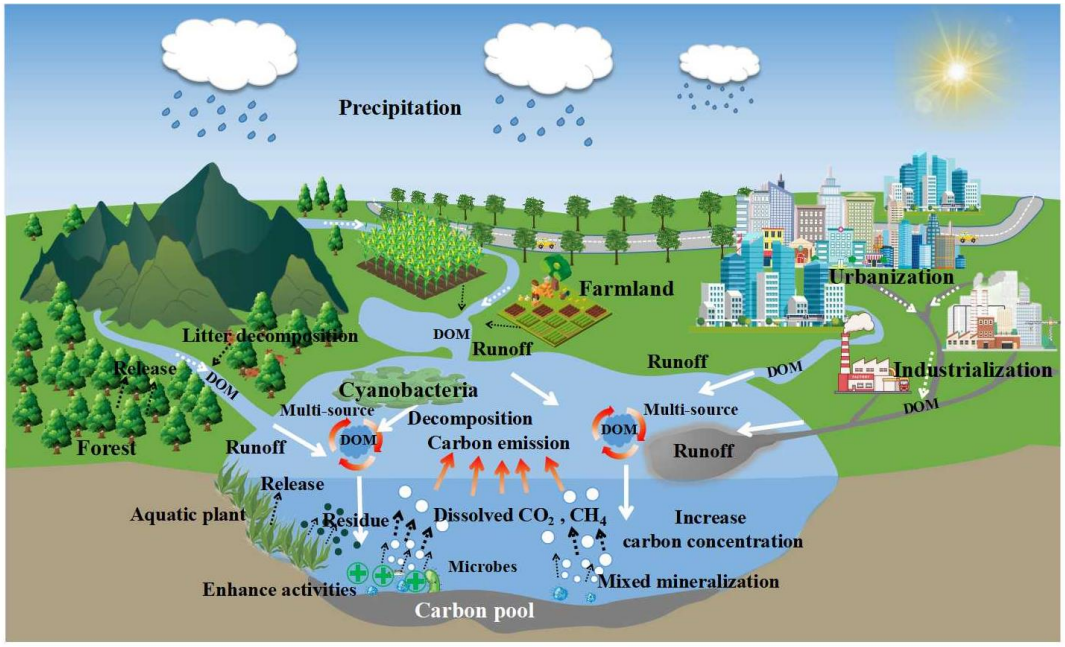

Fig. 3.12. A conceptual diagram of multi-source DOM and its potential mechanism on sediment carbon pool in lake basin.

4. Increased GHG emissions potentially driven by particulate organic carbon from oxic water of eutrophic lakes

4.1 Background

Lakes are transitional zones of permanent or periodic flooding between aquatic and terrestrial ecosystems and play an important role in the circulation of substances (Gudasz et al., 2010; Bastviken et al., 2011). Organic carbon (OC) in lake ecosystems mainly includes dissolved organic carbon (DOC) and particulate organic carbon (POC) (Ye et al., 2015; Shi et al., 2018). In particular, POC is an important component of the regional and global carbon cycle, and its biogeochemical process is key in defining the global carbon cycle and carbon, *i.e.*, CH_4 and CO_2 fluxes in freshwater lakes (Chanudet et al., 2020).

OC sources in freshwater lakes are autochthonous and allochthonous (Ankit et al., 2022). Autochthonous OC is mainly derived from aquatic plants and their degradation (De Kluijver et al., 2014; Yan et al., 2017). Allochthonous OC is mainly produced by terrestrial plants, degradation of soil organic matter, and humification (Solomon et al., 2015; Mitrovic et al., 2016). Various indices, such as the ratio of POC to chlorophyll-*a* (chl-*a*), the carbon isotopic composition ($\delta^{13}C_{poc}$), and the carbon to nitrogen ratio have been used to analyze the OC sources in freshwater lakes (Xu et al., 2015; Ma et al., 2022). Although it has been demonstrated that the trophic state of a lake leads to an uncertain estimate of the OC source and concentration, the relationship between the sources and concentrations of OC and the trophic state of lakes has not been e entirely revealed (Park et al., 2009; Wen et al., 2022). Lake eutrophication is a severe ecological problem, leading to an increase in OC concentration (Pelechata et al., 2016; Jiang et al., 2022). A high level of primary productivity, triggered by eutrophication, results in cyanobacterial blooms in eutrophic lakes (Isles et al., 2017). The accumulation of cyanobacteria rapidly increases POC in the surface sediment and overlying water (Zhao et al., 2021; Zhou et al., 2022a). Cyanobacterial residue on the sediment surface forms a “cyanobacterial detritus mat” that is suspended by wind and eddies, particularly in shallow lakes (Persaud et al., 2014). In eutrophic lakes, cyanobacterial-derived suspended particulate matter is an important POC component, conveying organic matter, and contributing to the change in the microenvironment (Ochs et al., 2010; Ye et al., 2015; Shi et al., 2017). POC participates in the carbon cycle as a carbon source and

eventually produces CH_4 and CO_2 (Bueno et al., 2020). Additionally, POC tends to adhere to aerobic heterotrophic microbes and inorganic ions (NH_4^+, Fe^{2+}, and HS^-) (Ochs et al., 2010; Zhou et al., 2019). Due to the oxidation of organic matter, the dissolved oxygen (DO) concentration in POC is significantly lower than that in the surrounding water (Ochs et al., 2010). Therefore, migration and transformation of POC create a micro-anaerobic environment inside, and such a redox condition changes the emission of CH_4 from the lake (Nakayam et al., 2018).

The global CH_4 emission flux from freshwater lakes is about 63.9 Tg/yr (Bastviken et al., 2011; Wang et al., 2022), and is expected to increase (Sepulveda-Jauregui et al., 2018). It is important to comprehensively understand the complex process of CH_4 emissions from lake sediments into the water column, including OC mineralization, carbon migration, and oxidation to accurately estimate CH_4 flux (Roland et al., 2017). In addition, a unique phenomenon, *e.g.*, the paradoxical supersaturation of CH_4 in oxygenated surface waters, *a.k.a.*, the methane paradox, should be understood (Repeta et al., 2016). The significant correlation between CH_4 emissions and OC concentrations in freshwater lakes, particularly the POC concentration, has attracted attention (Lennon et al., 2006; Zhou et al., 2020). Although autochthonous and allochthonous POC promote CH_4 production, the contribution of POC from autochthonous sources to CH_4 production is more significant in eutrophic lakes (Gudasz et al., 2012). Most autochthonous POC contains complex organic substances that can be degraded quickly, resulting in a low burial efficiency (Dai et al., 2005). The decomposition rate of allochthonous POC, particularly terrestrial POC, is slow, as it usually has a relatively high proportion of refractory organic matter (Grasset et al., 2018). Algae-derived POC accounts for a large proportion of OC and has a significant effect on the carbon cycle of eutrophic lakes (Jiang et al., 2015; Lammers et al., 2016). This propensity makes CH_4 emission fluxes under eutrophic conditions significantly higher than those under oligotrophic and mesotrophic conditions (Zhou et al., 2023), indicating that the trophic state is an important factor affecting the CH_4 emission flux, which leads to an increase in the concentration of POC in the overlying water (Xing et al., 2005; Zhou et al., 2020). In addition, recent studies have highlighted that CH_4 emissions from lakes are derived from overlying water that is highly oxygenated with POC (Ochs et al., 2010; Lenhart et al., 2016). The microenvironment created by abundant POC is a significant redox interface that provides extra space for CH_4 production (Zhou et al., 2019; Xu et al.,

2020). Ignoring the presence of POC results in an underestimate of CH_4 production and flux (Stackpoole et al., 2017). Additional descriptions regarding the composition and sources of POC and their effects on CH_4 production and flux in freshwater lakes are needed considering the intensification of eutrophication (Palma-Silva et al., 2014; Vincon-Leite et al., 2019).

Given the necessity for the POC effect on the production and flux of CH_4, for proposing a new perspective for methane paradox in eutrophic lakes. This study aimed to track the sources and composition of POC and to clarify the effect of POC on CH_4 emissions from freshwater lakes. Thus, the dissolved CH_4 and CO_2 concentrations in the overlying water and the emission fluxes from 18 shallow lakes in different trophic states were investigated along the Yangtze River basin. The concentrations of total phosphorus (TP), total nitrogen (TN), chlorophyll-*a* (chl-*a*), POC, and dissolved organic carbon (DOC) in the overlying water were synchronously analyzed. In addition, the $\delta^{13}C$ values of POC were determined in the overlying water to attain insight into the POC sources. These findings will help with the analysis of OC sources and estimating the carbon emissions in lakes of different trophic states.

4.2 Materials and methods

4.2.1 Study site and sample collection

Typical freshwater lakes along the Yangtze River basin were selected. The trophic states of the lakes in this basin vary greatly, and many lakes are in various states of eutrophication (Huang et al., 2016). Eighteen shallow freshwater lakes (<7 m deep) in the middle and lower reaches of the Yangtze River basin were selected based on the trophic level index (*TLI*) (Fig. 4.1). These lakes were classified into five trophic states, including oligotrophic ($TLI < 30$), mesotrophic ($30 \leq TLI < 50$), eutrophic ($50 \leq TLI < 60$), middle-eutrophic ($60 \leq TLI < 70$), and hyper-eutrophic ($TLI > 70$). All samples were collected from three sampling sites in each lake during July 2021, according to GB/T 14581-93 (China). The water depth at each sampling site was < 7 m; 5 L of water and 50 mL of gas were collected at each sampling site.

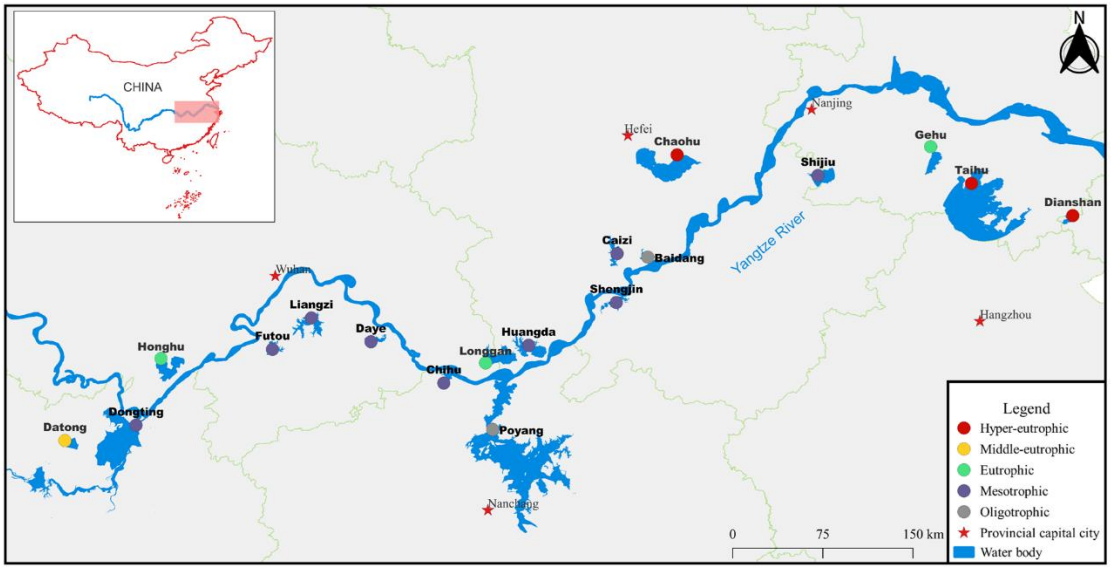

Fig. 4.1. The sample locations in different trophic state lakes along the Yangtze River.

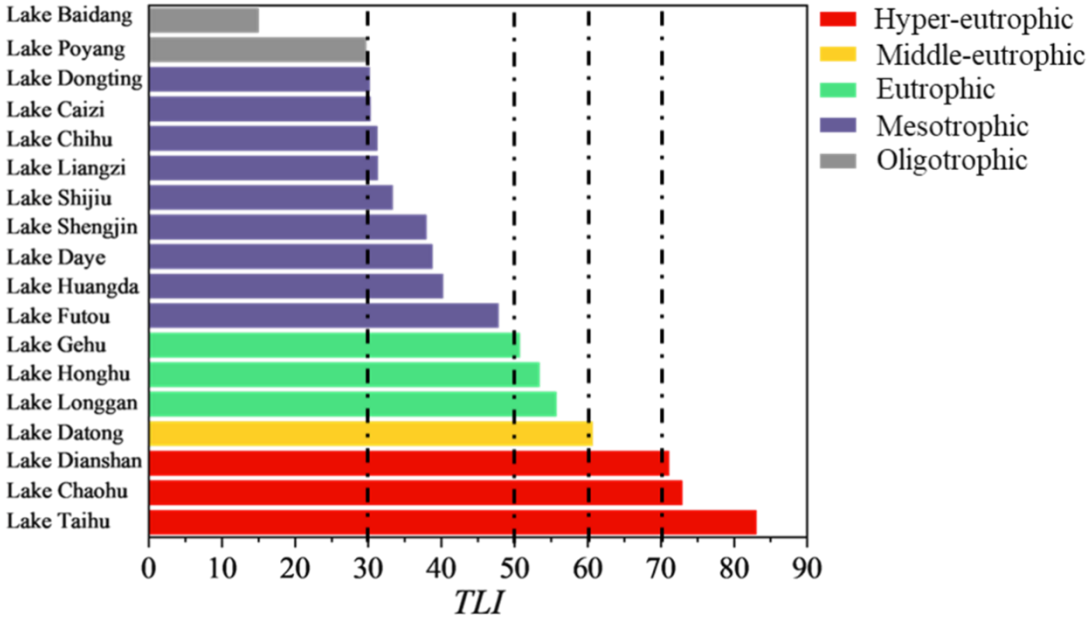

Fig. 4.2. The *TLI* values of different lakes along the Yangtze River in July 2021. The vertical dashed lines at TLIs of 30, 50, 60, and 70 represent the thresholds of oligotrophic-mesophilic, mesophilic-eutrophic, eutrophic-middle-eutrophic, and middle-eutrophic-hyper-eutrophic states.

The *in situ* DO and oxidation-reduction potential (ORP) in the overlying water were measured with a multiparameter sensor (YSI ProfessionalPlus, A Xylem; YSI Inc., Yellow Springs, OH, USA). An aerobic state of the shallow lakes in this study was defined as a DO concentration level > 2 mg/L (Diaz et al., 2001). Triplicate overlying water samples (30 cm below the water surface) were collected to measure nutrient concentrations. The headspace balance method was adopted to measure dissolved CH_4

and CO_2 concentrations. A water sample (300 mL) was gently and slowly poured into a 500 mL anaerobic bottle, and the excess gas was removed with 200 mL N_2 gas (99.999%). After 5 min of vigorous shaking, the headspace gas was extracted with a syringe and injected into an airbag (E-Switch, China) for storage. Gas flux samples were collected with a light-shielded floating static chamber.

4.2.2 Chemical analytical methods

The overlying water samples were used to determine the concentrations of total TP, TN, DOC, and chl-*a*. The TP concentration was measured using an ammonium molybdate spectrophotometric method after digestion with $K_2S_2O_8$ and NaOH (Ebina et al., 1983). The TN concentration was measured by an ultraviolet spectrophotometry method using a UV-Visible spectrophotometer (UV-6100, Mapada, Shang Hai Shi, China). The DOC concentration in the water was analyzed using a carbon analyzer (Anlaytik HT1300, Jena, Germany). Water samples for chl-*a* measurements were filtered through Mili CA membranes (0.45 μm pore size) at low pressure. Then, the filters were frozen and extracted using 10 mL of 95% acetone at −20℃. The optical densities of the extracts were determined at 630, 645, 663, and 750 nm using a UV-vis spectrophotometer (UV-6100, Mapada) with a 1 cm matched cell. The accuracy of the TN, TP, TOC, and chl-*a* concentrations was ±0.1 mg/L.

The overlying water samples (each 500 mL) were vacuum-filtered with a grade GF/F glass fiber filter membrane, which had been burned at 450℃ for 4 h, and the filter membrane was weighed with a 0.1 mg analytical balance before filtration. The filtered glass fiber filter membrane was frozen and then dried in a vacuum freeze dryer (Biosafer-10A, *Nanjing, Jiangsu,* China) after 24 h. The dried glass fiber filter membrane was fumigated with concentrated hydrochloric acid for 24 h to remove particulate inorganic carbon. The filter membrane was washed with deionized water and adjusted to neutral pH. POC concentrations were analyzed using a carbon analyzer (AnlaytikJena HT1300). The $\delta^{13}C$ values of POC were determined using an organic elemental analyzer (FLASH 2000, Thermo Fisher, Monza, Italy) (Xu et al., 2015).

Gas flux samples were collected every 10 min for 1 h using a light-shielded floating static chamber (38.5 cm × 30.5 cm × 18.5 cm), which provides unbiased water-gas exchange measurements (Peng et al., 2022). The CH_4 and CO_2 emission fluxes (*F*), estimated by the static chamber method, were calculated as follows:

$$F = \frac{V}{A} \times \frac{dC}{dt}$$

Where F is the CH_4 and CO_2 emissions fluxes ($\mu mol \cdot m^{-2} \cdot h^{-1}$); V is the static chamber volume (m^3); A is the static chamber surface area (m^2), and dC/dt is the slope of the gas concentration changing with time during sampling ($\mu mol \cdot m^{-3} \cdot h^{-1}$).

Gas samples collected from the 18 lakes were measured by gas chromatography (GC-2014, Shimadzu, Tokyo, Japan). Five mL of gas sample was withdrawn from the microsystem. The chamber and FID detector temperatures were 55℃ and 200℃, respectively. The carrier gas flow rate was 2 mL/min in 99.999% high-purity nitrogen. High-purity hydrogen and air were used as gases at flow rates of 40 and 400 mL/min, respectively. The detection limits were 0.2 ppm for CH_4 and 4.0 ppm for CO_2 with an error range of ±1%.

4.2.3 Statistical analysis

The Statistical Package for the Social Sciences 18.0 (SPSS 18.0; SPSS Inc., Chicago, IL, USA) was used for the statistical analysis. The correlation analysis was carried out using bivariate correlation analysis. A p-value < 0.05 was considered significant.

4.3 Results

4.3.1 The physicochemical environment and the trophic indices of the lakes

The 18 lakes investigated in this study were in different trophic states (oligotrophic, mesotrophic, eutrophic, middle-eutrophic, and hyper-eutrophic), indicating the presence of eutrophication in the shallow lakes along the Yangtze River basin (Fig. 4.2). The redox conditions in the overlying water of the lakes were aerobic overall. In the hyper-eutrophic lakes (Lake Taihu, Lake Chaohu, and Lake Dianshan), DO concentrations in the overlying water were 3.11, 2.92, and 3.17 mg/L (Fig. 4.3) with corresponding ORPs of 176.80, 168.20, and 86.80 mV (Fig. 4.4), respectively. The water temperature ranged from 26.5 to 32.4℃ in the lakes (Fig. 4.5).

The TP, TN, and chl-*a* concentrations in the overlying water were significantly different (Figs. 4.6 and 4.7). The TP and TN concentrations in the hyper-eutrophic lakes

were much higher than those in lakes of the other trophic states (oligotrophic, mesotrophic, eutrophic, and middle-eutrophic). The TP concentrations in Lake Taihu, Lake Chaohu, and Lake Dianshan, classified as hyper-eutrophic, were 0.69, 0.59, and 0.58 mg/L, respectively, displaying much higher TP concentrations than those in the other lakes (Fig. 4.6). The TN concentrations showed the same tendency as the TP concentrations, in which the highest TN concentration appeared in hyper-eutrophic Lake Taihu. The TN concentrations in Lake Taihu, Lake Chaohu, and Lake Dianshan were 6.34, 3.67, and 2.39 mg/L, respectively. The chl-*a* concentrations were distributed differently from the other trophic indices and varied widely among the lakes (Fig. 4.7). The chl-*a* concentrations were 124.80, 28.10, and 30.40 μg/L in Lake Taihu, Lake Chaohu, and Lake Dianshan, respectively.

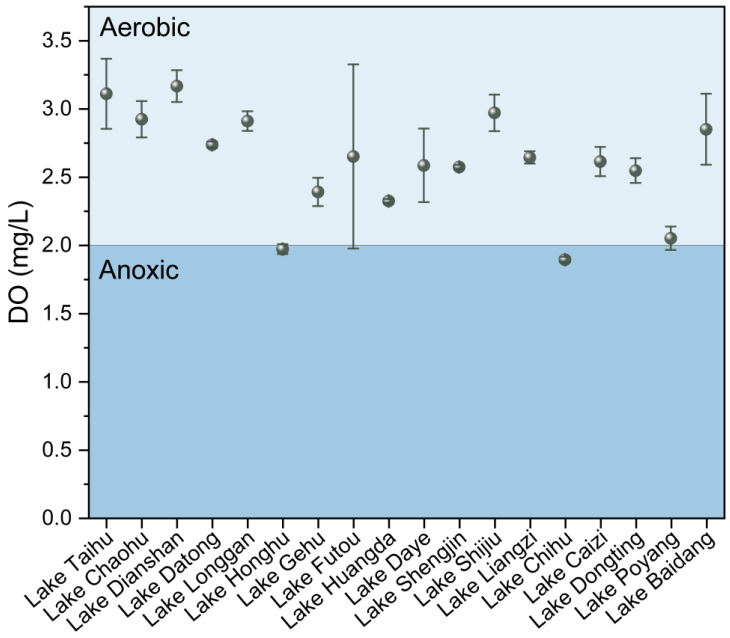

Fig. 4.3. The DO concentrations of overlying water in the investigated lakes in July 2021 along the Yangtze River.

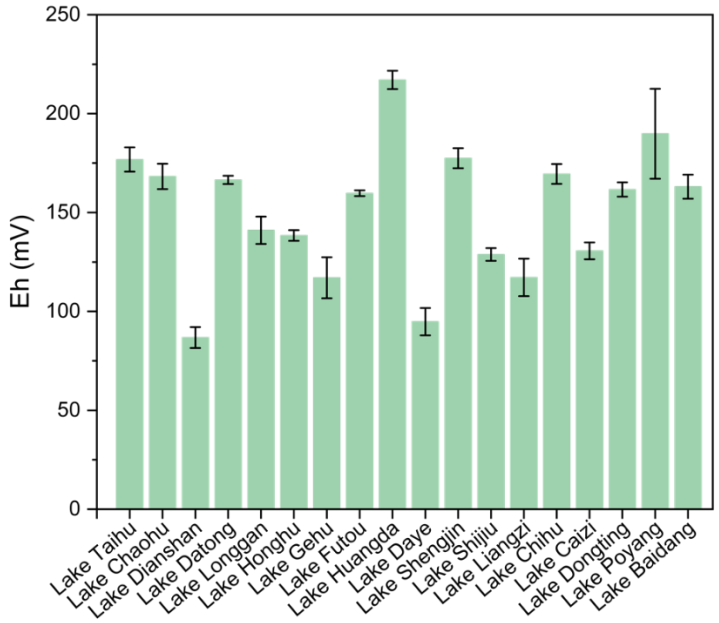

Fig. 4.4. The Eh of overlying water in the investigated lakes along the Yangtze River in July 2021

4.3.2 The POC, DOC, and $\delta^{13}C_{poc}$ concentrations in the overlying water

The POC and DOC concentrations in the overlying water of the lakes were similar (Fig. 4.8). The POC concentrations in the hyper-eutrophic lakes were higher than those in the other trophic state lakes. The highest and lowest POC concentrations were 25.01 mg/L and 1.98 mg/L in Lake Taihu (hyper-eutrophic) and Lake Poyang (oligotrophic), respectively. The DOC concentrations in the hyper-eutrophic lakes were much higher than those in the other trophic state lakes. The POC concentrations in a hyper-eutrophic state were 18.80, 15.90, and 22.30 mg/L in Lake Taihu, Lake Chaohu, and Lake Dianshan, respectively. The DOC concentration in Lake Datong (middle-eutrophic) was the lowest among all of the investigated lakes, reaching 2.05 mg/L. The $\delta^{13}C_{poc}$ values of the lakes ranged from−30.28‰ to −21.14‰ (Table 4.1). The highest $\delta^{13}C_{poc}$ value was −21.14‰ in Lake Daye (mesotrophic), while the lowest $\delta^{13}C_{poc}$ value was −30.28‰ in Lake Shijiu (mesotrophic).

4.3.3 Dissolved CH_4 and CO_2 concentrations in the overlying water

The dissolved CH_4 concentrations across all lakes ranged from 0.05 to 2.44 μmol/L and were correlated with *TLI* in the lakes ($R^2 = 0.67$) (Fig. 4.9). The dissolved CH_4

concentrations in the overlying water of the hyper-eutrophic lakes, *i.e.*, Lake Taihu, Lake Chaohu, and Lake Dianshan, were 2.11, 1.01, and 2.44 μmol/L, respectively. The lowest dissolved CH_4 was 0.05 μmol/L in Lake Huangda, classified as mesotrophic. The dissolved CO_2 concentrations were positively correlated with *TLI*, and dissolved CO_2 ranged from 4.05 to 98.90 μmol/L ($R^2 = 0.43$) (Fig. 4.9). In the hyper-eutrophic lakes, the concentration of dissolved CO_2 in Lake Taihu was 98.90 μmol/L, higher than Lake Chaohu at 76.50 μmol/L. The lowest dissolved CO_2 concentration was 4.05 μmol/L in Lake Huangda, which was similar to the dissolved CH_4.

Table. 4.1. The $\delta^{13}C_{poc}$ values, and the concentrations of POC, and DOC in overlying water of the investigated lakes along the Yangtze River basin

Lake name	$\delta^{13}C_{poc}$ (‰)	POC (mg L^{-1})	DOC (mg L^{-1})	Trophic state
Lake Taihu	-27.45 ± 2.1	25.0 ± 1.4	18.8 ± 2.3	Hyper-eutrophic
Lake Chaohu	-23.69 ± 1.6	18.4 ± 0.8	16.0 ± 1.2	Hyper-eutrophic
Dianshan	-23.04 ± 0.2	18.9 ± 2.1	22.3 ± 2.1	Hyper-eutrophic
Lake Datong	-26.9 ± 0.1	10.6 ± 1.3	2.1 ± 0.7	Middle-eutrophic
Lake Longgan	-24.51 ± 1.1	13.6 ± 1.1	10.7 ± 3.5	Eutrophic
Lake Honghu	-28.97 ± 0.2	4.3 ± 0.5	12.1 ± 0.4	Eutrophic
Lake Gehu	-26.63 ± 0.01	11.7 ± 0.8	10.5 ± 0.02	Eutrophic
Lake Futou	-27.54 ± 0.6	9.6 ± 0.6	2.5 ± 0.9	Mesotrophic
Lake Huangda	-28.2 ± 0.2	5.5 ± 0.4	2.7 ± 0.7	Mesotrophic
Lake Daye	-21.14 ± 1.0	10.9 ± 1.1	9.7 ± 0.8	Mesotrophic
Lake Shengjin	-30.27 ± 0.7	9.2 ± 1.0	2.8 ± 0.2	Mesotrophic
Lake Shijiu	-30.28 ± 0.5	9.4 ± 1.6	2.3 ± 0.3	Mesotrophic
Lake Liangzi	-26.98 ± 0.6	6.7 ± 0.5	2.2 ± 0.5	Mesotrophic
Lake Chihu	-29.42 ± 1.3	6.9 ± 1.1	7.7 ± 0.7	Mesotrophic
Lake Caizi	-28.17 ± 1.1	6.6 ± 1.3	4.6 ± 0.7	Mesotrophic
Lake Dongting	-29.65 ± 0.4	3.8 ± 0.3	2.3 ± 0.2	Mesotrophic
Lake Poyang	-27.76 ± 0.5	2.0 ± 0.1	3.7 ± 0.2	Oligotrophic
Lake Baidang	-28.07 ± 0.4	8.5 ± 1.6	7.3 ± 1.1	Oligotrophic

4.3.4 CH_4 and CO_2 emission fluxes

All of the lakes acted as a carbon emission source, and the carbon emission fluxes (CH_4 and CO_2) were noticeably different across the lakes (Fig. 4.10). The CH_4 emission fluxes ranged from 13.60 to 929.90 $\mu mol \cdot m^{-2} \cdot h^{-1}$ in the lakes. The CH_4 emission fluxes were 929.90, 830.90, and 563.60 $\mu mol \cdot m^{-2} \cdot h^{-1}$ in hypereutrophic Lake Taihu, Lake Chaohu, and Lake Dianshan, respectively (Table 4.2). The lowest CH_4 emission fluxes of 17.20 and 13.60 $\mu mol \cdot m^{-2} \cdot h^{-1}$ were observed in the oligotrophic lakes, *i.e.*, Lake Poyang and Lake Baidang, respectively. The CO_2 emission fluxes showed a similar tendency as the CH_4 emission fluxes (Fig. 4.10). The CO_2 emission fluxes of hyper-eutrophic Lake Taihu, Lake Chaohu, and Lake Dianshan were 7.20×10^3, 3.20×10^3,

and 2.70 × 10^3 μmol·m^{-2}·h^{-1}, respectively, which were higher than the less eutrophic lakes. The lowest CO_2 emission flux was 0.34 μmol·m^{-2}·h^{-1} in mesotrophic Lake Caizi.

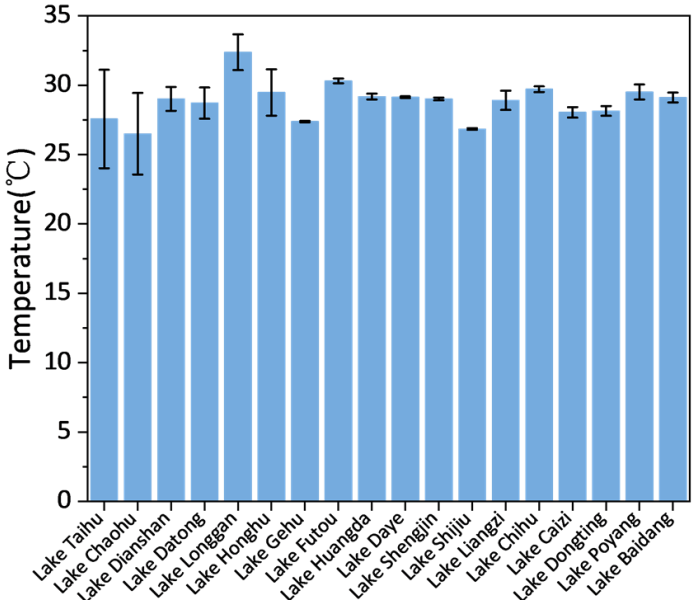

Fig. 4.5. The temperature of overlying water in the investigated lakes along the Yangtze River in July 2021.

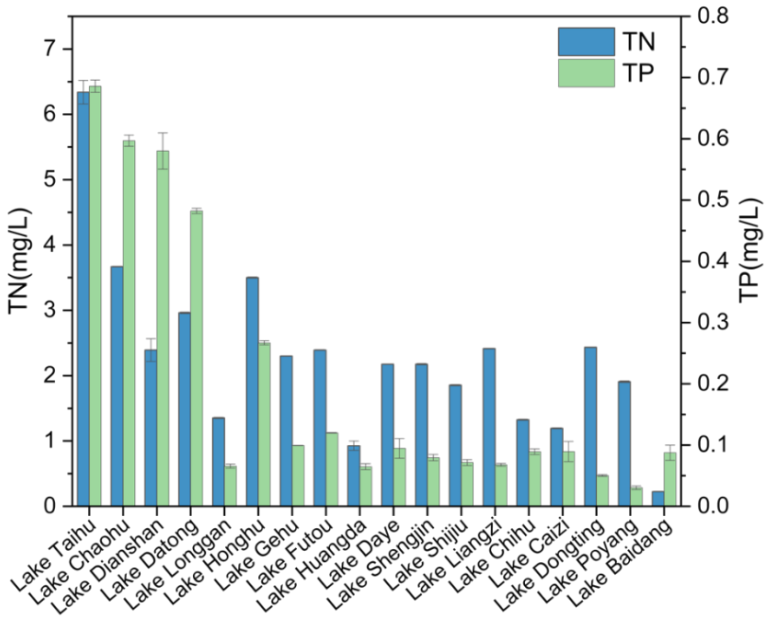

Fig. 4.6. The TN and TP concentrations of overlying water in the investigated lakes along the Yangtze River in July 2021.

Table. 4.2. The CH_4 and CO_2 emission flux of the investigated lakes along the Yangtze River basin

Lake name	CH_4 (μmol/m^2·h)	CO_2 (μmol/m^2·h)	Trophic state
Lake Taihu	929.9 ± 106.6	7222.5 ± 1197.3	Hyper-eutrophic
Lake Chaohu	830.9 ± 122.3	3180.8 ± 568.4	Hyper-eutrophic
Lake Dianshan	563.6 ± 90.6	2668.6 ± 50.2	Hyper-eutrophic
Lake Datong	483.6 ± 36.1	1969.8 ± 318.8	Middle-eutrophic
Lake Longgan	353.8 ± 4.1	1318.3 ± 60.0	Eutrophic
Lake Honghu	388.2 ± 111.2	1217.6 ± 221.8	Eutrophic
Lake Gehu	201.4 ± 55.1	1098.2 ± 116.8	Eutrophic
Lake Futou	188.5 ± 5.7	812.7 ± 20.6	Mesotrophic
Lake Huangda	205.4 ± 9.3	667.1 ± 10.5	Mesotrophic
Lake Daye	64.2 ± 10.4	415.7 ± 67.3	Mesotrophic
Lake Shengjin	42.1 ± 15.3	342.3 ± 38.9	Mesotrophic
Lake Shijiu	42.6 ± 4.9	41.4 ± 5.8	Mesotrophic
Lake Liangzi	42.2 ± 2.9	139.5 ± 19.9	Mesotrophic
Lake Chihu	52.42 ± 11.8	1476.3 ± 224.1	Mesotrophic
Lake Caizi	26.4 ± 5.0	0.3 ± 0.3	Mesotrophic
Lake Dongting	34.7 ± 3.4	26.9 ± 2.8	Mesotrophic
Lake Poyang	17.2 ± 5.6	468.7 ± 116.3	Oligotrophic
Lake Baidang	13.6 ± 2.9	5.7 ± 0.6	Oligotrophic

4.4 Discussion

Lakes are generally considered hot spots for CH_4 emissions. The CH_4 emissions range from 8 to 48 Tg/yr worldwide, accounting for 6–16% of total natural CH_4 emissions (Tranvik et al., 2009; Bastviken et al., 2011). With the input of exogenous nutrients (carbon, nitrogen, and phosphorus), the freshwater lakes investigated in this study were faced with severe eutrophication (Figs. 4.2 and 4.6). Eutrophication leads to cyanobacterial blooms (Fig. 4.7), and the decay of cyanobacteria promotes an increase in the POC concentration (Fig. 4.8), which likely destabilizes the carbon cycle in eutrophic lakes. POC was mainly derived from an endogenous source in the lakes we investigated (Table 4.1); cyanobacterial-derived carbon is likely the primary source of POC in shallow lakes with severe eutrophication (Ye et al., 2015; Shi et al., 2017). The increased POC concentration resulted in a significant increase in carbon production and emissions from the lakes (Figs. 4.11 and 4.12), particularly for dissolved CH_4 (R^2 = 0.51). The higher concentration of dissolved methane in oxic water in this study represents the typical methane paradox (Bartosiewicz et al., 2022). From the relationship among dissolved CH_4, DO, and POC concentrations, we hypothesized that the co-occurrence of a high concentration of POC potentially increases methane emissions from oxic waters of eutrophic lakes, which provides a new perspective to

explain the emergence of the methane paradox (Fig. 4.13).

The concentration and source of POC in the lakes were affected by many factors, including the trophic state, hydrological conditions, and temperature change (Sakai et al., 2013; Jiang et al., 2022). The decomposition of cyanobacteria generates a large amount of POC, and the cyanobacterial residue settles to the sediment surface and forms a "cyanobacterial detritus mat" (Qi et al., 2020). Shallow lakes are susceptible to wind and wave disturbances, which resuspend the sediment and organic debris (Sun et al., 2016). The $\delta^{13}C_{poc}$ ranged from −42‰ to −24‰, indicating that the POC was mainly derived from endogenous sources, and cyanobacterial decomposition will release a large amount of POC (Long et al., 2009; Zhou et al., 2019). In this study, the $\delta^{13}C_{poc}$ of the lakes ranged from −30.28‰ to −21.14‰, indicating that the POC was mainly from endogenous sources due to cyanobacterial growth in these shallow lakes along the Yangtze River basin (Table 4.1). The relationship between the POC concentration and *TLI* index underscores that intensifying eutrophication in shallow lakes increases the POC concentration (R^2 =0.84) (Fig. 4.11). In eutrophic lakes, the CO_2 source is restricted by the change in the lake environment with cyanobacterial-derived carbon as the main source of POC (Goni et al., 2003). The primary productivity of a lake is low at the early stage of eutrophication, and most of the CO_2 absorbed by cyanobacteria originates from the atmosphere (Goni et al., 2003; Dalu et al., 2016). The cyanobacterial-derived POC participates in the carbon cycle of the lakes, which contributes to the production and flux of CH_4 and CO_2 emissions from the lakes into the atmosphere (Wang et al., 2019; Liu et al., 2021). In the lakes we investigated, the DO concentrations were > 2 mg/L (Fig. 4.3), and were accompanied by a higher concentration of dissolved CH_4 (Fig. 4.9), particularly in the severely eutrophic lakes. This result was consistent with the definition of the methane paradox (Bartosiewicz et al., 2022). Current explanations for the methane paradox include diffusion from terrestrial sources and micro-anaerobic environments in aerobic water (Tang et al., 2014; Fernandez et al., 2016). These explanations assume that the methane paradox is premised on a sufficient source of OC and a high abundance of microorganisms (Mizandrontsev et al., 2020). Therefore, the carbon source provided by the cyanobacterial-derived POC in eutrophic lakes significantly contributed to the creation of the methane paradox (Table 4.1; Fig. 4.8).

Recent reports underscore that carbon emissions from shallow lakes to the

atmosphere have increased significantly (Wen et al., 2016; Yan et al., 2017). An *in situ* investigation showed that the intensification of lake eutrophication further promoted the carbon emission capacity of freshwater lakes (Figs. 4.9 and 4.10). Furthermore, this study determined that the dissolved concentrations and emission fluxes of CH_4 (R^2 = 0.51; 0.67) and CO_2 (R^2 = 0.44; 0.68) were positively correlated with the POC concentration, respectively (Fig. 4.12). CH_4 is a product of OC mineralization, and the composition of OC plays a decisive role in the mineralization rate (Clayer et al., 2020). Compared with the POC of allochthonous sources, the POC of autochthonous sources has a relatively simple organic structure, which results in faster conversion of autochthonous POC into CH_4 in an anaerobic environment (Grasset et al., 2018). CH_4 is released into the atmosphere from lakes by ebullition, diffusion, storage, and plant-mediated emissions (Bastviken et al., 2011). In hyper-eutrophic lakes, some of the CH_4 was dissolved when the CH_4 was discharged through the overlying water, which significantly increased the amount of dissolved CH_4 in the overlying water (Fig. 4.9). The aerobic environment and the high concentrations of dissolved CH_4 in the methane paradox resulted from this process (Fig. 4.13). Furthermore, due to the inhibitory effect of a high O_2 concentration and light, dissolved CH_4 is easily oxidized up to 50%, and, in extreme cases, up to 90% in overlying water (Yao et al., 2016; Thottathil et al., 2019). Therefore, the dissolved concentration and emission flux of CO_2 also represents the production of CH_4. This previous finding supports the increase in dissolved CO_2 and CO_2 fluxes observed in this study (Figs. 4.9 and 4.10), which was the final product of OC mineralization. The high CO_2 emission concentration indicates that microorganisms are highly active, thus the cyanobacterial-derived POC promotes the organic metabolic processes of microorganisms, particularly anaerobic microorganisms (Zhou et al., 2019). Although the growth of cyanobacteria absorbs CO_2, large amounts of CO_2 are released into the atmosphere from lakes (Goni et al., 2003). Studies have shown that the micro-anaerobic environment in oxic water induces the OC mineralization process, including the production of CH_4 and CO_2 (Schulz, et al., 2001). The formation of this micro-anoxic environment also affects the distribution of NO_3^- concentration and induces the nitrification process, leading to an increase in N_2O emissions (Xia et al, 2017). Because microorganisms attaching to the POC surface oxidize the organic matter in POC, a gradient of DO concentration is created inside and outside POC (Xia et al, 2017). The micro-anaerobic environment caused by POC in the aerobic water layer

provides an anaerobic environment for the organic metabolism of anaerobic microorganisms, which is an important reason for the occurrence of the methane paradox.

A concept is herewith proposed to clarify the sources of POC and their effect on carbon cycling, including a new perspective on the methane paradox (Fig. 4.13). Anthropogenic activities lead to eutrophication in freshwater lakes, which induces cyanobacterial blooms. The cyanobacterial-derived carbon increases the POC concentration, which mainly originates from autochthonous sources in shallow lakes. Methanogenesis occurs when the concentration of POC reaches a particular level (>10 mg/L), and forms a sufficient micro-anaerobic environment in the overlying water (Bizic-Ionescu et al., 2019; Zhou et al., 2019). Although the overlying water environment is primarily aerobic, the local anaerobic environment still provides the possibility for oxidation of CH_4. CH_4 and CO_2 produced in these micro-anaerobic zones within and on the surface of POC migrate into the aerobic water. Hence, POC positively contributes to methane paradox, which leads to carbon emission increased. These results reveal the main sources and functions of POC in lakes, which are of significance for estimating the lake carbon emission and predicting the climate warming trend.

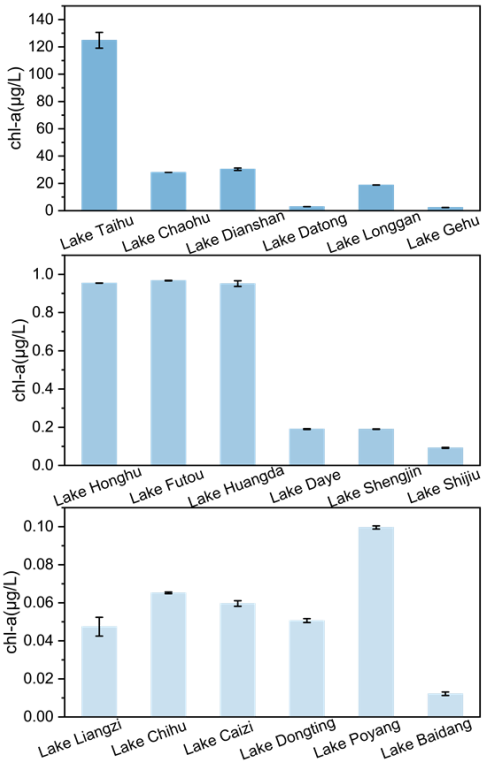

Fig. 4.7. The chl-a concentrations of different lakes overlying water in summer along the Yangtze River

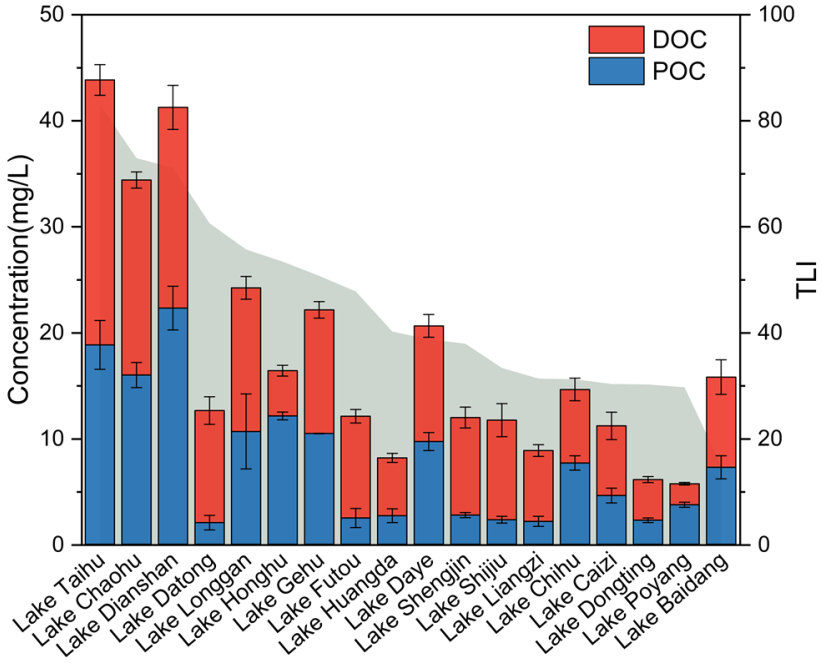

Fig. 4.8. The POC and DOC concentrations of overlying water in the investigated lakes along the Yangtze River in July 2021.

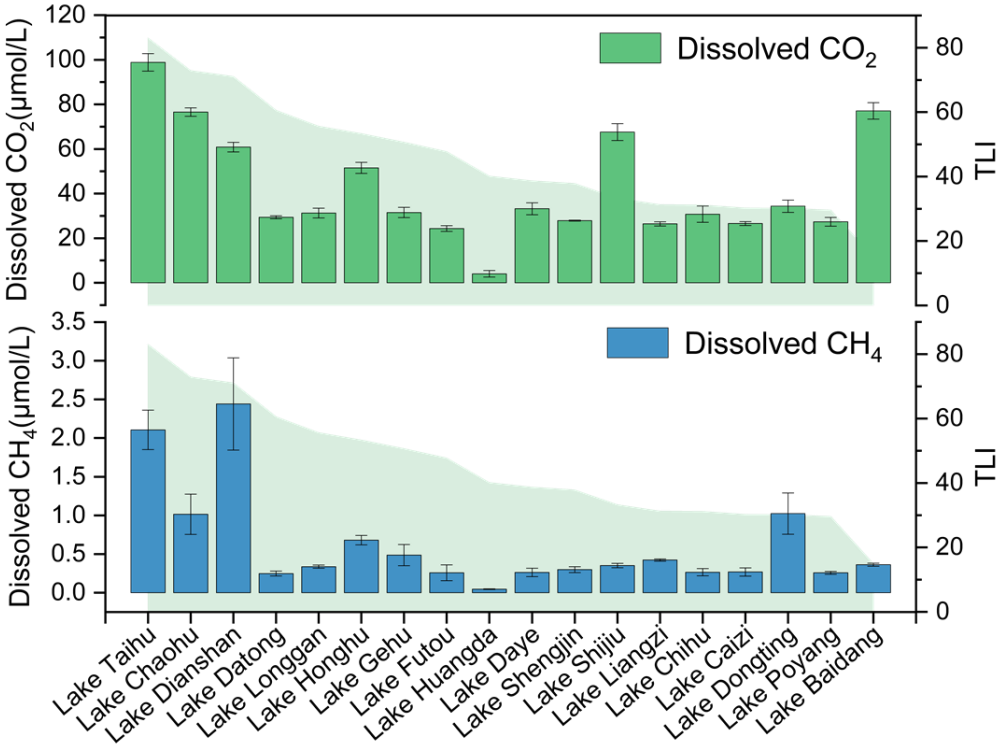

Fig. 4.9. The dissolved CO_2 and CH_4 concentrations of overlying water in the investigated lakes along the Yangtze River in July 2021.

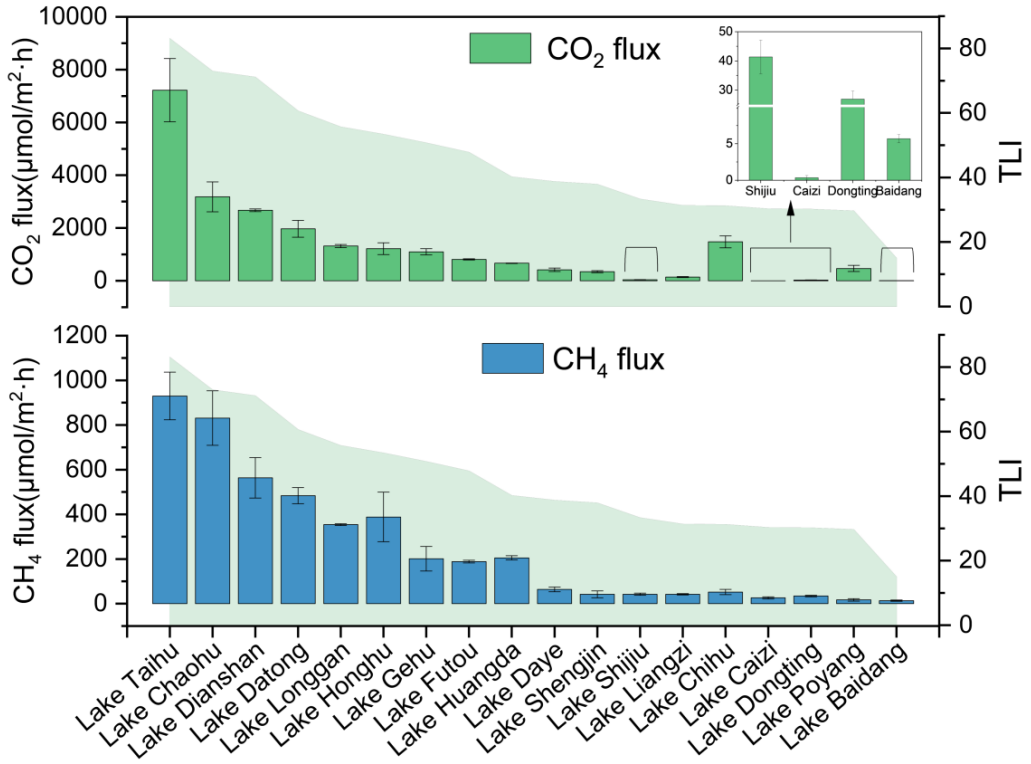

Fig. 4.10. The CH_4 and CO_2 flux in the investigated lakes along the Yangtze River in July 2021.

4.5 Summary

In this study, the OC concentrations, particularly POC, in the lakes were positively correlated with the increased trophic state, and the cyanobacterial-derived carbon contributed greatly, particularly POC. The intensification of lake eutrophication increased the concentration of POC in the overlying water, which was mainly derived from autochthonous sources. Cyanobacterial-derived POC provided a sufficient carbon source for the anaerobic metabolism of microbial organic matter, which maintained microbial activity at a high level and promoted the concentration flux of CH_4 and CO_2. Therefore, the increase in POC concentration caused by cyanobacterial-derived carbon significantly promoted the emissions of CH_4 and CO_2 from the shallow lakes as eutrophication intensified. In this study, high POC concentrations in the oxic overlying water of lakes in the middle and lower reaches of the Yangtze River were observed to be accompanied by high dissolved CH4 concentrations, revealing that the presence of POC may be cause of the methane paradox. These findings are important for evaluating the effect of POC on carbon emissions and the balance of freshwater shallow lakes.

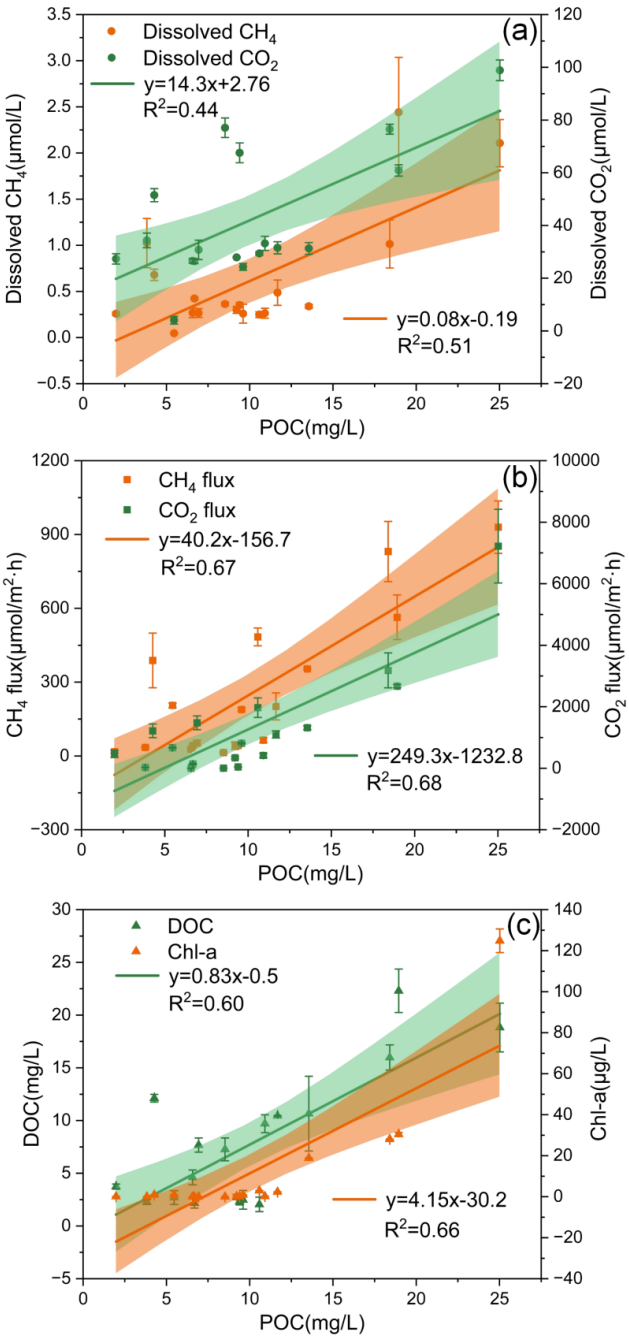

Fig. 4.12. Correlation analysis between POC concentration and dissolved CH_4, dissolved CO_2 (a), CH_4 flux, CO_2 flux (b), DOC concentration, chl-a concentration (c), respectively.

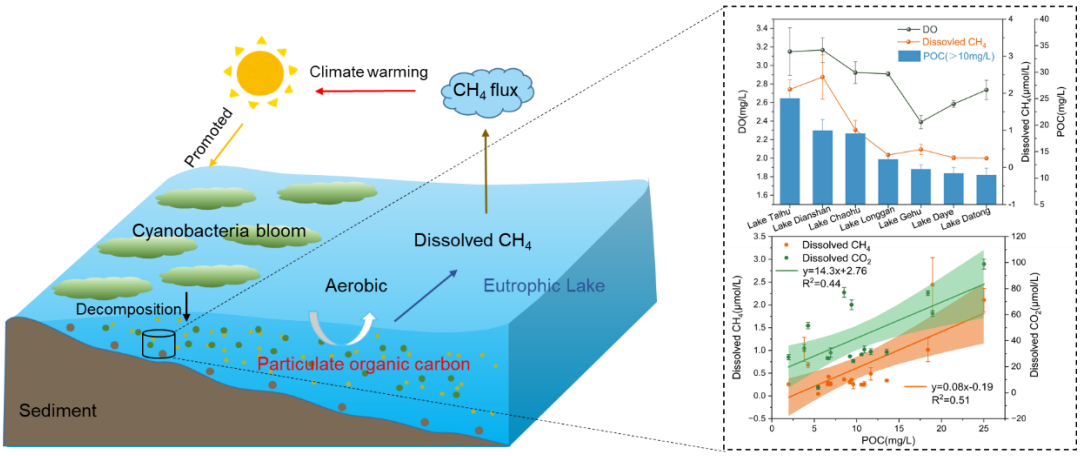

Fig. 4.13. A conceptual diagram of POC enhances CH_4 concentration in the oxic water of eutrophic lakes

5. Migration of GHG production hotspots in sediment of eutrophic lakes driven by cyanobacteria decomposition

5.1 Background

Lakes are recognized as significant natural contributors to global GHG emissions. It is estimated that lakes worldwide annually emit 8-48 Tg of CH_4 and 60-840 Tg of carbon dioxide (CO_2) annually into the atmosphere (Bastviken et al., 2004; Bastviken et al., 2008; Raymond et al., 2014). Previously, it has been identified bottom sediments as key zones for CH_4 and CO_2 production, primarily due to anaerobic conditions and the substantial accumulation of organic carbon (Einzmann et al., 2022). However, recent studies suggest that the decomposition of cyanobacteria induced by eutrophication significantly alters the physical and chemical properties of surface sediments (Zhou et al., 2022a). Changes in the characteristics of lake surface sediments, particularly resulting from eutrophic processes, have emerged as important factors that affect the accurate estimation of lake carbon emissions (Qi et al., 2020).

Surface sediments conventionally exhibit relatively higher oxygen concentrations compared to bottom sediments and are not traditionally considered primary zones for CH_4 production (Comer-Warner et al., 2019; Einzmann et al., 2022). However, several studies have proposed that eutrophication-induced cyanobacterial blooms lead to a significant accumulation of cyanobacterial residues on the sediment surface. This accumulation forms a “cyanobacteria detritus mat”, creating a suitable environment for methanogenic archaea to thrive on the surface sediments (Qi et al., 2020). Importantly, in comparison to decomposition processes involving aquatic plants, cyanobacterial residues typically contain more easily accessible forms of organic carbon, including low molecular weight organic acids, sugars, amino acids, and lipids. These forms provide resources for methanogenic archaea, leading to a faster decomposition rate (Villacorte et al., 2015; Bao et al., 2023). When cyanobacteria decompose, the introduction of cyanobacteria-derived carbon into lakes triggers co-metabolic effects, accelerating the breakdown of recalcitrant carbon, particularly in surface sediments where interactions occur between cyanobacteria-derived carbon and recalcitrant carbon (Deng et al., 2022). This co-metabolism markedly increases the mineralization rate of organic carbon, contributing substantially to CH_4 and CO_2 emissions from lakes (Ma et al., 2020; Deng et al., 2023). Furthermore, the accelerated decomposition of organic

carbon, driven by microbial activity, leads to a reduction in oxygen concentrations and significantly intensifies the rate of carbon metabolism in surface sediment (Qi et al., 2020; Ma et al., 2024). Therefore, surface sediments may exhibit heightened activity in CH_4 and CO_2 production processes.

The emission of CH_4 from lakes into the atmosphere is influenced by both CH_4 production and oxidation processes (Verpoorter et al., 2014; Zhou et al., 2022b). CH_4 and CO_2 generated through the mineralization of organic carbon in sediments are emitted into the atmosphere through various pathways, including ebullition, water column release, diffusive emission, and plant-mediated emission (Bastviken et al., 2004; Davidson et al., 2015). In lake ecosystems, as CH_4 produced in bottom sediments moves towards the surface sediments, between 50% and 90% of it is consumed through oxidation processes. This reduces the CH_4 concentration by the time it reaches the surface sediments (Alanna et al., 2017). The presence of increasing oxygen concentrations during its upward movement in sediments is a crucial factor that promotes methane oxidation (Hu et al., 2024). Methane oxidation plays a vital role in mitigating the greenhouse effect in lakes, as it converts most of the CH_4 into CO_2, resulting in increased CO_2 emissions (Miller et al., 2016; Yan et al., 2023). However, the formation of the cyanobacteria detritus mat on the surface sediment creates an anaerobic environment that inhibits the methane oxidation process in the surface sediments (Emerson et al., 2021; Perez-Coronel et al., 2022). While some research suggests anaerobic oxidation as a potential pathway for methane oxidation, aerobic oxidation processes primarily govern this mechanism in eutrophic freshwater lakes (Yang et al., 2019). Cyanobacteria residues consume and deplete oxygen from the surface sediments, potentially reducing methane oxidation losses (Cerbin et al., 2022). Traditionally, bottom sediments have been identified as hotspots for CH_4 production, as evidenced by in-situ experiments showing significantly higher CH_4 concentrations compared to the surface (Li et al., 2018; Einzmann et al., 2022). Nevertheless, changes in the lake's environmental conditions have led to surface sediments also being recognized as important sites for CH_4 production, indicating increased transmission efficiency (Murase et al., 2005; Xiao et al., 2017). Factors such as temperature and pressure, which are influenced by depth, play a role in determining the efficiency of gas transport (Gudasz et al., 2010; Emilson et al., 2018). Therefore, variations in the depth of areas with high CH_4 and CO_2 production can significantly alter the capacity to emit

carbon in lakes.

This study examines the influence of eutrophication on sediment carbon pools and explores the underlying mechanisms. The study collected water, sediment, and gas samples from seven lakes with varying trophic levels in the highly developed regions of the middle and lower reaches of the Yangtze River. Field investigations were conducted to measure the concentrations of dissolved CH_4 and CO_2, as well as their release fluxes in the overlying water. In addition, measurements of dissolved CH_4 and CO_2 concentrations were taken at different depths in the sediment pore-water. Furthermore, a series of microcosms were established using cyanobacteria, water, and sediment samples collected from the typical eutrophic Lake Taihu, to evaluate the impact of cyanobacterial carbon on the mineralization of organic carbon within the sediment. These findings provide valuable insights for accurately assessing the equilibrium of the lake sediment carbon pool and the associated carbon emissions in the context of increasing eutrophication conditions.

5.2 Materials and methods

5.2.1 Study site and sample collection

Seven shallow freshwater lakes (depth < 7m) located within the Yangtze River basin were selected and classified into three categories: mesotrophic ($30 < TLI < 50$), eutrophic ($50 < TLI < 60$), and hyper-eutrophic (($TLI > 70$)) based on the Trophic Level index (*TLI*) (Figs. 5.1 and 5.2). In July 2021, three sampling sites were designated in these lakes, all located over 300 m from the lake shore. Gas, water, and sediment samples were collected, with the water depth at each sampling point not exceeding 5 meters. Additionally, to simulate a typical eutrophic lake environment, samples of water, sediment, and cyanobacteria were collected from Lake Taihu to establish microcosmic systems. Detailed information about the lakes can be found in Table 5.1.

The gravity core sampler was be used to collect the sediment core at a depth of 0 to 24 cm, divided into 12 layers at 2 cm intervals. Overlying water samples from each lake were systematically collected 30 cm beneath the surface, in triplicate, to assess nutrient concentrations and concentrations of dissolved CH_4 and CO_2. Cyanobacteria were harvested from the cyanobacterial accumulation area using a plankton net with a mesh size of 250. Gas samples were systematically gathered at 10-minute intervals over

a period of one hour using light-shielded floating static chambers (38.5 cm × 30.5 cm × 18.5 cm), a method validated for delivering accurate assessments of water-gas exchange.

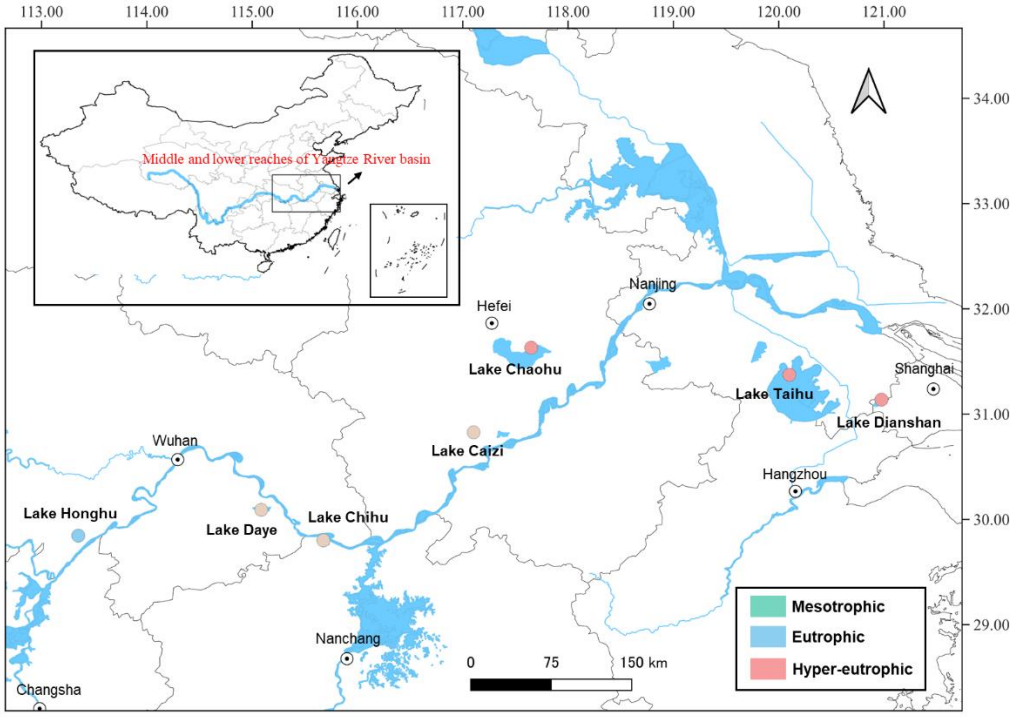

Fig. 5.1. Sampling sites in different trophic state lakes along the Yangtze River.

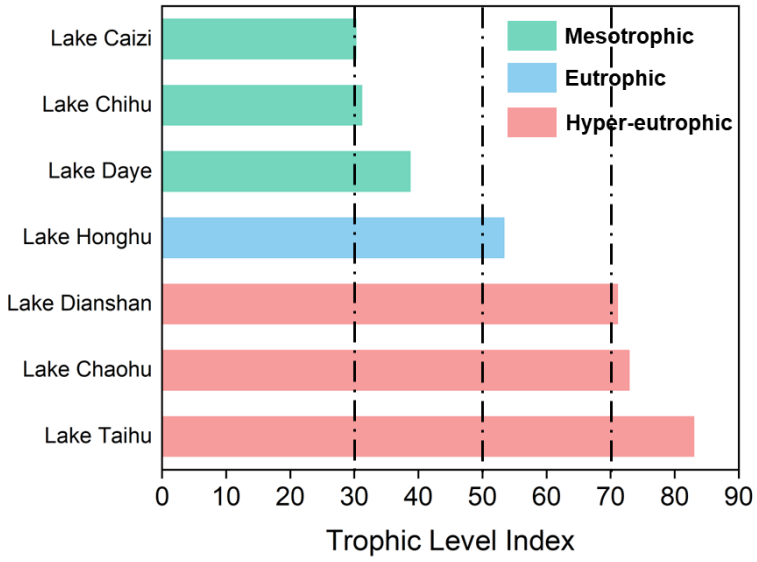

Fig. 5.2. The TLI values of different lakes along the Yangtze River. The vertical dashed lines at TLIs of 30, 50, and 70 represent the thresholds of oligotrophic-mesophilic, mesophilic-eutrophic, middle-eutrophic, and hyper-eutrophic states.

5.2.2 Microcosm system

The microcosm system consisted 156 plexiglass columns (8 cm diameter, 70 cm height), divided into four groups based on cyanobacterial density: K (no accumulation), A (4 cm), B (8 cm), and C (12 cm), each with three replicates. Each column contained in-situ lake water (20 cm) and sediment (20 cm), with varying cyanobacteria amounts. The cyanobacteria within the microcosmic system were labeled using $NaH^{13}CO_3$ (98 at. %^{13}C) inorganic salts. The $\delta^{13}C$ value of cyanobacteria before cultivation was -22.72‰, which decreased to -18.28‰ after cultivation. Before addition, cyanobacteria were washed to remove residual salts. Nitrogen gas was introduced into the headspace of the plexiglass columns for 20 minutes to ensure that the carbon in each treatment group originated solely from within the microcosm system. The rubber plug was sealed and further secured with silicone sealant, with a gas extraction pipe aperture reserved within the rubber plug. All samples were incubated in the dark at a constant temperature of 28±1°C in a water bath to simulate environmental conditions in Lake Taihu during algae blooms. Destructive sampling was conducted on days 0, 5, 10, 15, 20, 30, 40, 50, 70, 100, 140, 180, 270, and 360 over one year.

5.2.3 Chemical analytical methods

The microcosm system utilized a gravity core sampler to collect sediment core samples from depths of 0-20 cm, which were then divided into 5 layers with intervals of 4 cm each. The sediment core samples obtained in the field and microcosm were freeze-dried using freeze-drying machines (Biosafer-10A, China). After freeze-drying, the sediment samples were acidified with 1 mol/L hydrochloric acid and subsequently dried in an oven at 60 ℃ for 8 hours. The dried sediments were analyzed for total organic carbon (TOC) using a TOC analyzer (AnlaytikJena HT1300, Germany) in accordance with EPA 9060A guidelines, with an accuracy of TOC concentration to within 1%.

In this study, measurements were conducted to assess the CH_4 and CO_2 emissions at the water-gas interface, as well as to determine the concentrations of dissolved CH_4 and CO_2 in overlying water. Additionally, measurements were taken to determine the CH_4 and CO_2 concentrations in sediment pore-water of various depths. All gas samples were determined by gas chromatography (GC-2014, Shimadzu, Japan).

The emissions fluxes (F) of gas (CH_4 and CO_2) were determined by the static chamber method as follows:

$$F = \frac{V}{A} \times \frac{dC}{dt} \quad (1)$$

Where F is the gas emissions ($\mu mol \cdot m^{-2} \cdot h^{-1}$); V is the volume of the static chamber (m^3); A is the surface area of the static chamber (m^2), and dC/dt is the slope of the gas concentration changing with time during sampling ($\mu mol \cdot m^{-3} \cdot h^{-1}$).

To collect gas samples from water and measure dissolved CH_4 and CO_2 concentrations, 300 mL of water was slowly poured into an anaerobic bottle. Excess gas in the headspace was then removed by blowing N_2 for 3 minutes. The anaerobic bottles were agitated for 5 minutes before withdrawing the headspace gas using a syringe. The gas was injected into an airbag (E-Switch, China) for storage and later measured by gas chromatography.

To investigate the concentrations of dissolved CH_4 and CO_2 at various sediment depths, pore-water was extracted from sediment cores and analyzed using the static headspace method (Sun et al., 2022). Wet sediment core samples (1g each) were collected from different depths in both in-situ and microcosms, and placed in brown bottles (30 cm^3 in volume), and each sediment layer was sampled in triplicate. Subsequently, 20 mL of ultrapure water, previously deoxygenated through 5 min of vigorous aeration by N_2, was added to each bottle. After sealing, the brown glass bottles were shaken for 5 minutes and left to reach water and gas diffusion equilibrium. Finally, 5 mL of gas was extracted using a syringe and its concentration was measured by gas chromatography. The pore-water concentrations of CO_2 and CH_4 were calculated using Eq. (1) as described above.

The freeze-dried sediment core samples were treated with concentrated hydrochloric acid for 24 h to remove particulate inorganic carbon. After the treatment, the samples were washed extensively with deionized water to neutralize and adjust the pH to a neutral level. The $\delta^{13}C$ values of the sediment were determined using an organic elemental analyzer (FLASH 2000, Thermo Fisher, Monza, Italy) (Zhou et al., 2023a).

To investigate the impact of cyanobacterial decomposition on microorganisms in the sediment, sequencing and real-time reverse-transcriptase quantitative polymerase chain reaction (RT-qPCR) technologies were employed. The microbial communities were quantified with sets targeting ArBa515F_806R. Sediment samples were stored at -80°C in an ultra-low temperature freezer. Total genomic DNA was extracted using the

E.Z.N.A.® Soil DNA Kit (Omega Bio-Tek, Norcross, GA, USA). The quality of nucleic acids was assessed via 1% agarose gel electrophoresis, and concentrations were measured with a NanoDrop 2000 UV spectrophotometer (Thermo Scientific, USA). Bacterial communities were quantified through 16S rRNA gene analysis, following MIQE guidelines.

5.2.4 Statistical analysis

Data statistical analysis was conducted using Origin 2023 and SPSS 18.0. Prior to analysis, the normal distribution of the data was assessed to establish correlations. The Pearson correlation coefficient was employed for bivariate correlation analysis. Significant differences among variables were assessed through one-way analysis of variance (ANOVA) and independent sample t-tests.

5.3 Results

5.3.1 Trophic status and TOC concentration in the sediments of lakes

The investigated lakes in the field displayed a range of trophic state, with eutrophic lakes facing significant ecological challenges (Fig. 5.2). Among them, Lake Taihu, Lake Chaohu, and Lake Dianshan were in a hyper-eutrophic state, with Lake Taihu exhibiting the highest degree of eutrophication with a *TLI* of 83.1. The TOC concentration in sediments in hyper-eutrophic lakes was notably high, especially in the surface sediment layers (Fig. 5.3). The sediments of Lake Taihu had the highest TOC concentration, with the surface sediment reaching up to 68.4±114.9 g/kg. As the sediment depth increased, the TOC concentration gradually decreased, with a more pronounced trend observed in eutrophic lakes. In Lake Taihu, the most significant variation in TOC concentration with depth occurred in the range of -10 to -14 cm, where the TOC concentration decreased from 52.8±330.1 to 39.7±5.5 g/kg.

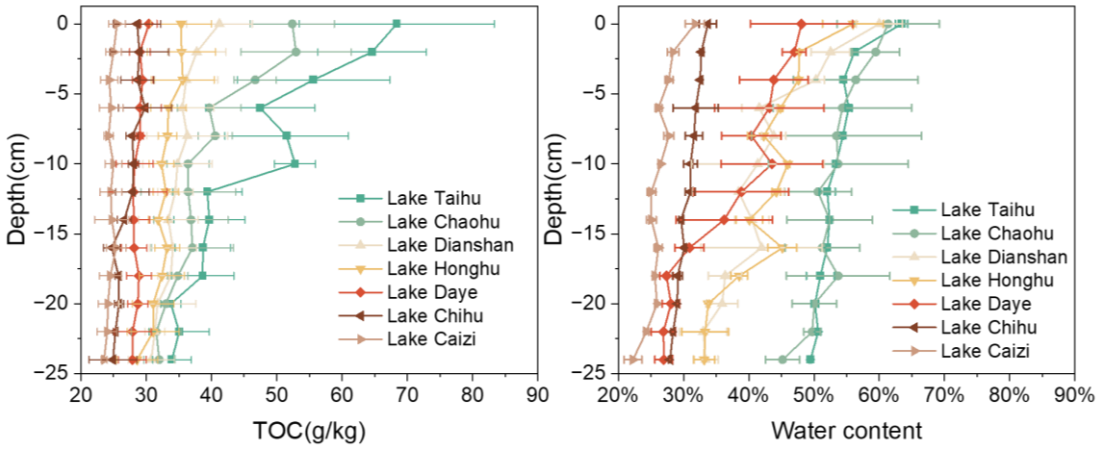

Fig. 5.3. The TOC concentration (left) and water content (right) in different depths of sediment in sediment of the investigated lakes along the Yangtze River.

5.3.2 Dissolved CH_4 and CO_2 in the water and their emissions in air-water fluxes of lakes

The emissions of CH_4 and CO_2 in air-water fluxes varied significantly among different lakes and displayed a positive correlation with the degree of lake eutrophication (Figs. 5.4 and 5.5). In these lakes, the CH_4 emissions in air-water fluxes ranged from 26.4±5.0 to 929.9±106.6 μmol/m^2·h, while CO_2 emissions ranged from 0.3±0.3 to 7222.5±1197.3 μmol/m^2·h. Among all investigated lakes, Lake Taihu had the highest emissions of CH_4 and CO_2 in air-water fluxes at 929.9±106.6 and 7222.5±1197.3 μmol/m^2·h, respectively. Conversely, the lowest emissions for CH_4 and CO_2 in air-water fluxes were observed in Lake Caizi at 26.4±5.0 and 0.3±0.3 μmol/m^2·h, respectively.

Dissolved CH_4 concentrations in the overlying water, ranging from 0.3±0.1 to 2.1±0.3 μmol/L, showed a positive correlation with the Trophic Level Index (*TLI*) of the studied lakes (Figs. 5.4 and 5.6). In a similar pattern, dissolved CO_2 concentrations varied from 26.6±0.9 to 98.9±3.9 μmol/L, mirroring the trends observed for CH_4. The peak concentration of dissolved CH_4, recorded at 2.4±0.6 μmol/L, was found in Lake Dianshan, while Lake Taihu registered the highest dissolved CO_2 concentration at 98.9±3.9 μmol/L.

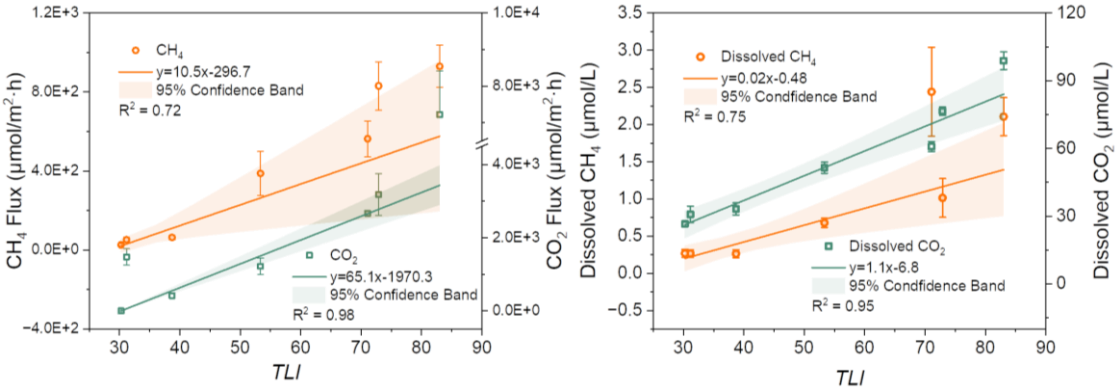

Fig. 5.4. Correlation analysis between Trophic Level index (*TLI*) and the CH_4, CO_2 flux (left), dissolved CH_4, CO_2 (right) of the investigated lakes along the Yangtze River, respectively.

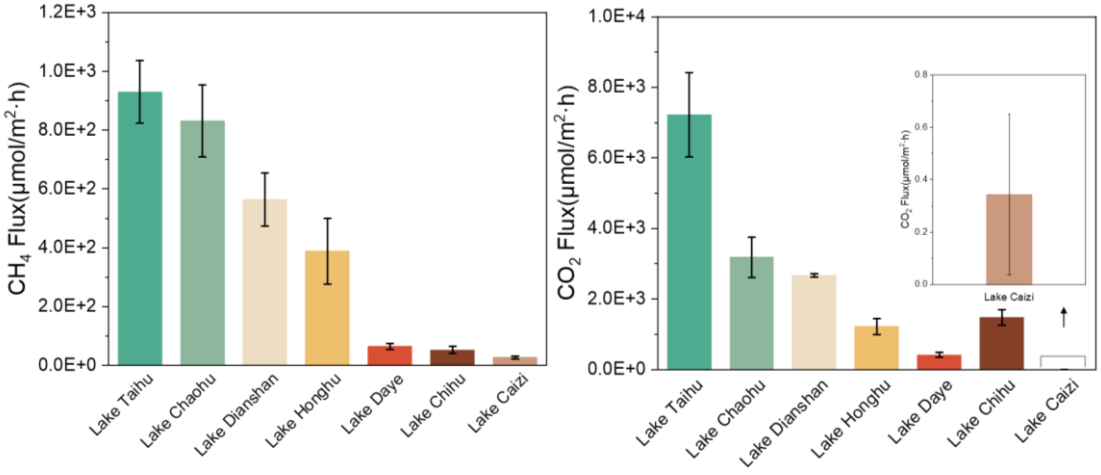

Fig. 5.5. The CH_4 (left) and CO_2 (right) flux in the investigated lakes along the Yangtze River.

5.3.3 Dissolved CH_4 and CO_2 in the pore-water of lakes

At a spatial scale, the dissolved CH_4 and CO_2 concentrations in pore-water from various lake sediments exhibited significant variation (Fig. 5.7a, b). Lake Taihu stood out as having particularly high concentrations of dissolved CH_4 and CO_2 in its pore-water. Specifically, the bottom sediment in the lake contained 2.2±0.3 μmol/L of dissolved CH_4 and 160.1±18.7 μmol/L of dissolved CO_2. Furthermore, the concentrations of dissolved CH_4 and CO_2 in the pore-water differed significantly at various depths in the sediment, gradually decreasing from the bottom to the surface. This decrease showed a strong negative correlation with depth (Fig. 5.7c). In lakes with hyper-eutrophic conditions, a slight increase in the dissolved CO_2 concentrations in the pore-water of surface sediments (-4–0 cm depth) was observed. For instance, at a depth

of -4 cm in Lake Dianshan, the concentration of dissolved CO_2 measured 88.1±16.7 μmol/L, while at the surface sediment, it registered at 96±16.8 μmol/L. Additionally, the TOC concentration in the sediment played a pivotal role in the production of CH_4 and CO_2. There existed a positive correlation between the TOC concentration and the concentration of dissolved CH_4 and CO_2 in the pore-water (Fig. 5.7d).

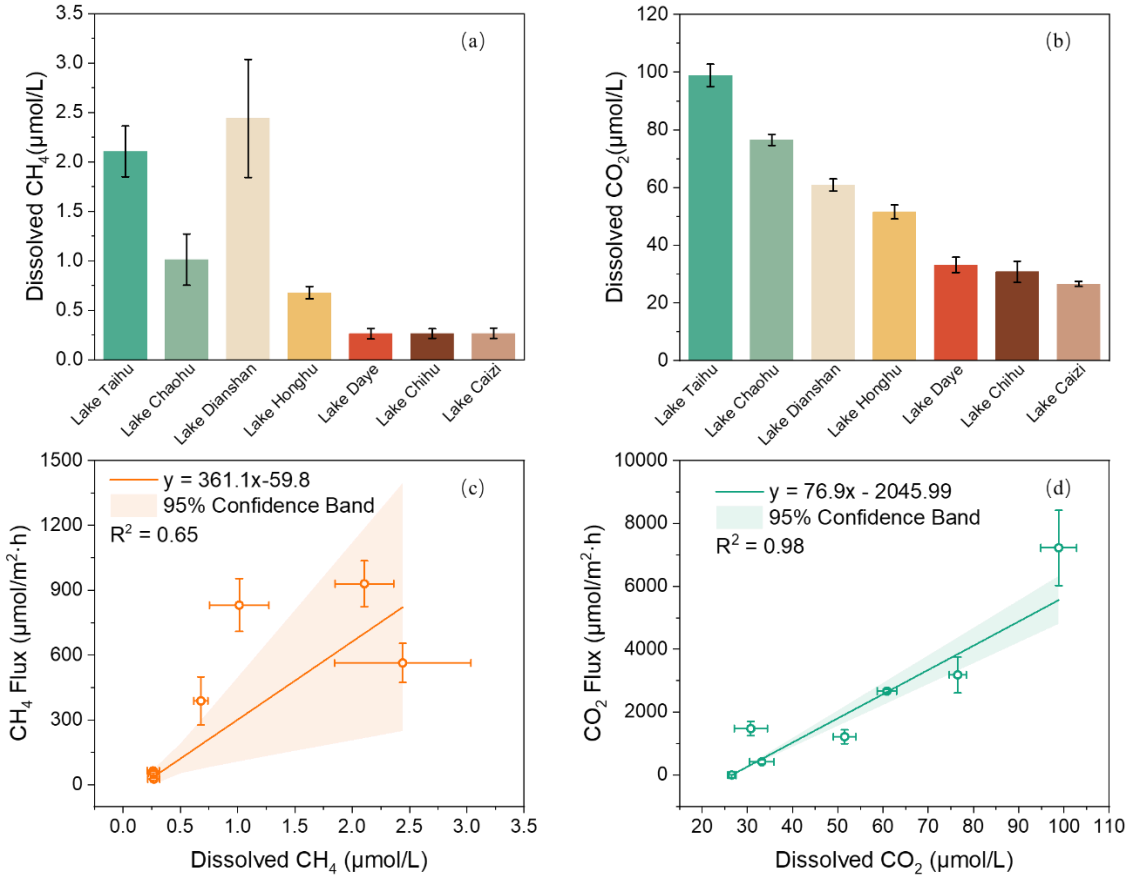

Fig. 5.6. The dissolved CH_4 (a) and CO_2 (b) flux in the investigated lakes along the Yangtze River, and the correlation between CH_4 flux and dissolved CH_4 (c), CO_2 flux and dissolved CO_2 (d), respectively.

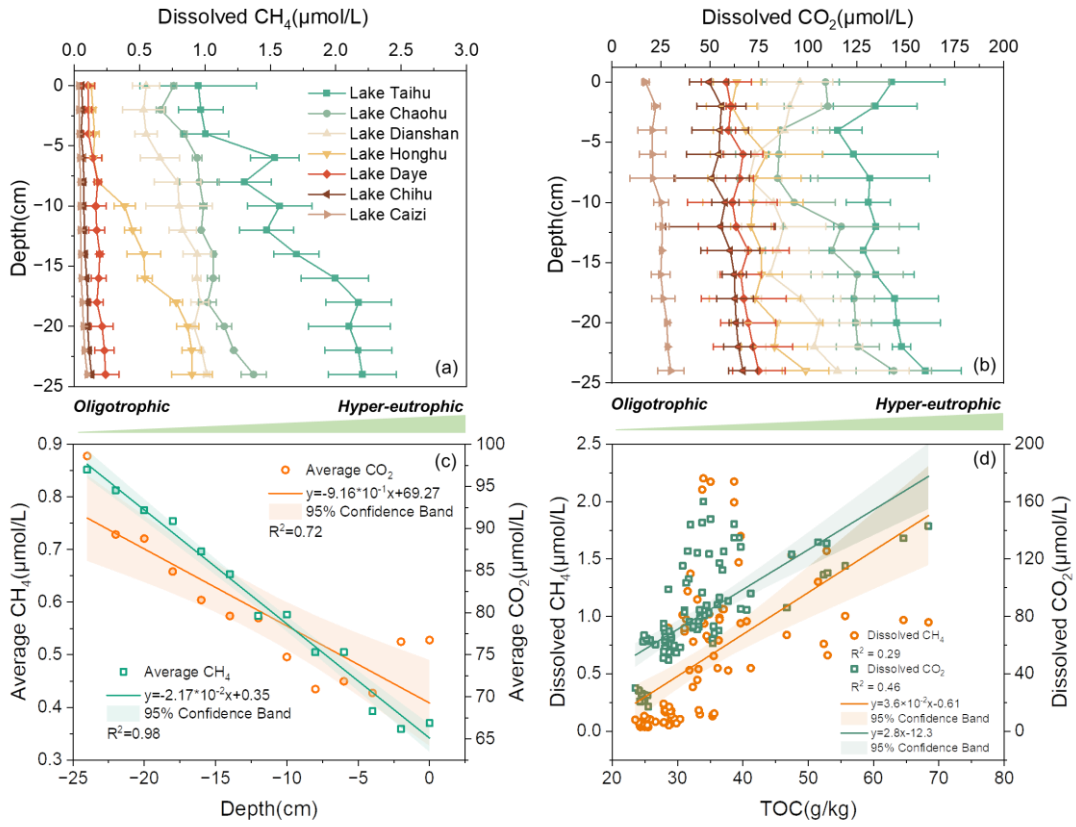

Fig. 5.7. The dissolved CH_4 (a) and CO_2 (b) concentrations in sediment at different depths, correlation analysis between depth and the dissolved CH_4, CO_2 in sediment (c), correlation analysis between Total Organic Carbon (TOC) and the dissolved CH_4, and CO_2 in sediment (d) of the investigated lakes along the Yangtze River.

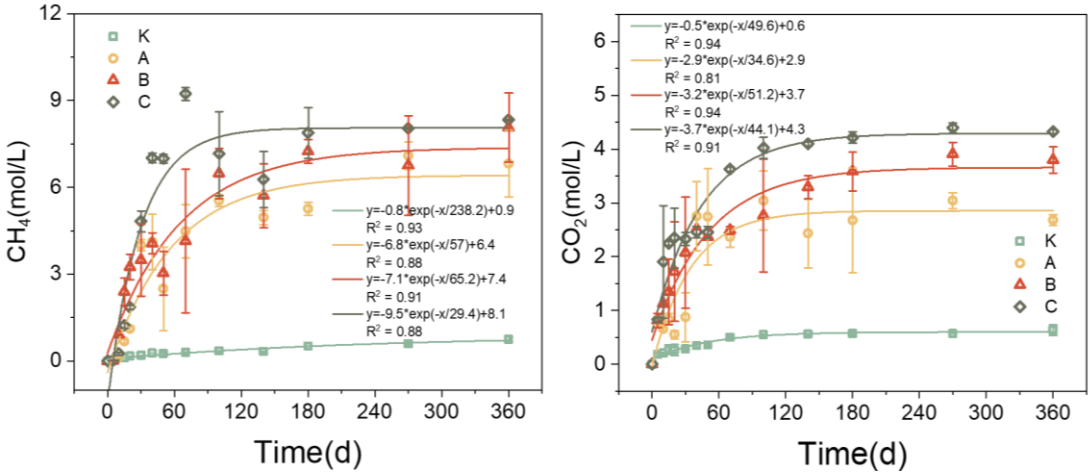

Fig. 5.8. Dynamics of cumulative CH_4 (left) and CO_2 (right) emissions in the microcosms during incubation under different cyanobacteria biomass.

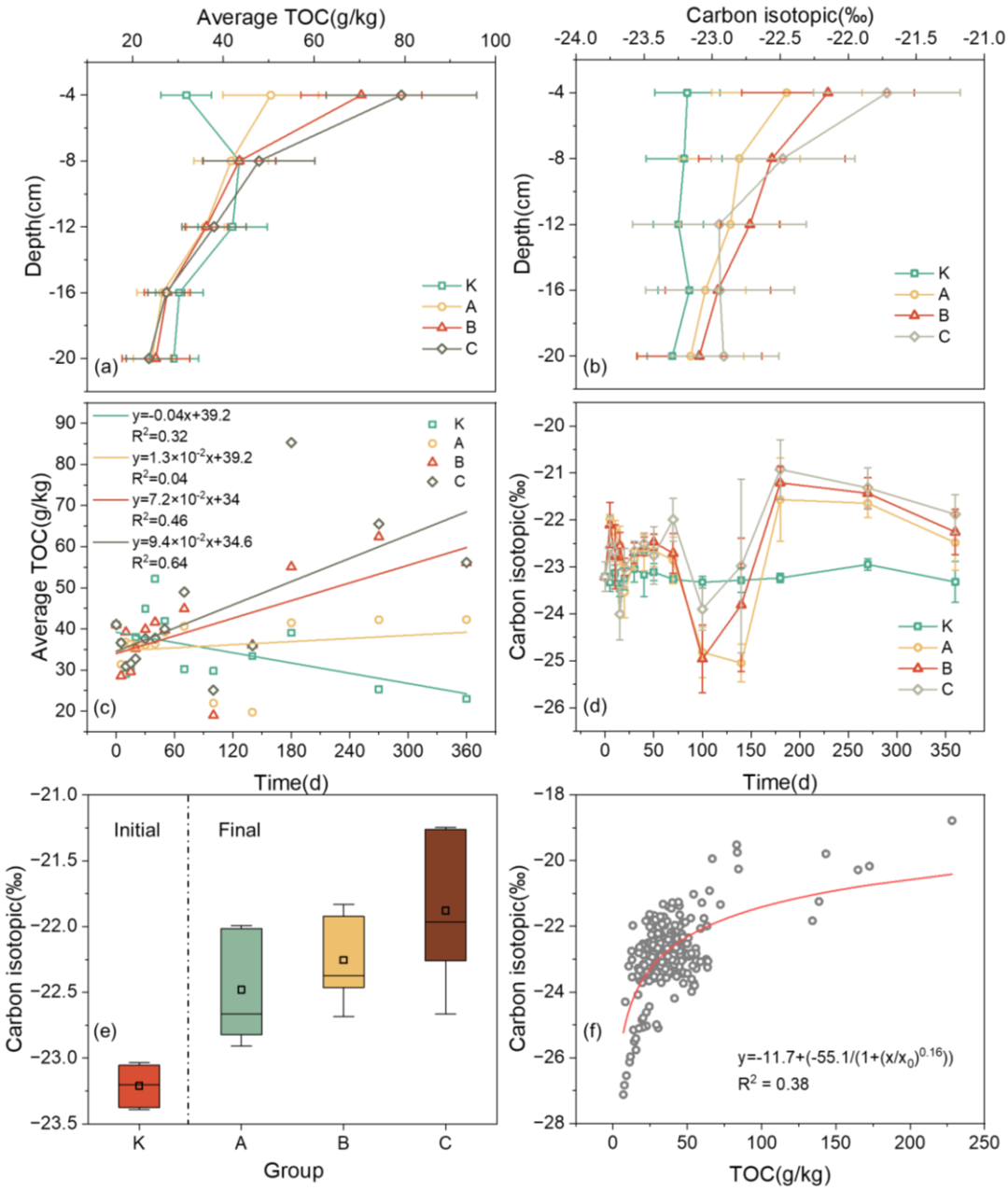

Fig. 5.9. Dynamics of average TOC concentration and average $\delta^{13}C$ values in different depths of sediment at temporal scale (a, b), average TOC concentration and average $\delta^{13}C$ values in sediment at temporal scale (c, d), initial and final $\delta^{13}C$ values in sediment (e), and correlation analysis between $\delta^{13}C$ values and TOC (f), during the incubation under different cyanobacteria biomass in microcosms of each group, respectively.

5.3.4 Cumulative CH_4 and CO_2 emissions in microcosms

During the decomposition of cyanobacteria, the cumulative concentrations of CH_4 and CO_2 in the microcosm system showed a continuous increase, eventually reaching a plateau (Fig. 5.8). In the initial 100 days of the experiment, there was a rapid increase in CH_4 and CO_2 concentrations, with group C showing the highest increase. At 100 days, the concentrations of CH_4 reached 7.2±1.5 mol/L, while the concentration of CO_2 reached 4.1±0.2 mol/L. The cumulative CH_4 and CO_2 concentrations were found to be correlated with the initial cyanobacteria biomass. Specifically, the experimental group with a higher initial accumulation of cyanobacteria exhibited a greater release of CH_4 and CO_2.

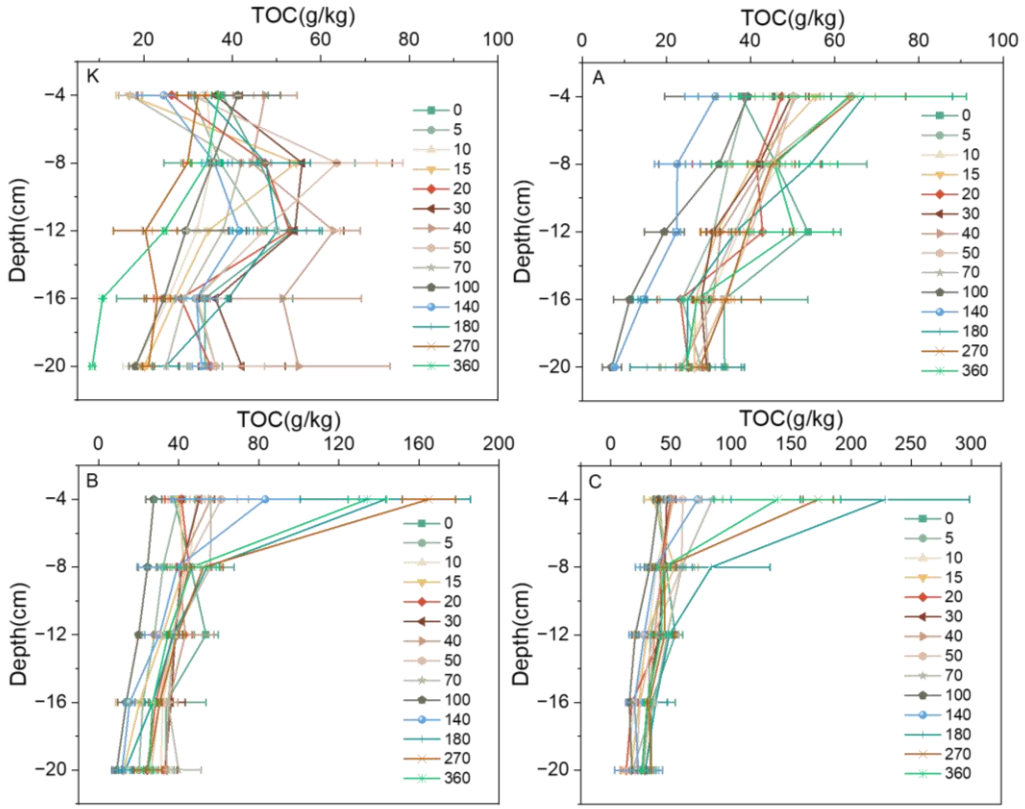

Fig. 5.10. Dynamics of TOC concentration in different depths of sediment during the incubation under different cyanobacteria biomass in microcosms, respectively.

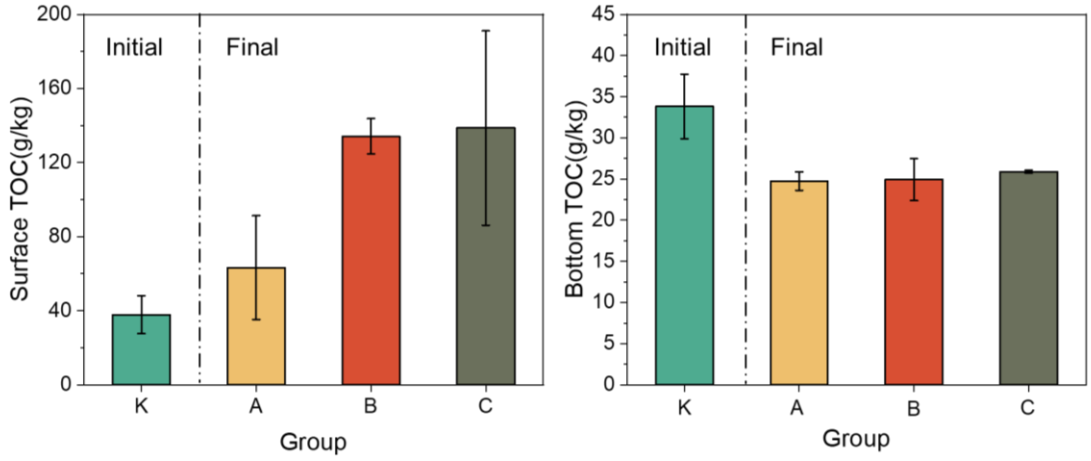

Fig. 5.11. Dynamics of initial and final TOC concentration in surface (left) and bottom (right) sediment during the incubation under different cyanobacteria biomass in microcosms, respectively.

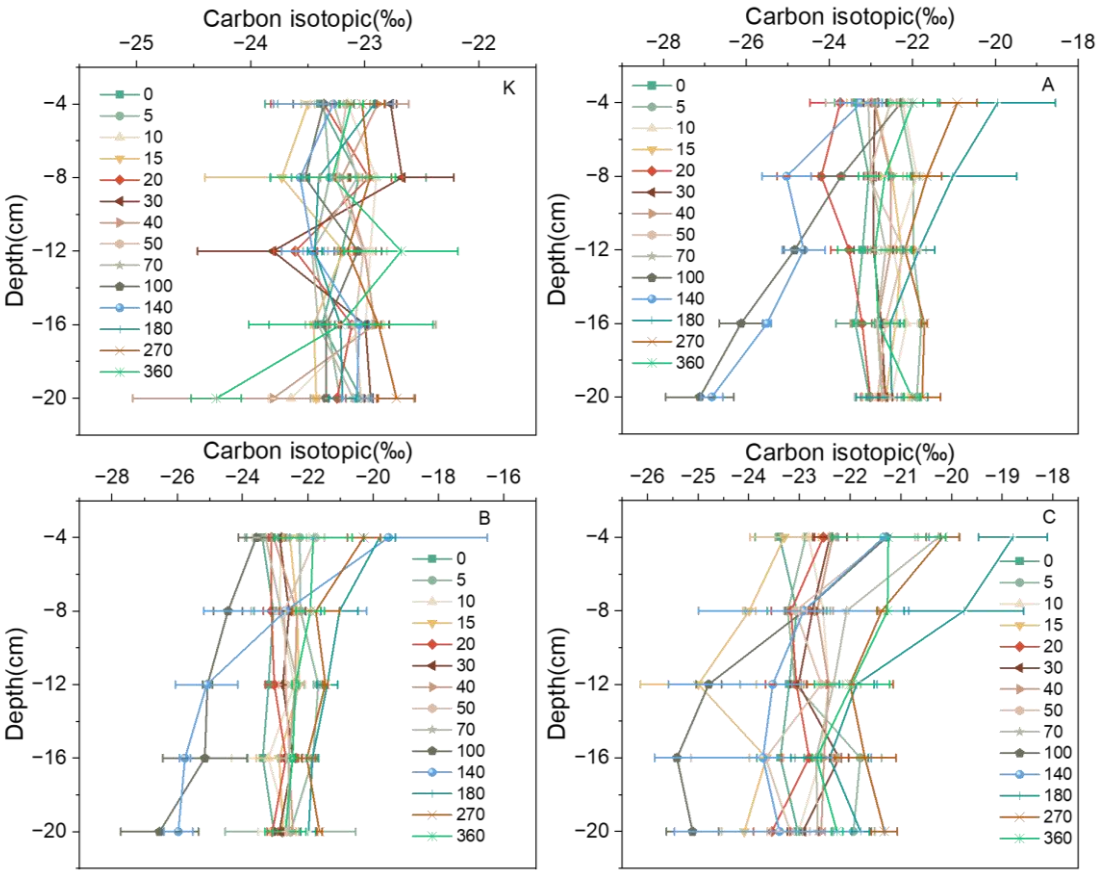

Fig. 5.12. Dynamics of $\delta^{13}C$ values in different depths of pore-water sediment during the incubation under different cyanobacteria biomass in microcosms, respectively.

5.3.5 TOC and $\delta^{13}C$ concentrations in sediments in microcosms

With the gradual decomposition of cyanobacteria, there was a concomitant increase in sediment TOC concentration. However, there were discernible differences among the experimental groups, indicating substantial variations in TOC concentration (Figs. 5.9, 5.10 and 5.11). The concentration of TOC in sediments showed a positive correlation with the magnitude of cyanobacteria accumulation, suggesting that a higher biomass of cyanobacteria led to an elevated TOC concentration in the sediment. On the 360th day, Group C displayed the highest concentration of sediment averaging 56.2±14 g/kg. Throughout the incubation period, the average TOC concentration in sediments decreased from the initial 41.1±12.3 to 22.9±1 g/kg in Group K without cyanobacteria. The concentration of TOC in surface sediments exhibited a notable increase. In Group C, the surface sediment exhibited an average TOC concentration of 79.3±16.6 g/kg, whereas the bottom layer displayed a notably lower concentration of 23.6±5 g/kg.

Cyanobacteria decomposition led to a notable increase in $\delta^{13}C$ in the sediment, indicating the incorporation of cyanobacteria-derived carbon into the sediment (Figs. 5.9 and 5.12). In the group characterized by cyanobacteria accumulation, there was a noticeable increase in the $\delta^{13}C$ value, demonstrating a positive correlation with the cyanobacteria biomass. On the 360th day, the average value of $\delta^{13}C$ in the sediment of Groups K, A, B, and C were -23.32±0.59 ‰, -22.48±0.44‰, -22.25±0.36‰, and -21.88±0.62‰, respectively. From 70d to 140d of incubation, there was a substantial decrease in the $\delta^{13}C$ value, reaching its lowest value in Group A at -25.05‰. The average $\delta^{13}C$ value showed a pronounced decrease as the sediment depth increased, as indicated by the TOC concentration in the sediment.

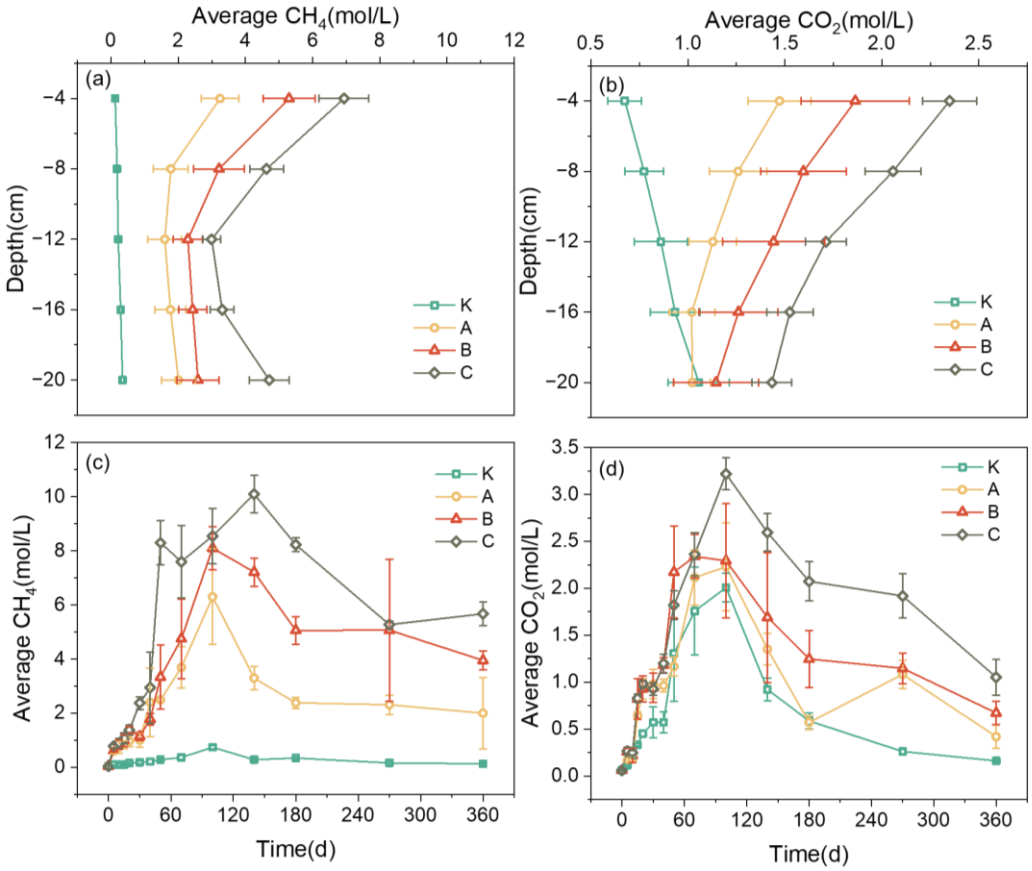

Fig. 5.13. Dynamics of average CH_4 and CO_2 concentration in different depths of sediment pore-water (a, b), average CH_4 and CO_2 concentration in sediment pore-water during the incubation at temporal scale (c, d) during the incubation under different cyanobacteria biomass in microcosms, respectively.

5.3.6 Dissolved CH_4 and CO_2 in the pore-water of microcosms

The dissolved CH_4 and CO_2 concentrations in pore-water exhibited a substantial increase during cyanobacteria decomposition, showing a positive correlation with the carbon derived from cyanobacteria (Figs. 5.13, 5.14, 5.15, and 5.16). However, the distribution pattern of dissolved CH_4 concentration in the sediment pore-water within the microcosm system differed from field investigations. In the microcosm system, higher concentrations of dissolved CH_4 were observed at the surface and bottom layers, while lower concentrations were found in the middle layer. In Group C, the average dissolved CH_4 concentration in the pore-water of surface sediment was 6.93±0.74 mol/L, whereas in the pore-water of bottom sediment it was 4.71±0.59 mol/L. The dissolved CH_4 concentration in the pore-water initially increased and reached a peak at 100 days of incubation. Group C displayed the highest dissolved CH_4 concentration,

peaking at 8.55±1.01 mol/L when it reached equilibrium.

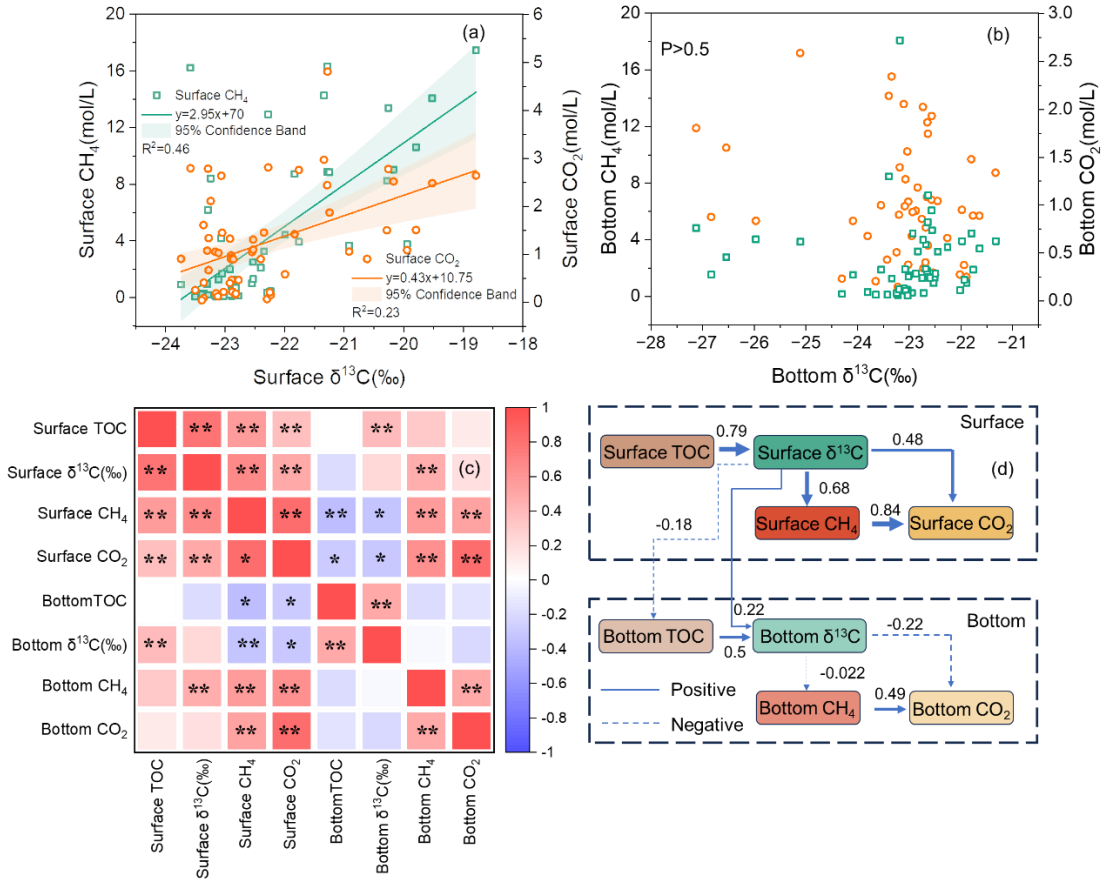

Fig. 5.14. Correlation analysis of dissolved CH_4 and CO_2 concentrations in sediments with surface $\delta^{13}C$ (a, b), correlation analysis of factors affecting dissolved CH_4 and CO_2 in surface and bottom sediment (c), and contribution of cyanobacteria-derived carbon on dissolved CH_4 and CO_2 in surface and bottom sediment (d).

The cyanobacteria decomposition also resulted in a peak in the dissolved CO_2 concentration in pore-water at 100 days. The average dissolved CO_2 concentration in the pore-water of sediment for each group was 2.01±0.15, 2.23±0.47, 2.29±0.61, and 3.22±0.17 mol/L, respectively. Subsequently, the dissolved CO_2 concentration gradually decreased and eventually stabilized at a certain concentration. The pattern of dissolved CO_2 concentration in the pore-water of sediment within the microcosm system was in contrast to field observations, as the concentration decreased gradually with increasing sediment depth. The CO_2 concentration in the pore-water of surface sediment in each group ranged from 0.68±0.09 to 2.35±0.14 mol/L, with higher concentrations corresponding to higher accumulation of cyanobacteria.

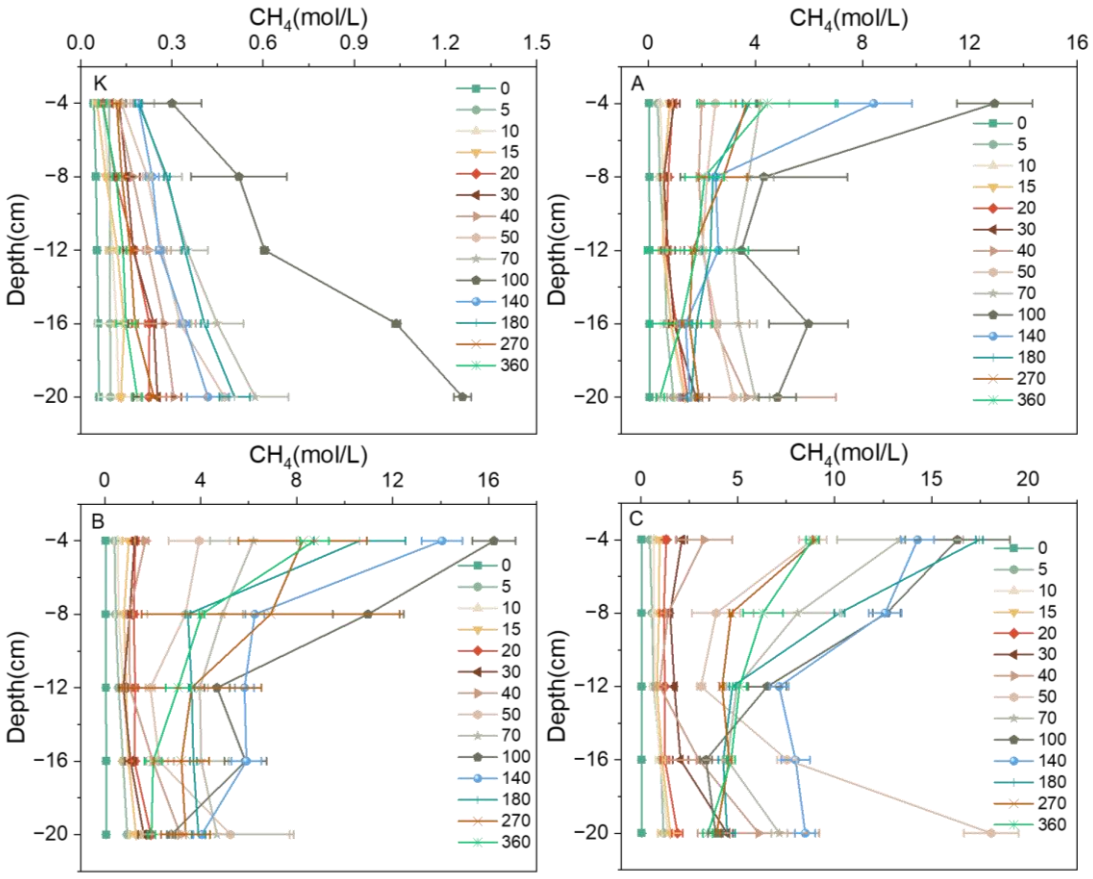

Fig. 5.15. Dynamics of CH_4 concentration in different depths of pore-water sediment during the incubation under different cyanobacteria biomass in microcosms.

5.3.7 Microbial communities in sediments of microcosms

The cyanobacteria decomposition caused changes in the structure of the microbial community in the sediment, resulting in a greater variety of species within these communities (Fig. 5.17). The composition of microbial communities in surface sediments differed markedly from those in bottom sediments.

In surface sediments, the accumulation of cyanobacteria led to a higher abundance of *Halobacterota* in the sediment, accounting for 32.3%, 24.1%, and 57.5% of the microbial composition in Groups A, B, and C, respectively. In the group without cyanobacteria accumulation, there were no significant changes observed in the microbial community structure within the sediment. The predominant microorganism remained *Proteobacteria*, initially, representing 24.1% and increasing to 28.5% in Group K.

In bottom sediments, *Proteobacteria* was the dominant species; however, the

proliferation of cyanobacteria resulted in a decrease in its abundance. The final abundance figures for *Proteobacteria* were 29.3%, 22.3%, 19.5%, and 19.7% of the microbial composition in Groups A, B, and C, respectively. Similar to surface sediments, no significant changes were observed in the microbial community structure within the bottom sediment in Group K.

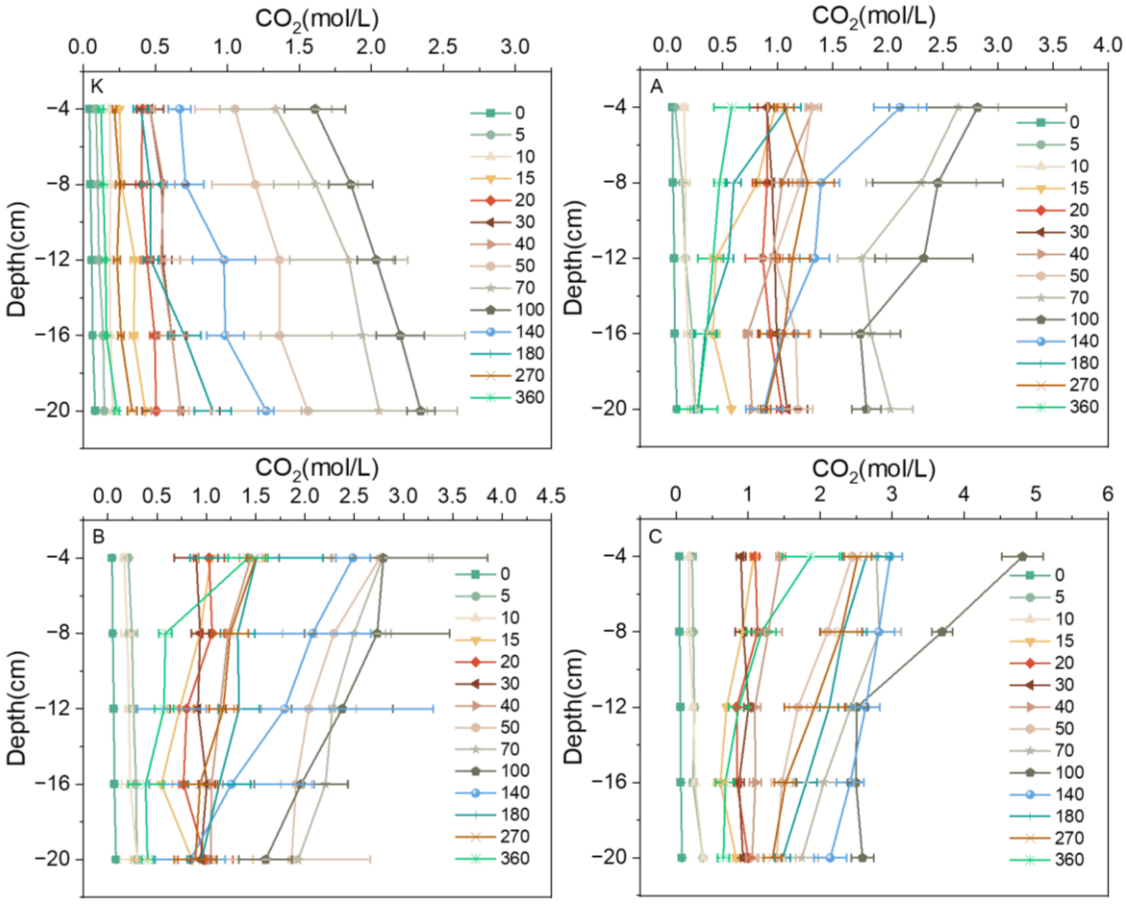

Fig. 5.16. Dynamics of CO_2 concentration in different depths of pore-water sediment during the incubation under different cyanobacteria biomass in microcosms.

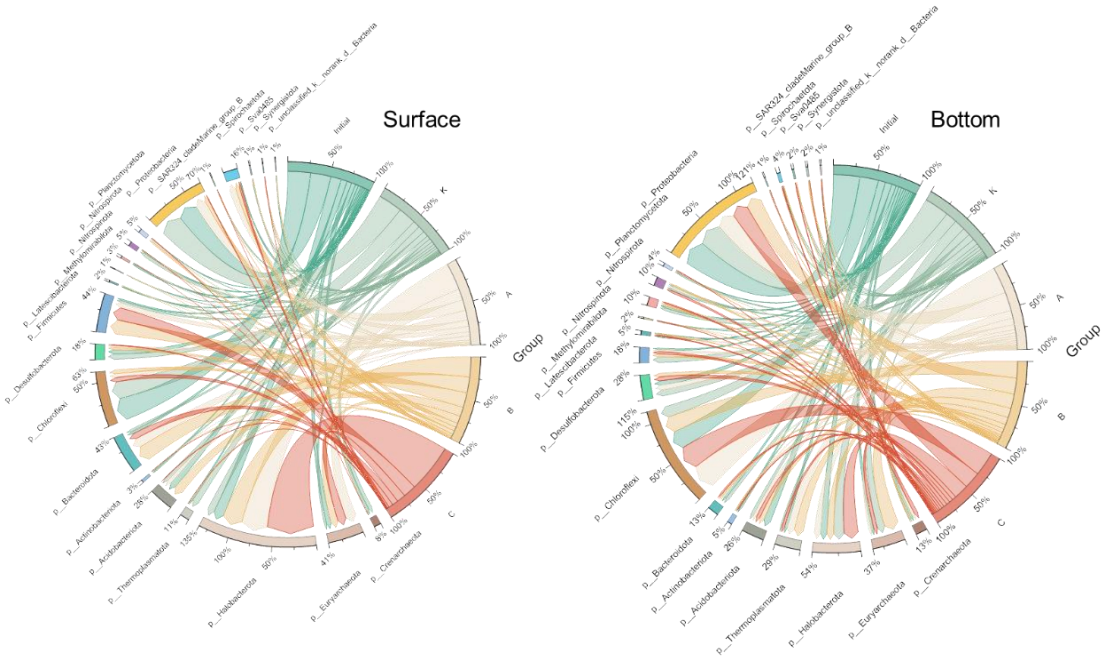

Fig. 5.17. The initial and finial community structures of microbial in the surface (left) and bottom (right) sediment under different cyanobacteria biomass in microcosms.

5.4 Discussion

5.4.1 Status of carbon emissions in lakes

Lakes, as significant natural sources of carbon emissions, release an estimated 117-212 Tg/y of CH_4 and 60-840 Tg/y of CO_2 into the atmosphere (Rosentreter et al., 2021; Raymond et al., 2014). As vital components of freshwater ecosystems, lakes play a crucial role in counterbalancing continental carbon sinks through CH_4 emissions, accelerating climate change and altering aquatic environments (Bastviken et al., 2011; Soued et al., 2022). The increasing eutrophication of lakes is believed to be a potential factor contributing to this phenomenon (Beaulieu et al., 2019; Zhou et al., 2022b). Currently, several studies have established bidirectional positive feedback loops between the escalation of lake eutrophication and the amplification of climate warming (Yan et al., 2017; Zhou et al., 2022a). Climate warming leads to higher temperatures, which in turn boosts the growth rates of cyanobacterial blooms by enhancing water body stability and prolonging thermal stratification duration (Ho et al., 2019). As cyanobacteria proliferation, their massive accumulation and subsequent decomposition accelerate CH_4 emissions by fostering an anaerobic reducing environment and enhancing the organic carbon mineralization process (Zhou et al., 2024). The average

emissions of CH_4 and CO_2 from the hyper-eutrophic lakes examined in this study were 774.8 and 4357.3 μmol/m^2·h, respectively, significantly higher than the 47.7 and 30.8 μmol/m^2·h in mesotrophic lakes (Figs. 5.4 and 5.5). Elevated eutrophication levels in lakes also result in increased concentrations of dissolved CH_4 and CO_2, indicating that various sources of organic carbons contribute to more intense organic carbon mineralization processes in eutrophic lakes (Zhou et al., 2023b). Our findings verify a rise in dissolved CH_4 and CO_2 concentrations in surface waters, particularly in lakes experiencing severe eutrophication, with average dissolved concentrations of 1.85 and 78.7 μmol/L, respectively (Figs. 5.4 and 5.6).

Current comprehensive research has confirmed the significant role of carbon derived from cyanobacteria, accelerating the release of carbon emissions and likely to strengthen further in the future (Torres et al., 2011; Zhou et al., 2023a). Studies on the positive effects of cyanobacteria-derived carbon on CH_4 and CO_2 have focused on increasing the supply of organic matter, creating an anaerobic environment, and promoting more active microbial activity (Paerl et al., 2013). However, with the continuous input of cyanobacteria-derived carbon in sediments (Zhou et al., 2023b), the influence of changes in sediment carbon pool structure and the physical and chemical environment on the mechanism of CH_4 and CO_2 production from organic carbon mineralization remains unexplored. Crucially, while methane oxidation in shallow lakes is typically vigorous, recent observations reveal an unexpected high in CH_4 emissions from these environments, which was consistent with the results of this study (Figs. 5.4 and 5.5). Consequently, it is imperative to thoroughly evaluate the impact of escalating eutrophication on the mechanisms of CH_4 and CO_2 production and emission during the organic carbon mineralization process.

5.4.2 Potential factors influencing carbon emissions in eutrophic lakes

In freshwater lakes, the transfer of CH_4 and CO_2 from sediments to the atmosphere is a complex process involving generation in sediments, release to overlying water, and eventual emission to the atmosphere (Zhou et al., 2023b). The presence of organic carbon in lake sediment's carbon pool is crucial in determining the rate and intensity of CH_4 and CO_2 production during organic matter mineralization (Wik et al., 2016; Peter et al., 2017). This study revealed a positive linear correlation between CH_4 (R^2 = 0.29) and CO_2 (R^2 = 0.46) concentrations in field sediments and the organic carbon content

in sediments (Fig. 5.7). Sediment bottoms are well-known as hotspots for CH_4 and CO_2 production, especially CH_4, due to the combination of anaerobic conditions, stable temperature and pH, and limited CH_4 oxidation (Einzmann et al., 2022). In-situ experiments in this study demonstrated that CH_4 and CO_2 concentrations in sediments increase with depth, particularly in lakes with low nutrient levels (Fig. 5.7). As CH_4 moves upward, significant losses occur due to oxygen-induced oxidation processes, which are crucial for managing carbon emissions from lakes effectively (Holgerson et al., 2016). The release of CH_4 and CO_2 from sediments into overlying water elevates dissolved concentrations of these gases, playing a vital role in regulating GHGs emissions (Holgerson et al., 2016). This study noted high CH_4 and CO_2 concentrations in overlying water, positively correlated with increased fluxes of CH_4 ($R^2 = 0.65$) and CO_2 ($R^2 = 0.98$) from water to the atmosphere (Figs. 5.4, 5.5, 5.6 and 5.8).

The escalation of eutrophication is leading to a notable rise in carbon emissions from lakes, largely due to higher levels of organic carbon stemming from cyanobacteria (Shi et al., 2017; Bartosiewicz et al., 2021). The continuous input of cyanobacteria-derived carbon disrupts the sediment carbon pool, leading to higher concentrations of TOC in the sediment (Figs. 5.9, and 5.10). This study found that the elevated TOC levels in the sediment spurred the production and release of both CH_4 and CO_2 (Figs. 5.7, 5.13, and 5.14). Increased organic carbon levels boost the activity of anaerobic microorganisms, which are key players in CH_4 and CO_2 production in sediments, promoting the anaerobic breakdown of organic carbon (Deng et al., 2019). It is proposed that the microbial co-metabolism of the sediment carbon pool, triggered by cyanobacterial organic carbon input, results in higher sediment carbon emissions (Deng et al., 2022). This process is driven by the fact that cyanobacteria-derived organic carbon alters the composition of the sediment carbon pool (Ma et al., 2022), mainly comprising unstable and easily decomposable carbon compounds with high primary productivity (Steffenhagen et al., 2012). As a result, metabolic processes and microbial activities in the sediment carbon pool become more active (Figs. 5.17 and 5.18). The presence of dissolved organic carbon is crucial in the transport of cyanobacteria-derived carbon into sediment, influencing the carbon dynamics within the sediment (Duan et al., 2022).

It has been reported that cyanobacteria outbreaks and their subsequent accumulation not only elevate organic carbon levels in freshwater lakes but also affect

the sediment carbon pool, which is essential for CH_4 and CO_2 production (Braeckman et al., 2019). This impact includes the formation of cyanobacterial detritus mats and alterations in the physicochemical environment (Woszcayk et al., 2017). While surface cyanobacterial detritus mats have been found in the sediments of eutrophic lakes (Qi et al., 2020), more research is necessary to fully comprehend their influence on the CH_4 and CO_2 production, particularly in specific areas where CH_4 and CO_2 are generated.

Table. 5.1. The sampling conditions of each lake along the Yangtze River basin

Lake	pH	DO (mg/L)	Temperature (℃)	*TLI*	Sediment type
Lake Taihu	7.81	0.55	27.9	83	Organic
Lake Chaohu	8.25	2.92	28.2	72.9	Organic
Lake Dianshan	8.93	3.17	31.7	71.1	Organic
Lake Honghu	8.27	1.97	31.3	53.4	Organic
Lake Daye	9.04	2.59	31.8	38.7	Organic
Lake Chihu	8.49	1.89	32.4	31.2	Organic
Lake Caizi	8.14	2.61	30.3	30.3	Organic

5.4.3 Effects of cyanobacteria-derived carbon on hotspots for CH_4 and CO_2

Eutrophication-induced cyanobacterial blooms have a significant impact on carbon emissions and the methanogenic zones in sediment. This results in the fromation of hotspots for CH_4 and CO_2 production, driven by the higher concentration of organic carbon in surface sediments and the creation of an anaerobic reducing environment (Figs. 5.7, 5.13, 5.14, and 5.18). The formation of cyanobacterial detritus mats, composed of cyanobacteria-derived carbon on sediment surfaces, plays a key role in this process (Yang et al., 2021). Using isotopic tracers, this study illustrated that the accumulation of cyanobacteria residues on sediment surfaces led to a marked rise in organic carbon concentrations (Figs. 5.9, 5.10 and 5.12). The cyanobacteria-derived organic carbon primarily enters the sediment carbon pool through gravitational sedimentation (Xu et al., 2015). The continuous influx and migration of cyanobacterial carbon into the sediment substantially raised the abundance of ^{13}C in the bottom sediment, accompanied by a significant increase in organic carbon concentration (Figs. 5.9, 5.10 and 5.12). Despite the rising concentration of organic carbon in bottom sediments, the levels and isotopic abundance of organic carbon in surface sediments remain notably higher, due to the considerable accumulation of surface cyanobacteria

residues. With sediment depth increases, there was a noticeable decrease in both the concentration and isotopic abundance of organic carbon (Figs. 5.9, 5.10, 5.11, and 5.12).

The sediment is the primary site for CH_4 and CO_2 production, as evidenced by multiple field studies. These gases decrease as they move upwards from the sediment bottom (Einzmann et al., 2022). CH_4 and CO_2 production in sediment necessitates an anaerobic setting, with their production being impeded by the micro-aerobic conditions present at the water-sediment interface (Lyautey et al., 2021). Notably, CH_4 undergoes oxidation in the presence of oxygen, and prior studies suggest that lake methane oxidation could potentially mitigate the greenhouse effect by up to 30% (Pimenov et al., 2014). However, our study challenges this concept, particularly in scenarios marked by substantial cyanobacteria accumulation (Fig. 5.18). Our findings demonstrate a significant link between CH_4 and CO_2 levels, and the quantities and isotopic compositions of organic carbon across various sediment depths. Surface sediments exhibited significantly higher CH_4 and CO_2 concentrations compared to bottom sediments (Figs. 5.9~5.16). The rich organic carbon content in cyanobacterial detritus mats acts as a plentiful carbon source (Figs. 5.13, 5.14 and 5.17), facilitating organic carbon metabolism and notably boosting CH_4 and CO_2 production in surface sediment (Figs. 5.9, 5.10, and 5.12). Concurrently, the decomposition of cyanobacterial detritus mats leads to low pH, and dissolved oxygen levels, establishing a distinctly anaerobic reducing environment at the water-sediment interface (Martinez-Cruz et al., 2018; Qi et al., 2020). Within this environment, anaerobic microorganisms flourish and partake in metabolic processes involving organic carbon (Figs. 5.17 and 5.18). Additionally, the anaerobic conditions further impede the oxidation process of CH_4, resulting in heightened CH_4 emissions (Steinsdottir et al., 2022).

Cyanobacterial detritus mats may enhance a more prominent co-metabolic effect in the surface layer of sediment, potentially leading to the upward movement of methanogenic hotspots within sediments (Figs. 5.9~5.14). Recently, the co-metabolic effect triggered by cyanobacterial carbon has been identified as a potential mechanism to increase lake carbon emissions. The breakdown of resistant organic carbon is a key component of this process (Liu et al., 2020; Deng et al., 2023). Shallow lakes tend to accumulate substantial amounts of plant debris in their surface sediments, primarily composed of resistant organic carbon, which can lead to a higher co-metabolic intensity (Deng et al., 2019). Co-metabolism involves the utilization of resistant organic carbon

in sediments, facilitating the transition of the lake carbon pool from a source to a sink (Ma et al., 2020; Deng et al., 2023). This study revealed a surprising decrease in organic carbon concentration in the bottom sediments of the experimental group supplemented with cyanobacteria, as opposed to the control group without cyanobacteria, demonstrating a co-metabolic effect (Fig. 5.11). Moreover, a rapid reduction in $\delta^{13}C$ abundance in sediment was observed alongside with peak CH_4 and CO_2 concentrations, potentially indicating the presence of a co-metabolic effect (Figs. 5.8, 5.9, and 5.13). The higher carbon content in algal sediments emerged as a key factor leading to elevated concentrations of CH_4 and CO_2 in the surface sediment layer, exceeding those found in deeper sediment layers (West et al., 2012). Additionally, this study observed that cyanobacteria decomposition significantly increased sediment water content, especially in surface sediments. Microcosms containing cyanobacteria had noticeably higher water content compared to those without (Fig. 5.19). The release of extracellular polysaccharides and mucus by cyanobacteria, followed by subsequent degradation processes, significantly contributed to the rise in sediment water content (Xu et al., 2018). This increase in water content hinders oxygen diffusion, fostering anaerobic bacterial growth and organic carbon mineralization, ultimately boosting CH_4 and CO_2 production in the sediment (Lu et al., 2021). Therefore, eutrophication-induced cyanobacteria significantly contribute to the upward movement of CH_4 and CO_2 production hotspots in sediments, enhancing the efficiency of carbon gas emissions. These insights contribute to more accurate assessments of lake carbon emissions and provide a theoretical foundation for lake management.

5.5 Summary

Eutrophication-driven cyanobacterial blooms significantly impact the CH_4 and CO_2 emission capacity of sediments by causing the migration of production hotspots. Field investigations in hypereutrophic lakes showed an unusual rise in CH_4 and CO_2 concentrations in the surface pore-water layer, which was confirmed by microcosm experiments. Cyanobacteria-derived carbon accumulates on the sediment surface, altering its physical and chemical properties and increasing water content. This influx of organic carbon boosts microbial activity, especially in surface sediments, leading to increased CH_4 and CO_2 production. The cyanobacterial residues create an environment with high organic carbon, anaerobic conditions, and elevated water content, enhancing

organic carbon mineralization. The migration of CH_4 and CO_2 hotspots towards the surface sediment reduces the travel path for carbon emissions. Additionally, the cyanobacterial deposits on the sediment surface hinder methane oxidation and may trigger microbial co-metabolism in the surface sediment, resulting in a significant increase in carbon emissions in the lake. These findings provide valuable insights into the assessment of the impact of cyanobacterial blooms on carbon emissions of the sedimentary carbon pool.

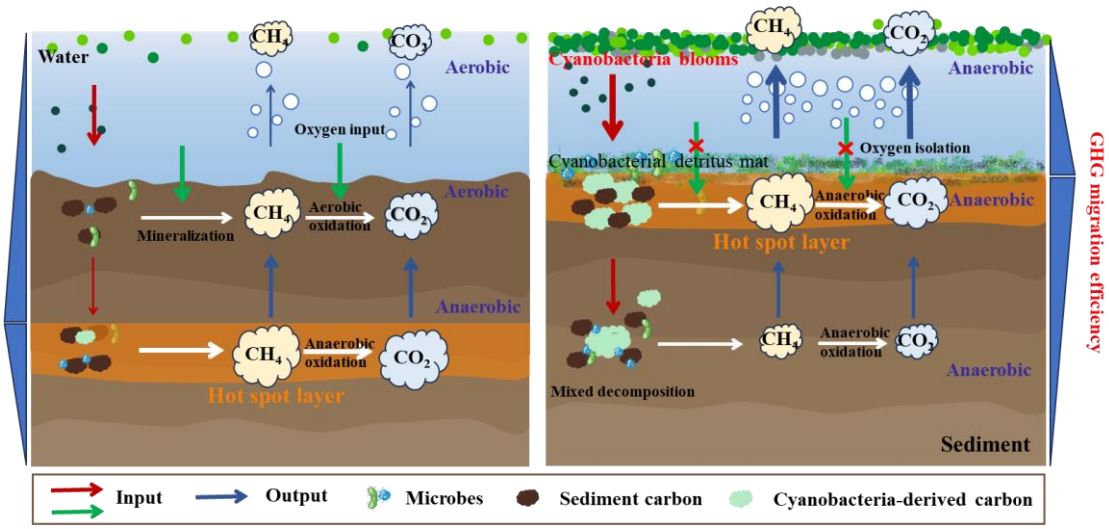

Fig. 5.18. A conceptual diagram of the mechanism of cyanobacteria decay changes the hot spots of carbon dioxide and methane production along vertical sediment profiles in eutrophic lakes.

6. Unexpected increase of sulfate concentrations and potential impact on GHG emissions in freshwater lakes

6.1 Background

During the last few decades, the sulfate (SO_4^{2-}) concentration in freshwater basins around the world has increased due to anthropologic activities (Baldwin et al., 2012). This increase is particularly significant in eutrophic lakes (Yu et al., 2013). Sulfur (S) in lakes primarily comes from various sources, such as the weathering of sulfur-bearing rocks, the oxidation of organic sulfur from terrestrial sources within the basin, the deposition of atmospheric SO_4^{2-} and SO_2 as acid rain, and the discharge of sulfur-containing wastewater (Ekholma et al., 2020). The rise in SO_4^{2-} concentration leads to an intensified occurrence of sulfate reduction, regarded as a critical metabolic pathway coupling to anaerobic organic compound degradation (Holmer et al., 2001). In lakes with low SO_4^{2-} concentrations, CH_4 production is generally the most important process in carbon mineralization (Holmer et al., 2001). Nevertheless, as SO_4^{2-} concentration continues to rise within the lake (Yu et al., 2013), its impact on both the sulfur and carbon cycles remains largely uncertain.

Currently, freshwater lakes also confront environmental issues, *e.g.*, eutrophication (Michalak et al., 2013). Lake Taihu as a representative eutrophic lake on a global scale an annual average CH_4 flux of 2106.3 $mmol \cdot m^{-2} \cdot yr^{-1}$, which is significantly higher than the average in Chinese lakes (531.5 $mmol \cdot m^{-2} \cdot yr^{-1}$) (Yang et al., 2011). Cyanobacterial blooms, a common phenomenon in eutrophic lakes, have been recognized as major contributors to CH_4 emissions (Paerl et al., 2012; Yan et al., 2017). Lakes experiencing cyanobacterial blooms emit considerably more CH_4 compared to those without blooms (Zhou et al., 2023). The blooms create an anaerobic environment by depleting dissolved oxygen (DO), which promotes the growth of anaerobic microorganisms (Shen et al., 2013). The decomposition of cyanobacteria releases substantial nutrients that serve as a substrate for the proliferation of anaerobic microorganisms (Yan et al., 2017). Additionally, the organic matter derived from cyanobacteria alters the microbial community structure, and influences CH_4 production and emissions (Handley et al., 2013; Shen et al., 2013; He et al., 2019). Hydrogenotrophic and acetoclastic methanogenesis are the primary pathways for CH_4

production in freshwater lakes. It has been observed that the severe cyanobacteria accumulation can trigger the emergence of the methylotrophic methane production pathway (Zhou et al., 2022a). Consequently, fluctuations in nutrient levels in lakes, which impact the availability of substrates and the overall physical and chemical environments, introduce uncertainties in predicting CH_4 emissions (Zhou et al., 2023).

Within marine ecosystems, sulfate reduction processes play a significant role in regulating CH_4 emissions. Anaerobic CH_4 oxidation is driven by sulfate reduction, which also competes with methanogenesis for available sources of organic carbon (Bowles et al., 2014). It is estimated that approximately 29% to 50% of organic carbon mineralization in marine sediments occurs through sulfate reduction, resulting in a reduction in CH_4 production (Zhou et al., 2022b). Consequently, sulfate reduction exerts a pivotal factor to mitigate CH_4 emissions (Zeng et al., 2019). In oceanic waters, SO_4^{2-} concentration is as high as 28 mM (Fike et al., 2015), while generally less than 800 μM in freshwater lakes, approximately 2~3 orders of magnitude lower than that in marine ecosystems. Therefore, the potential inhibitory effect of sulfate reduction on CH_4 emissions in freshwater lakes is often overlooked (Hausmann et al., 2016). As a sulfate concentration increases in eutrophic lakes (Yu et al., 2013), its influence on CH_4-producing processes may exceed previous estimations (Pester et al., 2012). In natural systems, the sulfate reduction processes are primarily facilitated by sulfate-reducing bacteria (SRB) (Zhou et al., 2022b). These bacteria engage in anaerobic respiration using SO_4^{2-} as an electron acceptor and utilize short-chain fatty acids like acetic and formic acid, along with other low molecular weight organic compounds and H_2 (Holmer et al., 2001). In lake sediments, SRB and methane-producing archaea (MPA) compete for fermentation resources, as they both have a preference for hydrogen and acetate. However, SRB have a higher affinity for these substrates compared to MPA (Li et al., 1996). Under oligotrophic conditions, the capacity of MPA to utilize these substrates is limited, ultimately retarding CH_4 production (Zhou et al., 2022b).

Due to low SO_4^{2-} concentrations typically observed in freshwater lakes, the abundance and activity of SRB are generally limited. As a result, this competitive interaction between SRB and MPA is often overlooked (Pester et al., 2012). However, progression of an increase in SO_4^{2-} concentrations in freshwater lakes accelerates the rate of sulfate reduction, leading to higher abundance and activity of SRB. This gives SRB a competitive advantage over MPA (Chen et al., 2016). Therefore, it is crucial to

investigate the effects of rising SO_4^{2-} concentrations on methane production in freshwater lakes.

This study aims to investigate the effect of increasing sulfate concentration on CH_4 emission and elucidate the underlying mechanisms. The SO_4^{2-} concentrations were measured in the overlying water of 9 lakes along the Yangtze River basin. Specifically, the data of SO_4^{2-} concentrations in the water column from the typical eutrophic Lake Taihu were collected over the past decades and onsite sampling was also implemented monthly for one year. To analyze the factors driving CH_4 emissions in eutrophic lakes, a random forest model was applied. Additionally, based on the observed SO_4^{2-} levels and the projected increase in Lake Taihu, a series of experiments were conducted using SO_4^{2-} addition microcosms at various concentrations (0, 30, 60, 90, 120, 150, and 180 mg/L). These experiments aimed to reveal the impact of increasing SO_4^{2-} concentrations in the overlying water on CH_4 production and emissions in eutrophic lakes, as well as to explore the underlying mechanisms. The findings from this study will contribute to the accurate assessment of CH_4 emission fluxes in eutrophic lakes.

6.2 Materials and methods

6.2.1 Study site and sample collection in the field

Under the dual influence of climate change and human activities, eutrophication has become the main ecological problem faced by lakes along the Yangtze River basin (Fig. 6.1). In this study, 9 lakes along the Yangtze River basin were selected and the in-situ investigation was conducted in July 2021. Lake Taihu, the third largest freshwater lake in China, is part of the Yangtze River basin. It has an average depth of 1.9 m and covers an area of 2340 m^2 (Qin et al., 2007; Mao et al., 2021). Over the past 70 years, SO_4^{2-} concentration in Lake Taihu has increased from 30 to 100 mg/L (Figs. 6.2a and 6.3). Rapid urbanization and industrialization discharged sulfur-containing pollutants as wastewater, entering the lake ecosystem along with surface runoff and atmospheric deposition (Yu et al., 2013).

This study collected the overlying water from 9 lakes along the Yangtze River basin, followed by filtrating the samples via 0.45 μm Nylon filters to determine the trophic index level (*TLI*) status and SO_4^{2-} concentrations. Two specific sites within the northwestern region of Lake Taihu were selected in consideration of cyanobacterial

bloom accumulation densities. The cyanobacteria accumulation area was located in Zhushan Bay (31°25’10’’N, 120°0’40’’E). The open area of the lake was located away from the reed zone (31°24’40’’N, 120°1’3’’E). Sampling was conducted at these two sites over a period of one year, from May 2020 to April 2021. Overlying water samples were collected every month, and sediment samples were collected four times in June, September, and December 2020 and March 2021.

Sediment cores were collected using a gravity core sampler, sealed at the upper and lower sides, and sectioned into 2 cm intervals, resulting in a total of 14 layers. Overlying water was collected 30 cm below the surface at the two areas. The incubator was used to store samples, and transported to the laboratory immediately. The sediment was then centrifuged at 1500 rpm using a CT15RT versatile refrigerated centrifuge (China) to obtain sediment pore-water.

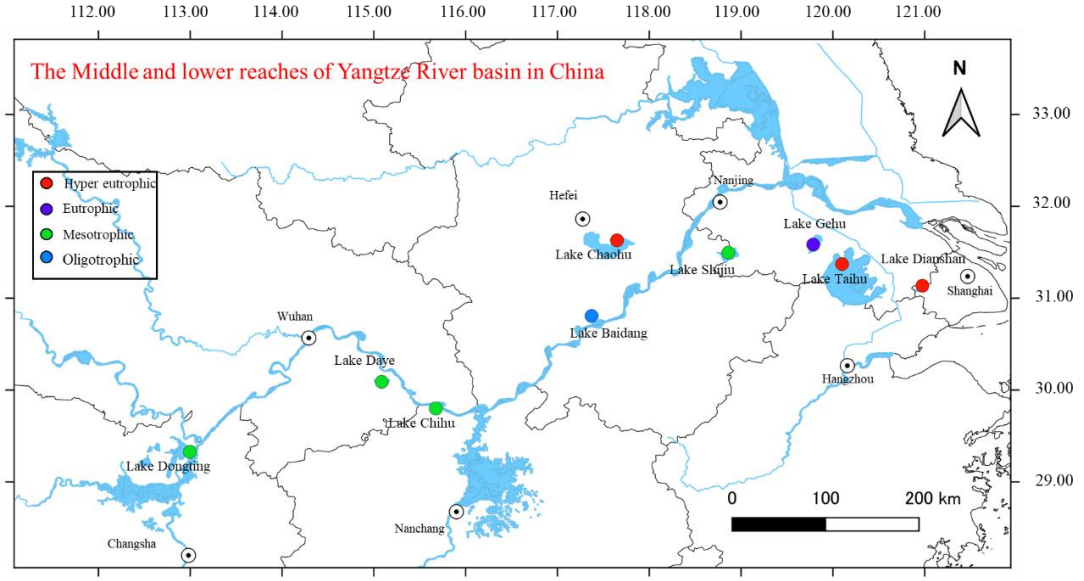

Fig. 6.1. Distribution of sampling site in the middle and lower reaches of the Yangtze River basin, China.

To construct the microcosm systems, the sediments and cyanobacteria samples were collected from eutrophic Lake Taihu in July 2020. Sediments were collected using a Peterson mud picker, while the fine mesh plankton (250 meshes) was used to collected and concentrated the cyanobacterial bloom scum. The scum was subsequently preserved in an incubator with ice packs and promptly transported to the laboratory. Sediment samples were meticulously mixed, homogenized, and sifted through a 100-mesh sieve into a polyethylene bag. The high-purity water and Na_2SO_4 were used to set up different gradient SO_4^{2-} concentration. The cyanobacteria samples

were rinsed and centrifuge at 1500 rpm for 5 minutes using CT15RT multi-function refrigerated centrifuge (China), then freeze-dried using biosafety-10a freeze-dryer.

6.2.2 Set up of microcosms

The microcosm systems were comprised of a total of 714 anaerobic bottles for seven treatments (Φ 75mm, length 180mm, and volume 500 mL), with each treatment including three replicates. To synchronize the release of organic matter from cyanobacteria decomposition with the sulfate reduction reaction, each anaerobic bottle contained sediment (100 g), water (200 mL), and cyanobacteria powder (0.11 g). These proportions were based on surface sediment composition, water depth, and a cyanobacteria accumulation density 2500 g/m^2 in Lake Taihu (Zhang et al., 2021). The concentrations of SO_4^{2-} in the seven microcosm systems were calibrated to follow the historical trend observed in Lake Taihu over the years, as depicted in Fig. 1a. To avoid interference from background SO_4^{2-} levels in the lake water, ultra-pure water was used to configure experimental water with initial SO_4^{2-} concentrations of 30, 60, 90, 120, 150, and 180 mg/L, with an additional control group devoid of SO_4^{2-}. All anaerobic bottles were carefully arranged within a controlled biochemical incubator, maintained at a precise temperature of 25 ℃ with darkness condition. Nitrogen purging was performed to minimize interference from atmosphere. A portion of the sediment was used for microbial determination and stored in a refrigerator at -80 ℃. Another portion of the sediment was flushed and centrifuged at 5000 rpm for 5 min using a CT15RT versatile refrigerated centrifuge (China) to obtain interstitial water. The remaining sediment and other samples were kept at 0-4 ℃ for less than 24 hours before analysis.

6.2.3 Chemical analytical methods

The concentrations of various parameters were measured using different methods. The calibrated probes (MP525, China) were used to determine the pH, DO, and oxidation-reduction potential (ORP) of overlying water. The UV-vis spectrophotometer (UV-6100, ma pada, China) was used to determine the concentration of total nitrogen (TN) (Raveh and Avnimelech et al., 1979). Total phosphorus (TP) concentration was assessed via colorimetric analysis following digestion with $K_2S_2O_8$ and NaOH (Ebina et al., 1983). Soil samples designated for total organic carbon (TOC) analysis were acidified to achieve a pH below 2.0 and subsequently examined utilizing a multi-N/C

analyzer (HT 1300, Analytik Jena, Germany). Water samples for dissolved total organic carbon (DOC) were analyzed with a multi-N/C analyzer (3100, Analytik Jena, Germany). All samples from the water column and pore water were subjected to filtration through 0.45 μm nylon filters prior to the quantification of SO_4^{2-} and $\sum S^{2-}$ concentrations. The concentrations of SO_4^{2-} and $\sum S^{2-}$ were detected using the turbidimetric method (Tabatabai et al., 1974), and methylene blue method, respectively (Cline et al., 1969). Acid volatile sulfate (AVS) was determined using the zinc cold diffusion method (Hsieh et al., 1997). The CH_4 and CO_2 concentration was determined using a gas chromatograph (Agilent,7890B, Germany).

6.2.4 Biological analysis

To elucidate variations in sedimentary MPA and SRB, cell copy numbers of MPA and SRB in the sediments were determined using real time quantitative PCR (qPCR) technology at both 0 and 38 days. The ultra-low temperature freezer was used to store the sediment sample at -80 ℃ promptly. Subsequently, total genomic DNA from each soil sample was extracted employing the E.Z.N.A. ®Soil DNA Kit (Omega Bio-Tek, Norcross, GA, USA), adhering closely to the manufacturer's protocol. Nucleic acid integrity and concentration were evaluated by 1% agarose gel electrophoresis and NanoDrop 2000 ultraviolet spectrophotometer (Thermo Scientific, USA), respectively.

The quantification of MPA and SRB in the sediments was conducted utilizing the quantitative polymerase chain reaction (qPCR) methodology. For MPA, the qPCR assay utilized primer sets targeting 1106f (5'-TTWAGT CAG GCAACG AGC-3') and 1378r (5'-TGT GCAAGG AGC AGG GAC-3'). For SRB, the qPCR assay utilized primer sets targeting DSR1F+ (5'-ACSCACTGGAAGCACGGCGG-3') and DSR-R (5'-GTGGMRCCG TGCAKRTTGG-3'). The ABI7300 qPCR instrument (Applied Biosystems, USA) was used to perform qPCR experiments, and the ChamQ SYBR Color qPCR Master Mix was used as a signal dye. The total volume of each reaction mixture was 20 μL, which comprised 2 μL of template DNA and 16.5 μL of ChamQ SYBR Color qPCR Master Mix. Standard plasmids containing target functional genes were continuously diluted 10 times to construct a standard curve for each gene. All agreements adhere strictly to the MIQE guidelines.

For the assessment of microbial community composition and diversity, the V3-V4 hypervariable regions of bacterial 16S rRNA genes were amplified using the universal

primers MLfF (5'-GGTGGTGTMGGATTCACACARTAYGCWAC AGC-3') and MLrR (5'-TTCATTGCRTAGTTWGGRTAGTT-3') as described by Zhou et al. (2022a). Subsequent to amplification, MiSeq sequencing was conducted on an Illumina MiSeq sequencer (Illumina, USA) via the Majorbio Cloud Platform (www.majorbio.com). Operational taxonomic units (OTUs) were clustered at a 97% similarity cutoff utilizing UCHIME (version 7.0.1090, http://www.drive5.com/uparse/), which also facilitated the identification and removal of chimeric sequences.

6.2.5 Model analysis and statistical analysis

The potential drivers (TN, TP, DOC, COD, pH, DO, SS, T, water level, and SO_4^{2-}) of CH_4 emission in Lake Taihu were obtained from "the National Earth System Science Data Center" (http://lake.geodata.cn/data/dataresource.html). Previous CH_4 emissions from Lake Taihu (2011.08 – 2015.03) were studied by Xiao et al., 2017. The random forest model was used to analyze these data and identify correlations in the R language environment. The steps involved importing data, splitting it into training and test sets, training and testing the model, evaluating its feasibility, and ultimately fitting and exporting the data. The data statistical analysis was performed with Origin 2023 and Social Sciences 18.0 (SPSS 18.0). Bivariate correlation analysis and one-way analysis of variance (ANOVA) were conducted.

6.3 Results

6.3.1 Spatial and temporal distribution of SO_4^{2-} concentrations in water and sediment

Over the past 70 years, there has been a significant increase in SO_4^{2-} concentrations in Lake Taihu, rising from 30 mg/L to over 100 mg/L. This upward trend is expected to continue in the future (Fig. 6.2a). The increase in concentrations does not seem to be directly influenced by seasonal variations, as there was a sharp fluctuation of 67.4 mg/L between the highest and lowest concentrations in 2021, compared to only 38.5 mg/L in the 2000s (Fig. 6.2b).

Both cyanobacterial bloom and DO concentrations demonstrated noticeable seasonal fluctuations, but the change of high and low concentration of two indexes with contrasting trends (Fig. 6.4). Severe cyanobacterial blooms were prevalent during the

summer, coinciding with reduced DO concentrations. On a spatial scale, the SO_4^{2-} concentration in the overlying water exhibited significant variations across the surveyed lakes along the Yangtze River basin (Fig. 6.2c). Notably, the hyper-eutrophic Lake Taihu and the oligotrophic Lake Baidang showcased the highest and lowest SO_4^{2-} concentrations at 90.3 mg/L and 12.8 mg/L, respectively, exhibiting the substantial difference in SO_4^{2-} concentration. The SO_4^{2-} concentration exhibited a positive correlation with the trophic state of the lakes (R^2 = 0.52), demonstrating an increase in line with eutrophication intensification (Fig. 6.2d).

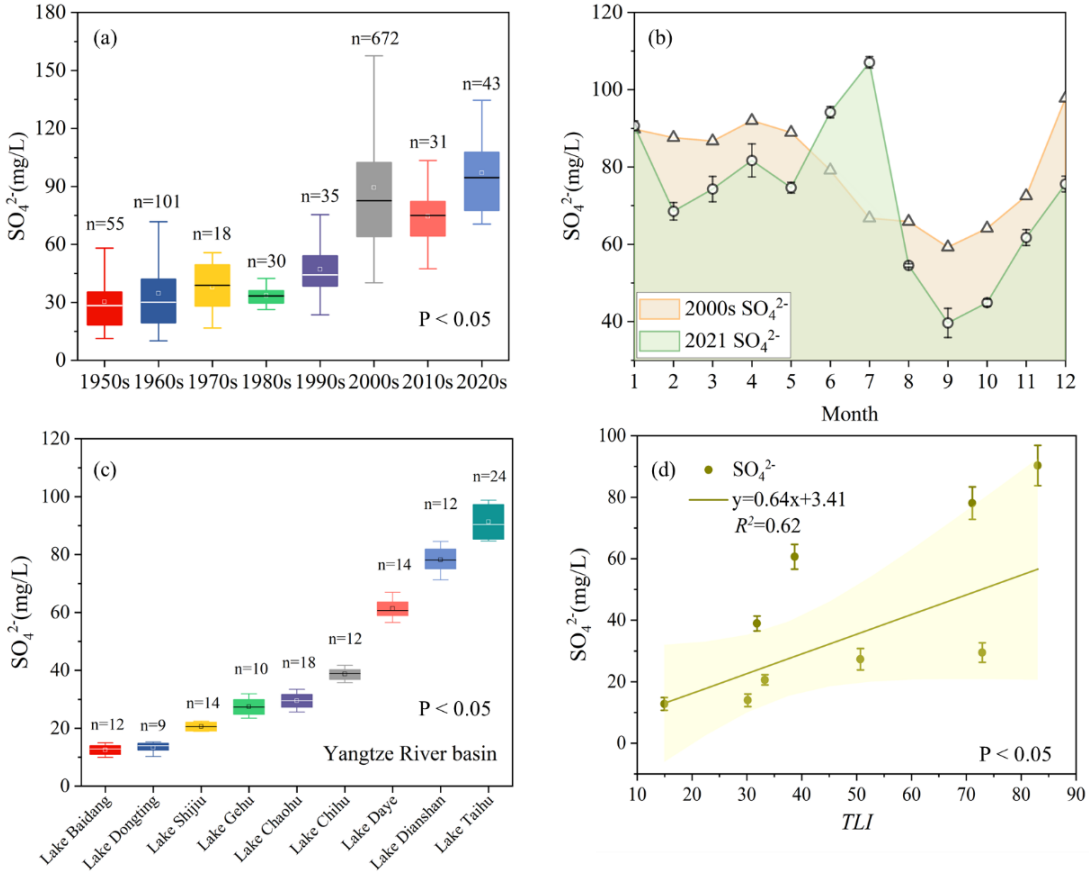

Fig. 6.2. The distribution of SO_4^{2-} concentration in the long-term trend (1950s-2020s) (a), the monthly trend of SO_4^{2-} concentration in Lake Taihu (b), and the lakes with different trophic levels along the Yangtze River basin (c, d).

6.3.2 Quarterly monitoring of SO_4^{2-} in sediment pore-water

The SO_4^{2-} concentration in the sediment pore-water displayed notable distinctions between the cyanobacteria accumulation area and the open lake area in Lake Taihu (Fig. 6.5). Except for March, the SO_4^{2-} concentration in the sediment pore-water in the cyanobacteria accumulation area consistently exceeded that of the open lake area. In

June, a pronounced difference in SO_4^{2-} concentration within the sediment pore-water was observed between the cyanobacteria accumulation and open lake area, especially at a sediment depth of 0-2 cm. This discrepancy reached a maximum value of 38.9 mg/L. The SO_4^{2-} concentration in sediment pore-water exhibited a decreasing trend as the sediment depth increased. It is worth noting that in the months of March and December, there were significant decreases in SO_4^{2-} concentration, with a sharp decrease observed at depths of 12-16 cm and 10-12 cm, respectively.

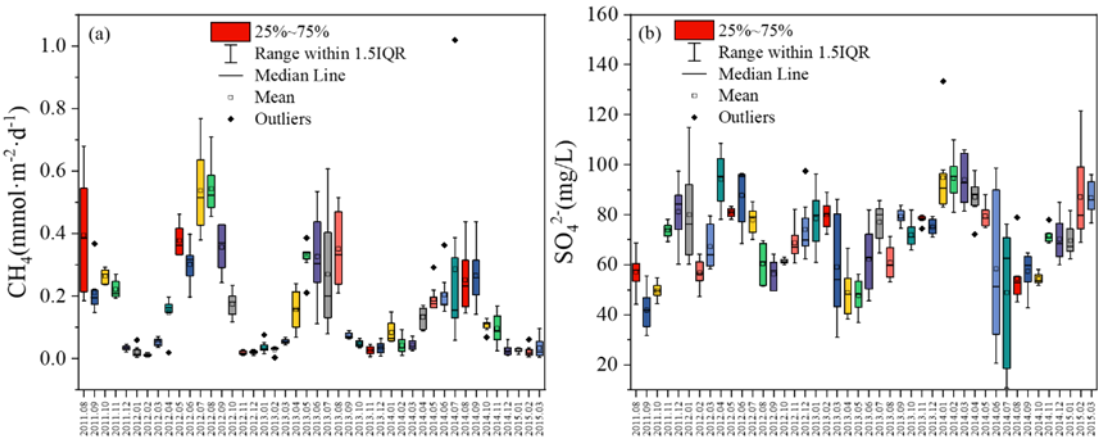

Fig. 6.3. Dynamic changes of CH_4 emissions (a) and SO_4^{2-} concentrations (b) in Lake Taihu from 2011.08 to 2015.03. (The data of CH_4 emissions were from Xiao et al., 2017, and the data of SO_4^{2-} concentrations were from National Earth System Science Data Center in China.)

6.3.3 Dynamic changes of CH_4 emissions and SO_4^{2-} concentrations

The CH_4 emission and SO_4^{2-} concentration in Lake Taihu showed significant seasonal variations from 2011 to 2015 (Figs. 6.3 and 6.6). The CH_4 emission occurred in summer, surpassing levels in other seasons. The highest recorded CH_4 emission flux was 0.54 mmol· m^{-2}·d^{-1} in the summer of 2012. In contrast, the SO_4^{2-} concentration consistently increased from 2011 to 2015, reaching a maximum recorded concentration of 100 mg/L. Interestingly, both the SO_4^{2-} concentration and CH_4 emission flux decreased in summer. A random forest model was used to analyze the factors influencing CH_4 emission. The predicted CH_4 emission flux exhibited a strong correlation (R^2 = 0.81) with the actual values, indicating a high level of consistency (Fig. 6.6). Both DO and SO_4^{2-} concentration exhibited a negative correlation with CH_4 emission flux, with their influence scores being only smaller than temperature.

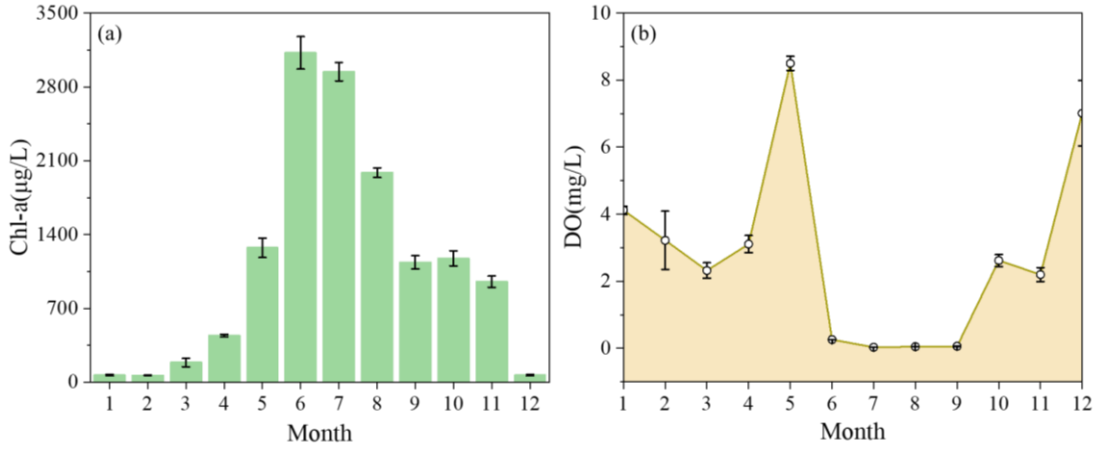

Fig. 6.4. The dynamics of Chl-a (a), and DO (b) concentrations in the overlying water of Lake Taihu.

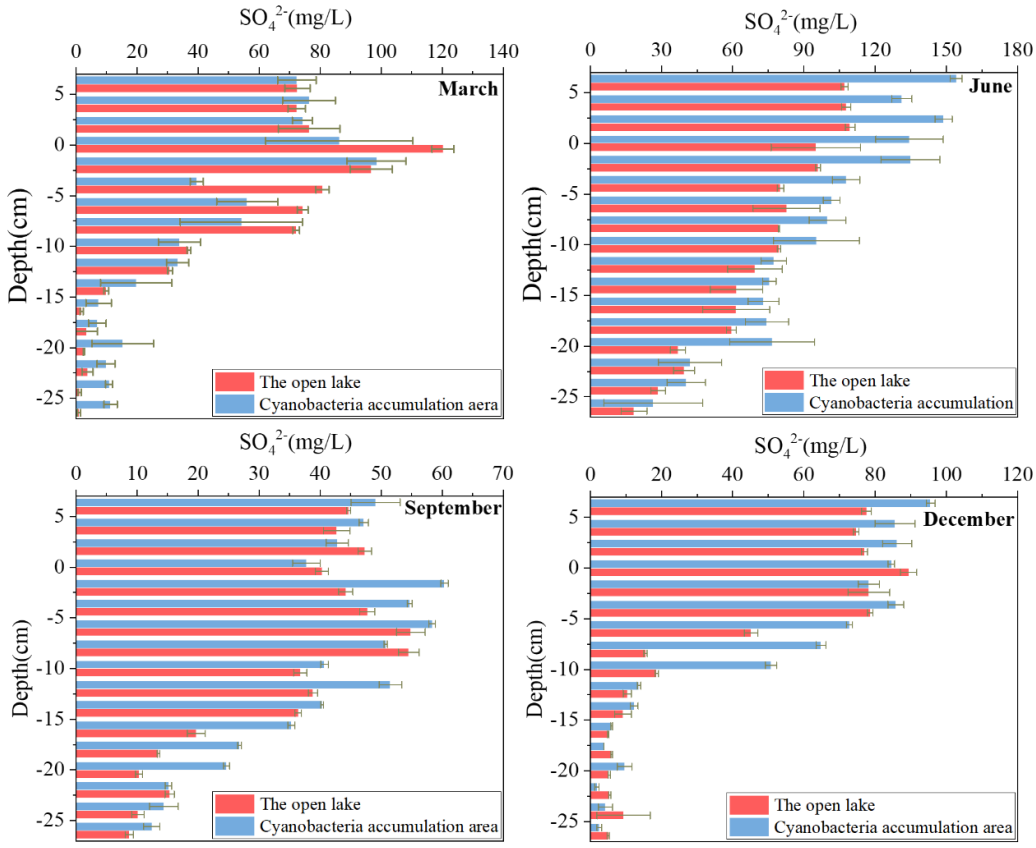

Fig. 6.5. Seasonal variations of SO_4^{2-} concentrations from 2020 to 2021 in sediment pore-water in cyanobacteria accumulation area and the open lake.

6.3.4 Dynamics of sulfur compound in water and sediment pore-water of microcosms

The microcosms displayed a pronounced reduction in sulfate during the early

incubation period, leading to a more rapid decline in SO_4^{2-} concentration in the sediment pore-water compared to the overlying water (Figs. 6.7, 6.5 and 6.8). In all the microcosms, the SO_4^{2-} concentration in the overlying water reached its lowest level after 18 days of incubation and remained stable thereafter. Simultaneously, the $\sum S^{2-}$ concentration in the overlying water initially increased, reaching its peak on the 7th day, followed by a subsequent decrease. Notably, the highest $\sum S^{2-}$ concentrations were measured as 0.61, 1.14, 1.55, 2.15, 3.15, and 3.59 mg/L in the treatments corresponding to initial SO_4^{2-} concentrations of 0, 30, 60, 90, 120, 150, and 180 mg/L, respectively (Figs. 6.7 and 6.8).

In sediment pore-water, a notable and sudden decrease in SO_4^{2-} concentration was observed. For treatments with initial SO_4^{2-} concentrations below 90 mg/L, the lowest concentration was reached on the first day, while the other treatments reached their lowest concentrations on the second day (Figs. 6.7 and 6.8). The cumulative $\sum S^{2-}$ concentration initially increased and then decreased, eventually stabilizing after 23 days. Within the various treatments, the treatment with an initial concentration of 180 mg/L SO_4^{2-} exhibited the highest concentration of $\sum S^{2-}$, which peaked at 0.23 mg/L. Throughout the cyanobacteria decomposition, the AVS concentration within the sediments exhibited a substantial increase in the microcosms (Fig. 6.9). This variation in AVS concentration in the sediment can be characterized by an initial increase, followed by a subsequent decrease, and ultimately converging towards a relatively stable concentration. The peak value of AVS concentration occurred on the 11th day and intensified with increasing initial SO_4^{2-} concentrations in the overlying water. Among the treatments with initial SO_4^{2-} concentrations of 0, 30, 60, 90, 120, 150, and 180 mg/L, the peak AVS concentrations were 4.8, 6.4, 6.9, 7.5, 7.8, 8.2, and 9.1 mg/kg, respectively (Fig. 6.9).

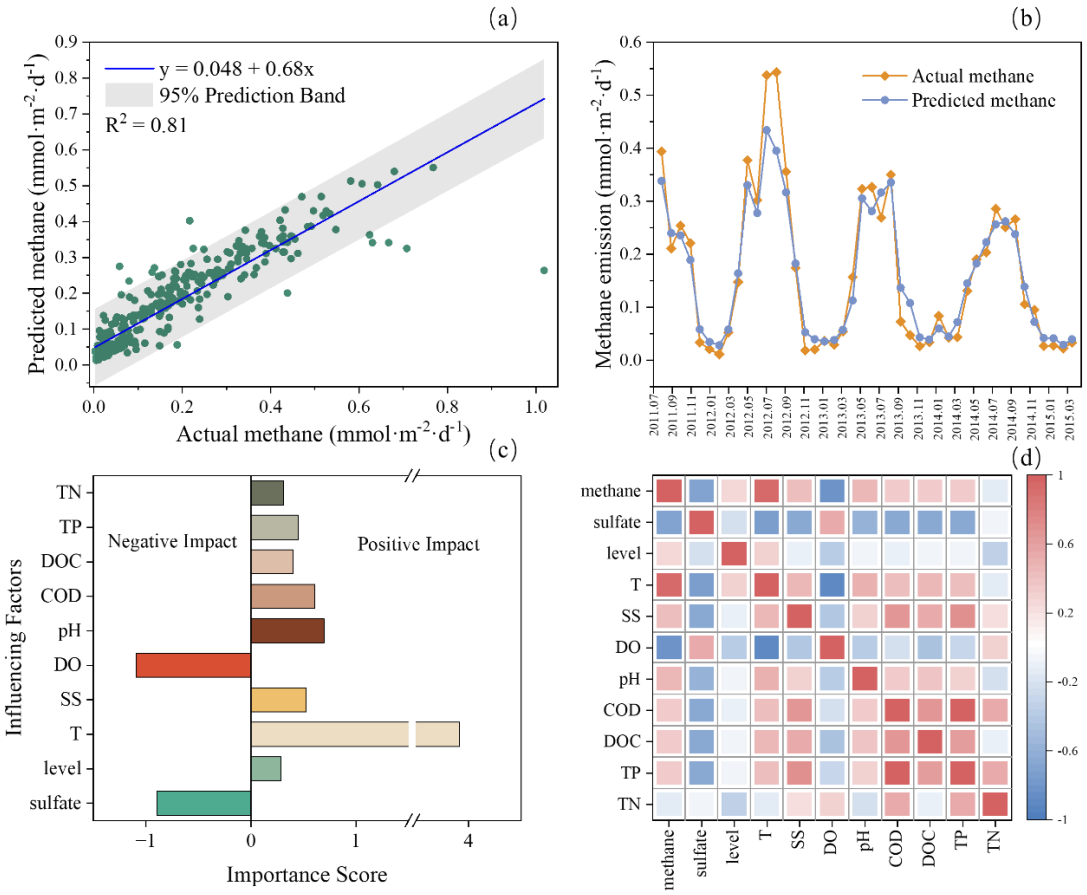

Fig. 6.6. The fitting of the predicted and actual methane emission (a, b), the weight of each influencing factors (c), and the correlation analysis between each index (d) based on the Random Forest model analysis.

6.3.5 Dynamics of CH_4 and CO_2 in microcosms

During the cyanobacteria decomposition, there was a substantial increase in CH_4 production and release in the microcosms (Fig. 6.10). Most of microcosms reached a relatively stable state by the 38th day, except for the treatment with initial SO_4^{2-} concentrations of 150 and 180 mg/L, which achieved stability by the 23rd day. On the 48th day, the treatments with initial SO_4^{2-} concentrations of 0 and 180 mg/L exhibited the highest and lowest CH_4 concentrations, measuring 3.9 ×10^3 and 1.9 ×10^3 μmol/L, respectively. The concentration of CH_4 decreased notably as the initial SO_4^{2-} concentrations increased. Additionally, the CO_2 concentrations in the microcosms increased due to cyanobacteria decomposition as shown in Fig. 4. A positive correlation was observed between CO_2 concentrations and initial SO_4^{2-} levels, with the highest concentration reaching a maximum value of 1.7 ×10^3 μmol/L in the treatment with the

highest initial SO_4^{2-} concentration (Fig. 6.10).

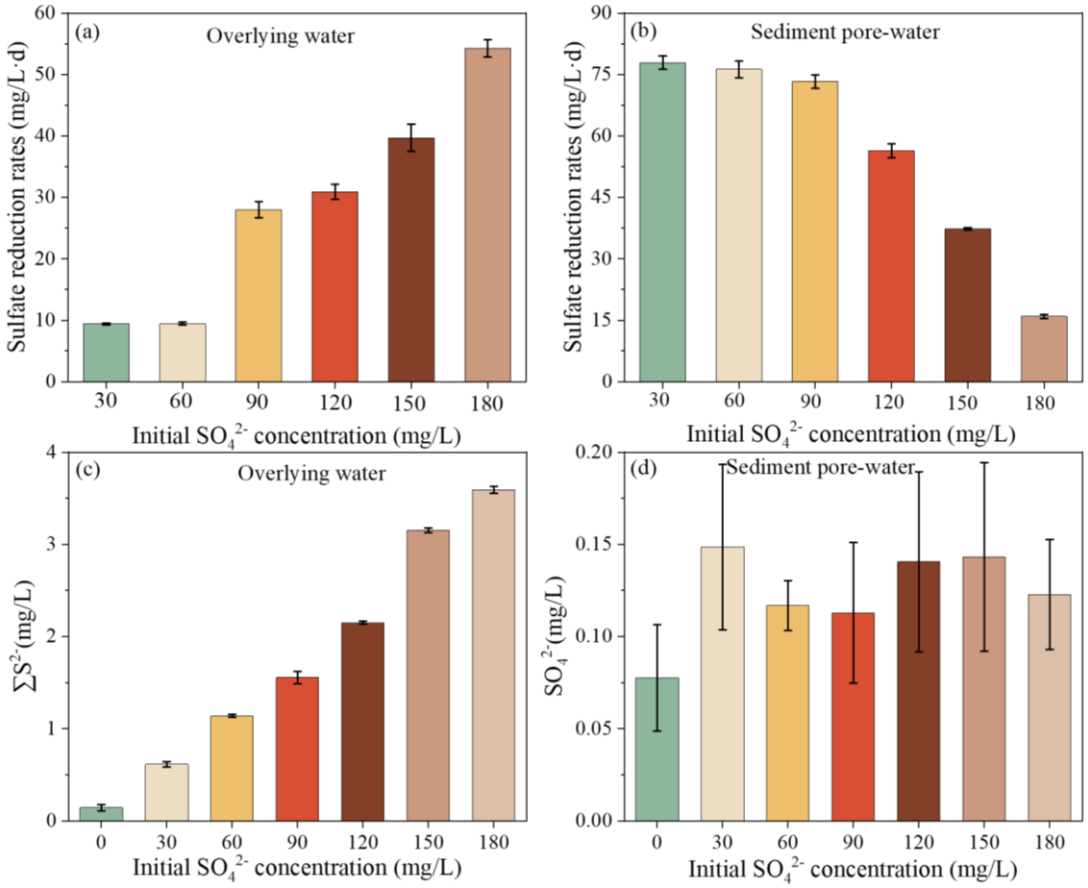

Fig. 6.7. The dynamics of the sulfate reduction rate in the overlying water (a), the sulfate reduction rate in the sediment pore-water (b), the $\sum S^{2-}$ concentration in the overlying water (c), the $\sum S^{2-}$ concentration in the sediment pore-water (d).

6.3.6 Dynamic changes in microorganisms of sediment in microcosms

During the cyanobacteria decomposition, there were significant fluctuations in the abundance of MPA and SRB, as shown in Fig. 6.11. Initially, the quantity of MPA was much higher at 3.16×10^8 copies/g compared to the abundance of SRB at 1.09×10^8 copies/g. However, as the decomposition progressed, the abundance of MPA decreased significantly, except in the control group. Among the treatments, the treatment with an initial SO_4^{2-} concentration of 180 mg/L exhibited the largest decrease in MPA abundance, with a decrease of 50.2% on the day 38 compared to the initial abundance. On the other hand, the abundance of SRB exhibited a positive correlation with the initial SO_4^{2-} concentrations. In particular, in the treatment with an initial SO_4^{2-}concentration of 180 mg/L, the abundance of SRB experienced the most prominent increase, rising

by 172.7% compared to its initial level by the 38th day.

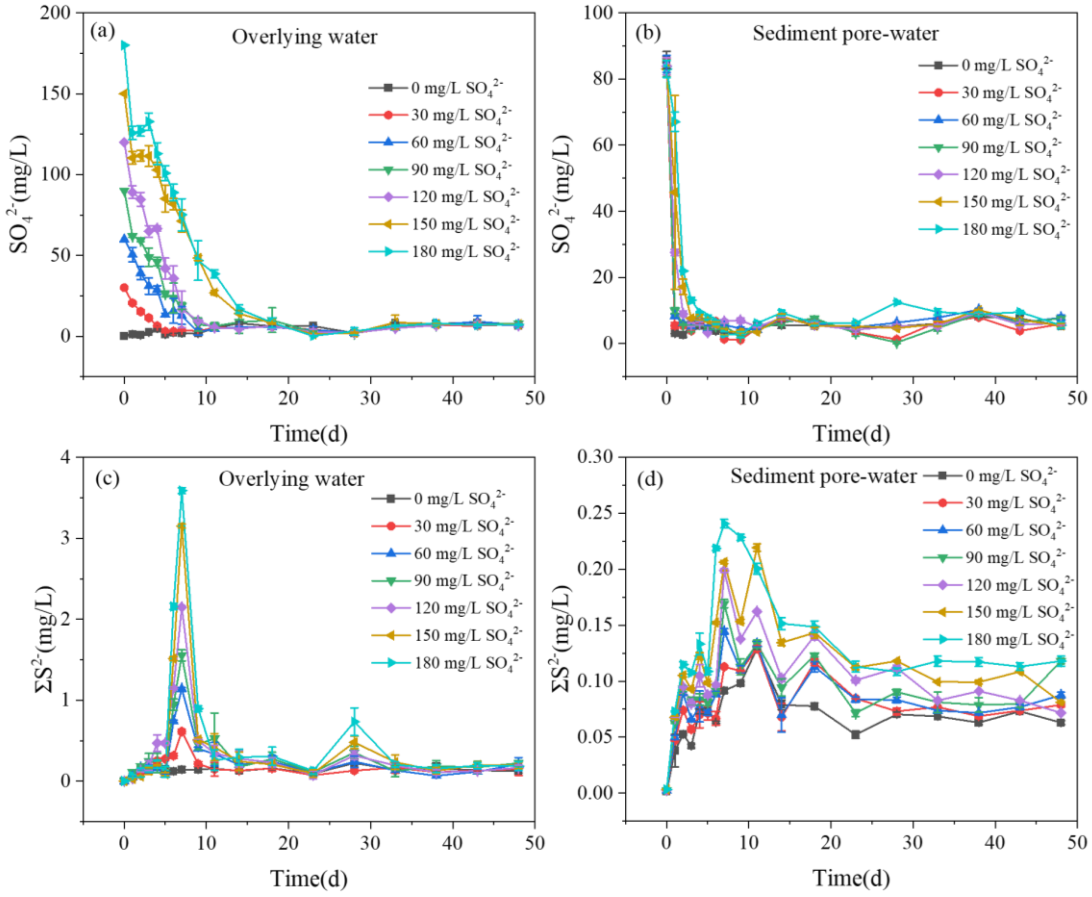

Fig. 6.8. The dynamics of SO_4^{2-} and $\sum S^{2-}$ concentrations in overlying water (a, b) and sediment pore-water (c, d) of microcosm.

During the incubation period, there were notable shifts in the community structure of MPA (Fig. 6.12). The MPA species included Methanomicrobiales, Methanobacteriales, Methanomassiliicoccales, and Methanosarcinales. Initially, Methanobacteriales were the predominant bacteria, accounting for 20.50% of the community. Methanomicrobiales and Methanomassiliicoccales accounted for 15.77% and 8.29% of the community, respectively. Conversely, Methanosarcinales exhibited the lowest abundance at only 4.61% of the total community. By the 38th day, the proportion of Methanosarcinales had decreased across all treatments. In the treatment with an initial SO_4^{2-} concentration of 180 mg/L, the relative abundance of Methanosarcinales slight decreased from 8.60% to 7.14%. Particularly noteworthy was the treatment without SO_4^{2-} at the beginning, which exhibited the most significant reduction in the proportion of Methanosarcinales.

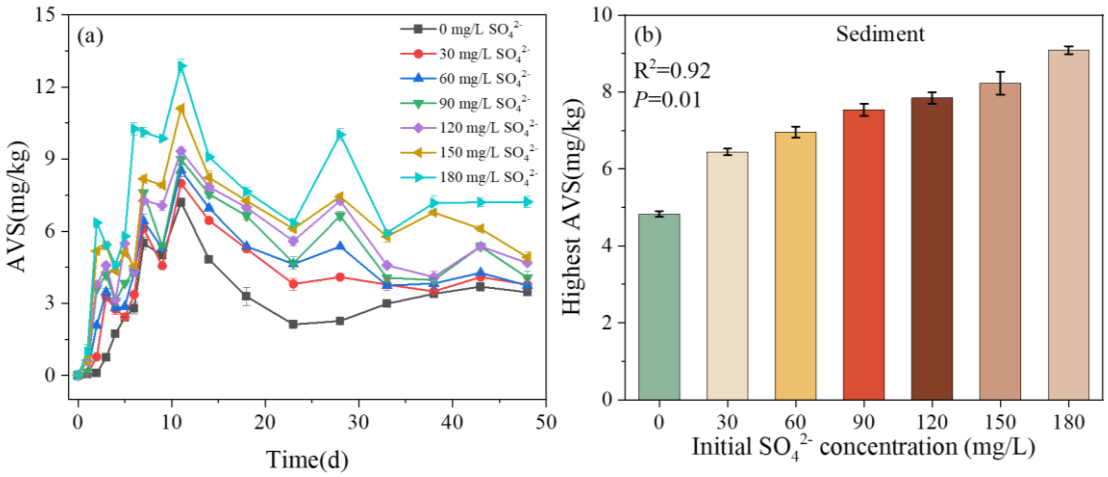

Fig. 6.9. The dynamics of AVS (a) and highest AVS concentrations (b) in sediments of microcosms.

6.4 Discussion

6.4.1 Temporal and spatial variations of SO_4^{2-} in freshwater lakes

In freshwater lakes, we observed a substantial increase in SO_4^{2-} concentrations and a trend that exhibited a positive correlation with eutrophication at both temporal and spatial scales (Fig. 6.2). Among the surveyed lakes, SO_4^{2-} concentrations exceeded 100 mg/L, marking a threefold increase compared to levels observed in the 1950s, and continue to exhibit an upward trend (Fig. 6.2a). The sulfur in lakes consists mainly of the anthropogenic and natural sources, with anthropogenic sources being the main contributor (Holmer et al., 2001). It has been reported that human activities are responsible for the significant increase in SO_4^{2-} concentrations in freshwater lakes over the past few decades (Wu et al., 2019). Of note that the SO_4^{2-} concentration in Lake Taihu has exhibited pronounced fluctuations throughout the year when compared to conditions two decades ago (Fig. 6.2b). The period from June to September was the main season for the breakout of cyanobacterial blooms (Fig. 6.4). After their decay DO in the water is rapidly consumed, leading to an anaerobic and strongly reducing environment (Bartosiewicz et al., 2021). Consequently, the SO_4^{2-} concentration in the water column was obviously reduced (Figs. 6.2 and 6.3). Conversely, in winter, the decrease in oxygen consumption by the degradation of fresh organic matter in the surface layer of sediments retards sulfate reduction reaction (Pan et al., 2018). In addition, the decay of cyanobacteria and other phytoplankton in winter releases $\sum S^2$

into the water (Wu et al., 2019). In the absence of cyanobacterial blooms, the water undergoes reoxygenation, and a portion of $\sum S^{2-}$ is oxidized to SO_4^{2-}, resulting in an obvious increase in SO_4^{2-} in the water during winter (Fig. 6.2). Our findings demonstrate that the presence of cyanobacterial blooms is one of the key factors driving the sulfate reduction process (Figs. 6.2, 6.5, 6.13 and 6.14).

Lake sediments serve as primary sites for sulfate reduction and sulfur reoxidation (Worner et al., 2019; Sandfeld et al., 2020). Due to wind disturbance and concentration diffusion, SO_4^{2-} from the overlying water diffuses into the sediments and participates in sulfate reduction as an electron acceptor (Zhao et al., 2021). It has been reported that 80%-90% of SO_2 is re-oxidized and transformed into SO_4^{2-} to sustain sulfate reduction (Fike et al., 2015; Wasmund et al., 2017). Cyanobacteria played an important role in this process, as they not only altered the physical and chemical conditions at the sediment-water interface (Fig. 6.13), but also released organic matter that stimulated the growth and activity of microbial communities, thereby influencing the microbial community structure (Figs. 6.11 and 6.12). Additionally, the decay and decomposition of cyanobacteria released substantial amounts of sulfur compounds, resulting in significant variations in SO_4^{2-} concentrations among different areas of the lake sediments (Figs. 6.5, 6.7, and 6.8). During the outbreak of cyanobacterial blooms, the SO_4^{2-} concentration in sediments, was notably higher compared to other months and varied with sediment depth (Fig. 6.5). This could be attributed to the deposition of sulfur compounds released during cyanobacteria decay, as well as the potential reoxidation processes within the sediments (Wasmund et al., 2017; Jorgensen et al., 2019). It has been observed that intense sulfate reduction reactions predominantly occur in the surface layer of the sediments, which could contribute to this phenomenon (Wu et al., 2019). In seasons without cyanobacteria, a relative dynamic equilibrium is established between the substances in the water and sediments, resulting in no significant difference in SO_4^{2-} concentrations between the cyanobacteria accumulation area and the open lake area (Figs. 6.5 and 6.12).

6.4.2 Potential drivers of sulfate reductions

The continuously escalating concentrations of SO_4^{2-} and recurrent outbreaks of cyanobacterial blooms have had a profound impact on intensifying sulfate reduction processes in eutrophic lakes (Zhao et al., 2019). This study postulates that the

decomposition of cyanobacteria is a prerequisite for sulfate reduction, as the reaction does not occur in the absence of cyanobacterial blooms (Fig. 6.15). During the decomposition of cyanobacteria, a large amount of nutrients is released, resulting in increases in TP, TN, and DOC concentrations in the water column (Fig. 6.14). These nutrients, originating from cyanobacteria decomposition, are crucial substrates for microbial growth and metabolic processes (Hansel et al., 2015; Zhu et al., 2021). In this study, the experimental microcosms supplemented with cyanobacteria exhibited a significant increase in the abundance of SRB (Figs. 6.11 and 6.16). Furthermore, the anaerobic environment created as a result of cyanobacteria decomposition provided favorable conditions for SRB growth (Fig. 6.13).

The increase in SO_4^{2-} concentration promoted sulfate reduction, with the reduction intensity being positively correlated with the initial SO_4^{2-} concentration (Figs. 6.7 and 6.8). SO_4^{2-} serves as a crucial substrate for the growth of SRB, which are key microorganisms driving the sulfate reduction process. It has been shown that an excess of SO_4^{2-} can stimulate SRB activity and increase the abundance of SRB, as reported by Gantzer et al. (2003) and Tripathi et al. (2021). Our findings align with these reports, showing that SRB abundance is positively associated with the initial SO_4^{2-} concentration (Figs. 6.11 and 6.17). SRB obtain energy through SO_4^{2-} metabolism, and their continuous growth may disrupt the sulfate reduction equilibrium, as highlighted in a recent study (Liu et al., 2022).

6.4.3 Potential factors in CH_4 emissions

Lakes are recognized as significant natural sources of CH_4 emissions, accounting for emissions ranging from 8 to 48 $Tg \cdot yr^{-1}$, which represents approximately 6-16% of all natural sources (Bastviken et al., 2004). CH_4 emissions in lakes are influenced by multiple factors, including substrate availability, water temperature, pH, and nutrient levels, and assessments of CH_4 emission must consider the synergistic effects of these factors (D'Ambrosio et al., 2021). This study not only confirmed the presence of numerous potential factors influencing CH_4 emissions but also unexpectedly discovered that increasing SO_4^{2-} concentrations in eutrophic lakes exert a significant inhibiting effect on CH_4 emissions (Fig. 6.6). Noticeably, CH_4 emissions from eutrophic lakes exhibit significant seasonal variations, with remarkably higher fluxes observed during the summer months than other seasons (Fig. 6.3b). The elevated temperatures in

summer stimulate MPA activities, leading to a significant enhancement in the rate of organic carbon mineralization (Fig. 6.3c, d). The cyanobacterial blooms during summer serve as a substrate for MPA, contributing to the rise in CH_4 emissions (Yan et al., 2017; D'Ambrosio et al., 2021). Previous studies have highlighted the existence of mutually reinforcing two-way feedback loops between cyanobacterial blooms, climate warming, and lake eutrophication (Davis et al., 2009). The decay of cyanobacterial blooms leads to the mineralization of cyanobacteria-derived organic carbon, resulting in the release of nutrients and CH_4 which perpetuates eutrophication and contributes to climate warming (Bartosiewicz et al., 2021; Yang et al., 2011).

In this study, CH_4 concentrations significantly increased in each microcosm system (Fig. 6.10), except for the one without cyanobacteria (Fig. 6.18). The decay and decomposition of cyanobacteria can weaken the function of lake sediments as a 'carbon sink,' potentially causing a reversal in the lake's ecological succession (Ma et al., 2020). Initially, a substantial amount of organic carbon is released into the water. However, in the later stages, as CH_4 concentrations continued to rise (Fig. 6.10), the organic carbon content in the overlying water significantly decreased (Fig. 6.14). The CH_4 production process is a pivotal mechanism for its release from sediments into the overlying water and the atmosphere, with MPA playing a decisive role in this process (Roland et al., 2017). The contribution to CH_4 production comes not only from the substantial release of organic carbon, which facilitates the carbon cycle, but also from the anaerobic reduction conditions created by cyanobacteria and the released nutrients that promote MPA growth (Figs. 6.11 and 6.16).

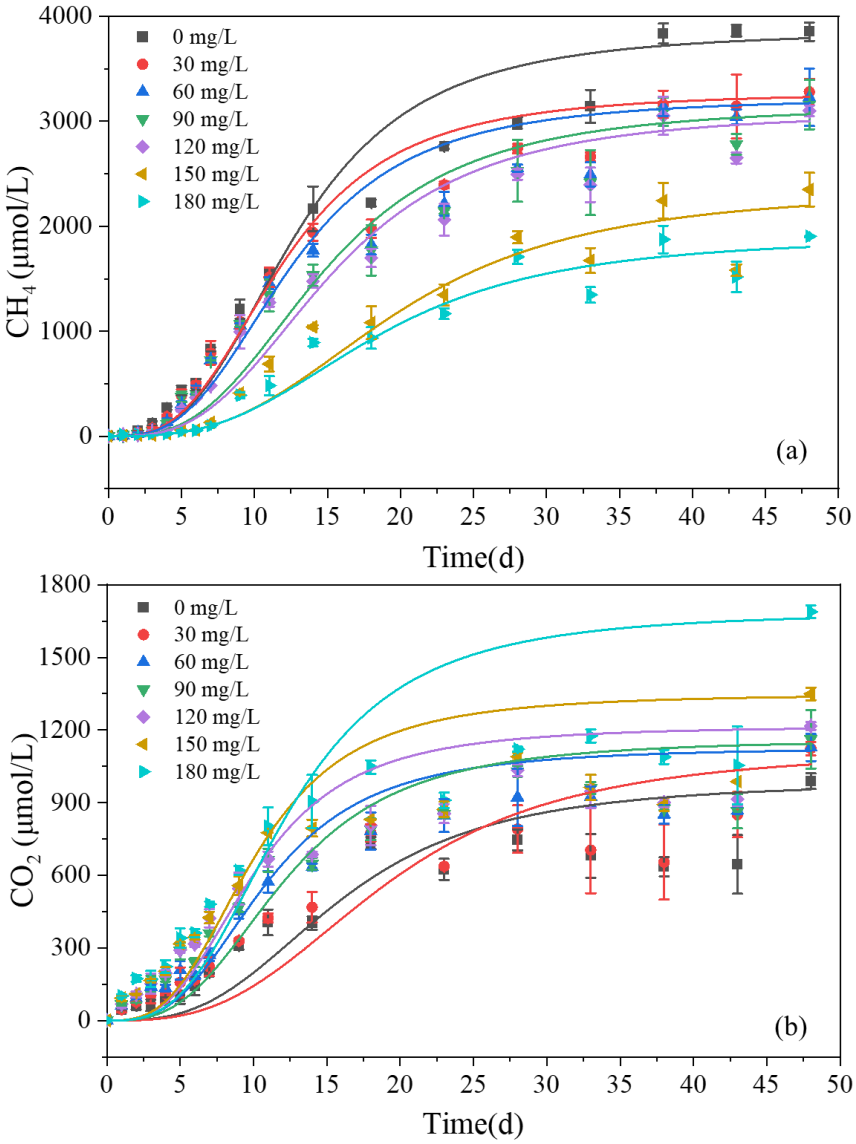

Fig. 6.10. The dynamics of CH_4 (a) and CO_2 (b) concentrations during the incubation in microcosms.

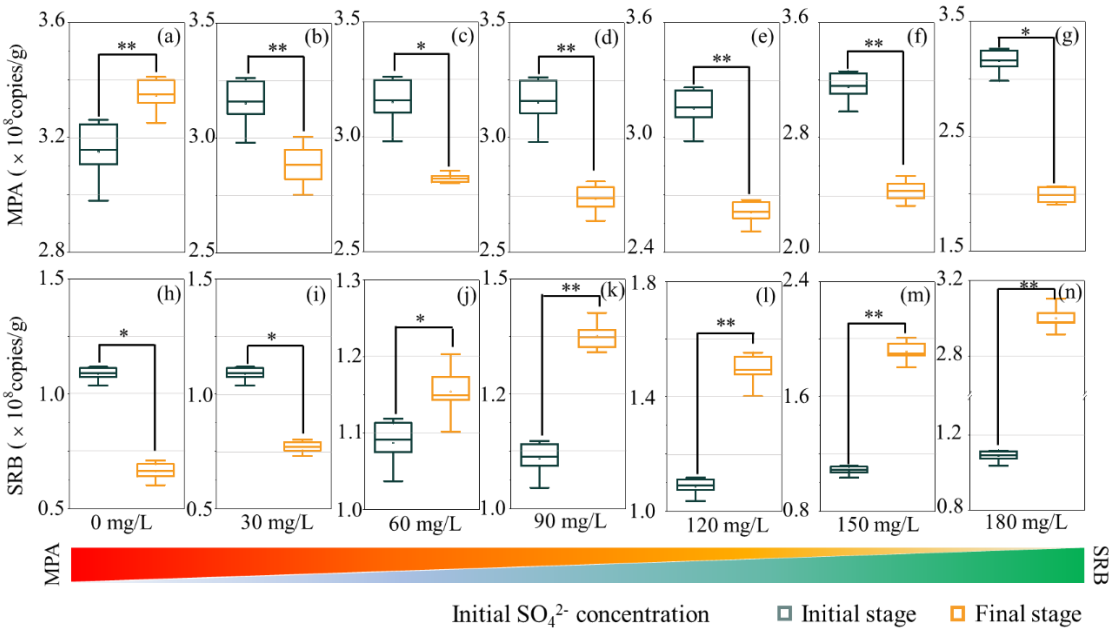

Fig. 6.11. The dynamics of SRB and MPA on initial stage and final stage in sediments of microcosms (* and ** indicate significant differences at $P < 0.05$ and $P < 0.01$, respectively).

6.4.4 The coupling mechanism of sulfate reduction and CH_4 production

With the continuous increase in SO_4^{2-} concentration, the inhibitory effect of sulfate reduction on CH_4 production becomes more pronounced (Figs. 6.2, 6.10, and 6.17). This study demonstrates that as SO_4^{2-} concentration rose, CH_4 concentration gradually decreased while CO_2 concentration steadily increased (Fig. 6.10). The influence of sulfate reduction on CH_4 production in marine and estuarine wetland ecosystems is primarily attributed to competition for organic carbon sources and the coupling of anaerobic CH_4 oxidation with sulfate reduction (Bowles et al., 2014). This process leads to sulfate reduction becoming the primary metabolic pathway for organic carbon, ultimately resulting in CO_2 being the main metabolic product of organic carbon (Jorgensen et al., 2019). It is important to note that the concentration of SO_4^{2-} in freshwater lakes is significantly lower than in the ocean (Fike et al.,2015). Consequently, the inhibitory effect of this process on CH_4 emissions in freshwater lakes has often been overlooked (Kopacek et al., 2006; Cabrol et al., 2020).

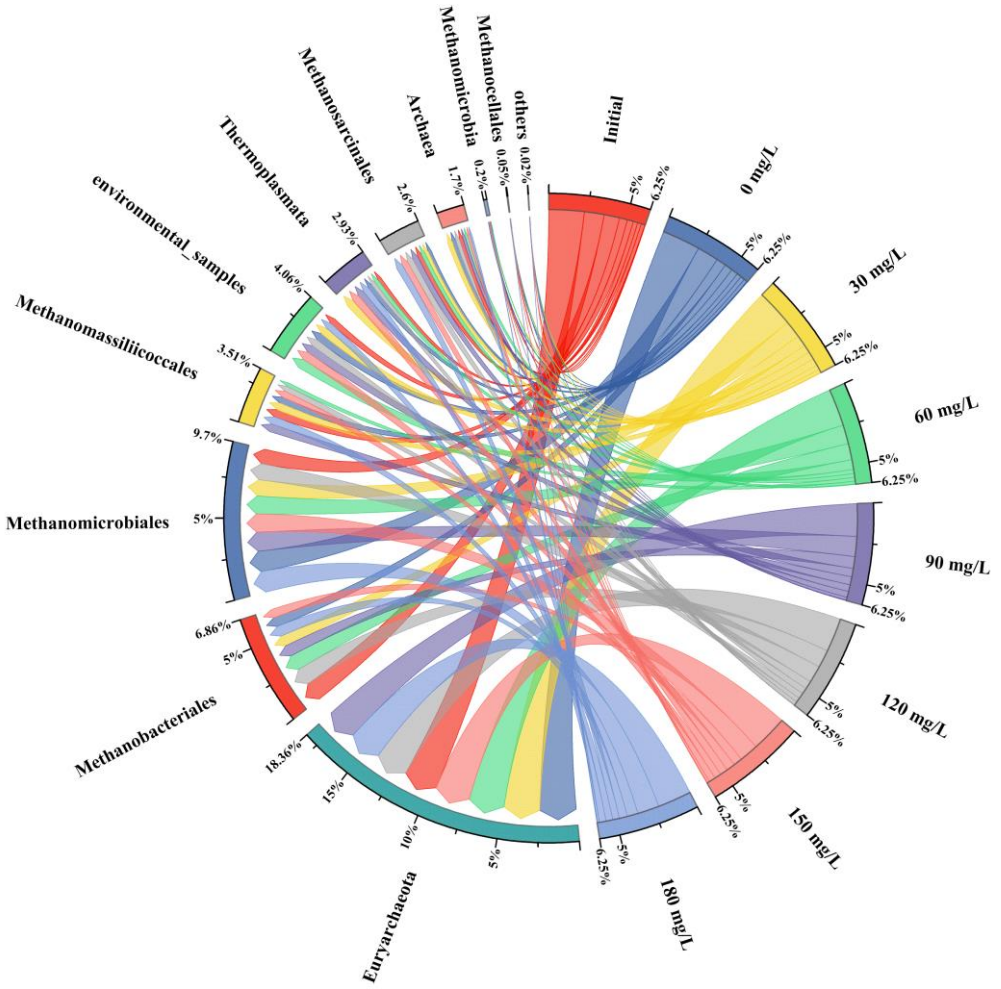

Fig. 6.12. Microbial community structure of MPA on initial stage and final stage in sediments in microcosms.

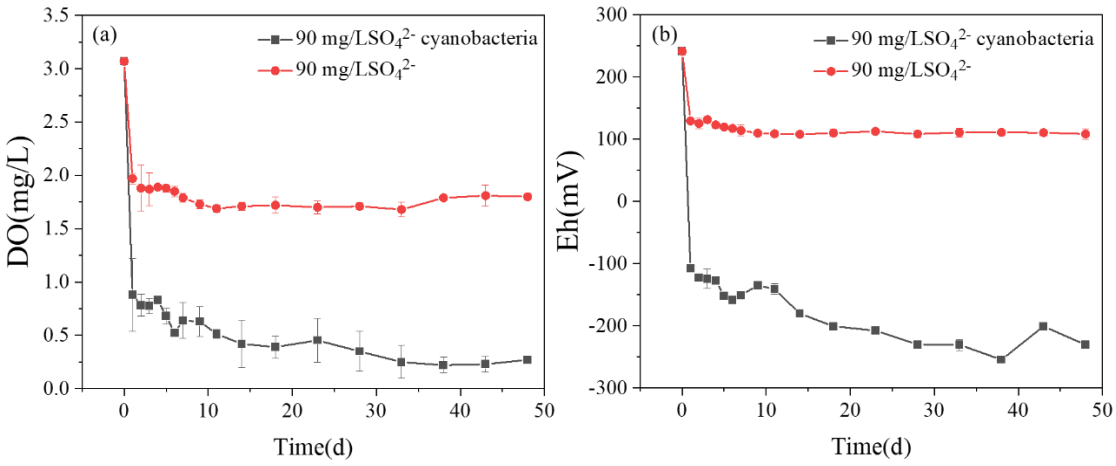

Fig. 6.13. The dynamics of DO (a), Eh (b) in 90 mg/L SO_4^{2-} with cyanobacteria and 90 mg/L SO_4^{2-} without cyanobacteria.

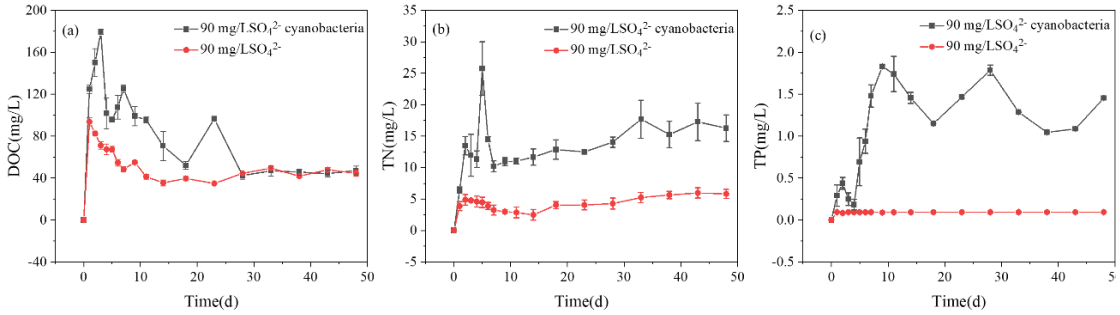

Fig. 6.14. The dynamics of DOC (a), TN (b) and TP (c) in 90 mg/L SO_4^{2-} with cyanobacteria and 90 mg/L SO_4^{2-} without cyanobacteria.

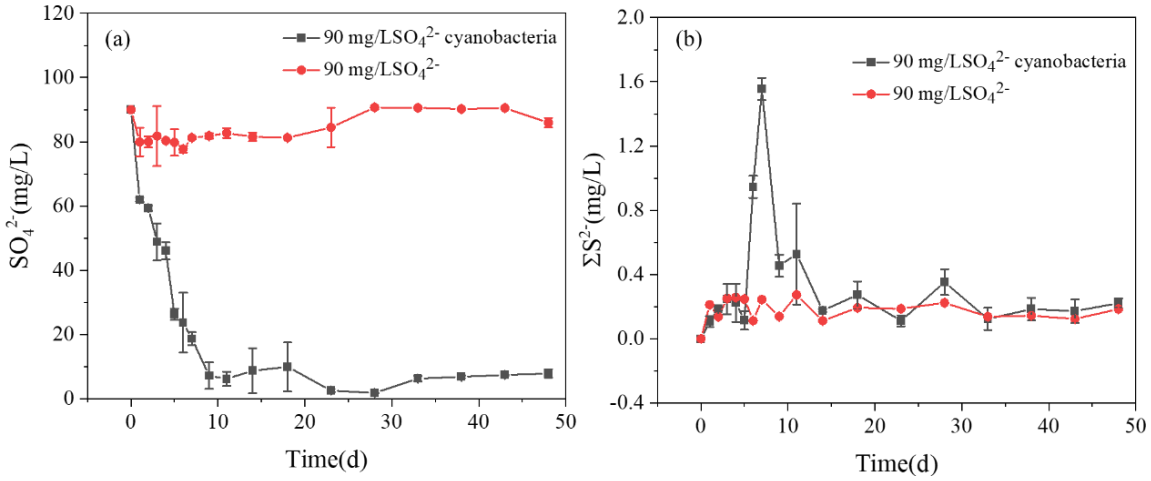

Fig. 6.15. The dynamics of SO_4^{2-} (a), $\sum S^{2-}$ (b) in 90 mg/L SO_4^{2-} with cyanobacteria and 90 mg/L SO_4^{2-} without cyanobacteria.

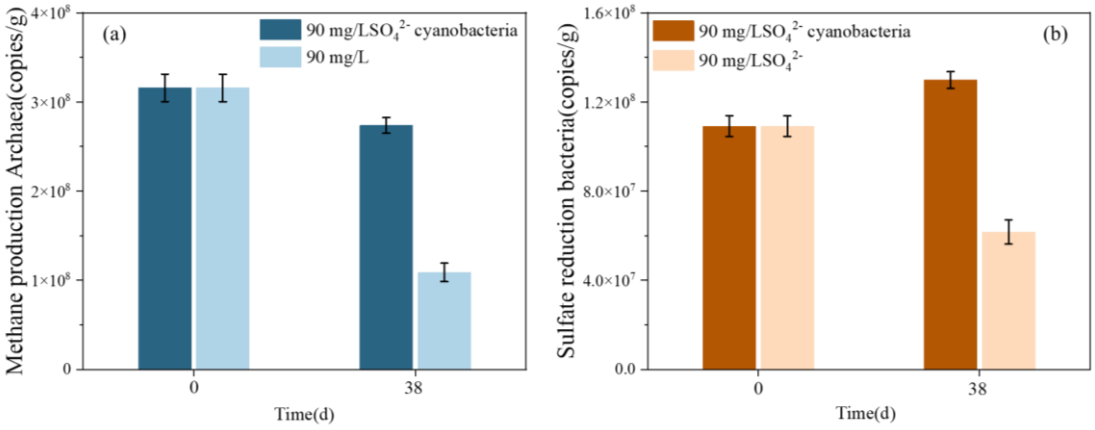

Fig. 6.16. The dynamics of MPA (a), and SRB (b), in 90 mg/L SO_4^{2-} with cyanobacteria and 90 mg/L SO_4^{2-} without cyanobacteria.

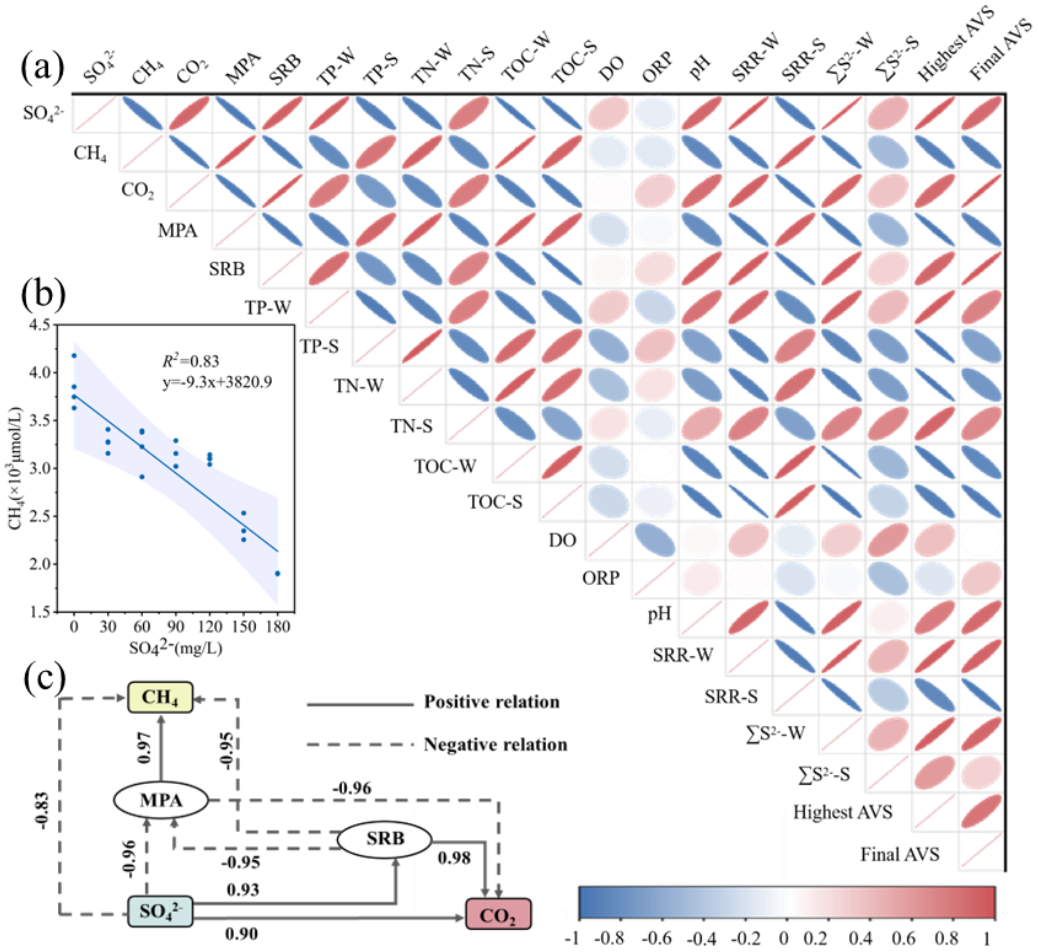

Fig. 6.17. Correlation analysis of each index (a), CH_4 and SO_4^{2-} concentration analysis (b), and structural equation modeling analysis (c). ("-W" and "-S" represent the samples in the overlying water and in the sediment, respectively)

This study revealed that the competition for substrate between SRB and MPA is the primary factor behind the inhibitory effect of sulfate reduction on CH_4 emissions (Figs. 6.6, 6.17, and 6.19). In lake sediments, SRB and MPA both have a strong affinity for common sediment substrates like H_2 and acetate, but SRB have a higher affinity for these substrates compared to MPA (Usman et al., 2020; Jantharadej et al., 2021). The SO_4^{2-} concentration can influence the growth of SRB, as they utilize H_2 and acetate as electron acceptors during sulfate reduction (Holmer et al., 2001; Rabus et al., 2004; Saxton et al., 2021). In lake ecosystems, methanogenesis primarily occurs through hydrogenotrophic and aceticlastic pathways, with MPA utilizing H_2 and acetic acid to produce CH_4 (Preheim et al., 2016). It has been indicated that changes in substrate availability and temperature are the primary factors influencing the methanogenesis pathway. Specifically, high temperatures and elevated organic matter content tend to favor the acetoclastic methanogenesis pathway (Yang et al., 2017). Under favorable

conditions, SRB can decrease the concentrations of these substrates, thus inhibiting the growth of MPA (Figs. 6.11 and 6.12), and ultimately suppressing CH_4 emissions (Figs. 6.10 and 6.17). When sulfate reduction is intense, non-competitive substrates like methyl compounds become the primary substrates for CH_4 production (Zhang et al., 2016). This finding aligns with previous evidence demonstrating that sulfate reduction affects CH_4 emissions through various pathways in marine and estuarine wetland systems (Pester et al., 2012; Bowles et al., 2014).

6.4.5 Negative impact of SO_4^{2-} concentrations on CH_4 emissions

In the context of lake ecosystems, the issue of CH_4 emissions from eutrophic lakes has become increasingly critical due to escalating eutrophication (Zhang et al., 2021). Surprisingly, this study, based on data analysis using the random forest model, found that the overlooked sulfate concentration in eutrophic lakes has a significant inhibitory effect on CH_4 emissions (Fig. 6.3). Further investigations showed that this phenomenon is likely driven by substrate competition among microorganisms (Figs. 6.10, 6.11, and 6.12). Moreover, the continuous increase in SO_4^{2-} concentration in eutrophic lakes, coupled with the disturbance caused by frequent cyanobacterial blooms, disrupts the balance of lake ecosystems (Paerl et al., 2012). It is important to note that neglecting the rise in SO_4^{2-} concentrations resulted in an overestimation of CH_4 emissions (Figs. 6.3, 6.10, 6.17 and 6.19). While cyanobacteria decomposition contributes to CH_4 emissions, the release of nutrients and the creation of anaerobic conditions also facilitate sulfate reduction (Paerl et al., 2012). Despite the inhibitory effect of rising sulfate levels, it only partially offsets the substantial increase in CH_4 emissions from cyanobacteria decomposition, overall, CH_4 emissions still rise (Figs. 6.10 and 6.18). This overlooked process is becoming more pronounced as sulfate levels increase rapidly, intensifying the inhibitory effect. This study underpinned positive correlation of SO_4^{2-} concentration with *TLI* in freshwater lakes, while SO_4^{2-} concentration was the lowest in summer when cyanobacteria outbreaks were severe, underscoring the occurrence of intensive sulfate reduction (Figs. 6.2, 6.6, and 6.19). Consequently, we have reason to believe that the overlooked sulfate reduction process in freshwater lakes plays an important role in slowing down CH_4 emissions during periods of high CH_4 emissions, such as summer. Based on the inhibitory effect of sulfate reduction on CH_4 emissions found in this study, future studies will prioritize quantifying its impact and evaluating

its potential in mitigating CH_4 emissions across global freshwater lakes. Additionally, when examining the combined impacts of different environmental variables on CH_4 emissions from lakes, sulfate concentration will be incorporated as a crucial factor in models utilized for CH_4 emission assessments.

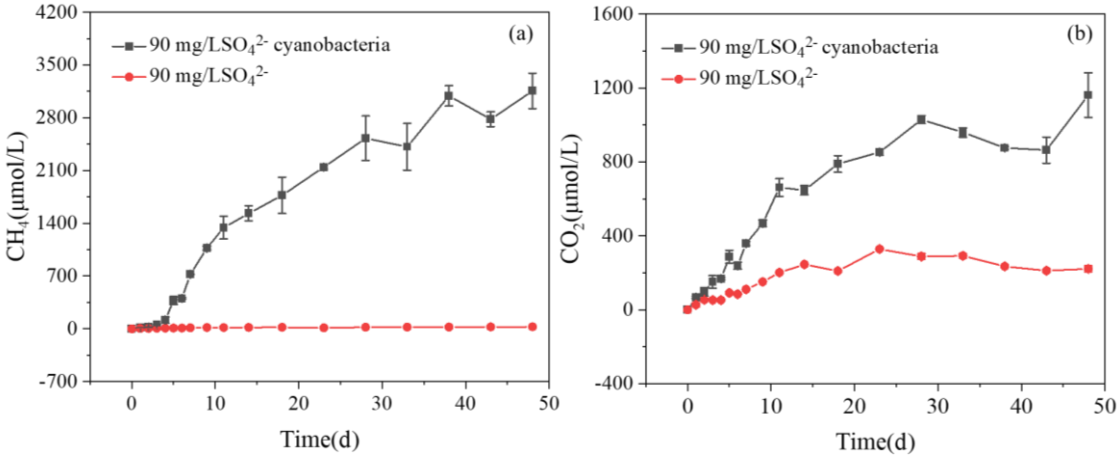

Fig. 6.18. The dynamics of CH_4 (a), and CO_2 (b) in 90 mg/L SO_4^{2-} with cyanobacteria and 90 mg/L SO_4^{2-} without cyanobacteria.

6.5 Summary

In the present study, we conducted a comprehensive investigation into the temporal and spatial dynamics of SO_4^{2-} concentrations within freshwater lakes. Our findings reveal a pronounced increase in SO_4^{2-} concentrations, which is closely associated with eutrophication processes. We found that cyanobacterial blooms played a critical role in stimulating sulfate reduction processes, as their decomposition released nutrients that promoted the SRB growth. An increase in SO_4^{2-} concentration further enhanced sulfate reduction, as evidenced by a positive correlation between the SRB abundance and the initial sulfate concentrations. Interestingly, we also discovered that higher SO_4^{2-} concentrations in eutrophic lakes inhibited CH_4 emissions. This inhibition can be attributed to the competition between SRB and MPA for substrates, with SRB demonstrating a strong affinity for substrates at high SO_4^{2-} levels. Our results highlight the importance of considering SO_4^{2-} concentrations when estimating CH_4 emissions in freshwater lakes, as the absence of this parameter may overestimate CH_4 emissions. We highlight the significance of sulfate reduction as a mitigation strategy for CH_4 emissions in eutrophic lakes and the necessity for further research to quantify its global impact.

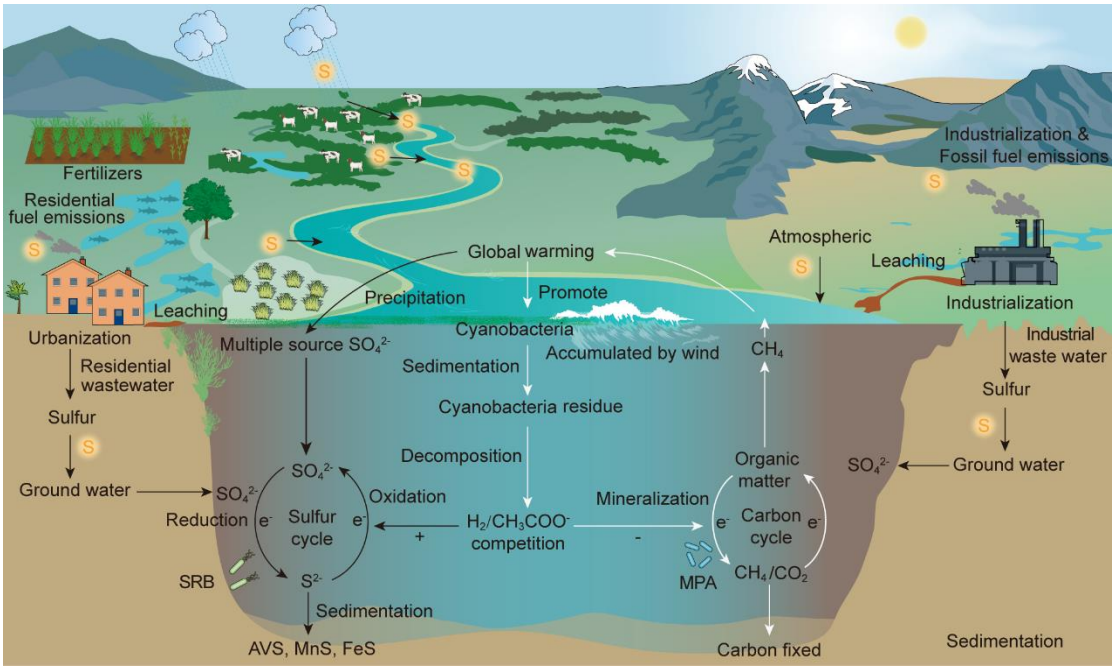

Fig. 6.19. A conceptual diagram of sulfate effects on CH_4 production during cyanobacteria decay processes in eutrophic lakes.

7. Conclusion and future study

7.1 Conclusion

This study focused on typical lakes in the middle and lower reaches of the Yangtze River basin, employing field investigations, laboratory simulations, and modeling analyses to explore the current state of GHG gross emissions and their potential influencing factors. The driving mechanisms of GHG gross emissions from these lakes were elucidated in detail, addressing aspects such as intensified eutrophication, increased endogenous carbon, exogenous carbon inputs, the impact of cyanobacteria blooms on sediment carbon reservoirs, and the biogeochemical coupling processes of carbon and sulfur. The specific findings are as follows:

(1) Lakes in the middle and lower reaches of the Yangtze River are currently facing severe eutrophication, as well as high GHG gross emissions. Eutrophication significantly enhances carbon emissions in shallow lakes by increasing carbon production potential, dissolved carbon concentrations, and release fluxes, particularly for CH_4. While DO negatively correlates with carbon release, temperature shows a positive correlation. This study indicates that the impact of eutrophication on carbon emissions varies across temporal and spatial scales. Due to the omission of seasonal variations in dissolved oxygen and temperature, spatial-scale assessments often lead to inaccuracies in carbon emission estimates. This study demonstrates that using summer data results in an overestimation of gross carbon emissions.

(2) DOM is the primary form of allochthonous carbon input in eutrophic lakes, with diverse sources and a complex structural composition. The multi-source input of DOM in Lake Taihu basin destabilizes sediment carbon pools by increasing carbon concentrations and promoting GHG gross emissions. Lignins and humic acids dominate the DOM composition, derived from terrestrial and aquatic plant decomposition, and exhibit a strong correlation with CH_4 and CO_2 emissions. The decomposition of mixed-source DOM can induce co-metabolic processes. The microbial mineralization of DOM intensifies under these conditions, further contributing to sediment carbon instability.

(3) This study highlights the role of POC, particularly cyanobacteria-derived POC, in driving CH_4 emissions and explaining the methane paradox. Cyanobacterial-derived POC provided a sufficient carbon source for the anaerobic metabolism of microbial organic matter, which maintained microbial activity at a high level and promoted the

concentration flux of CH_4 and CO_2. In this study, high POC concentrations in the oxic overlying water of lakes were observed to be accompanied by high dissolved CH_4 concentrations, revealing that the presence of POC may be cause of the methane paradox. These conditions intensify CH_4 and CO_2 emissions and reveal the significant contribution of POC to carbon emission.

(4) Cyanobacterial-derived organic carbon alters the physicochemical conditions and storage structure of the sediment carbon pool. Cyanobacteria-derived organic carbon in eutrophic lakes leads to the migration of CH_4 and CO_2 production hotspots from deep sediments to surface layers, reducing emission pathways and amplifying GHG gross emissions. The increased organic carbon and moisture content in surface sediments create an anaerobic microenvironment conducive to microbial activity, intensifying biogenic CH_4 and CO_2 production. Cyanobacterial deposits also hinder methane oxidation, further elevating emissions.

(5) Anthropogenic activities have significantly increased SO_4^{2-} concentrations in eutrophic lakes, which play a dual role in carbon cycling. Higher SO_4^{2-} concentrations inhibit CH_4 emissions by creating competition between SRB and MPA for substrates. Cyanobacterial blooms further stimulate sulfate reduction processes by releasing nutrients that promote SRB growth.

7.2 Perspective of GHG gross emission from eutrophic lakes

(1) The intensification of lake eutrophication disrupts the balance between the roles of lakes as carbon sinks and sources. In natural ecosystems, lake primarily function as carbon sinks. However, eutrophication and its progression led to increased carbon emissions. Although this rise has not yet fully shifted lakes from carbon sinks to carbon sources, studies suggest that the escalation of CH_4 emissions offset the continental carbon sink. With the continued intensification of eutrophication, the carbon sink function of lakes is expected to be further diminished, ultimately driving a transition from carbon sinks to carbon sources.

(2) The co-metabolism process induced by cyanobacteria blooms enhances lake GHG emissions while, mitigating lake degradation and sustaining ecological functions. The decay and decomposition of aquatic macrophytes, as well as the terrigenous litter input via hydrology process, leave behind a substantial amount of refractory organic matter in lakes. The continuous accumulation of this organic matter can lead to sediment

elevation, ultimately contributing to lake degradation, particularly in shallow lake systems in the middle and lower reaches of the Yangtze River basin. The co-metabolism process induced by cyanobacteria facilitates the mineralization of refractory organic matter in sediments. While this process enhances GHG production and emissions from lake sediments, it also slows sediment elevation, thereby helping to sustain lake ecosystem functions.

7.3 Limitation and future study

This study primarily focuses on the current states and potential driving mechanisms of GHG gross emissions from typical lakes in the middle and lower reaches of the Yangtze River Basin. However, there remain areas that require further research in the future, as follows:

(1) This study focuses on GHG gross emissions, without considering processes such as photosynthesis and respiration. Therefore, future research should account for the lake carbon sink processes to accurately quantify the net carbon emission flux of eutrophic lakes.

(2) The lakes selected for this study are primarily located in the middle and lower reaches of the Yangtze River, which have high baseline values and are significantly influenced by human activities, making them somewhat unique.

(3) The temporal scale analysis in this study mainly focuses on the typical eutrophic Lake Taihu, with limited data from other lakes. Future research should develop temporal-scale datasets for a wider range of lakes to expand the scope of temporal studies.

(4) This study does not precisely quantify the overall greenhouse gas emissions from different lake ecosystems. Future research should integrate machine learning, model analysis, and other methods to quantify greenhouse gas emissions across various basins and trophic states.

(5) Future studies should incorporate model analysis and advanced data science techniques to quantify the contributions of various drivers to lake greenhouse gas emissions. Additionally, they should predict changes in greenhouse gas fluxes and trends under future scenarios.

References

Alanna, L., Chuang, P.C., Singleton, M., Paytan, A., 2017. Sources of methane to an Arctic lake in Alaska: An isotopic investigation. Journal of Geophysical Research: Biogeosciences. 122(4), 753-766.

Ankit, Y., Muneer, W., Gaye, B., Lahajnar, N., Bhattacharya, S., Bulbul, M., Jehangir, A., Anoop, A., Mishra, P.K., 2022. Apportioning sedimentary organic matter sources and its degradation state: inferences based on aliphatic hydrocarbons, amino acids and delta $\delta^{15}N$. Environmental Research, 205: 112409.

Bai, L.L., Liu, X., Wu, Y.Q., Cheng, H.Y., Wang, C.H., Jiang, H.L., Wang, A.J., 2023. Distinct seasonal variations of dissolved organic matter across two large freshwater lakes in China: Lability profiles and predictive modeling. Journal of Environmental Management. 339, 117880.

Baldwin, D.S., Mitchell, A., 2012. Impact of sulfate pollution on anaerobic biogeochemical cycles in a wetland sediment. Water Research. 46(4), 965-974.

Bao, Y., Huang, T., Ning, C.W., Sun, T.T., Tao, P.L., Wang, J., Sun, Q.Y., 2023. Changes of DOM and its correlation with internal nutrient release during cyanobacterial growth and decline in Lake Chaohu, China. Journal of Environmental Sciences. 124, 769-781.

Bartosiewica, M., Venetz, J., Laeubli, S., Steiner, O.S., Bouffard, D., Zopfi, J., Lehmann, M.F., 2022. Detritus-hosted methanogenesis sustains the methane paradox in an alpine lake. Limnology and Oceanography, 68(1): 248-264.

Bartosiewicz, M., Maranger, R., Przytulska, A., Laurion, I., 2021. Effects of phytoplankton blooms on fluxes and emissions of greenhouse gases in a eutrophic lake. Water Research. 196, 116985.

Bastviken, D., Cole, J., Pace, M., Tranvik, L., 2004. Methane emissions from lakes: Dependence of lake characteristics, two regional assessments, and a global estimate. Global Biogeochemical Cycles, 18, GB4009.

Bastviken, D., Cole, J.J., Pacw, M.L., Van de Bogert, M.C., 2008. Fates of methane from different lake habitats: connecting whole-lake budgets and CH_4 emissions. Journal of Geophysical Research-Biogeosciences, 113(G2), G02024.

Bastviken, D., Tranvik, L.J., Downing, J.A., Crill, P.M., Enrich-prast, A., 2011. Freshwater methane emissions offset the continental carbon sink. Science,

331(6013), 50.

Beaulieu, J.J., DelSontro, T., Downing, J.A., 2019. Eutrophication will increase methane emissions from lakes and impoundments during the 21st century. Nature Communications. 10, 1375.

Begum, M.S., Bogard, M.J., Butman, D.E., Chea, E., Kumar, S., Lu, X.X., Nayna, O.K., Ran, L.S., Richey, J.E., Tareq, S.M., Xuan, D.T., Yu, R.H., Park, J.H., 2021. Localized pollution impacts on greenhouse gas dynamics in three anthropogenically modified Asian River systems. Journal of Geophysical Research: Biogeosciences. 126(5), e2020JG006124.

Bertolet, B.L., Olson, C.R., Szydlowski, D.K., Solomon, C.T., Jones, S.E., 2020. Methane and primary productivity in lakes: divergence of temporal and spatial relationships. Journal of Geophysical Research-Biogeosciences, 125(9), e2020JG005864.

Bianchini, I., d a Cunha-Santino, M.B., 2018. Contribution of humic substances as a sink and source of carbon in tropical floodplain lagoons. 18(4), 1232-1241.

Bizic-Ionescu, M., Ionescu, D., Gunthel, M., Tang, K.W., Grossart, H.P., 2019. Oxic methane cycling: New evidence for methane formation in oxic lake water. Biogenesis of Hydrocarbons. 379-400.

Borrel, G., Jezequel, D., Biderre-Petit, C., Morel-Desrosiers, N., Morel, J.P., Peyret, P., Fonty, G., Lehours, A.C., 2011. Production and consumption of methane in freshwater lake ecosystems. Research in Microbiology, 162(9), 832-847.

Bowles, M.W., Mogollón, J.M., Kasten, S., Zabel, M., Hinrichs, K.U., 2014. Global rates of marine sulfate reduction and implications for sub–sea-floor metabolic activities. Science. 344(6186), 889-891.

Braeckman, U., Pasotti, F., Vazquez, S., Zacher, K., Hoffmann, R., Elvert, M., Marchant, H., Buckner, C., Quartino, M.L., Mac Cormack, W., Soetaert, K., Wenzhofer, F., Vanreusel, A., 2019. Degradation of macroalgal detritus in shallow coastal Antarctic sediments. Limnology and Oceanography. 64(4), 1423-1441.

Bueno, C.D., Frascareli, D., Gontijo, E.S.J., van Geldern, R., Rosa, A.H., Friese, K., Barth, J.A.C., 2020. Dominance of in situ produced particulate organic carbon in a subtropical reservoir inferred from carbon stable isotopes. Scientific Reports, 10(1), 13187.

Cabrol, L., Thalasso, F., Gandois, L., Sepulveda-Jauregui, A., Martinez-Cruz, K.,

Teisserenc, R., Tananaev, N., Tveit, A., Svenning, M.M., Barretet, M., 2020. Anaerobic oxidation of methane and associated microbiome in anoxic water of Northwestern Siberian lakes. Science of the Total Environment. 736, 139588.

Carlson, R.E., 1997. A trophic state index for lakes. Limnology and Oceanography 22, 361-369.

Cerbin, S., Perez, G., Rybak, M., Wejnerowski, L., Konowalczyk, A., Helmsing, N., Naus-Wiezer, S., Meima-Franke, M., Pytlak, L., Raaijmakers, C., Nowak, W., Bodelier, P.L.E., 2022. Methane-derived carbon as a driver for cyanobacterial growth. Frontiers in Microbiology. 13, 837198.

Chanudet, V., Gaillard, J., Lambelain, J., Demarty, M., Descloux, S., Felix-Faure, J., Poirel, A., Dambrine, E., 2020. Emission of greenhouse gases from French temperate hydropower reservoirs. Aquatic Sciences, 82(3): 51.

Chen, M., Li, X.H., He, Y.H., Song, N., Cai, H.Y., Wang, C.H., Li, Y.T., Chu, H.Y., Krumholz, L.R., Jiang, H.L., 2016. Increasing sulfate concentrations result in higher sulfide production and phosphorous mobilization in a shallow eutrophic freshwater lake. Water research. 96, 94-104.

Clayer, F., Gelinas, Y., Tessier, A., Gobeil, C., 2020. Mineralization of organic matter in boreal lake sediment: rates, pathways, and nature of the fermenting substrates. Biogeosciences, 17(18): 4571-4589.

Cline, J.D., 1969. Spectrophotometric determination of hydrogen sulfide in natural waters. Limnology and Oceanography. 14, 454-458.

Culbertson, A.M., Martin, J.F., Aloysius, N., Ludsin, S.A., 2016. Anticipated impacts of climate change on 21st century Maumee River discharge and nutrient loads. Journal of Great Lakes Research. 42(6), 1332-1342.

D'Ambrosio, S. L., Harrison, J.A., 2021. Methanogenesis exceeds CH_4 consumption in eutrophic lake sediments. Limnology and Oceanography Letters. 6(4), 173-181.

Dai, J.H., Sun, M.Y., Culp, R.A., Noakes, J.E., 2009. A laboratory study on biochemical degradation and microbial utilization of organic matter comprising a marine diatom, land grass, and salt marsh plant in estuarine ecosystems. Aquatic Ecology, 43(4), 825-841.

Dalu, T., Richoux, N.B., Froneman, P.W., 2016. Nature and source of suspended particulate matter and detritus along an austral temperate river-estuary continuum, assessed using stable isotope analysis. Hydrobiologia, 767(1): 95-110.

Davidson, T.A., Audet, J., Svenning, J.C., Lauridsen, T.L., Sondergaard, M., Landkildehus, F., Larsen, S.E., Jeppesen, E., 2015. Eutrophication effects on greenhouse gas fluxes from shallow-lake mesocoms override those of climate warming. Global Change Biology, 21(12), 4449-4463.

Davis, T. W., Berry, D. L., Boyer G. L., Gobler C. J., 2009. The effects of temperature and nutrients on the growth and dynamics of toxic and non-toxic strains of microcystis during cyanobacteria blooms. Harmful algae. 8(5), 715-725.

De Kluijver, A., Schoon, P.L., Downing, J.A., Schouten, S., Middelburg, J.J., 2015. Stable carbon isotope biogeochemistry of lakes along a trophic gradient. Biogeosciences, 11(22): 6265-6276.

Deng, X.W., Qi, M., Ren, R., Liu, J.R., Sun, X.X., Xie, P., Chen, J., 2019. The relationship between odors and environmental factors at bloom and non-bloom area in Lake Taihu, China. Chemosphere. 218, 569-576.

Deng, Y., Wu, Y.T., Liu, G., Xu, X.G., Ma, J., Yan, Y., Wang, G.X., 2022. Species evenness affects algae driven co-metabolism with aquatic plant residues. Carbon Research. 1, 26.

Deng, Y., Yan, Y., Wu, Y.T., Liu, G., Ma, J., Xu, X.G., Wang, G.X., 2023. Response of aquatic decomposition to invasive algal organic matter mediated by the co-metabolism effect in eutrophic lakes. Journal of Environmental Management. 329, 117037.

Derimendjian, L., Lambert, T., Morana, C., Bouillon, S., Descy, J.P., Okello, W., Borges, A.V., 2020. Dissolved organic matter composition and reactivity in lake Victoria, the world's largest trophical lake. Biogeochemistry. 150(1), 61-83.

Diaz, R.J., 2001. Overview of hypoxia around the world. Journal of Environmental Quality, 30(2): 275-281.

Diaz-Torres, O., Lugo-Melchor, O.Y., de Anda, J., Pacheco, A., Yebra-Montes, C., Gradilla-Hernandez, M.S., Senes-Guerrero, C., 2022. Bacterial dynamics and their influence on the biogeochemical cycles in a subtrophical hypereutrophic lake during the Rainy season. Frontiers in Microbiology. 13, 832477.

Duan, Z.P., Tan, X., Ali, I., Wu, X.G., Cao, J., Xu, Y.X., Shi, L., Gao, W.P., Ruan, Y.L., Chen, C., 2022. Comparison of organic matter (OM) pools in water, suspended particulate matter, and sediments in eutrophic Lake Taihu, China: Implication for dissolved OM tracking, assessment, and management. Science of the Total

Environment. 845, 157257.

Ebina, J., Tsutsui, T., Shirai, T., 1983. Simultaneous determination of total nitrogen and total phosphorus in water using peroxodisulfate oxidation, Water Research, 17(12), 1721-1726, 1983.

Einzmann, T., Schroll, M., Kleint, J.F., Greule, M., Keppler, F., 2022. Application of concentration and 2-dimensional stable isotope measurements of methane to constrain sources and sinks in a seasonally stratified freshwater lake. Frontiers in Environmental Science. 10, 865862.

Ejarque, E., Khan, S., Steniczka, G., Schelker, J., Kainz, M.J., Battin, T.J., 2018. Climate-induced hydrological variation controls the transformation of dissolved organic matter in a subalpine lake. Limnology and Oceanography. 63(3), 1355-1371.

Ekholma, P., Lehtoranta, J., Taka, M., Sallantaus, T., Riihimäki, J., 2020. Diffuse sources dominate the sulfate load into Finnish surface waters. Science of the Total Environment. 748, 141297.

Emerson, J.B., Varner, R.K., Wik, M., Parks, D.H., Neumann, R.B., Johnsom, J.E., Singleton, C.M., Woodcroft, B., Tollerson, R., Owusu-Dommey, A., Binder, M., Freitas, N.L., Crill, P.M., Saleska, S.R., Tyson, G.W., Rich, V.I., 2021. Diverse sediment microbiota shape methane emission temperature sensitivity in Arctic lakes. Nature Communications. 12(1), 5815.

Emilson, E.J.S., Carson, M.A., Yakimovich, K.M., Osterholz, H., Dittmar, T., Gunn, J.M., Mykytczuk, N.C.S., Basiliko, N., Tanentzap, A.J., 2018. Climate-driven shifts in sediment chemistry enhance methane production in northern lakes. Nature Communications. 9, 1801.

Farjalla, V.F., Marinho, C.C., Faria, B.M., Amado, A.M., Esteves, F.D., Bozelli, R.L., Giroldo, D., 2009. Synergy of fresh and accumulated organic matter to bacterial growth. Microbial Ecology. 57(4), 657-666.

Fernandez, J.E., Peeters, F., Hofmann, H., 2016. On the methane paradox: transport from shallow water zones rather than in situ methanogenesis is the major source of CH_4 in the open surface water of lakes. Journal of Geophysical Research: Biogeosciences, 121(10), 2717-2726.

Fike, D.A., Bradley, A.S., Rose, C.V., 2015. Rethinking the ancient sulfur cycle. Annual Review of Earth and Planetary Science. 43, 593-622.

Gantzer, C.J., Stefan, H.G., 2003. A model of microbial activity in lakes sediments in response to periodic water-column mixing. Water Research. 37(12), 2833-2846.

Goni, M.A., Teixeira, M.J., Perkey, D.W., 2003. Sources and distribution of organic matter in a river-dominated estuary (Winyah Bay, SC, USA). Estuarine Coastal and Shelf Science, 57(5-6): 1023-1048.

Gontijo, E.S.J., Herzsprung, P., Lechtenfeld, O.J., Bueno, C.D., Barth, J.A.C., Rosa, A.H., Friese, K., 2021. Muti-proxy approach involving ultrahigh resolution mass spectrometry and self-organising maps to investigate the origin and quality of sedimentary organic matter across a subtropical reservoir. Organic Geochemistry. 151, 104165.

Grasset, C., Mendonca, R., Saucedo, G.V., Bastviken, D., Roland, F., Sobek, S., 2018. Large but variable methane production in anoxic freshwater sediment upon addition of allochthonous and autochthonous organic matter. Limnology and Oceanography, 63(4): 1488-1501.

Gudasz, C., Bastviken, D., Premke, K., Steger, K., Tranvik, L.J., Constrained microbial processing of allochthonous organic carbon in boreal lake sediments. Limnology and Oceanography, 57(1): 163-175.

Gudasz, C., Bastviken, D., Steger, K., Premke, K., Sobek, S., Tranvik, L.J., 2010. Temperature-controlled organic mineralization in lake sediments. Nature, 466(7305): 478-U3.

Guillemette, F., von Wachenfeldt, E., Kothawala, D.N., Bastviken, D., Tranvik, L.J., 2017. Preferential sequestration of terrestrial organic matter in boreal lake sediments. Journal of Geophysical Research: Biogeosciences. 122(4), 863-874.

Guo, X.J., Yu, H.B., Yan, Z.C., Gao, H.J., Zhang, Y.Z., 2018. Tracking variations of fluorescent dissolved organic matter during wastewater treatment by accumulative fluorescence emission spectroscopy combined with principal component, second derivative and canonical correlation analyses. Chemosphere. 194, 463-470.

Habicht, K.S., Miller, M., Cox, R.P., Frigaard, N.U., Tonolla, M., Peduzzi, S., Falkenby, L.G., Andersen, J.S., 2011. Comparative proteomics and activity of a green sulfur bacterium through the water column of Lake Cadagno, Switzerland. Environmental Microbiology. 13(1), 203-215.

Hall, S.J., Silver, W.L., Timokhin, V.I., Hammel, K.E., 2015. Lignin decomposition is sustained under fluctuating redox conditions in humid tropical forest soils. Global

Change Biology. 21(7), 2818-2828.

Handley, K.M., VerBerkmoes, N.C., Steefel, C.I., Williams, K.H., Sharon, I., Miller, C.S., Frischkorn, K.R., Chourey, K., Thomas, B.C., Shah, M.B., 2012. Biostimulation induces syntrophic interactions that impact C, S and N cycling in a sediment microbial community. The ISME Journal. 7(4), 800-816.

Hansel, C. M., Lentini, C.J., Tang, Y.Z., Johnston, D.T., Wankel, S.D., Jardine, P.M., 2015. Dominance of sulfur-fueled iron oxide reduction in low-sulfate freshwater sediments. The ISME Journal. 9(11), 2400-2412.

Hassan, M., Talbot, J., Arsenault, J., Martinez-Cruz, K., Sepulveda-Jauregui, A., Hoyo-Santillan, J., Lapierre, J.F., 2023. Linking dissolved organic matter to CO_2 and CH_4 concentrations in Canadian and Chilean peatland pools. Global Biogeochemical Cycles. 37(4), e2023GB007715.

Hausmann, B., Knorr, K.-H., Schreck, K., Tringe, S.G., del Rio, T.G., Loy, A., Pester, M., 2016. Consortia of low-abundance bacteria drive sulfate reduction-dependent degradation of fermentation products in peat soil microcosms. The ISME Journal. 10(10), 2365-2375.

He, Z., Xu, S., Zhao, Y., Pan, X., 2019. Methane emissions from aqueous sediments are influenced by complex interactions among microbes and environmental factors: a modeling study. Water Research, 166, 115086.

Ho, J.C., Michalak, A.M., Pahlevan, N., 2019. Widespread global increase in intense lake phytoplankton blooms since the 1980s. Nature, 574(7780), 667-683.

Holgerson, M.A., Raymond, P., 2016. Large contribution to inland water CO_2 and CH_4 emissions from very small ponds. Nature Geoscience, 9(3), 222-226.

Holmer, M., Storkholm, P., 2001. Sulphate reduction and sulphur cycling in lake sediments: a review. Freshwater Biology. 46, 431-451.

Hong, Z.C., Ma, H., Zhang, T., Wang, Q.R., Chang, Y.L., Song, Y.Y., Li, Z., Cui, F.Y., 2023. Joint role of land cover types and microbial processing on molecular composition of dissolved organic matter in inland lakes. Science of the Total Environment. 857, 159522.

Hosen, J.D., McDonough, O.T., Febria, C.M., Palmer, M.A., 2014. Dissolved organic matter quality and bioavailability changes across an urbanization gradient in Headwater streams. Environmental Science & Technology. 48(14), 7817-7824.

Hopkins, D.W., Sparrow, A.D., Elberling, B., Gregorich, E.G., Novis, P.M., Greenfield,

L.G., Tilston, E.L., 2006. Carbon, nitrogen and temperature controls on microbial activity in soils from an Antarctic dry valley. Soil Biology & Biochemistry. 38(10), 3130-3140.

Hsieh, Y.P., Shieh, Y.N., 1997. Analysis of reduced inorganic sulfur by diffusion methods: improved apparatus and evaluation for sulfur isotopic studies. Chemical Geology. 137(3), 255-261.

Hu, H., Chen, J., Zhou, F., Nie, M., Hou, D.Y., Liu, H., Delgado-Baquerizo, M., Ni, H.W., Huang, W.G., Zhou, J.Z., Song, X.W., Cao, X.F., Sun, B., Zhang, J.B., Crowther, T.W., Liang, Y.T., 2024. Relative increases in CH_4 and CO_2 emissions from wetlands under global warming dependent on soil carbon substrates. Nature Geoscience. 17, 26-31.

Huang, J.C., Gao, J.F., Zhang, Y.J., 2016. Eutrophication prediction using a markov chain model: Application to Lakes in the Yangtze River Basin, China. Environmental Modeling & Assessment, 21(2): 233-246.

Huisman, J., Sharples, J., Stroom, J.M., Visser, P.M., Kardinaal, W.E.A., Verspagen, J.M., Sommeijer, B., 2004. Changes in turbulent mixing shift competition for light between phytoplankton species. Ecology, 85(11), 2960-2970.

IPCC, 2014. Climate change 2014 Synthesis Report Summary Chapter for Policymakers. Ipcc, p. 31.

Isles, P.D.F., Xu, Y.Y., Stockwell, J.D., Scgroth, A.W., 2017. Climate-driven changes in energy and mass inpuuts systematically alter nutrient oncentration and stoichiometry in deep and shallow regions of Lake Champlain. Biogeochemistry. 133(2): 201-217.

Jantharadej, K., Limpiyakorn, T., Kongprajug, A., Mongkolsuk, S., Sirikanchana, K., Suwannasilp, B.B., 2021. Microbial community compositions and sulfate-reducing bacterial profiles in malodorous urban canal sediments. Archives of Microbiology. 203(5), 1981-1993.

Jiang, G.J., Ma, R.H., Loiselle, S.A., Duan, H.T., Su, W., Cai, W.X., Huang, C.G., Yang, J., Yu, W., 2015. Remote sensing of particulate organic carbon dynamics in a eutrophic lake (Taihu Lake, China). Science of the Total Environment, 532: 245-254.

Jiang, G.J., Su, W., Zhang, C.C., Deng, W., Wang, X.R., Yang, Z.X., Lv, X.L., Lu, C.Q., Li, S.Y., Ma, R.H., Huang, X.H., Ye, L.J., Wang, M., Yu, W., 2022. Satellite

determining dominant sources of particulate carbon across different eutrophic waters. Ecological Indicators, 142: 109302.

Jin, H., Yoon, T.K., Begum, M.S., Lee, E.J., Oh, N.H., Kang, N., Park, J.H., 2018. Longitudinal discontinuities in riverine greenhouse gas dynamics generated by dams and urban wastewater. Biogeosciences. 15(20), 6349-6369.

Jin, X., 1995. Lake environment in China. Ocean Press, Beijing.

Jorgensen, B.B., Findlay, A.J., Pellerin, A., 2019. The biogeochemical sulfur cycle of marine sediments. Frontiers in microbiology. 10, 849-849.

Jung, B.J., Jeanneau, L., Alewell, C., Kim, B., Park, J.H., 2015. Downstream alteration of the composition and biodegradability of particulate organic carbon in a mountainous, mixed land-use watershed. Biogeochemistry. 122(1), 79-99.

Kopacek, J., Turek, J., Hejzlar, J., Kana, J., Porcal, P., 2006. Element fluxes in watershed-lake ecosystems recovering from acidification: Plesne Lake, the Bohemian Forest, 2001-2005. Biologia. 61, S427-S440.

Kumar, A., Mishra, S., Bakshi, S., Upadhyay, P., Thakur, T.K., 2022. Response of eutrophication and water quality drivers on greenhouse gas emissions in lakes of China: A critical analysis. Ecohydrology, e2483.

Lambert, T., Bouillon, S., Darchambeau, F., Morana, C., Roland, F.A.E., Descy, J.P., Borges, A.V., 2017. Effects of human land use on the terrestrial and aquatic sources of fluvial organic matter in a temperate river basin (The Meuse River, Belgium). Biogeochemistry. 136(2), 191-211.

Lambert, T., Perolo, P., Escoffier, N., Perga, M.E., 2022. Enhanced bioavailability of dissolved organic matter (DOM) in human-disturbed streams in Alpine fluvial networks. Biogeosciences. 19(1), 187-200.

Lammers, J.M., Schubert, C.J., Middelburg, J.J., Reichart, G.J., 2016. Carbon flows in eutrophic Lake Rotsee: a ^{13}C-labelling experiment. Biogeochemistry, 131(1-2): 147-162.

Lenhart, K., Klintzsch, T., Langer, G., Nehrke, G., Bunge, M., Schnell, S., Keppler, F., 2016. Evidence for methane production by the marine algae Emiliania huxleyi. Biogeosciences, 13(10): 3163-3174.

Lennon, J.T., Faiia, A.M., Feng, X.H., Cottingham, K.L., 2006. Relative importance of CO_2 recycling and CH_4 pathways in lake food webs along a dissolved organic carbon gradient. Limnology and Oceanography, 51(4): 1602-1613.

Li, J., Takii, S., Kotakemori, R., 1996. Sulfate reduction in profundal sediments in lake Kizaki. Hydrobiologia. 333, 201-208.

Li, L.L., Xue, B., Yao, S.C., Tao, Y.Q., Yan, R.H., 2018a. Spatial-temporal patterns of methane dynamics in Lake Taihu. Hydrobiologia, 822(1), 143-156.

Li, Y., Xu, C., Zhang, W.L., Lin, L., Wang, L.F., Niu, L.H., Zhang, H.J., Wang, P.F., Wang, C., 2020. Response of bacterial community in composition and function to the various DOM at river confluences in the urban area. Water Research. 169, 115293.

Li, Z.C., Zhao, Y.P., Xu, X.G., Han, R.M., Wang, M.Y., Wang, G.X., 2018b. Migration and transformation of dissolved carbon during accumulated cyanobacteria decomposition in shallow eutrophic lakes: a simulated microcosm study. PEERJ, 6, e5922.

Liu, B.G., Peng, Y., Yu, M.T., Zhou, M.C., Zhang, L.Q., Chen, L., Jia, R.Y., Zhou, C.Q., Wu, Y.T., Xu, X.G., Wang, G.X., 2022. The insignificant effect of increased sulfate concentration on nitrogen dynamics in eutrophic lakes: the neglected role of iron ions. Marine and Freshwater Research. 73(11), 1369-1378.

Liu, D., Du, X.Y., Yu, S.J., Luo, J.H., Duan, H.T., 2019. Human activities determine quantity and composition of dissolved organic matter in lakes along the Yangtze River. Water Research. 168, 115132.

Liu, L., Fang, Y.C., Wang, Y., Xiang, H., Sun, X.L., 2022. Effects of photodegradation on carbon components of different land use types in typical fault subsidence lakes: Taking Xingyu Lake as an example. Fresenius Environmental Bulletin. 31(4), 4382-4394.

Liu, M.D., Wu, T., Zhao, X.Y., Zan, F.Y., Yang, G., Miao, Y.Q., 2021. Cyanobacteria blooms potentially enhance volatile organic compound (VOC) emissions from a eutrophic lake: Field and experimental evidence. Environmental Research, 202, 111664.

Liu, S.L., Trevathan-Tackett, S.M., Lewis, C.J.E., Huang, X.P., Macreadie, P.I., 2020. Macroalgal blooms trigger the breakdown of seagrass blue carbon. Environmental Science & Technology. 54(22), 14750-14760.

Long, M.A., Wu, J.L., 2009. Environmental significance from organic carbon and its isotope of Angulinao lake sediment. Journal of Natural Resources. 24(6), 1099-1104.

Lu, X., Zhou, X.T., Xu, Y.F., Ruan, A.D., Yu, Z.B., 2021. The investigation of the connections among hydrogeological factors and the emissions of two greenhouse gases in lake sediment. Water Resources Research. 57(5), e2020WR029375.

Luo, J.W., Zhou, Q.X., Hu, X.G., Zeng, H., Deng, P., He, C., Shi, Q., 2022. Lake chemodiversity driven by natural and anthropogenic factors. Environmental Science & Technology. 56(9), 5910-5919.

Lyautey, E., Billard, E., Tissot, N., Jacquet, S., Domaizon, I., 2021. Seasonal dynamics of abundance, structure, and diversity of methanogens and methanotrophs in lake sediments. Microbial Ecology. 82(3), 559-571.

Ma, H.H., Zhu, Y.R., Jiang, J., Bing, X.J., Xu, W.N., Hu, X.Y., Zhang, S.L., Shen, Y.Q., He, Z.Q., 2022. Characteristics of inorganic and organic phosphorus in Lake Sha sediments from a semiarid region, Northwest China: Sources and bioavailability. Applied Geochemistry, 137: 105209.

Ma, J., He, F., Yan, X.C., Shi, R.J., Ji, M., Xu, B., Wu, X.D., Li, Z.C., Xu, X.G., Wang, G.X., 2022. Stoichiometric flexibility regulates the co-metabolism effect during organic carbon mineralization in eutrophic lacustrine sediments. Journal of Oceanology and Limnology. 40(5), 1974-1984.

Ma, J., Xu, X.G., Yu, C.C., Liu, H.C., Wang, G.X., Li, Z.C., Xu, B., Shi, R.J., 2020. Molecular biomarkers reveal co-metabolism effect of organic detritus in eutrophic lacustrine sediments. Science of the Total Environment, 698, 134328.

Ma, J., Zhou, M.C., Peng, Y., Tuo, Y., Zhou, C.Q., Liu, K.X., Huang, Y.L., He, F., Lai, Q.Y., Zhang, Z.H., Kinouchi, T., Li, S.Y., Xu, X.G., Wu, X.D., Lin, X.W., Li, W.X., Wang, G.X., 2024. Instability in a carbon pool driven by multiple dissolved organic matter sources in a eutrophic lake basin: Potential factors for increased greenhouse gas emissions. Journal of Environmental Management. 350, 119697.

Ma, Y.M., Mao, R., Li, S.Y., 2021. Hydrological seasonality largely contributes to riverine dissolved organic matter chemical composition: Insights from EEM-PARAFAC and optical indicators. Journal of Hydrology. 595, 125993.

Mao, Z.G., Gu, X.H., Cao, Y., Luo,J.H., Zeng, Q.F., Chen, H.H., Jeppesen, E., 2021. How does fish functional diversity respond to environmental changes in two large shallow lakes? Science of the total environment. 753, 142158.

Martin, N., McEachern, P., Yu, T., Zhu, D.Z., 2013. Model development for prediction and mitigation of dissolved oxygen sags in the Athabasca River, Canada. Science

of the Total Environment. 443, 403-412.

Martinez-Cruz, K., Sepulveda-Jauregui, A., Casper, P., Anthony, K.W., Smemo, K.A., Thalasso, F., 2018. Ubiquitous and significant anaerobic oxidation of methane in freshwater lake sediments. Water Research. 144, 332-340.

Medeiros, P.M., Seidel, M., Ward, N.D., Carpenter, E.J., Gomes, H.R., Niggemann, J., Krusche, A.V., Richey, J.E., Yager, P.L., Dittmar, T., 2015. Fate of the Amazon River dissolved organic matter in the tropical Atlantic Ocean. Clobal Biogeochemical Cycles. 29(5), 677-690.

Michalak, A.M., Anderson, E.J., Beletsky, D., Boland, S., Bosch, N.S., Bridgeman, T.B., DePinto, J.V., 2013. Record-setting algal bloom in Lake Erie caused by agricultural and meteorological trends consistent with expected future conditions. Proceedings of the National Academy of Sciences of the United States of America. 110 (16), 6448-6452.

Miller, S.M., Miller, C.E., Commane. R., Chang, R.Y.W., Dinardo, S.J., Henderson, J.M., Karion, A., Lindaas, J., Melton, J.R., Miller, J.B., Sweeney, C., Wofsy, S.C., Michalak, A.M., 2016. A multiyear estimate of methane fluxes in Alaska from CARVE atmospheric observations. Global Biogeochemical Cycles. 30(10), 1441-1453.

Mitrovic, S.M., Baldwin, D.S., 2016. Allochthonous dissolved organic carbon in river, lake and coastal systems: transport, function and ecological role. Marine and Freshwater Research, 67(9): 1-4.

Mizandrontsev, I.B., Kozlov, V.V., Ivanov, V.G., Kucher, K.M., Korneva, E.S., Granin, N.G., 2020. Vertical distribution of methane in Baikal water. Water Resources, 47(1): 122-129.

Mostofa, K.M.G., Li, W., Wu, F.C., Liu, C.Q., Liao, H.Q., Zeng, L., Xiao, M., 2018. Environmental characteristics and changes of sediment pore water dissolved organic matter in four Chinese lakes. Environmental Science and Pollution Reearch. 25(3), 2783-2804.

Murase, J., Sakai, Y., Kametani, A., Sugimoto, A., 2005. Dynamics of methane in mesotrophic Lake Biwa, Japan. Ecological Research. 20(3), 377-385.

Musenze, R.S., Fan, L., Grinham, A., Werner, U., Gale, D., Udy, J., Yuan, Z.G., 2016. Methane dynamics in subtropical freshwater reservoirs and the mediating microbial communities. Biogeochemistry, 128(1-2), 233-255.

Nakayam, T., Pelletier, G.J., 2018. Impact of global major reservoirs on carbon cycle changes by using an advanced eco-hydrologic and biogeochemical coupling model. Ecological Modelling, 387: 172-186.

Ni, M.F., Ma, Y.M., Wang, Z.K., Wang, X.D., Zhu, S.X., 2022. A distinctive mode of dissolved organic carbon biodegradation in karst lakes and reservoirs: Evidence from trophic controls and compositional transformations. 368, 133217.

Ochs, C.A., Capello, H.E., Pongruktham, O., 2010. Bacterial production in the lower mississippi River: importance of suspended sediment and phytoplankton biomass. Hydrobiologia, 637(1): 19-31.

Paerl, H.W., Otten, T.G., 2013. Harmful cyanobacterial blooms: causes, consequences, and controls. Microbial Ecology. 65(4), 995-1010.

Paerl, H.W., Paul., V.J., 2012. Climate change: links to global expansion of harmful cyanobacteria. Water Research, 46(5), 1349-1363.

Palma-Silva, C., Marinho, C.C., Albertoni, E.F., Giacomini, I.B., Barros, M.P.F., Furlanetto, L.M., Trindade, C.R.T., Esteves, F.D., 2014. Methane emissions in two small shallow neotropical lakes: The role of temperature and trophic level. Atmospheric Environment, 81: 373-379.

Pan, F., Liu, H.T., Guo, Z.R., Li, Z.W., Wang,B., Cai, Y., Gao, A. G., 2018. Effects of tide and season changes on the iron-sulfur-phosphorus biogeochemistry in sediment porewater of a mangrove coast. Journal of Hydrology. 568, 686-702.

Park, H.K., Byeon, M.S., Shin, Y.N., Jung, D.I., 2009. Sources and spatial and temporal characteristics of organic carbon in two large reservoirs with contrasting hydrologic characteristics. Water Resources Research, 45: W11418.

Pelechata, A., Pelechaty, M., Pukacz, A., 2016. Factors influencing cyanobacteria community structure in Chara-lakes. Ecological Indicators, 71, 477-490.

Peng, Y., Zhou, C.Q., Jin, Q., Ji, M., Wang, F.Y., Lai, Q., Shi, R.J., Xu, X.G., Chen, L.G., Wang, G.X., 2022. Tidal variation and litter decomposition co-affect carbon emissions in estuarine wetlands. Science of the Total Environment, 839, 156357.

Perez, M.T., Rofner, C., Sommaruga, R., 2015. Dissolved organic monomer partitioning among bacterial groups in two oligotrophic lakes. Environmental Microbiology Reports, 7(2), 265-272.

Persaud, A.D., Paterson, A.M., Ingram, R., Yao, H.X., Dillon, P.J., 2014. Potential factors leading to the formation of cyanobacterial scums in a mesotrophic softwater

lake in Ontario, Canada. Lake and Reservoir Management, 30(4): 331-343.

Pester, M., Knorr, K.H., Friedrich, M.W., Wagner, M., Loy, A., 2012. Sulfate-reducing microorganisms in wetlands-fameless actors in carbon cycling and climate change. Frontiers in Microbiology. 3, 72.

Peter, S., Agstam, O., Sobek, S., 2017. Widespread release of dissolved organic carbon from anoxic boreal lake sediments. Inland Waters. 7(2), 151-163.

Perez-Coronel, E., Beman, J.M., 2022. Multiple sources of aerobic methane production in aquatic ecosystems include bacterial photosynthesis. Nature Communications. 13(1), 6454.

Platka, D.R., Frank, A.H., Kohler, I., Castiglione, K., van Geldern, R., Geldern, R., Barth, J.A.C., 2022. Balance of carbon species combined with stable isotope ratios show critical switch towards bicarbonate uptake during cyanobacteria blooms. Science of the Total Environment, 807(3), 151067.

Pimenov, N.V., Kalmychkov, G.V., Veryasov, M.B., Sigalevich, P.A., Zemskaya, T.I., 2014. Microbial oxidation of methane in the sediments of central and southern Baikal. Microbiology. 83(6), 773-781.

Preheim, S.P., Olesen, S.W., Spencer, S.J., 2016. Surveys, simulation, and single-cell assays relate function and phylogeny in a lake ecosystem. Nature Microbiology. 1(9), 16130.

Qi, C., Zhang, L.M., Fang, J.Q., Lei, B., Tang, H.X., Wang, Z.S., Si, Z.J., Wang, G.X., 2020. Benthic cyanobacterial detritus mats in lacustrine sediment: Characterization and odorant producing potential. Environmental Pollution. 256, 113453.

Rabus, R., Ruepp, A., Frickey, T., Rattei, T., Fartmann, B., Stark, M., Bauer, M., Zibat, A., Lombardot, T., Becker5, I., Amann, J., Gellner, k., Teeling, H., Leuschner, W.D., Glockner, F.O., Lupas, A.N., Amann, R., Klenk, H.P., 2004. The genome of Desulfotalea psychrophila, a sulfate-reducing bacterium from permanently cold Arctic sediments. Environmental Microbiology. 6(9), 887-902.

Raveh, A., Avnimelech, Y., 1979. Total nitrogen analysis in water, soil and plant material with persulphate oxidation. Water Research. 13(9), 911-912.

Raymond, P.A., Hartmann, J., Lauerwald, R., Sobek, S., McDonald, C., Hoover, M., Butman, D., Striegl, R., Mayorga, E., Humborg, C., Kortelainen, P., Durr, H., Meybeck, M., Ciais, P., Guth, P., 2014. Global carbon dioxide emissions from inland waters. Nature. 507(7492), 355.

Repeta, D.J., Ferron, S., Sosa, O.A., Johnson, C.G., Repeta, L.D., Acker, M., DeLong, E.F., Karl, D.M., 2016. Marine methane paradox explained by bacterial degradation of dissolved organic matter. Nature Geoscience, 9(12): 884.

Roland, F.A.E., Darchambeau, F., Morana, C., Bouillon, S., Borges, A.V., 2017. Emission and oxidation of methane in a meromictic, eutrophic and temperate lake (Dendre, Belgium). Chemosphere, 168, 756-764.

Rosentreter, J.A., Borges, A.V., Deemer, B.R., Holgerson, M.A., Liu, S.D., Song, C.L., Melack, J., Raymond, P.A., Duarte, C.M., Allen, G.H., Olefeldt, D., Poulter, B., Battin, TI., Eyre, B.D., 2021. Half of global methane emissions come from highly variable aquatic ecosystem sources. Nature Geoscience. 14(4), 225.

Sakai, Y., Karube, Z., Takeyama, T., Kohzu, A., Yoshimizu, C., Nagata, T., Tayasu, I., Okuda, N., 2013. Seasonal and site-specific variability in terrigenous particulate organic carbon concentration in near-shore waters of Lake Biwa, Japan. Limnology, 14(2): 167-177.

Sanches, L.F., Guenet, B., Marinho, C.C., Barros, N., Esteves, F.D., 2021. Global regulation of methane emission from natural lakes. Scientific Reports. 11(1), 21294.

Sandfeld, T., Marzocchi, Ugo., Petro, Caitlin., Schramm, Andreas., Risgaard-Petersen, N., 2020. Electrogenic sulfide oxidation mediated by cable bacteria stimulates sulfate reduction in freshwater sediments. The ISME Journal. 14(5), 1233-1246.

Saxton, M. A., Samarkin, V. A., Madigan, M.T., Bowles, M.W., Sattley, W. M., Schutte, C.A., Joye, S.B., 2021. Sulfate reduction and methanogenesis in the hypersaline deep waters and sediments of a perennially ice-covered lake. Limnology and Oceanography Letters. 66(5), 1804-1818.

Schulz, M., Faber, E., Hollerbach, A., Schroder, H.G., Gude, H., 2001. The methane cycle in the epilimnion of Lake Constance. Archiv Fur Hydrobiologie, 151(1): 157-176.

Sepulveda-Jauregui, A., Hoyos-Santillan, J., Martinez-Cruz, K., Anthony, K.M.W., Casper, P., Beimonte-Izquierdo, Y., Thalasso, F., 2018. Eutrophication exacerbates the impact of climate warming on lake methane emission. Science of the Total Environment, 636: 411-419.

Shamrin, A.M., Pestunov, D.A., Domysheva, V.M., Ivanov, V.G., Sakirko, M.V., Panchenko, M.V., 2019. Greenhouse gases, nutrients and fluorescent characteristics

of the lake Baikal water in the zones of spring homothermia formation. 25th International Symposium on Atmospheric and Ocean Optics: Atmospheric Physics, 11208, 112084E.

Shao, K.Q., Gao, G., Chi, K.X., Qin, B.Q., Tang, X.M., Yao, X., Dai, J.Y., 2013. Decomposition of microcystis blooms: implications for the structure of the sediment bacterial community, as assessed by a mesocosm experiment in Lake Taihu, China. Journal of Basic Microbiology, 53(6), 549-554.

Shen, Q.S., Liu, C., Zhou, Q.L., 2013. Effects of physical and chemical characteristics of surface sediments in the formation of shallow lake algae-induced black bloom. Journal of Environmental Sciences. 25(12), 2353-2360.

Shi, L.M., Huang, Y.X., Lu, Y.P., Chen, F.Z., Zhang, M., Yu, Y., Kong, F.X., 2018. Stocks and dynamics of particulate and dissolved organic matter in a large, shallow eutrophic lake (Taihu, China) with dense cyanobacterial blooms. Journal of Oceanology and Limnology, 36(3): 738-749.

Shi, L.M., Huang, Y.X., Zhang, M., Yu, Y., Lu, Y.P., Kong, F.X., 2017. Bacterial community dynamics and functional variation during the long-term decomposition of cyanobacterial blooms in-vitro. Science of the Total Environment, 598: 77-86.

Shi, R.J., Ma, J., Lv, C.X., Xu, X.G., Dang, X.Y., Jiang, Y.N., Ye, Z., Wu, Y.T., 2021. Accumulation and decomposition of cyanobacteria and reed debris in eutrophic lakes and its potential co-metabolism effects. Journal of Lake Science, 33(4), 1062-1071.

Shirokova, L.S., Kunhel, L., Rols, J.L., Pokrovsky, O.S., 2015. Experimental modeling of cyanobacteria bloom in a Thermokarst Lake: fate of organic carbon, trace metal, and carbon sequestration potential. Aquatic Geochemistry. 21(6), 487-511.

Smith, C.R., Sleighter, R.L., Hatcher, P.G., Lee, J.W., 2013. Molecular characterization of inhibiting biochar water-extractable substances using electrospray ionization fourier transform ion cyclotron resonance mass spectrometry. Environmental Science & Technology. 47(33), 13294-13302.

Solomon, C.T., Jones, S.E., Weidei, B.C., Buffam. I., Fork, M.L., Karlsson, J., Larsen, S., Lennon, J.T., Read, J.S., Sadro, S., Saros, J.E., 2015. Ecosystem consequences of changing inputs of terrestrial dissolved organic matter to lakes: current knowledge and future challenges. Ecosystems, 18(3): 376-389.

Song, J.M., Xu, Y.F., Hu, W.P., Ni, L.Y., 2008. Biogeochemistry of carbon in China seas

and lakes. p424-493.

Song, K.S., Wen, Z.D., Xu, J.Y., Yang, H., Lyu, L.L., Zhao, Y., Fang, C., Shang, Y.X., Du, J., 2018. Dissolved carbon in a large variety of lakes across five limnetic regions in China. Journal of Hydrology. 563, 143-154.

Song, N., Bai, L.L., Xu, H.C., Jiang, H.L., 2020. The composition differences of macrophyte litter-derived dissolved organic matter by photodegradation and biodegradation: Role of reactive oxygen species on refractory component. Chemosphere. 242, 125155.

Song, X.Y., Zhang, C.H., Su, X.Y., Zhu, L.J., Wei, Z.M., Zhao, Y., 2021. Characteristics of humic substance in lake sediments: The case of lakes in northeastern China. Journal of Hydrology. 603, 127079.

Soued, C., Harrison, J.A., Mercier-Blais, S., Prairie, Y.T., 2022. Reservoir CO_2 and CH_4 emissions and their climate impact over the period 1900-2060. Nature Geoscience. 15(9), 700.

Stackpoole, S.M., Butman, D.E., Clow, D.W., Verdin, K.L., Gaglioti, B.V., Genet, H., Striegl. R.G., 2017. Inland waters and their role in the carbon cycle of Alaska. Ecological Applications, 27(5): 1403-1420.

Steffenhagen, P., Zak, D., Schulz, K., Timmermann, T., Zerbe, S., 2012. Biomass and nutrient stock of submersed and floating macrophytes in shallow lakes formed by rewetting of degraded fens. Hydrobiologia. 692(1), 99-109.

Steinsdottir, H.G.R., Schauberger, C., Mhatre, S., Thamdrup, B., Bristow, L.A., 2022. Aerobic and anaerobic methane oxidation in a seasonally anoxic basin. Limnology and Oceanography. 67(6), 1257-1273.

Sun, H.Y., Yu, R.H., Liu, X.Y., Cao, Z.X., Li, X.W., Zhang, Z.Z., Wang, J., Zhuang, S., Ge, Z., Zhang, L.X., Sun, L.Q., Lorke, A., Yang, J., Lu, C.W., Lu, X.X., 2022. Drivers of spatial and seasonal variations of CO_2 and CH_4 fluxes at the sediment water interface in a shallow eutrophic lake. Water Research. 222, 118916.

Sun, Y.J., Lu, S.Q., Lin, W.Q., Wang, D.Z., Fan, J.Y., Li, Z., 2016. In-situ study on nutrient release fluxes from shallow lake sediments under wind-driven waves. Journal of Hydrodynamics, 28(2): 247-254.

Tabatabai, M. A., 1974. Rapid method for determination of sulfate in water samples. Environmental letters. 7, 237-243.

Tang, K.W., McGinnis, D.F., Ionescu, D., Grossart, H.P., 2016. Methane production in

oxic lake waters potentially increases aquatic methane flux to air. Environmental Science & Technology Letters, 3(6), 227-233.

Tang, K.W., McGinnis, D.F., Frindte, K., Bruchert, V., Grossart, H.P., 2014. Paradox reconsidered: methane oversaturation in well-oxygenated lake waters. Limnology and Oceanography, 59(1): 275-284.

Thottathil, S.D., Reis, P.C.J., Praire, Y.T., 2019. Methane oxidation kinetics in northern freshwater lakes. Biogeochemistry. 143(1), 105-116.

Tian, K., Kong, X.S., Yuan, L.H., Lin, H., He, Z.H., Yao, B., Ji, Y.L., Yang, J.B., Sun, S.C., Tian, X.J., 2019. Priming effect of litter mineralization: the role of root exudate depends on its interactions with litter quality and soil condition. Plant and Soil, 440(1-2), 457-471.

Torres, I.C., Inglett, K.S., Reddy, K.R., 2011. Heterotrophic microbial activity in lake sediments: effects of organic electron donors. Biogeochemistry. 104(1-3), 165-181.

Tranvik, L.J., Downing, J.A., Cotner, J.B., Loiselle, S.A., Striegl, R.G., Ballatore, T.J., Dillon, P., Finlay, K., Fortino, K., Knoll, L.B., Kortelainen, P.L., Kutser, T., Larsen, S., Laurion, I., Leech, D.M., McCallister, S.L., McKnight, D.M., Melack, J.M., Overholt, E., Porter, J.A., Prairie, Y., Renwick, W.H., Roland, F., Sherman, B.S., Schindler, D.W., Sobek, S., Tremblay, A., Vanni, M.J., Verschoor, A.M., von Wachenfeldt, E., Weyhenmeyer, G.A., 2009. Lakes and reservoirs as regulators of carbon cycling and climate. Limnology and Oceanography. 54(6), 2298-2314.

Tripathi, A.K., Thakur, P., Saxena, P., Rauniyar, S., Gopalakrishnan, V., Singh, R.N., Gadhamshetty, V., Gnimpieba, E.Z., Jasthi, B.K., Sani, R.K., 2021. Gene sets and mechanisms of sulfate-reducing bacteria biofilm formation and quorum sensing with impact on corrosion. Frontiers in Microbiology. 12, 754140.

Tong, Y.D., Xu, X.W., Qi, M., Sun, J.J., Zhang, Y.Y., Zhang, W., Wang, M.Z., Wang, X.J., Zhang, Y., 2021. Lake warming intensifies the seasonal pattern of internal nutrient cycling in the eutrophic lake and potential impacts on algal blooms. Water Research. 188, 116570.

Townsend-Small, A., Disbennett, D., Fernandez, J.M., Ransohoff, R.W., Mackay, R., Bourbonniere, R.A., 2016. Quantifying emissions of methane derived from anaerobic organic matter respiration and natural gas extraction in Lake Erie. Limnology and Oceanography, 61, S356-S366.

Usman, M., Shi, Z.j., Ren, S., Ngo, H.H., Luo, G.; Zhang, S.C., 2020. Hydrochar

promoted anaerobic digestion of hydrothermal liquefaction wastewater: Focusing on the organic degradation and microbial community. Chemical Engineering Journal. 399, 125766.

Valle, J., Gonsior, M., Harir, M., Enrich-Prast, A., Schmitt-Kopplin, P., Bastviken, D., Conrad, R., Hertkorn, N., 2018. Extensive processing of sediment pore water dissolved organic matter during anoxic incubation as observed by high-field mass spectrometry (FTICR-MS). Water Research. 129, 252-263.

Van der Kooij, D., Veenendaal, H.R., van der Mark, E.J., Dignum, M., 2017. Assessment of the microbial growth potential of slow sand filtrate with the biomass production potential test in comparison with the assimilable organic carbon method. Water Research. 125, 270-279.

Verpoorter, C., Kutser, T., Seekell, D.A., Tranvik, L.J., 2014. A global inventory of lakes based on high-resolution satellite imagery. Geophysical Research Letter. 41(18), 6396-6402.

Villacorte, L.O., Ekowati, Y., Neu, T.R., Kleijn, J.M., Winters, H., Amy, G., Schippers, J.C., Kennedy, M.D., 2015. Characterization of algal organic matter produced by bloom-forming marine and freshwater algae. Water Research. 73, 216-230.

Vincon-Leite, B., Casenave, C., 2019. Modeling eutrophication in lake ecosystems: A review. Science of the Total Environment, 651: 2985-3001.

Wadham, J.L., Arndt, S., Tulaczyk, S., Stibal, M., Tranter, M., Telling, J., Lis, G.P., Lawson, E., Ridgwell, A., Dubnick, A., Sharp, M.J., Anesio, A.M., Butler., C.E.H., 2012. Potential methane reservoirs beneath Antarctica. Nature, 488(7413), 633-637.

Walter, K.M., Smith. L.C., Chapin, F.S., 2007. Methane bubbling from northern lakes: present and future contributions to the global methane budget. Philosophical Transactions of the Royal Society A-Mathematical Physical and Engineering Sciences, 365(1856), 1657-1676.

Wan, L.L., Cao, L., Song, C.L., Cao, X.Y., Zhou, Y.Y., 2023. Regulation of the nutrient cycle pathway and the microbial loop structure by different types of dissolved organic matter in lakes. Environmental Science & Technology. 57(1), 297-309.

Wang, J., Wei, Z.P., Chu, Y.X., Tian, G.M., He, R., 2022. Eutrophic levels and algae growth increase emissions of methane and volatile sulfur compounds from lakes. Environmental Pollution, 306: 119435.

Wang, J.Y., Chen, G.J., Kang, W.G., Hu, K., Wang, L., 2019. Impoundment intensity

determines temporal patterns of hydrological fluctuation, carbon cycling and algal succession in a dammed lake of Southwest China. Water Research, 148: 162-175.

Wang, S.Y., Gao, Y., Jia, J.J., Lu, Y., Sun, K., Ha, X.R., Li, Z.X., Deng, W.Q., 2022. Vertically stratified water source characteristics and associated driving mechanisms of particulate organic carbon in a large floodplain lake system. Water Research. 209, 117963.

Wang, P.F., Ma. J.J., Wang, X., Tan, Q.Q., 2020. Rising atmospheric CO_2 levels result in an earlier cyanobacterial bloom-maintenance phase with higher algal biomass. Water Research, 185, 116267.

Wasmund, K., Mußmann, M., Loy, A., 2017. The life sulfuric: microbial ecology of sulfur cycling in marine sediments. Environmental Microbiology Reports. 9(4), 323-344.

Wasswa, J., Driscoll. C.T., Zeng, T., 2022. Contrasting impacts of photochemical and microbial processing on the photoreactivity of dissolved organic matter in an Adirondack Lake watershed. 56(3), 1688-1701.

Wen, Z.D., Shang, Y.X., Song, K.S., Liu, G., Hou, J.B., Lyu, L., Tao, H., Li, S.J., He, C., Shi, Q., He, D., 2022. Composition of dissolved organic matter (DOM) in lakes responds to the trophic state and phytoplankton community succession. Water Research, 224: 119073.

West, W.E., Coloso, J.J., Jones, S.E., 2012. Effects of algal and terrestrial carbon on methane production rates and methanogen community structure in a temperate lake sediment. Freshwater Biology. 57(5), 949-955.

Williams, C.J., Frost, P.C., Morales-Williams, A.M., Larson, J.H., Richardson, W.B., Chiandet, A.S., Xenopoulos, M.A., 2016. Human activities cause distinct dissolved organic matter composition across freshwater ecosystems. Global Change Biology. 22(2), 613-626.

Wik, M., Varner, R.K., Anthony, K.W., Maclntyre, S., Bastviken, D., 2016. Climate-sensitive northern lakes and ponds are critical components of methane release. Nature Geoscience. 9(2), 99.

Worner, S., Pester, M., 2020. The active sulfate-reducing microbial community in littoral sediment of oligotrophic lake constance. Frontiers in microbiology. 10, 247.

Wu, S.J., Zhao, Y.P., Chen, Y.Y., Dong, X.M., Wang, M.Y., Wang, G.X., 2019. Sulfur cycling in freshwater sediments: A cryptic driving force of iron deposition and

phosphorus mobilization. Science of the Total Environment. 657, 1294-1303.

Xia, X.H., Liu, T., Yang, Z.F., Michalski, G., Liu, S.D., Jia, Z.M., Zhang, S., 2017. Enhanced nitrogen loss from rivers through coupled nitrification-denitrification caused by suspended sediment. Science of the Total Environment., 579, 47-59.

Xiao, K.Q., Beulig, F., Kjeldsen, K.U., Jorgensen, B.B., Risgaard-Petersen, N., 2017. Concurrent methane production and oxidation in surface sediment from Aarhus Bay, Denmark. Frontiers in Microbiology. 8, 1198.

Xiao, Q.T., Duan, H.T., Qin, B.Q., Hu, Z.H., Zhang, M., Qi, T.C., Lee, X.H., 2022. Eutrophication and temperature drive large variability in carbon dioxide from China's Lake Taihu. Limnology and Oceanography, 67(2), 379-391.

Xiao, Q.T., Zhang, M., Hu, Z.H., Gao, Y.Q., Hu, C., Liu, C., Liu, S.D., Zhang, Z., Zhao, J.Y., Xiao, W., Lee, X., 2017. Spatial variations of methane emission in a large shallow eutrophic lake in subtropical climate. Journal of Geophysical Research: Biogeosciences. 122(7), 1597-1614.

Xing, Y.P., Xie, P., Yang, H., Ni, L.Y., Wang, Y.S., Rong, K.W., 2005. Methane and carbon dioxide fluxes from a shallow hypereutrophic subtropical lake in China. Atmospheric Environment, 39(30), 5532-5540.

Xu, H., Paerl, H.W., Qin, B.Q., Zhu, G.W., Gao, G., 2010. Nitrogen and phosphorus inputs control phytoplankton growth in eutrophic Lake Taihu, China. Limnology and Oceanography. 55(1), 420-432.

Xu, H.C., Lin, H., Jiang, H.L., Guo, L.D., 2018. Dynamic molecular size transformation of aquatic colloidal organic matter as a function of pH and cations. Water Research. 144, 543-552.

Xu, J., Lei, S.H., Bi, S., Li, Y.M., Lyu, H., Xu, J.F., Xu, X.G., Mu, M., Miao, S., Zeng, S., Zheng, Z.B., 2020. Tracking spatio-temporal dynamics of POC sources in eutrophic lakes by remote sensing. Water Research, 168: 115162.

Xu, J., Lyu, H., Xu, X.G., Li, Y.M., Li, Z.C., Lei, S.H., Bi, S., Mu, M., Du, C.G., Zeng, S., 2019. Dual stable isotope tracing the source and composition of POM during algae blooms in a large and shallow eutrophic lake: All contributions from algae? Ecological Indicators. 102, 599-607.

Xu, L., Hu, Q., Jian, M.F., Mao, K., Liu, Z.T., Liao, W., Yan, Y.M., Shen, R.C., Zhong, A.W., 2023. Exploring the optical properties and molecular characteristics of dissolved organic matter in a large river-connected lake (Poyang Lake, China)

using optical spectroscopy and FT-ICR MS analysis. Science of the Total Environment. 879, 162999.

Xu, X.G., Li, W., Fujibayashi, M., Nomura, M., Nishimura, O., Li, X.N., 2015. Asymmetric response of sedimentary pool to surface water in organics from a shallow hypereutrophic lake: The role of animal consumption and microbial utilization. Ecological Indicators. 58, 346-355.

Xu, X.G., Shi, R.J., Lv, C.X., Liu, H.Z., Yang, W., Qian, S.H., Fujibayashi, M., Zhi, Y., Wang, G.X., Nomura, M., 2021. Hydrodynamic-Driven changes in the source and composition of sedimentary organic matter via Grain Size distribution in shallow lakes. Journal of Geophysical Research: Biogeosciences, 126(11): e2021JG006502.

Ya, M., Wu, Y.L., Wang, X.H., Wei, H.C., 2022. Fine particles and pyrogenic carbon fractions regulate PAH partitioning and burial in a eutrophic shallow lake. Environmental Pollution. 314, 120211.

Yan, F.P., Du, Z.H., Pu, T., Xu, Q., Wang, L., Ma, R.F., Zhang, C., Yu, Z.L., Li, C.L., Kang, S.C., 2023. Isotopic composition and emission characteristics of CO_2 and CH_4 in glacial lakes of the Tibetan Plateau. Environmental Research Letters. 18(9), 094025.

Yan, X.C., Xu, X.G., Ji, M., Zhang, Z.Q., Wang, Z.Q., Wang, M.Y., Wu, S.J., Wang, G.X., Zhang, C., Liu, H.C., 2019. Cyanobacteria blooms: A neglected facilitator of CH_4 production in eutrophic lakes. Science of the Total Environment, 651(466-474), 1.

Yan, X.C., Xu, X.G., Wang, M.Y., Wang, G.X., Wu, S.J., Li, Z.C., Sun, H., Shi, A., Yang, Y.H., 2017. Climate warming and cyanobacteria blooms: Looks at their relationships from a new perspective. Water Research, 125, 449-457.

Yao, M., Henny, C., Maresca, J.A., 2016. Freshwater bacteria release methane as a by-product of phosphorus acquisition. Applied Environmental Microbiology, 82(23), 6994-7003.

Yang, H., Xie, P., Ni, LY., Flower, R.J., 2011. Underestimation of CH_4 emission from freshwater lakes in China. Environmental Science & Technology. 45(10), 4203-4204.

Yang, Y.Y., Chen, J.F., Chen, X.L., Jiang, Q.S., Liu, Y., Xie, S.G., 2021. Cyanobacterial bloom induces structural and functional succession of microbial communities in

eutrophic lake sediments. Environmental Pollution. 284, 117157.

Yang, Y.Y., Chen, J.F., Tong, T.L., Li, B.Q., He, T., Liu, Y., Xie, S.G., 2019. Eutrophication influences methanotrophic activity, abundance and community structure in freshwater lakes. Science of the Total Environment. 662, 863-872.

Yang, Y.Y., Li, N.N., Wang, W., Li, B.X., Xie, S.G., Liu, Y., 2017. Vertical profiles of sediment methanogenic potenital and communities in two plateau freshwater lakes. Biogeosciences. 14(2), 341-351.

Ye, L.L., Wu, X.D., Liu, B., Yan, D.Z., Kong, F.X., 2015. Dynamics and sources of dissolved organic carbon during phytoplankton bloom in hypereutrophic Lake Taihu (China). Limnologica, 54: 5-13.

Yu, M.D., Liu, S.J., Li, G.W., Zhang, H., Xi, B.D., Tian, Z.F., Zhang, Y., He, X.S., 2020. Municipal wastewater effluent influences dissolved organic matter quality and microbial community composition in an urbanized stream. Science of the Total Environment. 705, 135952.

Yu, T., Zhang, Y., Wu, F,C., Meng, W., 2013. Six-decade change in water chemistry of large freshwater lake Taihu, China. Environmental Science & Technology. 47(16), 9093-9101.

Zeng, Q., Hao T.W., Mackey, H.R., van Loosdrecht, M.C.M., Chen, G.H., 2019. Recent advances in dissimilatory sulfate reduction: From metabolic study to application. Water Research. 150, 162-181.

Zhao, Y.P., Wu, S.J., Yu, M.T., Zhang, Z.Q., Wang, X., Zhang, S.Y., Wang, G.X., 2021. Seasonal iron-sulfur interactions and the stimulated phosphorus mobilization in freshwater lake sediments. Science of the Total Environment, 768, 144336.

Zhao, Z.L., Huang, C.C., Meng, L.Z., Lu, L.F., Wu, Y.F., Fan, R., Li, S.D., Sui, Z.W., Huang, T., Huang, C.L., 2021. Eutrophication and lakes dynamic conditions control the endogenous and terrestrial POC observed by remote sensing: Modeling and application. Ecological Indicators, 129: 107907.

Zhang, C., Cheng, S.G., Long, L., Xie, H., Mu, X.H., Zhang, W.L., 2018. Diel and seasonal methane flux across water-air interface of a subtrophic eutrophic pond. Toxicological and Environmental Chemistry, 100(4), 413-424.

Zhang, G.C., Elling, F.J., Nigro, L.M., Samarkin,V., Joye, S.B., Teske, A., Hinrichs, K.U., 2016. Multiple evidence for methylotrophic methanogenesis as the dominant methanogenic pathway in hypersaline sediments from the Orca Basin, Gulf of

Mexico. Geochimica et cosmochimica Acta. 187, 1-20.

Zhang, G.S., Yu, X.B., Gao, Y., Li, Y., Zhang, Q.J., Liu, Y., Rao, D.D., Lin, Y.M., Xia, S.X., 2018. Effects of water table on cellulose and lignin degradation of carex cinerascens in a large seasonal floodplain. Journal of Freshwater Ecology. 33(1), 311-325.

Zhang, H., Cui, K.P., Guo, Z., Li, X.Y., Chen, J., Qi, Z.G., Xu, S.Y., 2020. Spatiotemporal variations of spectral characteristics of dissolved organic matter in river flowing into a key drinking water source in China. Science of the Total Environment. 700, 134360.

Zhang, L., Sun, Q.X., You, Y., Zhang, K., Gao, C.D., Peng, Y.Z., 2021. Compositional and structurak characteristics of dissolved organic matter in overlying water of the Chaobai River and its environment significance. Environmental Science and Pollution Research. 28(42), 59673-59686.

Zhang, S.Y., Zhao, Y.P., Zhou, C.Q., Duan, H.X., Wang, G.X., 2021. Dynamic sulfur-iron cycle promoted phosphorus mobilization in sediments driven by the algae decomposition. Ecotoxicology, 30(8), 1662-1671.

Zhao, Y.P., Wu, S.J., Yu, M.T., Zhang, Z.Q., Wang, X., Zhang, S.Y., Wang, G.X., 2021. Seasonal iron-sulfur interactions and the stimulated phosphorus mobilization in freshwater lake sediments. Science of the Total Environment. 768, 144336.

Zhao, Y.P., Zhang, Z.Q., Wang, G.X., Li, X.J., Ma, J., Chen, S., Deng, H., Annalisa, O.H., 2019. High sulfide production induced by algae decomposition and its potential stimulation to phosphorus mobility in sediment. Science of the Total Environment. 650(1), 163-172.

Zhao, L.Y., Li, N., Huang, T.L., Zhang, H.H., Si, F., Li, K., Qi, Y.Z., Hua, F.Y., Huang, C., 2022. Effects of artificially induced complete mixing on dissolved organic matter in a stratified source water reservoir. Journal of Environmental Sciences. 111, 130-140.

Zhou, C.Q., Peng, Y., Yu, M.T., Deng, Y., Chen, L., Zhang, L.Q., Xu, X.G., Zhang, S.Y., Yan, Y., Wang, G.X., 2022a. Severe cyanobacteria accumulation potentially induces methylotrophic methane producing pathway in eutrophic lakes. Environmental Pollution, 292, 118443.

Zhou, C.Q., Peng, Y., Deng, Y., Yu, M.T., Chen, L., Zhang, L.Q., Xu, X.G., Zhao, F.J., Yan, Y., Wang, G.X., 2022b. Increasing sulfate concentration and sedimentary

decaying cyanobacteria co-affect organic mineralization in eutrophic lake sediments. Science of the Total Environment, 806, 151260.

Zhou, C.Q., Zhou, M.C., Jia, R.Y., Peng, Y., Zhao, F.J., Xu, R.Z., Liang, S.Y., Terada, A., Wang, G.X., Kinouchi, T., Xu, X.G., 2023a. Particulate organic carbon potentially increases methane emissions from oxic water of eutrophic lakes. Science of the Total Environment. 889, 164339.

Zhou, M.C., Zhou, C.Q., Peng, Y., Jia, R.Y., Zhao, Y.P., Liang, S.Y., Xu, X.G., Terada, A., Wang, G.X., 2023b. Space-for-time substitution leads to carbon emission overestimation in eutrophic lakes. Environmental Research. 219, 115175.

Zhou, C.Q., Zhou, M.C., Peng, Y., Xu, X.G., Terada, A., Wang, G.X., Zhong, H., Kinouchi, T., 2024. Unexpected increase of sulfate concentrations and potential impact on CH_4 budgets in freshwater lakes. Water Research. 261, 122018.

Zhou, Y.Q., Li, Y., Yao, X.L., Ding, W.H., Zhang, Y.B., Jeppesen, E., Zhang, Y.L., Podgorski, D.C., Chen, C.M., Ding, Y., Wu, H.W., Spencer, R.G.M., 2019. Response of chromophoric dissolved organic matter dynamics to tidal oscillations and anthropogenic disturbances in a large subtropical estuary. Science of the Total Environment. 662, 769-778.

Zhou, Y.Q., Xiao, Q.T., Yao, X.L., Zhang, Y.L., Zhang, M., Shi, K., Lee, X.H., Podgorski, D.C., Qin, B.Q., Spencer, R.G.M., Jeppesen, E., 2018. Accumulation of terrestrial dissolved organic matter potentially enhances dissolved methane levels in eutrophic lake Taihu, China. Environmental Science & Technology, 52(18), 10297-10306.

Zhou, Y.Q., Yao, X.L., Zhang, Y.L., Zhang, Y.B., Shi, K., Tang, X.M., Qin, B.Q., Podgorski, D.C., Brookes, J.D., Jeppesen, E., 2018. Response of dissolved organic matter optical properties to net inflow runoff in a large fluvial plain lake and the connecting channels. Science of the Total Environment. 639, 876-887.

Zhou, Y.W., Song, K., Han, R.M., Riya, S., Xu, X.G., Yeerken, S., Geng, S.X., Ma, Y., Terada, A., 2020. Nonlinear response of methane release to increased trophic state levels coupled with microbial processes in shallow lakes. Environmental Pollution, 265, 114919.

Zhou, Y.W., Xu, X.G., Han, R.M., Li, L., Feng, Y., Yeerken, S., Song, K., Wang, Q.L., 2019. Suspended particles potentially enhance nitrous oxide (N_2O) emissions in the oxic estuarine waters of eutrophic lakes: Field and experimental evidence.

Environmental Pollution, 252: 1225-1234.

Zhou, Y.W., Xu, X.G., Song, K., Yeerken, S., Deng, M., Liu, L., Riya, S.H., Wang, Q.L., Terada, A., 2021. Nonlinear pattern and algal dual-impact in N_2O emission with increasing trophic levels in shallow lakes. Water Research, 203, 117489.

Copyright

This thesis was published in the following Journals.

[1] **Zhou, C.Q**., Peng, Y., Zhou, M.C., Jia, R.Y., Liu, H.Z., Xu, X.G., Chen, L., Ma, J., Kinouchi, T., Wang, G.X., 2024. Cyanobacteria decay alters CH_4 and CO_2 produced hotspots along vertical sediment profiles in eutrophic lakes. Water Research, 265, 122319.

[2] **Zhou, C.Q**., Zhou, M.C., Peng, Y., Xu, X.G., Terada, A., Wang, G.X., Zhong, H., Kinouchi, T., 2024. Unexpected increase of sulfate concentrations and potential impact on CH_4 budgets in freshwater lakes. Water Research. 261, 122018.

[3] **Zhou, C.Q**., Xu, X.G., Peng, Y., Wang, G.S., Liu, H.Z., Jin, Q., Jia, R.Y., Ma, J., Kinouchi, T., Wang, G.X., 2024. Response of sulfate concentration to eutrophication on spatio-temporal scale in freshwater lakes. Science of the Total Environment. 953, 176142.

[4] **Zhou, C.Q**., Zhou, M.C., Jia, R.Y., Peng, Y., Zhao, F.J., Xu, R.Z., Liang, S.Y., Terada, A., Wang, G.X., Kinouchi, T., Xu, X.G., 2023. Particulate organic carbon potentially increases methane emissions from oxic water of eutrophic lakes. Science of the Total Environment. 889, 164339.

[5] Zhou, M.C., **Zhou, C.Q** (Co-first author)., Peng, Y., Jia, R.Y., Zhao, W.P., Liang, S.Y., Xu, X.G., Terada, A., Wang, G.X., 2023. Space-for-time substitution leads to carbon emission overestimation in eutrophic lakes. Environmental Research. 219, 115175.

[6] Ma, J., Zhou, M.C., Peng, Y., Tuo, Y., **Zhou, C.Q** (Corresponding author)., Liu, K.X., Huang, Y.L., He, F., Lai, Q.Y., Zhang, Z.H., Kinouchi, T., Li, S.Y., Xu, X.G., Wu, X.D., Lin, X.W., Li, W.X., Wang, G.X., 2024. Instability in a carbon pool driven by multiple dissolved organic matter sources in a eutrophic lake basin: Potential factors for increased greenhouse gas emissions. Journal of Environmental Management. 350, 119697.

Acknowledgement

As I write these words, a mix of emotions fills my heart. The days of the past are beyond reach, and the uncertainties of tomorrow weigh heavily. Three years have passed in the blink of an eye, and I extend my heartfelt gratitude to all those who have accompanied me sincerely along the way.

Firstly, I would like to express my heartfelt gratitude to my supervisor Prof. Tsuyoshi Kinouchi. I still vividly remember your encouragement and expectation when I first joined and shared my aspirations and research with you. I am deeply thankful for your patience and guidance, as well as your support and understanding during my moments of confusion in both my research and personal life. I will carry this encouragement and expectation with me as I continue striving forward.

Secondly, I would like to extend my heartfelt thanks to Prof. Xiaoguang Xu, who has been both a mentor and a friend to me. Thank you for your unwavering support and for going above and beyond to help me achieve what I aspire to and become the person I strive to be. I am especially grateful for your encouragement and companionship during countless challenging days and nights. In the days to come, I will continue to work hard and make you proud.

Additionally, I would like to express my sincere gratitude to the members of the defense committee, Prof. Nakamura (Suzukakeidai), Prof. Yoshimura, Prof. Nakamura (Ookayama), and Prof. Fuji. Your professional insights and comments during the defense process have immensely helpful in improving my thesis. I deeply appreciate your support and help.

I would also like to express my gratitude to all the members of the Kinouchi Lab for their companionship and encouragement over the past three years. The experiences we shared together are truly precious. My thanks also go to all the teachers and friends at MIFA, especially my Japanese teacher, Omatsu sensei, for teaching me Japanese and preparing thoughtful gifts. I wish you health and happiness in the years to come. I am deeply thankful to the Chinese members of Professor Terada's Lab at Tokyo University of Agriculture and Technology for the warmth and happiness they have brought into my life. Additionally, I would like to thank my friends at Institute of Science Tokyo, including Qiulin Xu, Haitian Zhang, and Rongzhen Cai, *etc*, as well as the friends I have met during my studies and life in Japan. Thank you for listening to me, supporting

me, and accompanying me throughout my journey.

My heartfelt gratitude extends to my parents, grandparents, and family members, whose unwavering support allowed me to focus on completing my doctoral research with peace of mind. I am equally grateful to my lifelong friends for standing by my side all these years.

Lastly, I want to thank myself. Thank you for persevering through countless days and nights, for your determination, and for striving to become the person you aspire to be. Thank you for your unwavering effort and resilience.

This research was supported by JST SPRING (JPMJSP2106), JASSO, and the National Natural Science Foundation of China (42077294).

Chuanqiao Zhou

Written in Japan, February 2025